Double soft theorem for generalised bi-adjoint scalar amplitudes

Md. Abhishek, Subramanya Hegde, Dileep P. Jatkar & Arnab Priya Saha,
arXiv: 2008.07271[hep-th]

[1] Harish-Chandra Research Institute, Allahabad, India - 211019

mdabhishek@hri.res.in, subramanyahegde@hri.res.in, dileep@hri.res.in, arnabpriyasaha@hri.res.in

Introduction

- In usual CHY formalism, we map the kinematic space of n-particle scattering to the moduli space of n-punctured Riemann sphere ($\mathbb{CP}^1$). CEGM formalism[2] generalises this to generalised bi-adjoint scalar amplitudes, defined as the integral on n-punctured $\mathbb{CP}^{k-1}$.
- Generalised scattering potential:

$$\mathcal{S}^{(k)} = \sum_{a_1<a_2<\cdots<a_k} s_{a_1 a_2\cdots a_k} \log |a_1 a_2 \cdots a_k|, \tag{1}$$

where $s_{a_1 a_2\cdots a_k}$ are generalized Mandelstam variables, and $|a_1 a_2 \cdots a_k|$ are the determinant of the $k \times k$ minor of $n \times k$ matrix with the inhomogeneous coordinates of the punctures $a_1, a_2, \cdots, a_k$ as entries.

- Scattering equations:

$$E_a^i := \frac{\partial \mathcal{S}^{(k)}}{\partial x_i^a} = 0. \tag{2}$$

- The n-point amplitude is given by,

$$m_n^{(k)}(\alpha|\beta) = \frac{1}{vol(SL(k,\mathbb{C}))} \int \prod_{a=1}^{n}\prod_{i=1}^{k-1} dx_i^a \prod_{a=1}^{n}\prod_{i=1}^{k-1} \delta(E_a^i) PT^{(k)}(\alpha) PT^{(k)}(\beta), \tag{3}$$

where the Parke-Taylor factor with canonical ordering,

$$PT^{(k)}(\mathbb{I}) = \frac{1}{|12\cdots k||2\cdots k+1|\cdots|n-k+1\, n-k+2\cdots n|}. \tag{4}$$

- The usual CHY bi-adjoint scalar amplitudes for n particle scattering are related to $\mathcal{A}_{n-3}$ cluster algebra. For a given general k and n value, CEGM amplitudes are related to $Gr(k,n)$ cluster algebra. These $k>2$ amplitudes do not have a physical intepretation, as of yet.

Soft theorems for k=2

Single soft limit

- Take n-th particle to be soft, and Mandelstam variables scale as,

$$s_{na} = \tau \hat{s}_{na}, \quad lim\, \tau \to 0, \quad a \in \{1,2,\cdots,n-1\}. \tag{5}$$

- Scattering equations,

$$E_a = \sum_{b=1, b\neq a}^{n-1} \frac{s_{ab}}{x_a - x_b} = 0, \qquad E_n = \tau \sum_{b=1}^{n-1} \frac{\hat{s}_{nb}}{x_n - x_b} = 0. \tag{6}$$

- We cansider soft limit in bi-adjoint scalar amplitude,

$$m_n^{(2)}(I|I) = \mathtt{S}_n^{(2)} m_{n-1}^{(2)}(I|I), \tag{7}$$

where the single soft factor,

$$\mathtt{S}_n^{(2)} = \frac{1}{\tau}\left[\frac{1}{\hat{s}_{n\,n-1}} + \frac{1}{\hat{s}_{n\,1}}\right]. \tag{8}$$

Double soft limit

- In the adjacent double soft limit, contributions from the degenerate solutions dominate over those of the non-degenerate ones.
- Take the adjacent n-th and (n-1)-th particles to be soft simultaneously, and Mandelstam variables scale as,

$$s_{na} = \tau \hat{s}_{na}, \quad s_{n-1\,a} = \tau \hat{s}_{n-1\,a} \quad s_{n\,n-1} = \tau^2 \hat{s}_{n\,n-1}, \quad a \in \{1,2,\cdots,n-2\}. \tag{9}$$

- Scattering equations,

$$E_a = \sum_{b=1, b\neq a}^{n-2} \frac{s_{ab}}{x_a - x_b} = 0,$$

$$E_{n-1} = \tau \sum_{b=1}^{n-2} \frac{\hat{s}_{n-1\,b}}{x_{n-1} - x_b} + \tau^2 \frac{\hat{s}_{n-1\,n}}{x_{n-1} - x_n} = 0, \quad E_n = \tau \sum_{b=1}^{n-2} \frac{\hat{s}_{n\,b}}{x_n - x_b} - \tau^2 \frac{\hat{s}_{n-1\,n}}{x_{n-1} - x_n} = 0. \tag{10}$$

- The simultaneous double soft factor,

$$\mathtt{S}_{DS}^{(2)} = \frac{1}{\tau^3} \frac{1}{\hat{s}_{n\,n-1}} \left[\frac{1}{\hat{s}_{n-1\,n-2} + \hat{s}_{n\,n-2}} + \frac{1}{\hat{s}_{n-1\,1} + \hat{s}_{n\,1}}\right]. \tag{11}$$

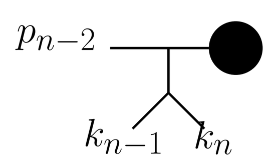

$$\frac{1}{s_{n-1\,n}} \times \frac{1}{s_{n-1\,n-2} + s_{n\,n-2}}$$

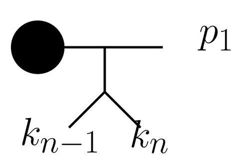

$$\frac{1}{s_{n-1\,n}} \times \frac{1}{s_{n-1\,1} + s_{n\,1}}$$

- The non-adjacent simultaneous double soft factor is subleading and scales as τ^{-2}.

Single soft theorem for generalised bi-adjoint scalars

Single soft limit for $k=3$

- For general $k \geq 3$, we will consider the regular solutions of the scattering equations because singular solutions will contribute in subleading order as shown in [3].
- In the single soft limit by taking the n-th puncture to be soft the scattering equantions become,

$$E_a^{(i)} = \sum_{\{b,c\}\neq\{a,n\}}^{n-2} \frac{s_{abc}}{|abc|}\frac{\partial}{\partial x_a^{(i)}}|abc| = 0, \quad E_n^{(i)} = \tau \sum_{1\leq a<b\leq n-1} \frac{\hat{s}_{abn}}{|abn|}\frac{\partial}{\partial x_n^{(i)}}|abn| = 0, \quad i=1,2. \tag{12}$$

- Here we have encounter two types of singularities collision and collinear singulaties.
- The single soft factor,

$$\mathtt{S}_n^{(3)} = \frac{1}{\tau^2}\frac{1}{\sum_{a=2}^{n-1}\hat{s}_{1\,a\,n}}\left(\frac{1}{\hat{s}_{1\,2\,n}} + \frac{1}{\hat{s}_{n-1\,n\,1}}\right) + \frac{1}{\sum_{a=1}^{n-2}\hat{s}_{n-1\,n\,a}}\left(\frac{1}{\hat{s}_{n-1\,n\,1}} + \frac{1}{\hat{s}_{n-2\,n-1\,n}}\right) + \frac{1}{\hat{s}_{n-2\,n-1\,n}\hat{s}_{n\,1\,2}}. \tag{13}$$

Single soft limit for arbitrary k

- In [3], the single soft factor for arbitrary k value was evaluated in terms of the generalised Mandelstam variables by an iterative procedure.
- The scaling of the soft factor can be seen to be $\tau^{-(k-1)}$.

Double soft theorem for $k=3$

- The scattering equations, with n-th and (n-1)-th punctures to be soft, are,

$$E_a^{(i)} = \sum_{b,c\neq a,n-1,n} \frac{s_{abc}}{|abc|}\frac{\partial}{\partial x_a^{(i)}}|abc|, \quad \forall a,$$

$$E_{n-1}^{(i)} = \tau \sum_{a,b\neq n-1,n} \frac{\hat{s}_{ab\,n-1}}{|ab\,n-1|}\frac{\partial}{\partial x_{n-1}^{(i)}}|ab\,n-1| + \tau^2 \sum_{a=1}^{n-2} \frac{\hat{s}_{a\,n-1\,n}}{|a\,n-1\,n|}\frac{\partial}{\partial x_{n-1}^{(i)}}|a\,n-1\,n| = 0,$$

$$E_n^{(i)} = \tau \sum_{a,b\neq n-1,n} \frac{\hat{s}_{ab\,n}}{|ab\,n|}\frac{\partial}{\partial x_n^{(i)}}|ab\,n| + \tau^2 \sum_{a=1}^{n-2} \frac{\hat{s}_{a\,n-1\,n}}{|a\,n-1\,n|}\frac{\partial}{\partial x_n^{(i)}}|a\,n-1\,n| = 0, \quad i=1,2. \tag{14}$$

- In this limit the adjacent degenerate configuration gives leading order contribution.
- The double soft factor, when the two soft punctures collide in the degenerate limit,

$$\begin{aligned}\mathtt{S}_{\mathrm{DS}}^{(3)} =& \frac{\tau^{-6}}{\sum_{a=1}^{n-2}\hat{s}_{a\,n-1\,n}}\left(\frac{1}{\hat{s}_{n-1\,n\,1}} + \frac{1}{\hat{s}_{n-2\,n-1\,n}}\right) \\ &\times \Bigg[\frac{1}{(\hat{s}_{n-3\,n-2\,n-1} + \hat{s}_{n-3\,n-2\,n})(\hat{s}_{n-1\,12} + \hat{s}_{n12})} \\ &+ \frac{1}{\sum_{a=1}^{n-3}(\hat{s}_{a\,n-2\,n-1} + \hat{s}_{a\,n-2\,n})}\left(\frac{1}{\hat{s}_{n-3\,n-2\,n-1} + \hat{s}_{n-3\,n-2\,n}} + \frac{1}{\hat{s}_{n-2\,n-1\,1} + \hat{s}_{n-2\,n\,1}}\right) \\ &+ \frac{1}{\sum_{a=2}^{n-2}(\hat{s}_{a\,n-1\,1} + \hat{s}_{an1})}\left(\frac{1}{\hat{s}_{n-2\,n-1\,1} + \hat{s}_{n-2\,n\,1}} + \frac{1}{\hat{s}_{n-1\,12} + \hat{s}_{n12}}\right)\Bigg].\end{aligned} \tag{15}$$

- The configuration, when the soft punctures are collinear to one hard puncture, produces subleading contribution compared to the case when two soft punctures collide.

Simultaneous double soft theorem for arbitrary k

- For arbitrary k value, the leading order double soft factor comes from the degenerate configuration. The degenerate solution of the scattering equation comes from two different situations,
  1. when two adjacent punctures, say n-th and $(n-1)$-th, on $\mathbb{CP}^{(k-1)}$ infinitesimally approach each other,
  2. when two adjacent soft punctures and $(k-2)$ number of hard punctures lie in a codimension one subspace.
- For the above both cases the determinant $|a_1 a_2 \cdots a_k| \sim \mathcal{O}(\tau)$, where the parameter τ defines the soft limit in terms of the generalized Mandelstam variables given below,

$$\begin{aligned} s_{a_1\,a_2\cdots\,a_{k-1}\,n} &= \tau\, \hat{s}_{a_1\,a_2\cdots a_{k-1}\,n}, \\ s_{a_1\,a_2\cdots\,a_{k-1}\,n-1} &= \tau\, \hat{s}_{a_1\,a_2\cdots a_{k-1}\,n-1}, \\ s_{a_1\,a_2\cdots\,a_{k-2}\,n-1\,n} &= \tau^2\, \hat{s}_{a_1\,a_2\cdots a_{k-2}\,n-1\,n}. \end{aligned} \tag{16}$$

- In the leading order the configuration(1), mentioned above, dominates over the other for degenerate adjacent case. The non-degenerate solutions contribute in further lower order in the adjacent double soft factor.
- The simultaneous double soft factor for the adjacent soft external states n and $(n-1)$ is,

$$\mathtt{S}_{\mathrm{DS}}^{(k)} = \frac{1}{\sum_{1\leq a_1\cdots<a_{k-2}\leq n-2} s_{a_1\cdots a_{k-2}\,n-1\,n}} \mathtt{S}^{(k-1)}\left(s_{a_1\cdots a_{k-2}\,m} \to s_{a_1\cdots a_{k-2}\,n-1\,n}\right)\, \mathtt{S}^{(k)}, \tag{17}$$

where the single soft factor $\mathtt{S}^{(k-1)}$ for $k-1$ is defined with m as the composite level for '$n-1\ n$' and $\mathtt{S}^{(k)}$ is the single soft factor for k, but with the shifted generalised Mandelstam variable $(s_{a_1\cdots a_{k-1}\,n} + s_{a_1\cdots a_{k-1}\,n-1})$.

- The leading simultaneous double soft factor for the adjacent case scales as $\tau^{-3(k-1)}$ as $\tau \to 0$, and the non-adjacent double soft factor contributes in the subleading order for arbitrary k-value.

Conclusions and future directions

- Relation between the $Gr(3,6)$ amplitude and four point one-loop integrand in cubic biadjoint scalar field theory is studied in [1].
- Factorisations of the amplitude can be given in the moduli space using the CEGM classification of boundaries of the moduli space.
- Appearance of the higher order poles could be a signature of composite particles or multiparticle states contributing to the amplitude.
- It would be interesting to generalise our results to multiple soft theorem.
- Study of subalgebras of cluster algebra from CEGM moduli space maybe interesting for applications to $Gr(4,n)$ amplitudes relevant for the study of SYM amplitudes.

References

[1] Md. Abhishek, Subramanya Hegde, and Arnab Priya Saha. One-loop integrand from generalised scattering equations. *JHEP*, 05:012, 2021.

[2] Freddy Cachazo, Nick Early, Alfredo Guevara, and Sebastian Mizera. Scattering Equations: From Projective Spaces to Tropical Grassmannians. *JHEP*, 06:039, 2019.

[3] Diego García Sepúlveda and Alfredo Guevara. A Soft Theorem for the Tropical Grassmannian. 9 2019.

Acknowledgements

We are grateful to Subhroneel Chakrabarti, Alok Laddha, R. Loganayagam, Biswajit Sahoo, and Ashoke Sen for several important and illuminating discussions.

MANCHESTER 1824
The University of Manchester

A New Form of QCD Coherence Using Glauber-SCET

Aditya Pathak
The University of Manchester

Abstract

Amplitude-level factorization has been long understood in terms of a product of loop-expanded soft-gluon currents and hard scattering matrix element, both of which are IR divergent. A more recent work by Angeles-Martinez, Forshaw and Seymour (AMFS) expressed the factorization in an ordered evolution approach involving IR finite one-loop insertions where the virtual momentum is constrained in a highly non-trivial way by the k_T of the adjacent real emissions. The proof of AMFS result at one-loop in QCD, however, involves many diagrams, and only after summing over all the diagrams does the correct ordering variable emerge. This highlights the difficulty in extending the result to higher orders. We present using effective operators in the Glauber-SCET Lagrangian, an elegant and a significantly compact proof of the AMFS result, involving only a few diagrams, that offers clean physical insights and makes higher order extension of the AMFS result tractable.

1 Introduction

1.1 Amplitude for ordered soft gluon emissions

Consider amplitude for N ordered soft gluon emissions from n hard partons with momenta $\{p_i\}$ with

$$\{p_i^\mu\} \gg q_1^\mu \gg \ldots \gg q_N^\mu \tag{1}$$

$$\big|M_N\big] = (g\mu^\epsilon)^N \mathbf{J}(q_N)\ldots\mathbf{J}(q_1)\big|\mathcal{M}(p_1,\ldots,p_n)\big]\,, \tag{2}$$

Both the hard matrix element and soft gluon amplitudes have the loop expansion:

$$\big|\mathcal{M}(p_1,\ldots,p_n)\big] = \big|M_0^{(0)}\big] + \big|M_0^{(1)}\big] + \ldots\,, \qquad \mathbf{J}(q) = \mathbf{J}^{(0)}(q) + \mathbf{J}^{(1)}(q) + \ldots\,, \tag{3}$$

At one-loop accuracy, we have

$$\mathbf{J}^{(1)}(q_{m+1}) = \frac{1}{2}\sum_{j=1}^{n+m}\sum_{k=1}^{n+m}\mathbf{d}_{jk}^{(1)}(q_{m+1})\,, \quad \big|M_0^{(1)}\big] = \sum_{i=2}^{n}\sum_{j=1}^{i-1}\mathbf{I}_{ij}(0,\omega_{ij})\big|M_0^{(0)}\big]\,, \quad \omega_{ij} \equiv 2p_i\cdot p_j\,, \tag{4}$$

IR divergent soft gluon emission and virtual corrections:

$$\mathbf{d}_{ij}^{(1)}(q) \equiv \frac{\alpha_s}{2\pi}\frac{c_\Gamma}{\epsilon^2}\mathbf{T}_q\cdot\mathbf{T}_i\left(\frac{e^{-\mathrm{i}\pi\tilde\delta_{ij}}}{e^{-\mathrm{i}\pi\tilde\delta_{iq}}e^{-\mathrm{i}\pi\tilde\delta_{jq}}}\frac{4\pi\mu^2}{(q_\perp^{(ij)})^2}\right)^\epsilon\mathbf{d}_{ij}(q)\,, \qquad \mathbf{I}_{ij}(0,\omega_{ij}) \equiv \frac{\alpha_s}{2\pi}\frac{c_\Gamma}{\epsilon^2}\mathbf{T}_i\cdot\mathbf{T}_j\left(e^{-\mathrm{i}\pi\tilde\delta_{ij}}\frac{4\pi\mu^2}{\omega_{ij}}\right)^\epsilon\,,$$

Which IR divergences survive in the multiple, ordered soft gluon amplitude?

1.2 The AMFS Result

Angeles-Martinez, Forshaw and Seymour [1] (AMFS) re-expressed the result in an ordered evolution approach, involving ***IR finite* one-loop insertions** bounded by k_T of soft gluon emissions.

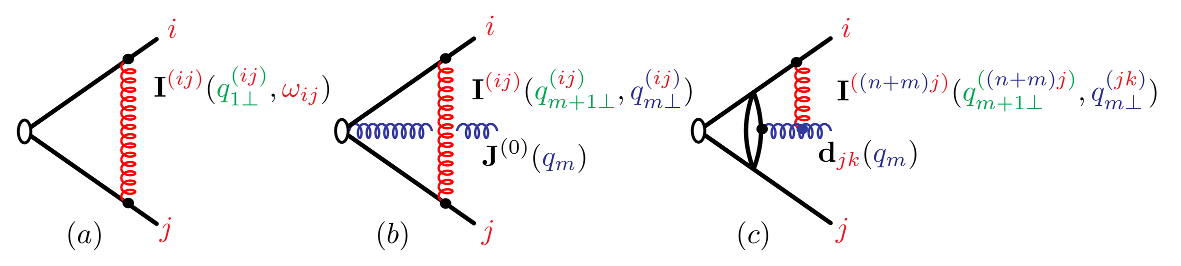

Figure 1: The three lines in the AMFS result

$$\begin{aligned}\big|M_N^{(1)}\big] &= (g\mu^\epsilon)^N\left(\prod_{k=1}^{N}\mathbf{J}^{(0)}(q_k)\right)\left(\sum_{i=2}^{n}\sum_{j<i}\mathbf{I}^{(ij)}(q_{1\perp}^{(ij)},\omega_{ij})\right)\big|M_0^{(0)}\big]\\ &+ (g\mu^\epsilon)^N\sum_{m=1}^{N}\left(\prod_{k=m+1}^{N}\mathbf{J}^{(0)}(q_k)\right)\left(\sum_{i=2}^{n+m-1}\sum_{j<i}\mathbf{I}^{(ij)}(q_{m+1\perp}^{(ij)},q_{m\perp}^{(ij)})\right)\left(\prod_{\ell=1}^{m}\mathbf{J}^{(0)}(q_\ell)\right)\big|M_0^{(0)}\big]\\ &+ (g\mu^\epsilon)^N\sum_{m=1}^{N}\left(\prod_{k=m+1}^{N}\mathbf{J}^{(0)}(q_k)\right)\left(\sum_{j,k=1}^{n+m-1}\mathbf{I}^{(n+m)j}(q_{m+1\perp}^{((n+m)j)},q_{m\perp}^{(jk)})\mathbf{d}_{jk}(q_m)\right)\left(\prod_{\ell=1}^{m-1}\mathbf{J}^{(0)}(q_\ell)\right)\big|M_0^{(0)}\big]\,,\end{aligned} \tag{5}$$

where

$$\mathbf{I}^{(ij)}(a,b) = \frac{\alpha_s}{2\pi}\mathbf{T}_i\cdot\mathbf{T}_j\left[\left(\frac{4\pi\mu^2}{b^2}\right)^\epsilon\left(1+\mathrm{i}\pi\tilde\delta_{ij}-\epsilon\ln\frac{2p_i\cdot p_j}{b^2}\right)-\left(\frac{4\pi\mu^2}{a^2}\right)^\epsilon\left(1+\mathrm{i}\pi\tilde\delta_{ij}-\epsilon\ln\frac{2p_i\cdot p_j}{a^2}\right)\right]. \tag{6}$$

Features:

1. **Virtual loop-momentum bounded** by k_T of adjacent real emissions.
2. **Novel amplitude level QCD coherence** where the IR divergences originating only from the very last, softest, gluon emission remain, and the rest cancel.
3. **Markovian** in nature **but cannot be exponentiated**! No analog in SCET
4. **Interesting memory effect**: In the last line k_T of the last emission must be evaluated in the rest frame of its *parent-dipole*, (jk)

1.3 Derivation using QCD graphs (Very Complicated!)

Focus on the imaginary part of one-loop diagrams by evaluating ***cut diagrams***.

- Involves **many diagrams with careful grouping**
- **Only after summing** over all the diagrams does the correct ordering variable emerge
- **Extremely hard to extend to higher orders**!

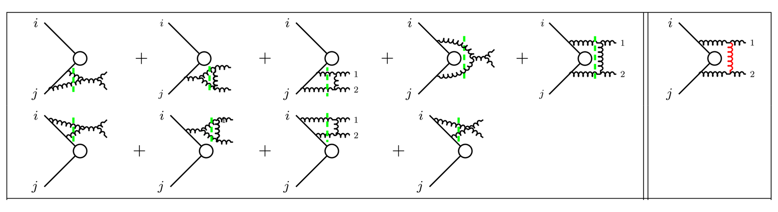

Figure 2: Graphs for cuts through soft gluons

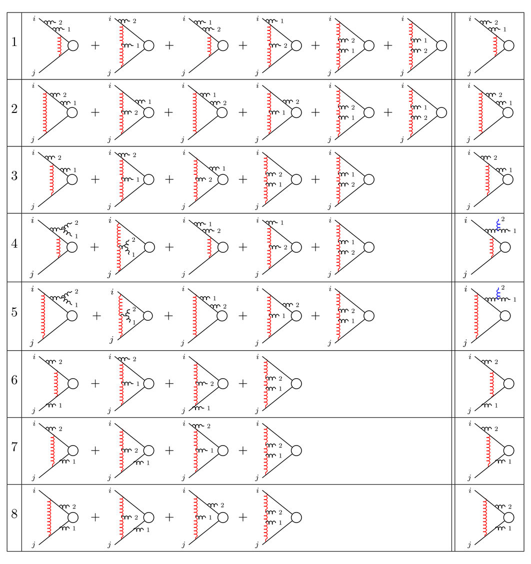

Figure 3: Grouping of 2 real emission diagrams in QCD graphs for cuts through hard partons

2 Derivation using Glauber-SCET

Derive the AMFS result in Eq. (5) in Soft Collinear Effective Theory with Glauber operators [2] **with only a handful of diagrams**.

1. Hard scattering operator with Soft Wilson lines:

$$O_n = \sum_\Gamma\int\left(\prod_{i=1}^{n}d\omega_i\right)\big[O_n^{(0)}(\{\omega_i,n_i\})\big|\prod_{i=1}^{n}\mathbf{S}_{n_i}\big|\mathcal{C}_{n,\Gamma}(\{\omega_i\})\big]\,. \tag{7}$$

2. Glauber operators:

$$O_{n_i s n_j}^{ij} = \mathbf{O}_{n_i}^{i}\cdot\frac{1}{\mathcal{P}_\perp^2}\hat{\mathbf{O}}_s^{(n_i n_j)}\frac{1}{\mathcal{P}_\perp^2}\cdot\mathbf{O}_{n_j}^{j}\,, \qquad O_{n_i s}^{ij} = \mathbf{O}_{n_i}^{i}\cdot\frac{1}{\mathcal{P}_\perp^2}\mathbf{O}_s^{n_i,j} \tag{8}$$

3. Correspondence between QCD and SCET result:

$$\begin{aligned}&\big[\{C_j\}\cup\{a_i\}\big|(g\mu^\epsilon)^N\mathbf{J}(q_N)\ldots\mathbf{J}(q_1)\big|\mathcal{M}(p_1,\ldots,p_n)\big]\\ &= \sum_\Gamma\int\left(\prod_{i=1}^{n}d\omega_i\right)\Big[\{C_j\}\cup\{a_i\}\Big|\langle\{p_i\},\{q_j\}\big|\Big(\mathrm{T}\,O_n^{(0)}(\{\omega_i,n_i\})\prod_{i=1}^{n}\mathbf{S}_{n_i}e^{\mathrm{i}\int d^4x' O_G(x')}\Big)\big|0\rangle\big|\mathcal{C}_{n,\Gamma}(\{\omega_i\})\Big]\,.\end{aligned} \tag{9}$$

Glauber graphs allow us to ***efficiently calculate the imaginary part*** of the amplitude.

2.1 Derivation using a recursive EFT sequence

Step 1: Amplitude for single gluon emission

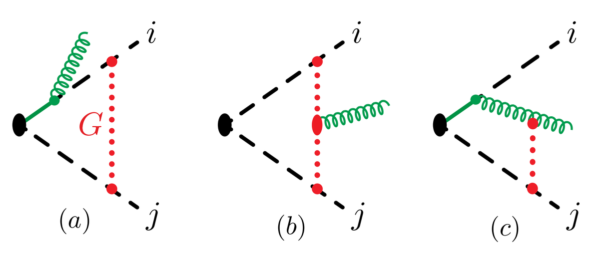

Combine the matrix element with the **Wilson coefficient**:

$$\mathrm{Im}\big|\mathcal{C}_n^{[1]}(\{\omega_i\},\mu)\big] = \sum_{i=1}^{n}\sum_{j<i}\mathbf{C}^{(ij)}(\mu,\omega_{ij})\big|M_0\big]\,, \qquad \mathbf{C}^{(ij)} = \mathrm{Im}\big[\mathbf{I}^{(ij)}\big]\,. \tag{10}$$

One gluon emission at one loop:

$$\begin{aligned}&\mathrm{Im}\Big(\big[\{a_i\},C_1\big|\langle(q_1,\varepsilon_1),\{p_i\}|O_n(\{\omega_i,n_i\})|0\rangle\big|\mathcal{C}_n(\{\omega_i\},\mu)\big]\Big)^{[1]}\\ &= \big[\{a_i\},C_1\big|\Big(g\,\varepsilon_1\cdot\mathbf{J}^{(0)}(q_1)\times\mathrm{Im}\big|\mathcal{C}_n^{[1]}(\{\omega_i\},\mu)\big] + G_{1(a+b+c)}(m,q_1,\mu)\times\mathrm{Re}\big|\mathcal{C}_n^{[0]}(\{\omega_i\},\mu)\big]\Big)\\ &= g\big[\{a_i\},C_1\big|\Big(\varepsilon_1\cdot\mathbf{J}^{(0)}(q_1)\sum_{i=1}^{n}\sum_{j<i}\mathbf{C}^{(ij)}(q_{1\perp}^{(ij)},\omega_{ij})\\ &\qquad + \sum_{i=1}^{n}\Big[\sum_{j<i}\mathbf{C}^{(ij)}(m,q_{1\perp}^{(ij)})\,\varepsilon_1\cdot\mathbf{J}^{(0)}(q_1) + \sum_{j\neq i}\mathbf{C}^{(q_1 j)}(m,q_{1\perp}^{(ij)})\,\varepsilon_1\cdot\mathbf{d}_{ji}(q_1)\Big]\Big)\big|M_0\big]\,.\end{aligned} \tag{11}$$

Step 2: Resolve the soft emission and update the hard scattering and Glauber operators

$$O_{n+1}^{\text{hard scatter}} = \int\left(\prod_{i=1}^{n+1}d\omega_i\right)\big[O_{n+1}(\{\omega_1,n_1,\omega_i,n_i\})\big|\mathcal{C}_{n+1}(\{\omega_1,\omega_i\},\mu)\big]\,. \tag{12}$$

$$\big[O_{n+1}(\{\omega_1,n_1,\omega_i,n_i\})\big| \equiv \big[O_n(\{\omega_i,n_i\})\big|\left[g\sum_{i=1}^{n}\frac{n_i\cdot\mathcal{B}^a_{n_1\perp,\omega_1}}{n_i\cdot q_1}\mathbf{T}_i^a\right]\,. \tag{13}$$

Calculate the imaginary part of the **Wilson coefficient for the low energy EFT** by one-loop Glauber graphs:

$$\begin{aligned}&\mathbf{J}^{(0)}(q_1)\mathrm{Im}\big|\mathcal{C}_{n+1}^{[1]}(\{q_{1\perp}^{(ij)},\omega_i\},\mu)\big] = \mathbf{J}^{(0)}(q_1)\sum_{i=1}^{n}\sum_{j<i}\mathbf{C}^{(ij)}(q_{1\perp}^{(ij)},\omega_{ij})\big|M_0\big]\\ &+ \sum_{i=1}^{n}\Big(\sum_{j<i}\mathbf{C}^{(ij)}(\mu,q_{1\perp}^{(ij)})\mathbf{J}^{(0)}(q_1) + \sum_{j\neq i}\mathbf{C}^{(q_1 i)}(\mu,q_{1\perp}^{(ij)})\mathbf{d}_{ij}(q_1)\Big)\big|M_0\big]\,.\end{aligned} \tag{14}$$

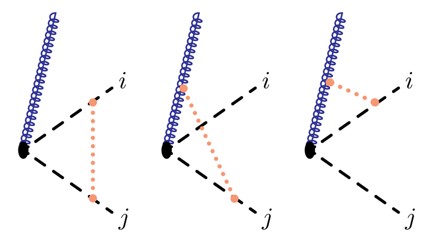

Step 3: Recycle the single gluon emission result and derive AMFS by induction

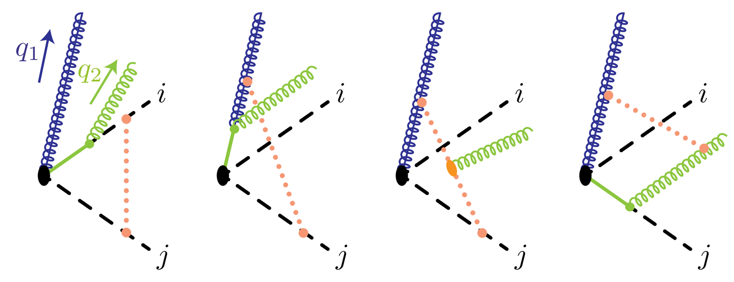

Two soft gluon emissions at one-loop:

$$\begin{aligned}&\mathrm{Im}\Big[\{C_1,C_2\}\cup\{a_i\}\Big|\langle(q_2,\varepsilon_2),(q_1,\varepsilon_1),\{p_i\}|O_{n+1}(\{q_{1\perp}^{(ij)},n_1,\omega_i,n_i\})|0\rangle\Big|\mathcal{C}_{n+1}(\{q_{1\perp}^{(ij)},\omega_i\},\mu)\Big]^{[1]}\\ &= g^2\,\varepsilon_{2\nu}\varepsilon_{1\mu}\Big[\mathbf{J}_2^\nu(q_2,q_1)\mathbf{J}^{(0)\mu}(q_1)\sum_{i=1}^{n}\sum_{j\neq i}\mathbf{C}^{(ij)}(q_{1\perp}^{(ij)},\omega_{ij})\\ &\qquad + \mathbf{J}_2^\nu(q_2,q_1)\sum_{i=1}^{n}\Big(\sum_{j<i}\mathbf{C}^{(ij)}(q_{2\perp}^{(ij)},q_{1\perp}^{(ij)})\Big)\mathbf{J}^{(0)\mu}(q_1) + \sum_{j\neq i}\mathbf{C}^{(q_1 i)}(q_{2\perp}^{(q_1 i)},q_{1\perp}^{(ij)})\,\mathbf{d}_{ij}^\mu(q_1)\Big)\\ &\qquad + \sum_{i=1}^{n+1}\Big(\sum_{j<i}\mathbf{C}^{(ij)}(m,q_{2\perp}^{(ij)})\mathbf{J}_2^\nu(q_2,q_1) + \sum_{j\neq i}\mathbf{C}^{(q_2 i)}(m,q_{2\perp}^{(ij)})\,\mathbf{d}_{ij}^\nu(q_2)\Big)\mathbf{J}^{(0)\mu}(q_1)\Big]\,.\end{aligned} \tag{15}$$

SCET derivation is thus a lot more compact!

2.2 Derivation using double soft emission amplitude in SCET

The **grouping of QCD graphs** is already ***implicit in the SCET graphs***!

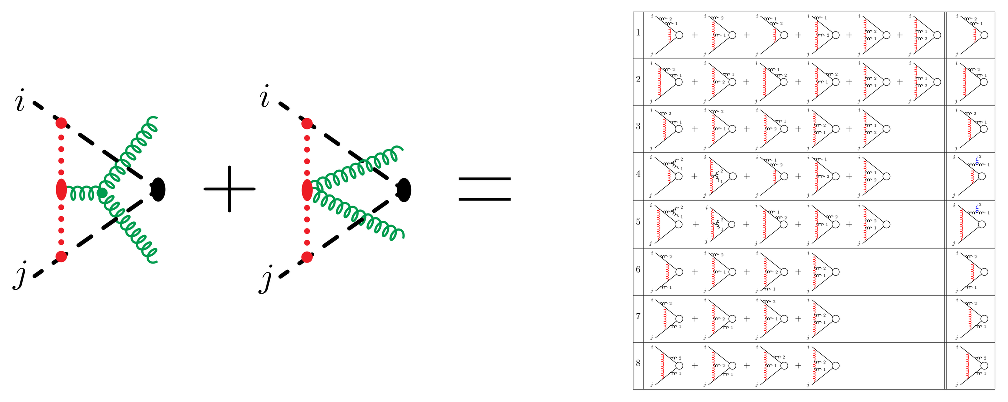

The AMFS result can also be derived by evaluating ***two emission diagrams in SCET***:

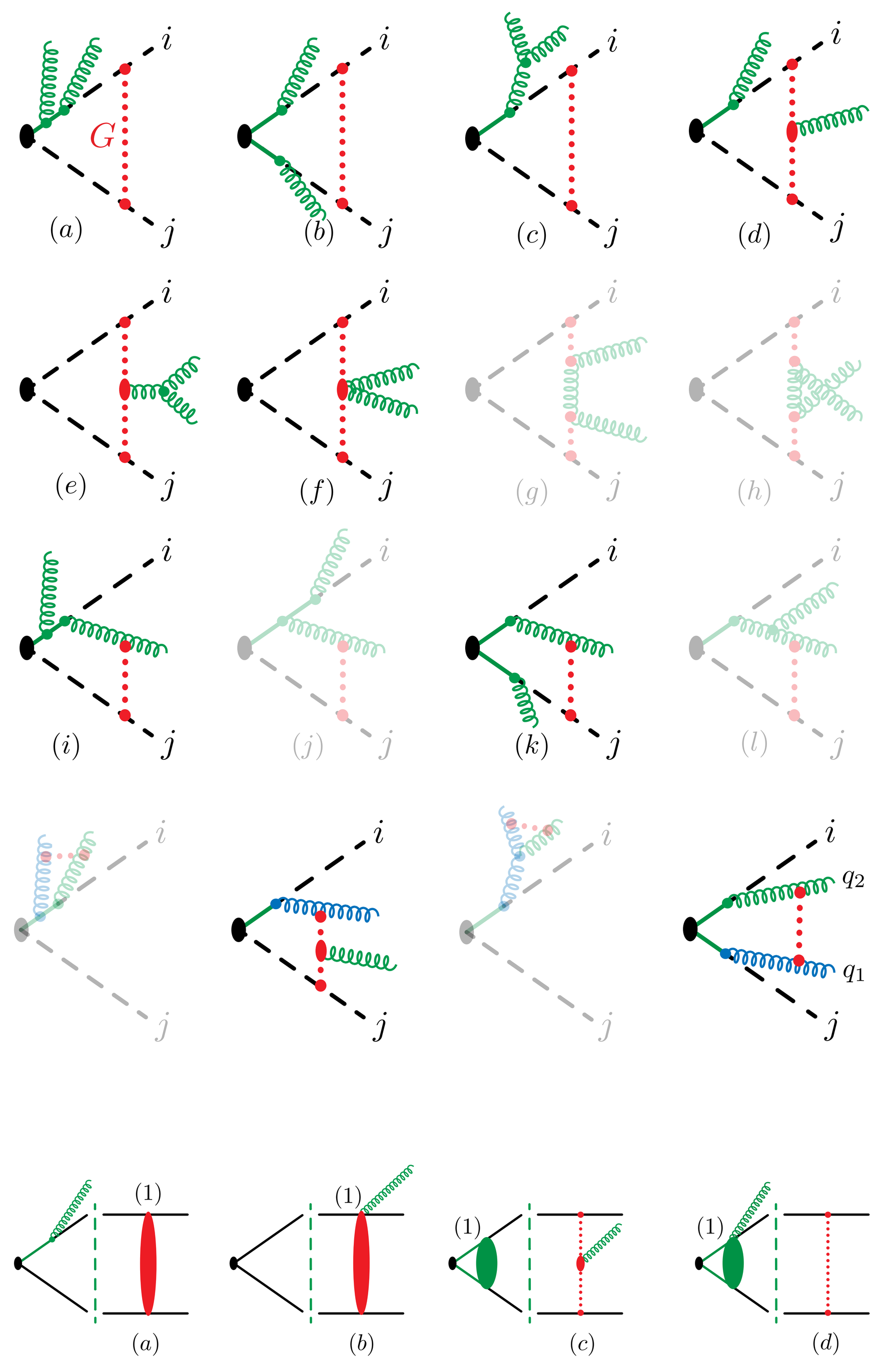

Figure 4: Diagrams needed for extension of AMFS result to two-loops. Additional diagrams not shown include one-loop corrections to the n-s forward scattering and soft emission diagrams involving 3 Wilson lines.

3 Conclusions

1. Rederived the AMFS result using Glauber SCET operators
2. Considered a sequence of EFTs where each time a new soft emission is resolved to become a collinear direction.
3. Each SCET diagram contributes to a specific term in AMFS and there are a lot fewer diagrams to consider even with two emissions.
4. The SCET derivation thus has made it possible for us to envisage a tractable way forward in extending the AMFS result to higher orders.

References

[1] R. Ángeles Martínez, J. R. Forshaw and M. H. Seymour, *Ordering multiple soft gluon emissions*, *Phys. Rev. Lett.* **116** (2016) 212003 [1602.00623].

[2] I. Z. Rothstein and I. W. Stewart, *An Effective Field Theory for Forward Scattering and Factorization Violation*, *JHEP* **08** (2016) 025 [1601.04695].

[3] A. Pathak, *A new form of QCD coherence for multiple soft emissions using Glauber SCET*, *To appear soon* (2021) .

[4] J. R. Forshaw, J. Holguin and A. Pathak, *Coulomb gluons will generally destroy coherence*, *To appear soon* (2021) .

[5] R. Ángeles-Martínez, J. R. Forshaw and M. H. Seymour, *Coulomb gluons and the ordering variable*, *JHEP* **12** (2015) 091 [1510.07998].

The Chirality-Flow Formalism for SM Amplitudes

Andrew Lifson, Lund University, Amplitudes 2021 poster

In collaboration with Joakim Alnefjord, Christian Reuschle, and Malin Sjödahl (based on hep-ph:2003.05877 (EPJC) and hep-ph:2011.10075 (EPJC))

Aim of Chirality Flow

Explore if spinor-helicity $\simeq su(2) \oplus su(2)$ calculations can be done analogously to colour flow $\equiv su(3)$

Ex: Calculate $ee \to \gamma\gamma$ in One Line

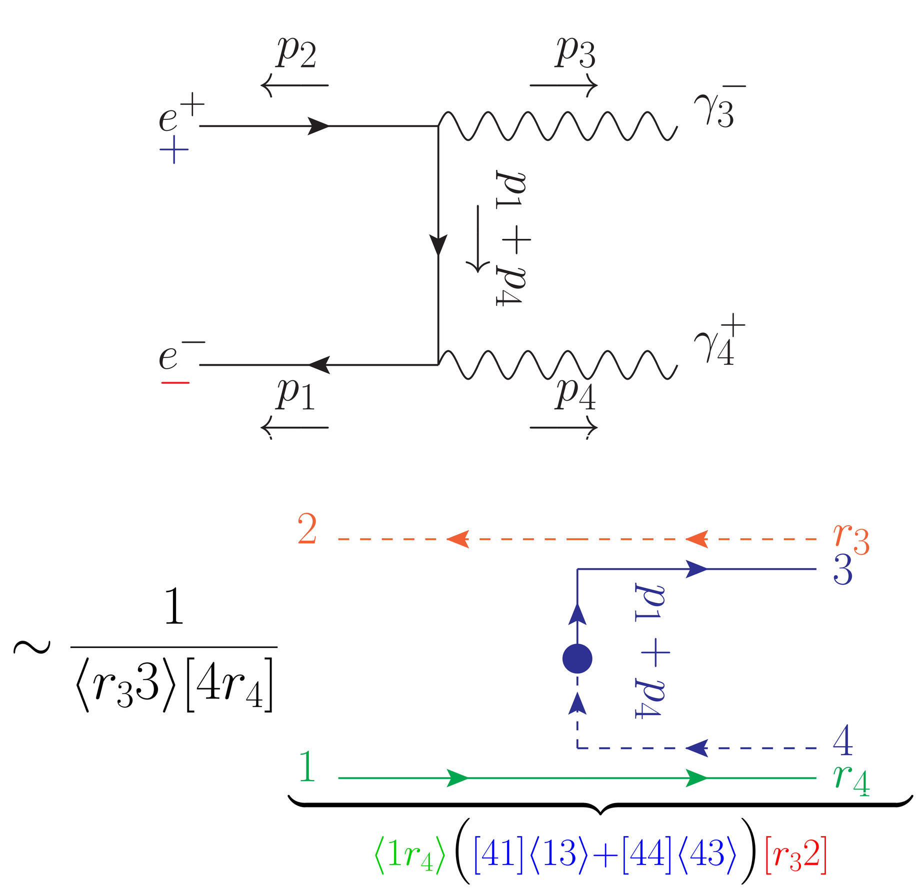

In above and below examples:

Feynman diagram in black

Coloured flow lines $\equiv$ coloured inner products

Inner products $\equiv$ well known complex numbers

Ex: 10-pt Feynman Diagram in One Line

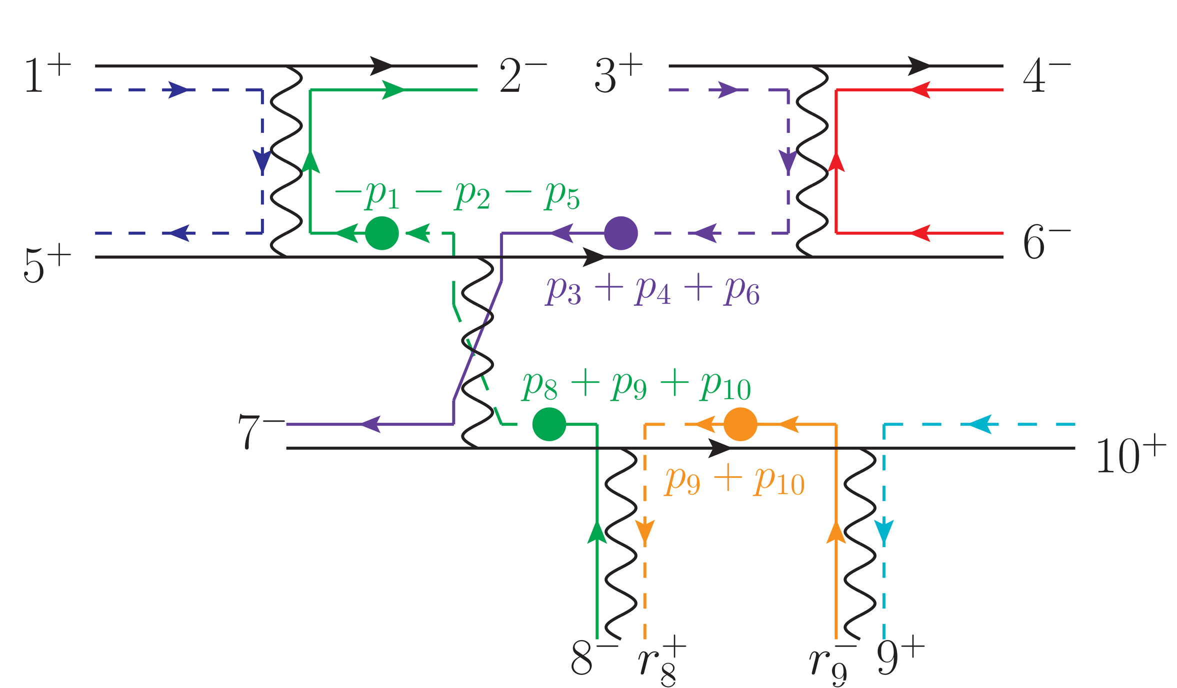

$$= \underbrace{(\sqrt{2}ei)^8}_{\text{vertices}} \underbrace{\frac{(-i)^3}{s_{12}\, s_{34}\, s_{8\,9\,10}}}_{\text{photon propagators}} \underbrace{\frac{(i)^4}{s_{125}\, s_{346}\, s_{8\,9\,10}\, s_{9\,10}}}_{\text{fermion propagators}} \underbrace{\frac{1}{[8 r_8]\langle r_9 9\rangle}}_{\text{polarization vectors}} [15]\langle 64\rangle[10\ 9]$$

$$\times \Big(\langle r_9 9\rangle[9 r_8] + \langle r_9 10\rangle[10 r_8]\Big)\Big(\underbrace{[33]}_{0}\langle 37\rangle + [34]\langle 47\rangle + [36]\langle 67\rangle\Big)$$

$$\times \Big(-\langle 89\rangle[91]\langle 12\rangle - \langle 89\rangle[95]\langle 52\rangle - \langle 8\,10\rangle[10\ 1]\langle 12\rangle - \langle 8\,10\rangle[10\ 5]\langle 52\rangle\Big)$$

Key Conclusion of Chirality Flow

You can (often) **go from Feynman diagram to complex number in one line**

Spinor-Helicity Basics

Massless **spinors** either left and right chiral (use chiral basis, $\gamma^5 = \mathrm{diag}(-1,1)$):

$$u^+(p) = v^-(p) = \begin{pmatrix} 0 \\ |p\rangle \end{pmatrix} \qquad u^-(p) = v^+(p) = \begin{pmatrix} |p] \\ 0 \end{pmatrix}$$

$$\bar{u}^+(p) = \bar{v}^-(p) = \big([p|\ 0\big) \qquad \bar{u}^-(p) = \bar{v}^+(p) = \big(0\ \langle p|\big)$$

Vectors ($r \equiv$ arbitrary ref spinor, $\tau^\mu = \sigma^\mu/\sqrt{2}$):

$$\epsilon^\mu_+(p,r) = \frac{\langle r|\bar{\tau}^\mu|p]}{\langle rp\rangle}, \qquad \epsilon^\mu_-(p,r) = \frac{[r|\tau^\mu|p\rangle}{[pr]}$$

$$\sqrt{2}p^\mu\tau_\mu \equiv \not{p} = |p]\langle p|, \qquad \sqrt{2}p^\mu\bar{\tau}_\mu \equiv \bar{\not{p}} = |p\rangle[p|$$

Algebraic identities remove vector indices, e.g.

$$\underbrace{\langle i|\bar{\tau}^\mu|j][k|\tau_\mu|l\rangle = \langle il\rangle[kj]}_{\text{Fierz identity}}, \qquad \underbrace{\langle i|\bar{\tau}^\mu|j] = [j|\tau^\mu|i\rangle}_{\text{Charge Conjugation}}$$

Amplitude $\equiv$ function of Lorentz-invariant spinor inner products (numbers)

$$\langle ij\rangle = -\langle ji\rangle \equiv \langle i||j\rangle \text{ and } [ij] = -[ji] \equiv [i||j],$$

$$\langle ij\rangle \sim [ij] \sim \sqrt{2p_i \cdot p_j}$$

Chirality Flow for 3-pt Amplitudes

You can use flow lines to find 3-pt amplitudes

3-pt Ampiltude Rules

- Begin with minimum number of lines which satisfies little-group scaling
- Only solid or dotted lines allowed, move lesser type to denominator and change line type
- Multiply by 1 to add lines until Lorentz-invariant found
- Cannot connect lines in a way to give 0 or ∞

Lund University

Chirality-Flow Simplifies Spinor-Helicity Calculations

Drawing and connecting lines simpler than keeping track of indices

Chirality Flow Building Blocks

Left-chiral spinors $\equiv$ dotted lines

Right-chiral spinors $\equiv$ solid lines

Inner products defined as:

$$\langle i|^{\alpha}|j\rangle_{\alpha} \equiv \langle ij\rangle = -\langle ji\rangle = \qquad [i|_{\dot\beta}|j]^{\dot\beta} \equiv [ij] = -[ji] =$$

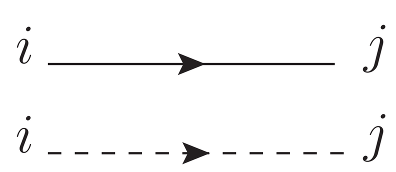

Vectors replaced by double lines (cf. colour flow)

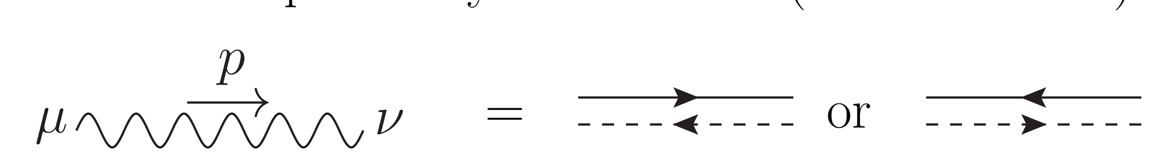

Momenta represented by momentum dot ($p = \sum_i p_i$, $p_i^2 = 0$)

$$\sqrt{2}p^\mu\bar{\tau}_\mu = \sum_i |i\rangle[i| = \qquad , \qquad \sqrt{2}p^\mu\tau_\mu = \sum_i |i]\langle i| =$$

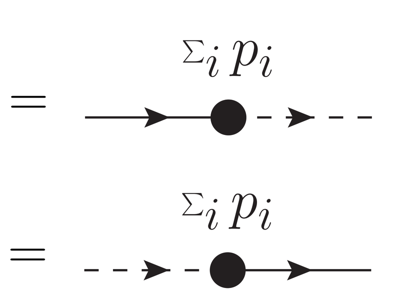

Important Takeaway

You can use these replacements to create new set of Feynman rules

3-pt Chirality-Flow Ex:

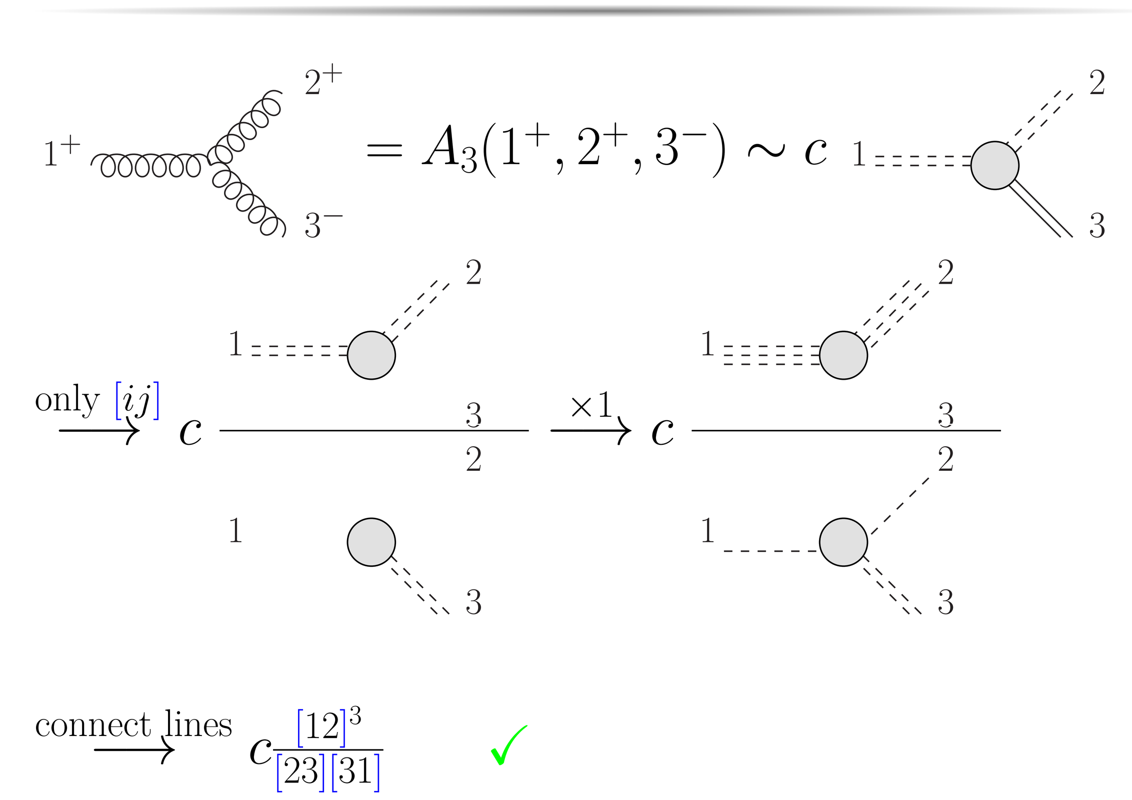

Ex: (Massless) QED Chirality-Flow Rules

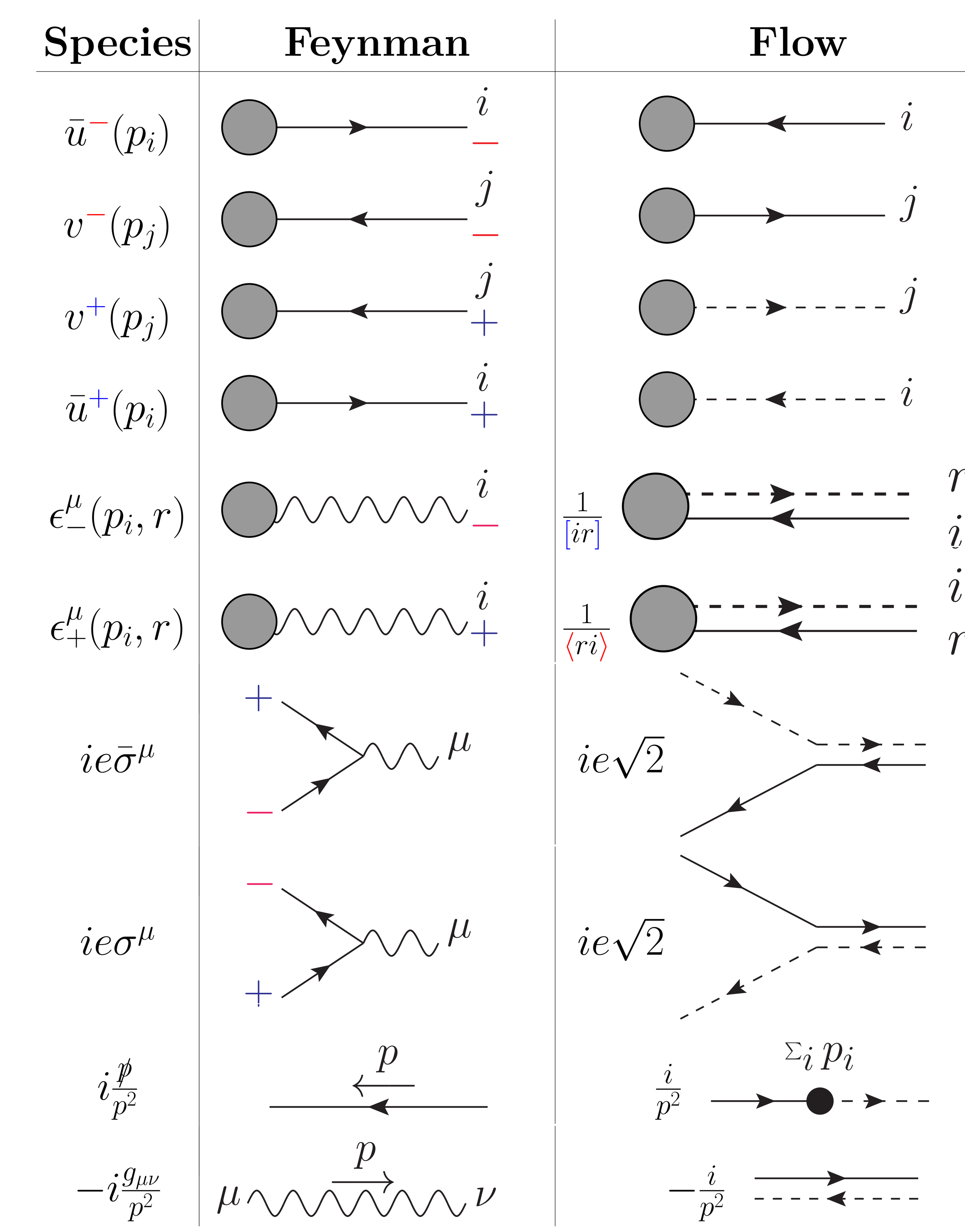

Application of Chirality-Flow Rules

- Draw and connect flow lines *without* arrows
- Choose single arrow direction and follow it through diagram (vector double lines have arrows opposing)
- Read off inner products

Conclusions

- Chirality flow offers shortest journey from Feynman diagram to complex number
- Calculations often performed in a single step, *without* algebraic manipulations
- Full standard model at tree level understood

LAPLACE'S METHOD FOR THE CALCULATION OF SCALAR TWO-LOOP FEYNMAN DIAGRAMS OF ELASTIC SCATTERING

A.Mileva, N.Chudak, O.Potienko

Department of Theoretical and Experimental Nuclear Physics,

Odessa Polytechnic State University, Odessa ,Ukraine

yourspersonaljesus@gmail.com

This study is devoted to the possibility of applying the Laplace method to the calculation of the contributions of Feynman diagrams with loops to the amplitude of elastic scattering of particles. We consider a two-loop diagram and the simplest model with the scalar particles interacting and exchanging with scalar particles. Using the Feynman's identity, the analytical expression corresponding to this diagram can be reduced to a seven-dimensional integral containing the Dirac delta function. It is taken into account by moving to seven -dimensional spherical variables. After that the integrand may be represented as

$$A = \lim_{\varepsilon \to +0} \int_0^{\pi/2} d\theta_1 \int_0^{\pi/2} d\theta_2 \int_0^{\pi/2} d\theta_3 \int_0^{\pi/2} d\theta_4 \int_0^{\pi/2} d\theta_5 \int_0^{\pi/2} d\theta_6 \frac{F(\theta)}{\left(Z(\theta)+i\varepsilon\right)^3} \qquad (1)$$

Here θ denotes the whole set of quantities $\theta_1, \theta_2, \theta_3, \theta_4, \theta_5, \theta_6$. The function $F(\theta)$ has no singularities within the integration domain, but the function $Z(\theta)$ turns to zero in some part of the integration domain. As a result, one cannot perform the passage to the limit before integration and cannot effectively apply the numerical integration methods. However, the integral (1) can be written as:

$$A = \frac{1}{2} \lim_{\varepsilon \to +0} \frac{\partial^4}{\partial \varepsilon^4} \int_0^{\pi/2} d\theta_1 \int_0^{\pi/2} d\theta_2 \int_0^{\pi/2} d\theta_3 \int_0^{\pi/2} d\theta_4 \int_0^{\pi/2} d\theta_5 \int_0^{\pi/2} d\theta_6 F(\theta)\left(\left(Z(\theta)+i\varepsilon\right)\ln\left(Z(\theta)+i\varepsilon\right)-\left(Z(\theta)+i\varepsilon\right)\right). \qquad (2)$$

As can be seen from (2), the region in which $Z(\theta)=0$ now makes a zero contribution to the integral. Therefore, one can now apply the Laplace' s method to calculate the integral of the real and imaginary parts of the integrand. The maximization of the moduli of the real and imaginary parts showed that the the location of the maximum points does not depend on ε . In addition, some variables reach the maximum at the boundary $\pi/2$, while some others – at the values less than this limit. Next we represent the integral (2) in the form

$$\begin{aligned} A = {} & \frac{1}{2} \lim_{\varepsilon \to +0} \frac{\partial^4}{\partial \varepsilon^4} \int_0^{\pi/2} d\theta_1 \int_0^{\pi/2} d\theta_2 \int_0^{\pi/2} d\theta_3 \int_0^{\pi/2} d\theta_4 \int_0^{\pi/2} d\theta_5 \int_0^{\pi/2} d\theta_6 \times \\ & \times \exp\left(\ln\left(\mathrm{Re}\left(F(\theta)\left(\left(Z(\theta)+i\varepsilon\right)\ln\left(Z(\theta)+i\varepsilon\right)-\left(Z(\theta)+i\varepsilon\right)\right)\right)\right)\right) + \\ & + \frac{1}{2} \lim_{\varepsilon \to +0} \frac{\partial^4}{\partial \varepsilon^4} \int_0^{\pi/2} d\theta_1 \int_0^{\pi/2} d\theta_2 \int_0^{\pi/2} d\theta_3 \int_0^{\pi/2} d\theta_4 \int_0^{\pi/2} d\theta_5 \int_0^{\pi/2} d\theta_6 \times \\ & \times \exp\left(\ln\left(\mathrm{Im}\left(F(\theta)\left(\left(Z(\theta)+i\varepsilon\right)\ln\left(Z(\theta)+i\varepsilon\right)-\left(Z(\theta)+i\varepsilon\right)\right)\right)\right)\right). \end{aligned}$$

and substitute the exponent with its Taylor series near the point where the maximum value of the moduli of each term is reached. For those variables for which the maximum is reached at the boundary value, the expansion can be limited to linear terms only, and to the second order – for the rest. After that, the integral can be easily calculated.

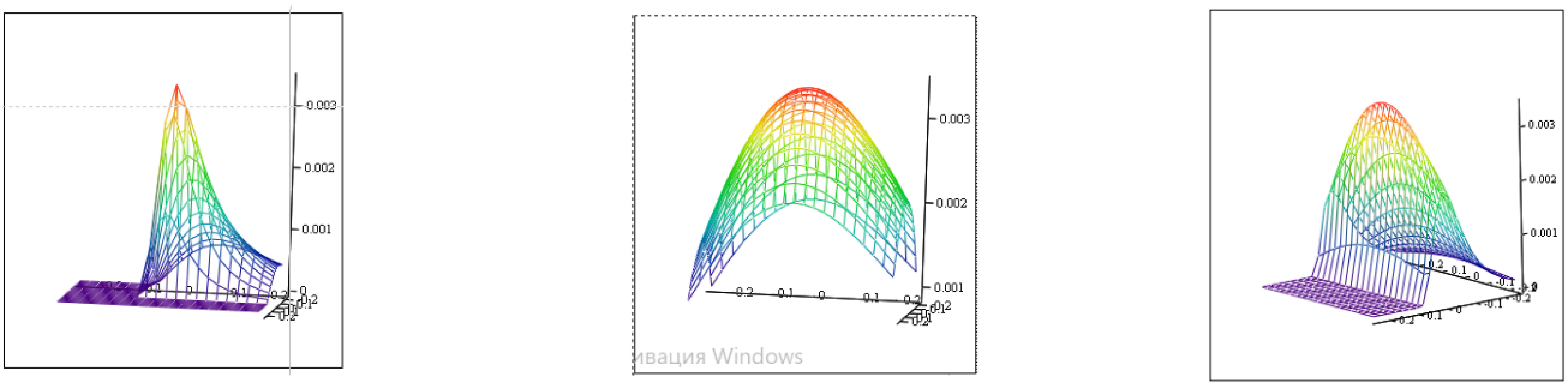

POSITIVITY BOUNDS WITH GRAVITY

ANNA TOKAREVA
(UNIVERSITY OF JYVÄSKYLÄ, FINLAND)

POSITIVITY BOUNDS

The general idea

- to find out which EFT can be UV completed by a good theory and which - cannot

What do we mean by 'good'?

- Lorenz-invariant $\Rightarrow \mathcal{A} = \mathcal{A}(s,t,u)$
- unitary $\Rightarrow Im\,\mathcal{A} > 0$
- satisfying causality $\Rightarrow \mathcal{A}(s,t,u)$ is analytic everywhere except real axes
- local $\Rightarrow$ polynomial boundedness (Froissart-Martin bound)

$$\lim_{|s|\to\infty} \left|\frac{\mathcal{A}(s,t)}{s^2}\right| = 0, \quad t < 4m^2.$$

Weakly coupled string theory leads to the similar properties of amplitudes.

What is positive?

Example: forward limit $t = 0$

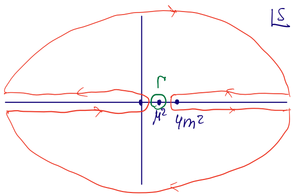

$$\Sigma_{IR} = \frac{1}{2\pi i}\int_\Gamma ds \frac{\mathcal{A}(s)}{(s-\mu^2)^3} =$$

$$= \int_{4m^2}^\infty \frac{ds}{\pi}\left(\frac{Im\mathcal{A}(s)}{(s-\mu^2)^3} + \frac{Im\mathcal{A}^+(s)}{(s-4m^2+\mu^2)^3}\right)$$

$$\Sigma_{IR} = \frac{1}{2}\mathcal{A}''(s) > 0$$

POSITIVITY BOUNDS

Improved positivity bounds

Part of the rhs integrals still can be computed in the effective theory

$$\Sigma_{IR} = \frac{1}{2}\mathcal{A}''(s) > \int_{4m^2}^{\Lambda^2}\frac{ds}{\pi}\left(\frac{Im\mathcal{A}(s)}{(s-\mu^2)^3} + \right.$$

$$\left. + \frac{Im\mathcal{A}^+(s)}{(s-4m^2+\mu^2)^3}\right)$$

Issues with massless particles

- Branch cuts divide the complex plane $\Rightarrow$ contours should be chosen in a different way
- Froissart-Martin bound can be no longer satisfied
- IR singularities
- the function in the RHS is positive definite only for $\mu < 4m^2$

To resolve the last issue we can use instead:

$$\Sigma_{IR} = \frac{1}{2\pi i}\int_\Gamma \frac{s^3\mathcal{A}(s, t\to -0)}{(s^2+\delta^2)^3} =$$

$$= \int_{4m^2}^\infty ds\left(\frac{2s^3 \mathrm{Im}\mathcal{A}(s,t\to -0)}{2\pi(s^2+\delta^2)^3}\right)$$

Issues with gravitons

Infrared singularities

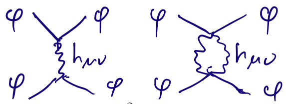

$$\mathcal{A}(s,t)|_{t\to 0} = \frac{s^2}{t} + s^2\log(t) + \mathcal{A}_\circ(s) + \mathcal{O}(t).$$

CANCELLING INFRARED SINGULARITIES

Twice substracted dispersive relation

2→2 scattering for scalars through the graviton exchange

$$\Sigma = \sum \mathrm{Res}\frac{s^3\mathcal{A}(s)}{(s^2+\delta^2)^3} = \frac{a}{t} + b\log t + (\text{finite at } t\to 0)$$

From the other side,

$$\Sigma = \int_{4m^2}^\infty dz\left(\frac{z^3 \mathrm{Im}\mathcal{A}(z+i\epsilon, t\to -0)}{2\pi(z^2+\delta^2)^3} + \frac{(z-4m^2)^3\mathrm{Im}\mathcal{A}^\times(z+i\epsilon,t\to -0)}{2\pi((z-4m^2)^2+\delta^2)^3}\right)$$

The only source for $t\to 0$ divergences is an infinite part of the integral. This can be achieved if

$$\mathrm{Im}\mathcal{A}(s,t) = r(t)\,(\alpha' s)^{2+l(t)}\left(1 + \frac{\zeta}{\log(\alpha' s)}\right)$$

The form of infrared divergences fixes the behaviour of the amplitude in UV at $s\to\infty$, $t\to 0$.

Positivity bounds after cancellation of IR divergences: example

$$S = \int d^4x\sqrt{|g|}\left(-\frac{R}{2\kappa^2} + \frac{1}{2}\partial_\mu\phi\partial^\mu\phi\right)$$

$$\mathcal{A}(s,0^-) = -\frac{\kappa^2 s^2}{t} - \frac{33\kappa^4 s^2}{24\pi^2}\left(\log(s)+\log(-s)\right) - \frac{33\kappa^4 s^2}{24\pi^2}\log(t)$$

$$\Sigma = -\frac{\kappa^2}{t} - \frac{33\kappa^4}{24\pi^2}\left(\frac{3}{2} + \log(t) + \log(\delta^2)\right)$$

Cancelling the divergences determines $r(0)\alpha'^2 \sim -l'(0)\kappa^2$ and $r(0)\alpha'^2\zeta \sim \kappa^4$, which fixes $\zeta > 0$

Conclusions

- Low energy theories can be constrained from the requirement to have good UV completion (Lorentz invariance, unitarity, causality, locality)
- In the massless limit, extra assumptions about UV physics are needed to cancel IR divergencies - Regge form of the amplitude
- This allows to justify the bounds obtained without gravity
- Inclusion of graviton scatterings typically make the positivity bounds weaker, due to terms with unknown signs left after cancellation of the poles
- Renormalizable theory with gravity can have lower cutoff than expected (Planck mass)

Based on M. Herrero -Valea, R. Santos-Garcia, AT, 2011.11652

Soft factors in the presence of small negative Λ

Arpita Mitra

Department of Physics, IISER Bhopal, India

arpitamitra89@gmail.com

(In collaboration with N. Banerjee, A. Bhattacharjee and K. Fernandes; arXiv:2102.06165, arXiv:2008.02828)

Introduction & Motivation

- Soft theorems on asymptotically flat spacetimes relate scattering amplitudes with soft particles to amplitudes without soft particles by a soft factor.

$$\langle \text{out}|a^{\text{f}}_{+}(\omega\hat{x})\mathcal{S}|\text{in}\rangle = S^{\text{f}}\langle \text{out}|\mathcal{S}|\text{in}\rangle$$

where we assumed a single soft particle inserted in the 'out' state

- In the soft photon case, for $p_{(a)}$, Q_a the hard particle momenta and charges; k, ε the momentum and polarization of the soft photon, the leading soft factor is

$$S^{\text{f}\,(0)}_{\text{em}} = \left[\sum_{a=\text{out}} \frac{p_{(a)}.\epsilon_+}{p_{(a)}.k}Q_a - \sum_{a=\text{in}} \frac{p_{(a)}.\epsilon_+}{p_{(a)}.k}Q_a\right] \equiv \frac{1+z\bar{z}}{\sqrt{2}\omega}\left[\sum_{a=\text{out}}\frac{1}{z-z_a}Q_a - \sum_{a=\text{in}}\frac{1}{z-z_a}Q_a\right]$$

- We also have large gauge Ward identities across $\mathcal{I}^{\pm}$

$$4\int d^2w\,\partial_{\bar{w}}\varepsilon^{\text{f}}\langle \text{out}|\partial_w\mathcal{N}^{\text{f}}\mathcal{S}|\text{in}\rangle = \left[\sum_{a=\text{in}} Q_a\varepsilon^{\text{f}}(z_a\,,\bar{z}_a) - \sum_{a=\text{out}} Q_a\varepsilon^{\text{f}}(z_a\,,\bar{z}_a)\right]\langle \text{out}|\mathcal{S}|\text{in}\rangle$$

- Equivalent to soft photon theorem with the following gauge parameter ϵ^f and derivable soft photon number mode $\mathcal{N}^f$ on asymptotically flat spacetimes [1,2]

$$\varepsilon^{\text{f}}(w\,,\bar{w}) = \frac{1}{w-z}$$

$$\partial_w\mathcal{N}^{\text{f}} = -\frac{\sqrt{2}}{8\pi}\frac{1}{1+w\bar{w}}\lim_{\omega\to 0}\left[\omega a^{\text{f}}_{+}(\omega\hat{x}) + \omega a^{\text{f}}_{-}(\omega\hat{x})^{\dagger}\right]$$

- Rich IR structure for massless theories (IR triangle) relating large gauge transformations, soft theorems and memory effects in soft radiative fields across $\mathcal{I}^{\pm}$.
- Interesting developments in AdS: Extensions of BMS to ΛBMS symmetries on AdS spacetimes [3]; soft photon Ward identity realized as CFT Ward identity [4]
- First principles derivations are not well understood primarily due to absence of asymptotic states and the existence of a mass gap.
- Key insights possible from classical scattering:
  Classical limits of soft theorems derivable from scattering processes with
  A) large impact parameters, B) radiated energy <<< energy of scattering bodies.

Classical Soft theorems [5]:

$$\lim_{\omega\to 0}\epsilon^{\mu\nu}\tilde{h}_{\mu\nu}(\omega,\vec{x}) = -i\frac{e^{i\omega R}}{4\pi R}S_{\text{gr}}\,, \quad \lim_{\omega\to 0}\epsilon^{\mu}\tilde{a}_{\mu}(\omega\,,\vec{x}) = -i\frac{e^{i\omega R}}{4\pi R}S_{\text{em}}$$

in the $\omega\to 0$ limit (long wavelength limit), for $\tilde{a}_\mu$ ($\tilde{h}_{\mu\nu}$) the Fourier transformed classical radiative electromagnetic (gravitational) field, with polarization ϵ^μ ($\epsilon^{\mu\nu}$) and S_{em} (S_{gr}) the classical limit of the soft factor

- In $d=4$ dimensions : derivation of universal subleading $\ln\omega^{-1}$ contribution from long range interactions of massless fields.
- Our plan: Scatter a probe particle on a AdS black hole spacetime to determine (perturbative) Λ corrections of known flat spacetime soft factors.
- Corrections realized across $\mathcal{I}^{\pm}$ of flat patch around the center of AdS spacetime; hard particles trajectories uncorrected by AdS potential to l^{-2} order.

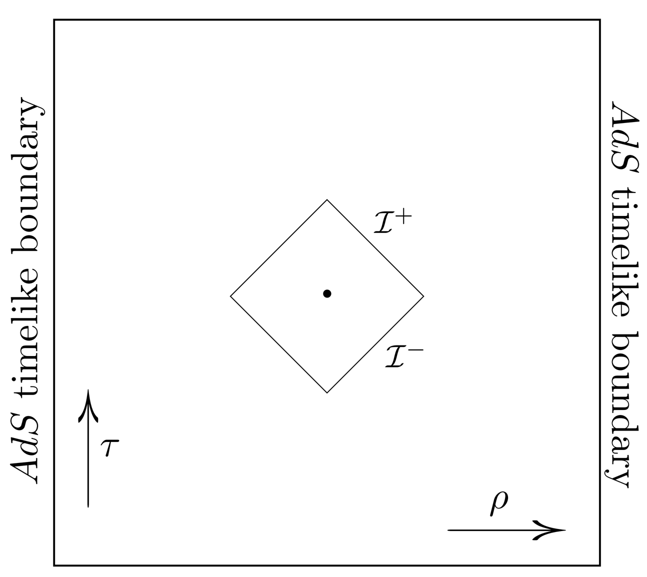

Procedure

- Scatter a point particle with charge Q and mass M on a Reissner-Nordström AdS spacetime (BH charge $\tilde{Q}$ and mass $\tilde{M}$). Gives soft photon and graviton corrections.
- Large impact parameter scattering with leading l^{-2} corrections $\Rightarrow$ scattering on linearized spacetime with $\sqrt{G}\tilde{Q}\leq G\tilde{M}\ll r\ll l$ (confined to flat patch in AdS).
- Solve perturbed Einstein and Maxwell equations about the linearized spacetime.
- Derived $h_{ij}(t,\vec{x})$ and $a_i(t,\vec{x})$ solutions using Synge's worldline formalism.
- Fourier transform and take soft limit to derive soft factors in frequency space.

Results

- $\omega\to 0$ limit is formally not defined on asymptotically AdS due to mass gap.
- We consider a *double scaling limit*: Provides $\omega\to 0$ contributions from l^0 terms and l^{-2} contributions that survive $\omega\to 0$ and $l\to\infty$ with $\omega l=\gamma$ finite.
- We find soft factor results in frequency space

$$S_{\text{em}} = S^{\text{f}}_{\text{em}} + S^{l}_{\text{em}}\,,\ \text{with}\quad S^{\text{f}}_{\text{em}} = S^{\text{f}\,(0)}_{\text{em}} + S^{\text{f}\,(1)}_{\text{em}}\quad \&\quad S^{l}_{\text{em}} = S^{l\,(0)}_{\text{em}} + S^{l\,(1)}_{\text{em}}\ \text{, where}$$

$$S^{\text{f}\,(0)}_{\text{em}} = Q\sum_{a=1}^{2}(-1)^{a-1}\frac{\epsilon_\mu p^\mu_{(a)}}{p_{(a)}.k},\quad S^{\text{f}\,(1)}_{\text{em}} = iQ\sum_{a=1}^{2}(-1)^{a-1}\frac{\epsilon_\nu k_\rho j^{\rho\nu}_{(a)}}{p_{(a)}.k}$$

$$S^{l\,(0)}_{\text{em}} = \frac{Q}{4l^2}\sum_{a=1}^{2}(-1)^{a-1}\frac{\epsilon_\mu p^\mu_{(a)}}{p_{(a)}.k}\frac{\vec{p}^{\,2}_{(a)}}{\left(p_{(a)}.k\right)^2},\quad S^{l\,(1)}_{\text{em}} = i\frac{Q}{4l^2}\sum_{a=1}^{2}(-1)^{a-1}\frac{\epsilon_\nu k_\rho j^{\rho\nu}_{(a)}}{p_{(a)}.k}\frac{\vec{p}^{\,2}_{(a)}}{\left(p_{(a)}.k\right)^2}$$

- $S^{\text{f}\,(0)}_{\text{em}}$ and $S^{\text{f}\,(1)}_{\text{em}}$ go like ω^{-1} and $\ln\omega^{-1}$ respectively, while $S^{l\,(0)}_{\text{em}}$ and $S^{l\,(1)}_{\text{em}}$ go like $\gamma^{-2}\omega^{-1}$ and $\gamma^{-2}\ln\omega^{-1}$

Likewise, the soft graviton soft factor corrections are $S^{l}_{\text{gr}} = S^{l\,(0)}_{\text{gr}} + S^{l\,(1)}_{\text{gr}}$, with

$$S^{l\,(0)}_{\text{gr}} = \frac{1}{2l^2}\sum_{a=1}^{2}\frac{\epsilon_{\mu\nu}p^\mu_{(a)}p^\nu_{(a)}}{p_{(a)}.k}\frac{\vec{p}^{\,2}_{(a)}}{\left(p_{(a)}.k\right)^2}\left(3+\frac{\vec{p}^{\,2}_{(a)}}{p^2_{(a)}}\right),$$

$$S^{l\,(1)}_{\text{gr}} = i\frac{1}{2l^2}\sum_{a=1}^{2}\frac{\epsilon_{\mu\nu}p^\mu_{(a)}k_\rho j^{\rho\nu}_{(a)}}{p_{(a)}.k}\frac{\vec{p}^{\,2}_{(a)}}{\left(p_{(a)}.k\right)^2}\left(3+\frac{\vec{p}^{\,2}_{(a)}}{p^2_{(a)}}\right)$$

- Results can be realized as perturbed asymptotically flat spacetime Ward identities.
- The leading soft factors $S^{(0)}$ are universal. Therefore we can consider corrections to the well known soft photon Ward identity for a massless scattering process.
- Soft factors involve $1/l^2$ corrections; hard particles do not $\Rightarrow$ Soft modes and gauge parameter involve $1/l^2$ corrections (strongly constraining the Ward identities).
- Soft photon case : Asymptotic boundary of $l\to\infty$ for hard particles not corrected $\Rightarrow$ corrected Ward identity realized at $\mathcal{I}^{\pm}$ of flat patch in the Figure.

$$4\int d^2w\left[\partial_{\bar{w}}\varepsilon^{\text{f}}(w\,,\bar{w})\langle \text{out}|\partial_w\mathcal{N}^{l}(w\,,\bar{w})\mathcal{S}|\text{in}\rangle + \partial_{\bar{w}}\varepsilon^{l}(w\,,\bar{w})\langle \text{out}|\partial_w\mathcal{N}^{\text{f}}(w\,,\bar{w})\mathcal{S}|\text{in}\rangle\right]$$
$$= \left[\sum_{a=\text{in}} Q_a\varepsilon^{l}(z_a\,,\bar{z}_a) - \sum_{a=\text{out}} Q_a\varepsilon^{l}(z_a\,,\bar{z}_a)\right]\langle \text{out}|\mathcal{S}|\text{in}\rangle\,,$$

- The gauge parameter and soft photon mode are corrected

$$\varepsilon(w\,,\bar{w}) = \varepsilon^{\text{f}}(w\,,\bar{w}) + \frac{1}{l^2}\varepsilon^{l}(w\,,\bar{w})\,;\qquad \partial_w\mathcal{N} = \partial_w\mathcal{N}^{\text{f}} + \frac{1}{l^2}\left(\partial_w\mathcal{N}^{l}_1 + \partial_w\mathcal{N}^{l}_2\right)$$

with

$$\varepsilon^{l}(w\,,\bar{w}) = \frac{(1+z\bar{z})^2(1+w\bar{w})^2}{(\bar{w}-\bar{z})^2\,(w-z)^3}\,,\qquad \partial_w\mathcal{N}^{l}_1 = -\frac{16\sqrt{2}}{8\pi(1+z\bar{z})}\lim_{\omega\to 0}\left[\omega^3 a^{l}_{+}(\omega\hat{x}) + \omega^3 a^{l}_{-}(\omega\hat{x})^{\dagger}\right]\,,$$

$$\partial_w\mathcal{N}^{l}_2 = \frac{\sqrt{2}}{8\pi}\frac{(1+z\bar{z})^2}{(\bar{w}-\bar{z})}\frac{w}{(w-z)^2}\lim_{\omega\to 0}\left[\omega a^{\text{f}}_{+}(\omega\hat{x}) + \omega a^{\text{f}}_{-}(\omega\hat{x})^{\dagger}\right]$$

Outlook & Open questions

- Ward identity from conformal Ward Identity on AAdS at large l [Ongoing]
- Soft limits depend on asymp. flat spacetime embeddings in global spacetimes.
- Status of soft factor corrections to all orders in l [Open]
- Connections of (conformal) Ward identities with celestial amplitudes

References

1) A. Strominger, "On BMS Invariance of Gravitational Scattering," JHEP **07**, 152 (2014)
2) T. He, P. Mitra, A. P. Porfyriadis and A. Strominger, "New Symmetries of Massless QED," JHEP **10**, 112 (2014)
3) G. Compère, A. Fiorucci and R. Ruzziconi, "The Λ-BMS$_4$ group of dS$_4$ and new boundary conditions for AdS$_4$," Class. Quant. Grav. **36** (2019) no.19, 195017
4) E. Hijano and D. Neuenfeld, "Soft photon theorems from CFT Ward identites in the flat limit of AdS/CFT," JHEP **11**, 009 (2020)
5) A. Laddha and A. Sen, "Logarithmic Terms in the Soft Expansion in Four Dimensions," JHEP **10**, 056 (2018)

PRINCETON UNIVERSITY

On-Shell Symmetry Breaking and the Higgs Mechanism

Brad Bachu

Department of Physics, Princeton University

AMPLITUDES 2021 AUGUST 16th–20th NIELS BOHR INSTITUTE COPENHAGEN

Introduction

We show that 'on-shell' techniques are sufficient to reproduce the physics of spontaneous symmetry breaking and the Higgs mechanism, without reference to Lagrangians, quantum fields, and a scalar field acquiring a vacuum expectation value.

In particular, we use helicity and spin spinors, along with group factors (required by consistent factorization) to specify three-particle amplitudes in the IR and UV. We then discover familiar constraints by demanding that high energy (HE) limit of the IR amplitudes match onto UV amplitudes. This work generalizes and extends that presented in Refs. [1, 2]

Scattering Amplitudes as Little Group Tensors

A particle is labeled by its momentum, p, and representation under global symmetry groups, σ, and transforms under some representation of the **little group**.

- For **massless** particles, the little group is $SO(2) = U(1)$, and its representations are specified by its helicity, h. 'Helicity spinors' transform under the little group as,

$$|\lambda\rangle_\alpha \to w^{-1}|\lambda_\alpha\rangle \quad \text{and} \quad |\tilde{\lambda}]_{\dot\alpha} \to w|\tilde{\lambda}_{\dot\alpha}]\,. \tag{1}$$

- For **massive** particles, the little group is $SO(3) = SU(2)$, and its representations are labeled by its spin, S. 'Spin spinors' transform under the little group as,

$$|\lambda\rangle^I_\alpha \to (W^{-1})^I{}_J|\lambda\rangle^J_\alpha \quad \text{and} \quad |\tilde{\lambda}]^I_{\dot\alpha} \to W^I{}_J|\tilde{\lambda}]^J_{\dot\alpha}\,. \tag{2}$$

Scattering amplitudes, $\mathcal{M}$, constructed from helicity and spin spinors, are Lorentz invariant and under the little group,

$$\mathcal{M}(p_a, \rho_a) \to \prod_a (D_{\rho_a\rho'_a}(W))\mathcal{M}((\Lambda p)_a, \rho'_a) \tag{3}$$

where, for massless particles $D_{\rho_a\rho'_a}(W) = \delta_{\sigma_a,\sigma'_a}\delta_{h_a,h'_a}w^{-2h_a}$ and $\rho_a = (h_a, \sigma_a)$, and for massive particles $D_{\rho_a\rho'_a}(W) = \delta_{\sigma_a,\sigma'_a}W^{I_1}_{I'_1}\ldots W^{I_{2S}}_{I'_{2S}}$ and $\rho_a = (\{I_1, \ldots, I_{2S}\}, \sigma_a)$.

The IR

There are d_H massless adjoint gluons from the symmetry group $H \subset G$, with an associated Lie algebra spanned by,

$$\mathfrak{h} = \{X^1, X^2, \ldots, X^{\alpha_1}, X^{\beta_1}, X^{\gamma_1}, \ldots, X^{d_H}\}\,, \tag{4}$$

such that

$$[X^{\alpha_1}, X^{\beta_1}] = h^{\alpha_1\beta_1}{}_{\gamma_1}X^{\gamma_1}\,. \tag{5}$$

There are $(d_G - d_H)$ massive vectors arising from the 'broken' generators $\{X^{(d_H+1)_0}, \ldots, X^{\alpha_0}, X^{\beta_0}, X^{\gamma_0}, \ldots, X^{(d_G-d_H)_0}\}$. A general three massive vector amplitude,

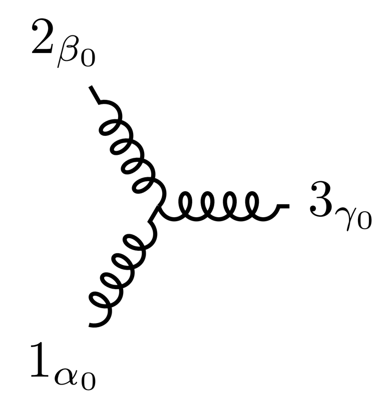

$$\frac{h^{\alpha_0\beta_0\gamma_0}}{m_{\alpha_0}m_{\beta_0}m_{\gamma_0}}\langle\mathbf{12}\rangle[\mathbf{12}]\langle\mathbf{3}|p_1 - p_2|\mathbf{3}] + \text{ cyc. }]\,. \tag{6}$$

The UV

There are d_G massless adjoint gluons from the symmetry group $G = G_1 \times G_2 \times \cdots \times G_n$. Each subgroup G_i has an associated coupling g_i, which we use to rescale the generators $g_i\tilde{T}^i = T^i$. The Lie algebra is then spanned by,

$$\mathfrak{g} = \{T^1, T^2, \ldots, T^a, T^b, T^c, \ldots, T^{d_G}\}\,, \tag{7}$$

which follow the commutation relation

$$[T^c, T^b] = f^{cb}{}_dT^d\,. \tag{8}$$

We have N_ϕ massless scalars, labeled by $\{I, J\}$. Three particle amplitudes in the UV are,

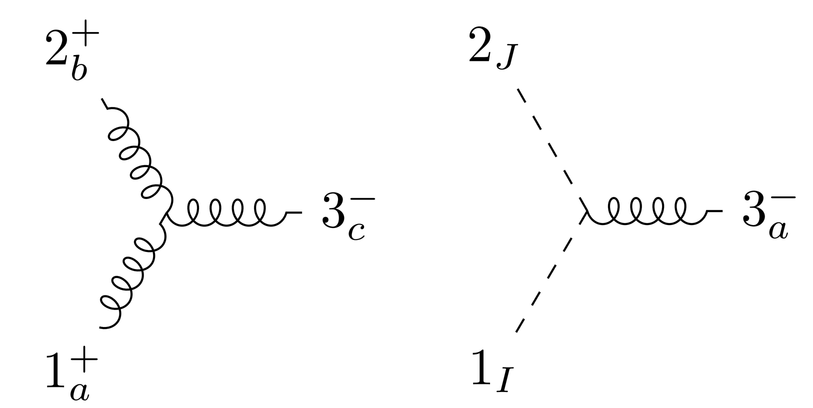

$$f^{abc}\frac{\langle 12\rangle^3}{\langle 31\rangle\langle 23\rangle} \qquad (T^a)_{IJ}\frac{\langle 31\rangle\langle 23\rangle}{\langle 12\rangle} \tag{9}$$

Matching the High Energy Limit of the IR onto UV

$\mathcal{O} \in SO(d_G)$ matches a linear combination of adjoint labels in the UV to the IR. $U \in SO(N_\phi)$ matches a linear combination of scalars in the UV to the longitudinal component of a massive vector in the IR.

Two massive vectors and one massless gluon:

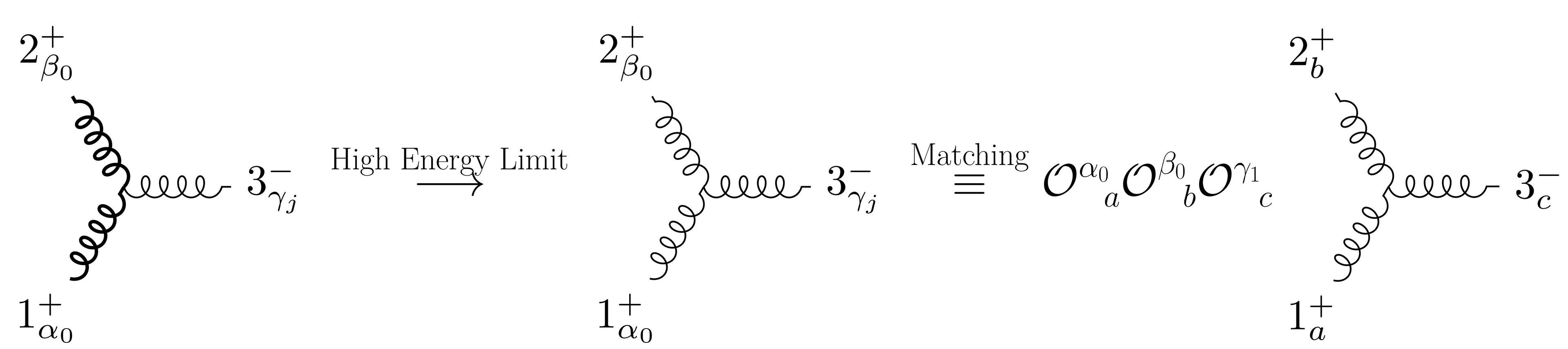

$$h^{\alpha_1\beta_1\gamma_1}\frac{\langle 12\rangle^3}{\langle 31\rangle\langle 23\rangle} \equiv \mathcal{O}^{\alpha_0}{}_a\mathcal{O}^{\beta_0}{}_b\mathcal{O}^{\gamma_1}{}_c f^{abc}\frac{\langle 12\rangle^3}{\langle 31\rangle\langle 23\rangle} \tag{10}$$

Three massive vectors:

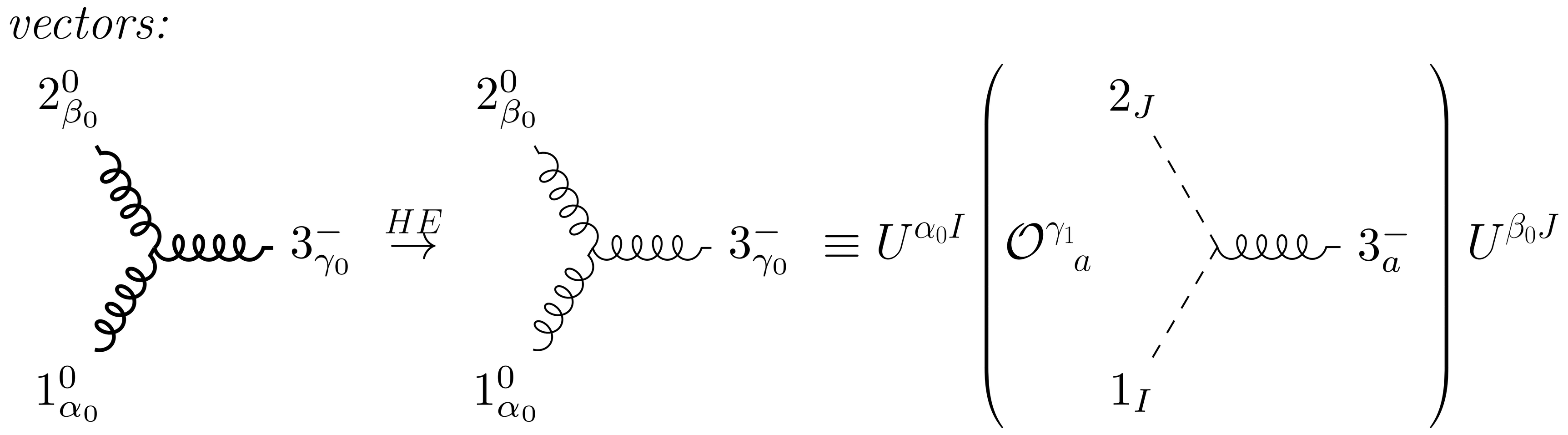

$$h^{\alpha_0\beta_0\gamma_0}\frac{((m^{\gamma_0})^2 - (m^{\alpha_0})^2 - (m^{\beta_0})^2)}{m_{\alpha_0}m_{\beta_0}}\frac{[23][31]}{[12]} \equiv U^{\alpha_0 I}(\mathcal{O}^{\gamma_0}{}_aT^a)_{IJ}U^{\beta_0 J}\frac{[23][31]}{[12]} \tag{11}$$

Results

From Eq. (10), we learn that, the coupling constants and generators in the IR are related to those of the UV via,

$$h^{\alpha\beta\gamma} = \mathcal{O}^\alpha{}_a\mathcal{O}^\beta{}_b\mathcal{O}^\gamma{}_cf^{abc}$$
$$X^\alpha = \mathcal{O}^\alpha{}_aT^a\,. \tag{12}$$

From Eq. (11), we have that

$$h^{\alpha_0\beta_0\gamma_0}\frac{((m^{\gamma_0})^2 - (m^{\alpha_0})^2 - (m^{\beta_0})^2)}{m_{\alpha_0}m_{\beta_0}} \equiv U^{\alpha_0 I}(\mathcal{O}^{\gamma_0}{}_aT^a)_{IJ}U^{\beta_0 J}\,, \tag{13}$$

which is solved by the ansatz

$$m^{\alpha_0}U^{\alpha_0 I} = (X^{\alpha_0})^{IJ}V_J\,, \tag{14}$$

for some $d_R = N_\phi$ dimensional vector V_J. This is the on-shell incarnation of the massive vector 'eating' the combination $(T^a)^{IJ}\phi_JV_I$. Furthermore, for massless vectors γ_1,

$$m^{\gamma_1} = 0 \Rightarrow (X^{\gamma_1})^{IJ}V_J = 0 \tag{15}$$

which tell us massless particles in the IR correspond to generators of unbroken symmetries. The mass matrix, for massive vectors and massless gluons in the IR are collectively given by,

$$(m^\alpha)^2\delta^{\alpha\beta} = VX^\alpha X^\beta V \tag{16}$$

Outlook

A similar analysis is executed for massive fermions in the IR and massless fermions in the UV, which requires the introduction of Yukawa couplings and mass mixing matrices.

References

[1] Nima Arkani-Hamed, Tzu-Chen Huang, and Yu-tin Huang. Scattering Amplitudes For All Masses and Spins. 9 2017.

[2] Brad Bachu and Akshay Yelleshpur. On-Shell Electroweak Sector and the Higgs Mechanism. *JHEP*, 08:039, 2020.

Acknowledgements

I thank Akshay Yelleshpur and Nima Arkani-Hamed for guidance at all stages of the project. I am supported in part by the Government of the Republic of Trinidad and Tobago.

The Wilson Loop - Large Spin OPE Dictionary

Carlos Bercini[1], Vasco Gonçalves[1,2], Alexandre Homrich[1,3,4], Pedro Vieira[1,3]

[1]ICTP South American Institute for Fundamental Research, IFT-UNESP
[2]Centro de Física do Porto e Departamento de Física e Astronomia, Faculdade de Ciências da Universidade do Porto
[3]Perimeter Institute for Theoretical Physics
[4]Walter Burke Institute for Theoretical Physics, California Institute of Technology

Introduction

In appendix B of [1] a duality was proposed between the n-point correlation functions of large spin single trace twist-two operators in planar $\mathcal{N}=4$ SYM and the expectation value of null polygonal Wilson loops with $2n$ sides. The simplest non-trivial example of such duality would relate three point functions and the null hexagon Wilson loop

$$\langle \mathcal{O}_{J_1}(x_1,\epsilon_1)\mathcal{O}_{J_2}(x_2,\epsilon_2)\mathcal{O}_{J_3}(x_3,\epsilon_3)\rangle \longleftrightarrow \mathbb{W}(U_1,U_2,U_3)$$

GOAL: Find the dictionary relating the variables on both sides of this equation: the spins J_j and polarization vector ϵ_j on the left hand side and the hexagon cross-ratios U_i on the right hand side.
We find this map between the OPE and Wilson loop variables by composing two other maps:

- The $\epsilon(\ell)$ map
- The $U(\ell)$ map

Combining the two maps, we get the desired $\epsilon(U)$ dictionary as summarized in the discussion section. Finally, to completely nail down the relation above with all precise kinematical and normalization factors we analyzed further the null six point correlator through an analytic bootstrap perspective.

The $\ell(\epsilon)$ map

The three point function described above can be parametrized as follows

$$\langle \mathcal{O}_{J_1}\mathcal{O}_{J_2}\mathcal{O}_{J_3}\rangle = \sum_{\ell_i}\left(\frac{C^{J_1,J_2,J_3}_{\ell_1,\ell_2,\ell_3}V_{1,23}^{J_1-\ell_2-\ell_3}V_{1,23}^{J_1-\ell_2-\ell_3}V_{2,31}^{J_2-\ell_3-\ell_1}V_{3,21}^{J_3-\ell_1-\ell_2}}{(x_{12}^2)^{\frac{\kappa_1+\kappa_2-\kappa_3}{2}}(x_{23}^2)^{\frac{\kappa_2+\kappa_3-\kappa_1}{2}}(x_{13}^2)^{\frac{\kappa_1+\kappa_3-\kappa_2}{2}}H_{23}^{-\ell_1}H_{31}^{-\ell_2}H_{12}^{-\ell_3}}\right)$$

In the large spin limit, the sum over tensor structures in the three point function is dominated by a saddle point so that given some polarizations ϵ_i there will be effectively a single ℓ_i contributing:

$$\frac{H_{2,3}}{V_{2,31}V_{3,1,2}} = \frac{\ell_1^2}{(J_3-\ell_1-\ell_2)(J_2-\ell_1-\ell_3)}$$
$$\frac{H_{3,1}}{V_{3,12}V_{1,2,3}} = \frac{\ell_2^2}{(J_1-\ell_2-\ell_3)(J_3-\ell_2-\ell_1)}$$
$$\frac{H_{1,2}}{V_{1,23}V_{2,3,1}} = \frac{\ell_3^2}{(J_2-\ell_3-\ell_1)(J_2-\ell_3-\ell_2)}$$

The $U(\ell)$ map

Next we turn to the OPE decomposition of six point functions in the so-called snowflake channel. The starting point is given by 6 sums (3 are spin sums and 3 are polarization sums) and the 3 integrals that appear in the representation of the conformal block). We proceed as follows:

- Take $x_{12}^2, x_{34}^2, x_{56}^2 \to 0$, which projects into leading twist.
- Take $x_{23}^2, x_{45}^2, x_{61}^2 \to 0$, which projects into large spin.
- Replace the six sums by integrals over spins and polarizations, resulting in nine integrals.
- Perform six of those integrals by saddle point, leaving only the integration over spins left to be done and obtaining the $\ell(U)$ map.

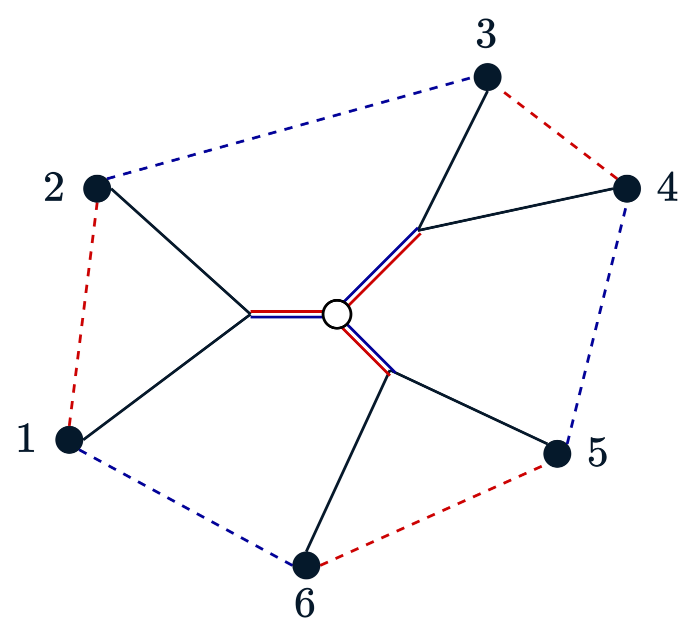

$$\ell_1 = \frac{J_2J_3}{J_2+J_3+J_1\sqrt{\frac{U_2}{U_1U_3}}}$$
$$\ell_2 = \frac{J_1J_3}{J_1+J_3+J_2\sqrt{\frac{U_1}{U_2U_3}}}$$
$$\ell_3 = \frac{J_1J_2}{J_1+J_2+J_3\sqrt{\frac{U_3}{U_1U_2}}}$$

The $C_{123} \leftrightarrow \mathbb{W}$ relation

We took the limit where all points approach the boundary of a null hexagon. But because we did it in two steps the final six point correlator is not manifestly cyclic invariant. By imposing cyclic symmetry of our correlator under $x_i \to x_{i+1}$ we can further constraint the structure constant to be.

$$\hat{C}^{J_1,J_2,J_3}_{\ell_1,\ell_2,\ell_3} = \mathcal{N}\left(\prod_{i=1}^{3}\left(\frac{J_i\ell_i}{2\ell_{i+1}\ell_{i-1}}\right)^{\frac{\gamma_i}{2}}\right)\times\mathbb{W}(U_1,U_2,U_3) \qquad (1)$$

Conclusions

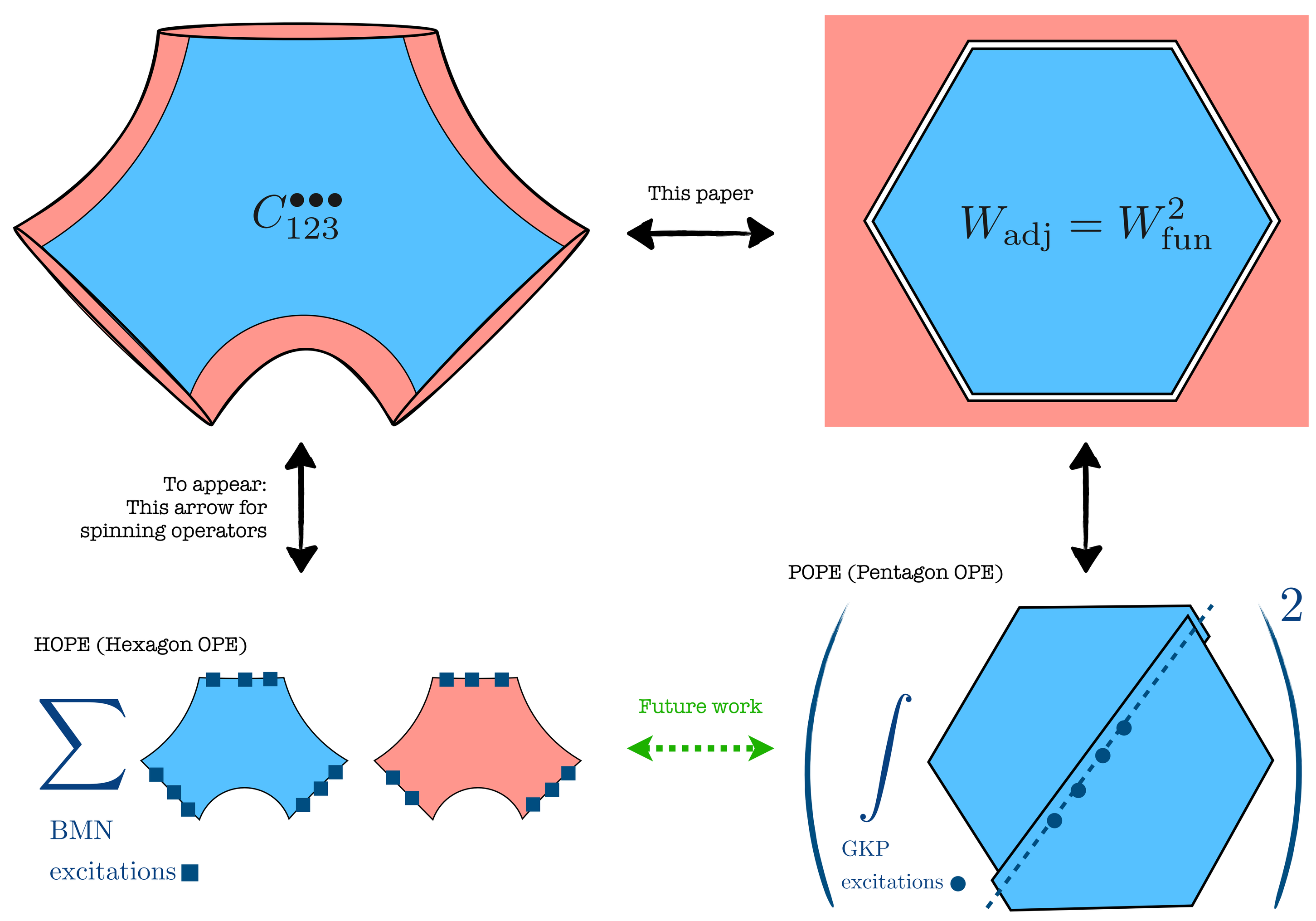

Top arrow: Large spin three-point function/hexagon Wilson loop duality [1].**Left arrow:** Three point functions can be decomposed in terms of two hexagons [3].**Right arrow:** Wilson loops can be decomposed in terms of two pentagons [2].**Bottom arrow:** The top duality hints at a transmutation of hexagons into pentagons in the large spin limit.
A basis question in the above mentioned duality is how are the variables related. The answer is our main result, it reads

$$\frac{\langle L_{i+1},R_{i+1}\rangle\langle L_{i+2},R_{i+2}\rangle}{\langle L_{i+1},R_{i+2}\rangle\langle L_{i+2},R_{i+1}\rangle} = \left(1-\frac{1+\frac{J_{i+2}}{J_{i+1}}+\frac{J_i}{J_{i+1}}\sqrt{\frac{U_i}{U_{i+1}U_{i+2}}}}{1+\frac{J_{i+1}}{J_i}+\frac{J_{i+2}}{J_i}\sqrt{\frac{U_{i+2}}{U_iU_{i+1}}}}\right)\left(1-\frac{1+\frac{J_{i+1}}{J_{i+2}}+\frac{J_i}{J_{i+2}}\sqrt{\frac{U_i}{U_{i+1}U_{i+2}}}}{1+\frac{J_{i+2}}{J_i}+\frac{J_{i+1}}{J_i}\sqrt{\frac{U_{i+1}}{U_iU_{i+2}}}}\right)$$

References

[1] L. F. Alday, D. Gaiotto, J. Maldacena, A. Sever, and P. Vieira. An Operator Product Expansion for Polygonal null Wilson Loops. *arXiv: 1006.2788.*

[2] B. Basso, A. Sever, and P. Vieira. Spacetime and Flux Tube S-Matrices at Finite Coupling for N=4 Supersymmetric Yang-Mills Theory. *arXiv:1303.1396.*

[3] T. Fleury and S. Komatsu. Hexagonalization of Correlation Functions. *arXiv:1611.05577.*

Underlying simplicity in two dimensional scattering

Patrick Dorey and **Davide Polvara**

Abstract

The S-matrices for a large class of (1+1)-dimensional integrable quantum field theories have been conjectured in the past following the bootstrap program. Though this approach has been able by itself to generate exact expressions for amplitudes that have passed different perturbative checks, a full understanding of how integrability manifests itself in perturbation theory is still a mystery. This poster aims to show, in Lagrangians with an arbitrary number of interacting bosons, under what conditions on the masses and couplings Feynman diagrams contributing to production processes sum to zero.

The bound state region

We focus on a class of integrable theories in (1+1) dimensions described by a scalar Lagrangian of the form

$$L = \frac{1}{2}\partial_\mu \phi_a \partial^\mu \phi_a - \frac{1}{2} m_a^2 \phi_a^2 - \frac{1}{3!} C_{abc}\phi_a\phi_b\phi_c - \frac{1}{4!} C_{abcd}\phi_a\phi_b\phi_c\phi_d - \dots$$

On-shell momentum associated to the j-particle ⟶ $p_j = m_j(\cosh\theta_j, \sinh\theta_j) = m_j(\cos u_j, i\sin u_j) \cong m_j e^{iu_j}$ (Rapidity; $\theta_j = iu_j$)

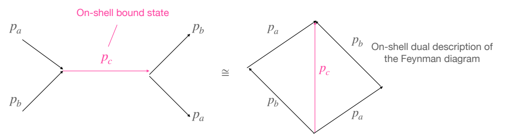

On the pole positions momenta can be represented by complex numbers having absolute values equal to the masses of the associated particles and arguments given by their rapidities

Cancellation of non-elastic processes in integrable theories

- Poles in non-allowed processes of the form $a + b \to c + d$ cancel through a **flipping rule**.
- If for a choice of external momenta an internal propagator goes on-shell, generating a pole, then there must be a propagator in another channel going on-shell for the same choice of external momenta.
- In this way there are always copies (or triplets) of poles that cancel each other, so that non-elastic processes do not occur.

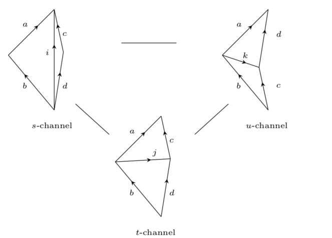

Additional constraints on the scattering: Simply-laced scattering conditions

A theory respects "simply-laced scattering conditions" if in 2 to 2 non-diagonal scattering the poles cancel in pairs (flip s/t, s/u or t/u) and in 2 to 2 diagonal processes the poles are due to only one on-shell bound state propagator at a time

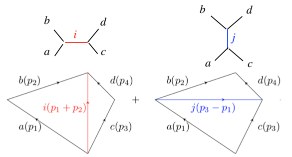

$$\simeq \frac{1}{s - m_i^2}\left(\frac{C_{abi}C_{icd}}{\Delta_{abi}\Delta_{icd}} - \frac{C_{acj}C_{jbd}}{\Delta_{acj}\Delta_{jbd}}\right) \qquad \left.\frac{dt}{ds}\right|_{s=m_i^2} = -\frac{\Delta_{acj}\Delta_{jbd}}{\Delta_{abi}\Delta_{icd}}$$

We impose that the residue at the pole is zero

➡ $C_{abc} = f_{abc}\Delta_{abc}$ with $f_{abi}f_{icd} - f_{acj}f_{jbd} = 0$

Provided these "simply-laced scattering conditions", if we additionally impose the cancellation of production processes of the from $2 \to 3$ we discover that all the parameters f_{ijk} need to have the same absolute value

$$f_{abc} = \pm f$$

Outlook on cancellation of 5-point processes

$A + B \to D + F + G$

We parametrise the propagators of the first diagram

$L^2 - m_L^2 = (x + a_1)\delta$

$E^2 - m_E^2 = (x + a_2)\delta$

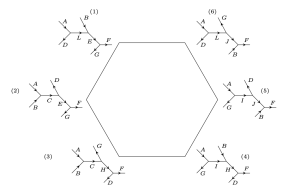

and take the limit $\delta \to 0$ in which a double pole appears.

a_1 and a_2 : fixed parameters

x : free variable

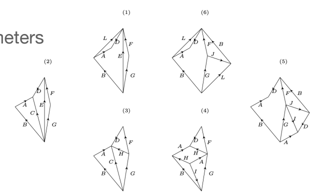

In a 5-point process there exists an entire network of singular diagrams connected by flipping internal propagators canceling each other

$$M_5 = \frac{1}{\delta^2}\left[\frac{a_1 - a_2}{(x+a_1)(x+a_2)} + \frac{a_2 - a_3}{(x+a_2)(x+a_3)} + \dots + \frac{a_N - a_1}{(x+a_N)(x+a_1)}\right]$$
$$= \frac{1}{\delta^2}\left[\frac{1}{x+a_1} + \frac{1}{x+a_2} - \frac{1}{x+a_2} + \frac{1}{x+a_3} + \dots - \frac{1}{x+a_N} + \frac{1}{x+a_1}\right] = 0$$

Loop simplicity

The S-matrix of some diagonal processes $(a + b \to a + b)$ present higher order poles. They correspond to have more propagators on-shell simultaneously internally to the loop.

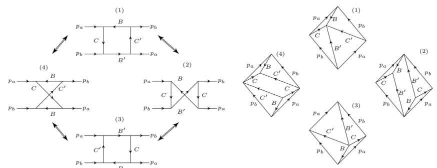

Once we find a Feynman diagram generating a singularity, by flipping loop propagators, we can find an entire network of graphs contributing to the pole. In the present case we consider a second order pole.

On the second order pole the loops can be cut into particular products of tree level graphs and the result can be derived from tree level properties.

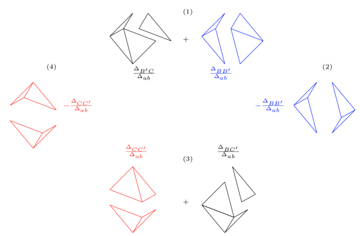

Diagrams that differ by one flipped propagator (the coloured ones) cancel in the sum and the final result is obtained by summing just the black graphs.

Summing all the contributions at the pole we obtain a universal result for the residue

$$S_{ab}(\theta) = \frac{1}{(\theta - i\theta_0)^2}\frac{f^4}{64}$$

Check out https://sagex.paradox-chaos.com/#/exhibition-hub/BeyondFeynmanDiagrams/4 to generate from yourself a 2-loop network in an interactive game!

Results

- We have found necessary and sufficient conditions to have absence of particle production at tree level for scalar Lagrangians
- We have proven that such conditions are universally satisfied by all the affine Toda theories
- In known integrable models, such as affine Toda theories, we have shown a similar simplicity also at loop level; loops can be decomposed into tree level diagrams, many cuts cancel each other in the sum and the final result is reproduced by few surviving terms

Acknowledgments *This project has received funding from the European Union's Horizon 2020 research and innovation programme under the Marie Skłodowska-Curie grant agreement No. 764850 (SAGEX.)*

Amplituhedron Like Geometries

Gabriele Dian (Durham University, UK)

Based on joint work with Paul Heslop arXiv:2106.09372

SAGEX Scattering Amplitudes: from Geometry to Experiment

Durham University

Correlator/Amplitude duality

The main motivaiton for studing the product of super amplitudes is that these objects emerge naturaly from a limit of the correlator of super stress energy tensor multiples

$$\left(\prod_{i=1}^{n} D_i^4\right) G_n = \langle \mathcal{O}(x_1,\theta_1)\cdots\mathcal{O}(x_n,\theta_n)\rangle$$

$$\lim_{x_{i,i+1}^2\to 0} G_n/G_{n;0}^{(0)} = (\mathcal{A}_n/\mathcal{A}_n^{\text{MHV tree}})^2$$

The right hand side corresponds to the square of the super amplitude and it can be decomposed into sectores with fixed NMHV degree as

$$(\mathcal{A}^2)_{n,k} = \sum_{k'=0}^{k} \mathcal{A}_{n,k'}\mathcal{A}_{n,k-k'}$$

Notation

	geometry	bosonised superspace	superspace
amplituhedron	$\mathscr{A}_{n,k,l}$	$A_{n,k,l}$	$\mathcal{A}_{n,k,l}$
amplituhedron-like	$\mathscr{H}_{n,k,l}^{(f;l')}$	$H_{n,k,l}^{(f;l')}$	$\mathcal{H}_{n,k,l}^{(f;l')}$

Hedron geometry

Amplituhedron-like geometries are the generalization of the amplituhedron to non-maximal winding number.

$$\mathscr{H}_{n,k}^{(f)} := \left\{ Y \in Gr(k,k+4) \;\middle|\; \begin{array}{ll} \langle Y i i+1 j j+1\rangle > 0 & 1 \le i < j-1 \le n-2 \\ \langle Y i i{+}1 1 n\rangle (-1)^f > 0 & 1 \le i < n-1 \\ \{\langle Y 123 i\rangle\} & \text{has } f \text{ sign flips as } i = 4,..,n \end{array} \right\}$$
$$\text{for } Z \in Gr_+(k+4,n)$$

For n minimal, the following alternative definition can be used

$$\mathscr{H}_{n,n-m}^{(f);\text{alt}} := \begin{cases} Y = \begin{pmatrix} C_1 \\ C_2 \end{pmatrix} \cdot Z \mid C_1 \in Gr_>(f,n) \,\wedge\, C_2 \in \text{alt}(Gr_>)(n-m-f,n) & \text{for } g_{n,f} \text{ even} \\ Y = \begin{pmatrix} C_1 \\ C_2 \end{pmatrix} \cdot Z \mid C_1 \in Gr_<(f,n) \,\wedge\, C_2 \in \text{alt}(Gr_>)(n-m-f,n) & \text{for } g_{n,f} \text{ odd} \end{cases}$$

The union of all amplituhedron-like geometres for a given k correspond to the squared amplituhedron, which can more intrinsecally be defined as the union of the following two regions

$$\mathscr{H}_{n,k,l}^{\pm} := \left\{ Y,(AB)_1,..,(AB)_l \;\middle|\; \begin{array}{ll} \langle Y i i+1 j j+1\rangle > 0 & 1 \le i < j-1 \le n-2 \\ \pm\langle Y i i{+}1 1 n\rangle > 0 & 1 \le i < n-1 \\ \langle Y (AB)_j i i{+}1\rangle > 0 & \forall\, j,\ \forall i = 1,..,n{-}1 \\ \pm\langle Y (AB)_j 1 n\rangle > 0 & \forall\, j \\ \langle (AB)_i (AB)_j\rangle > 0 & \forall i \neq j \end{array} \right\}$$

Main Result

Tree level

$$H_{n,n-4}^{(f)} = A_{n,f} * A_{n,n-f-4}\ .$$

Loop level

$$H_{n,n-4,l}^{(k',l')} = \binom{l}{l'} A_{n,k',l'} * A_{n,n-k'-4,l-l'}\ .$$

Product of Amplitudes

The bosonized super twistor allows to express the dependence of the amplitude on the Grassmann odd super variables as determinants of k+4 matrices.

$$\int d^4\phi \langle 12345\rangle^4 = \prod_{I=A}^{4}(\langle 1234\rangle \chi_5^A + \text{cyclic})$$

In this formulation is not obvious how the product of amplitudes can be computed. We conjecture that the following formula gives the right equivalent of the product in bosonized space

$$\left(\prod_{a=1}^{m}\langle I_a\rangle_{k_1+m}\right) * \left(\prod_{b=1}^{m}\langle J_b\rangle_{k_2+m}\right) = \frac{(-1)^{(k_1k_2+k_2)m}}{m!}\sum_{\sigma\in S_m}\prod_{a=1}^{m}\langle Y(I_a\cap J_{\sigma(a)})\rangle_{k_1+k_2+m}$$

As an example, here is the expression for the 6 point NMHV amplitude squared

$$(A_{6,1})^{*2} = 2\left([12345]*[12356]+[12345]*[13456]+[13456]*[12356]\right) =$$
$$= 2\langle 123456\rangle^4 \frac{\langle 1245\rangle\langle 2361\rangle\langle 3456\rangle + \langle 2356\rangle\langle 3412\rangle\langle 4561\rangle + \langle 3461\rangle\langle 4523\rangle\langle 5612\rangle}{\prod_{i=1}^{3}\langle i(i{+}1)(i{+}3)(i{+}4)\rangle\prod_{i=1}^{6}\langle i(i{+}1)(i{+}2)(i{+}3)\rangle}$$

Oriented Canonical Form

The canonical form of a geometry is defined to be the unique differential form with dlog divergency on the boundary and maximal residues equal to ±1,0. A region possessing a canonical form is called a positive geometry. The canonical form of the amplituhedron is the bosonized super amplitude. To compute geometrically the square of the super amplitude we need to modify the definition of the canonial form since its maximal residues can take different values. An important observation is that the union of positve geometries is not always a positive geometry itself. The key point is that as soon as positive geometries touch, there is the possibility of the maximal residues at intersecting points summing to values differing from 1,0.

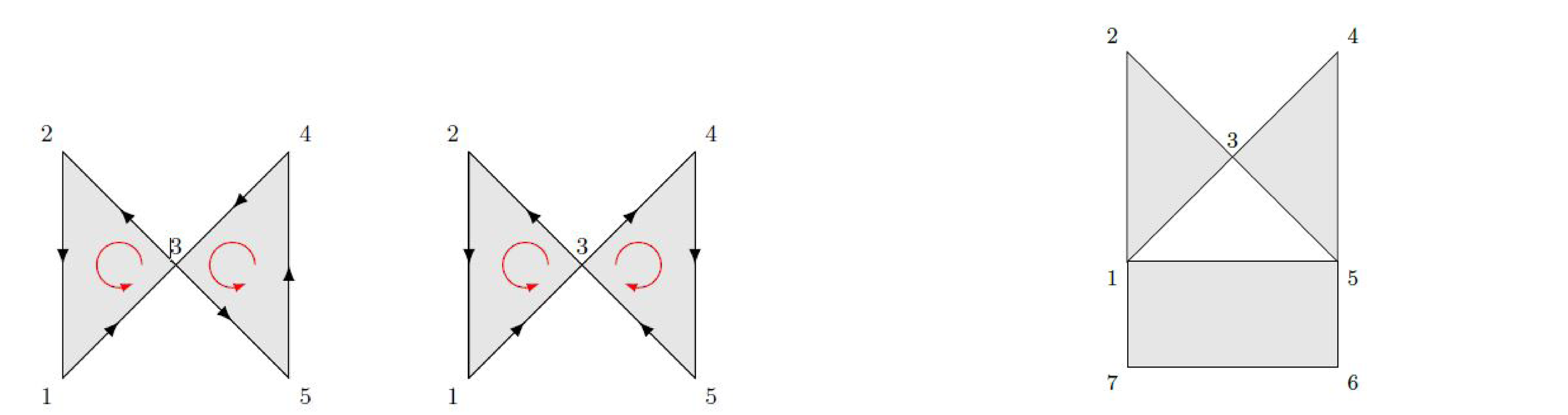

Not a positive geometry — Positive geometry — Not a positive geometry (for any choice of orientations)

We define the oriented canonical form of a region triangulated by a set of positive geometries having all the same orientation as the sum of the canonical form of the elements in the triangulation. We conjecture that the oriented caonical form of the squared amplituhedron gives the square of the super amplitude.

This project has received funding from the European Union's Horizon 2020 research and innovation programme under the Marie Sklodowska-Curie grant agreement No.764850 "SAGEX".

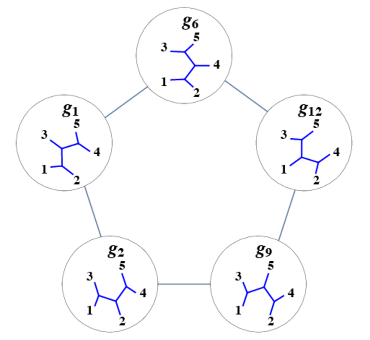

CONSTRUCTING HIGH-LOOP FORM FACTORS VIA COLOR-KINEMATICS DUALITY

GUANDA LIN , GANG YANG AND SIYUAN ZHANG ArXiv:2106.05280

MOTIVATION

The motivations are (i) explore high-loop structure of color-kinematics duality[1, 2] (ii) form factors in N=4 SYM provide maximally transcendental part in QCD Higgs amplitudes[3]

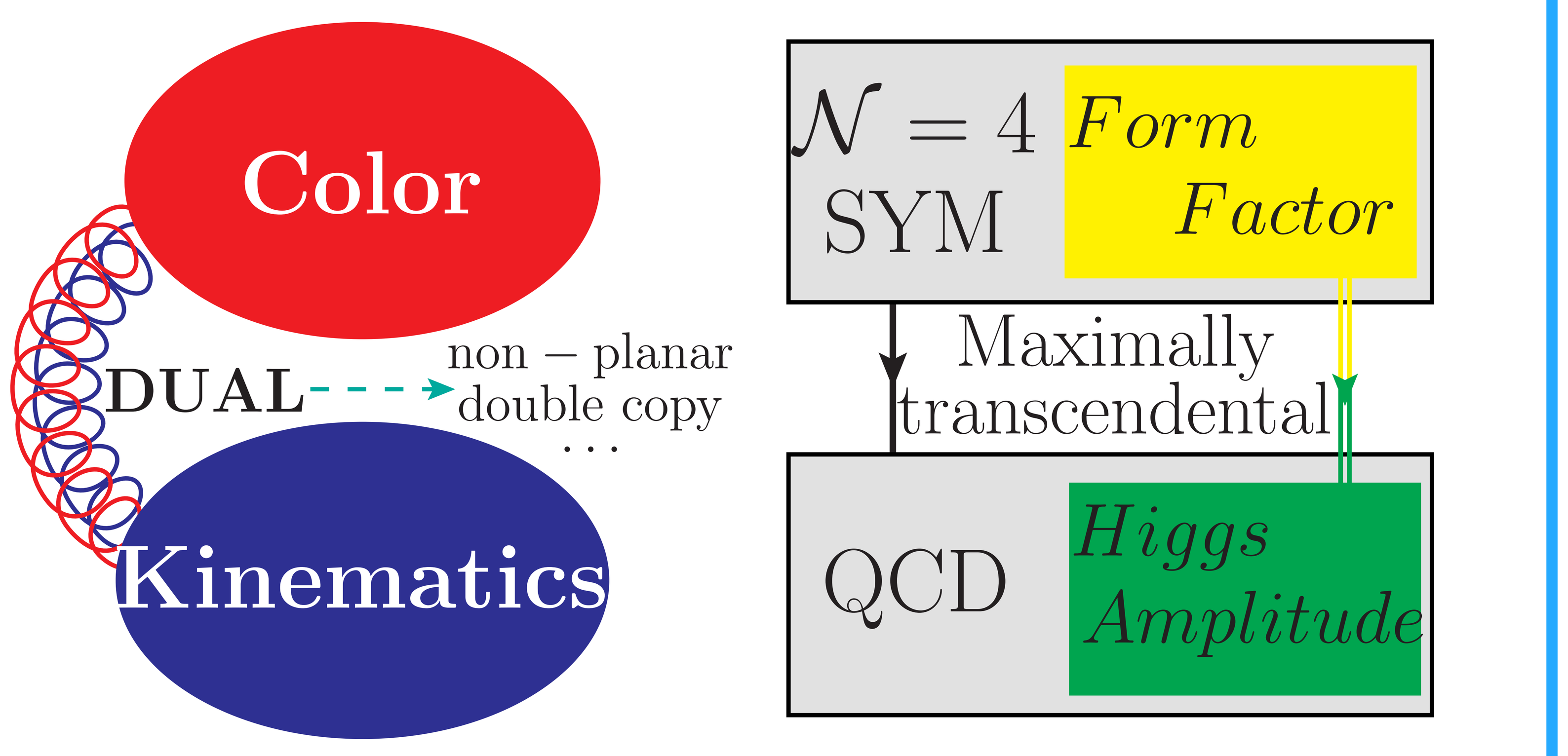

GENERAL STRATEGY

TARGET:

A representation of form factor integrand manifesting color-kinematics duality as

$$\mathbf{F}_{\mathcal{O}}^{(L)}=\mathcal{F}_{\mathcal{O}}^{(0)}\sum_{\sigma}\sum_{\Gamma_i\text{ cubic}}\int\prod_{j}^{L}d^D\ell_j\frac{1}{S_i}\frac{C_i\,N_i}{\prod_{\alpha_i}P_{\alpha_i}^2},$$

where the crucial conditions are kinematics numerators N_i satisfy dual Jacobi relations parallel to color Jacobi relations for C_i

$$C_s=C_t+C_u \quad\Rightarrow\quad N_s=N_t+N_u$$

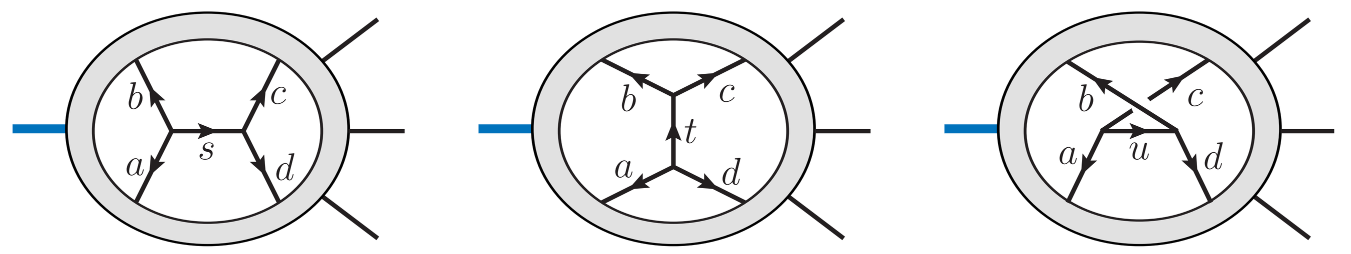

STRATEGY:

Our computation strategy can be shown by the flow chart

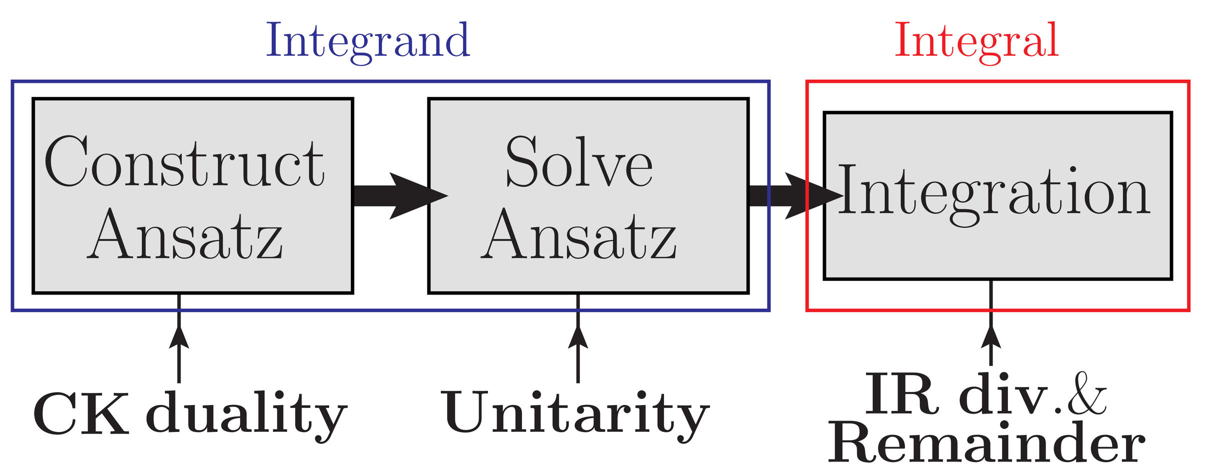

THREE-POINT THREE-LOOP FORM FACTOR

We consider the three-loop three-point super form factors of $\mathrm{tr}(\phi^2)$, *i.e.* $\mathbf{F}^{(3)}_{\mathrm{tr}(\phi^2)}(\Phi_1,\Phi_2,\Phi_3)$ as an example.

☐ **Construct Ansatz**

1.Topologies and masters

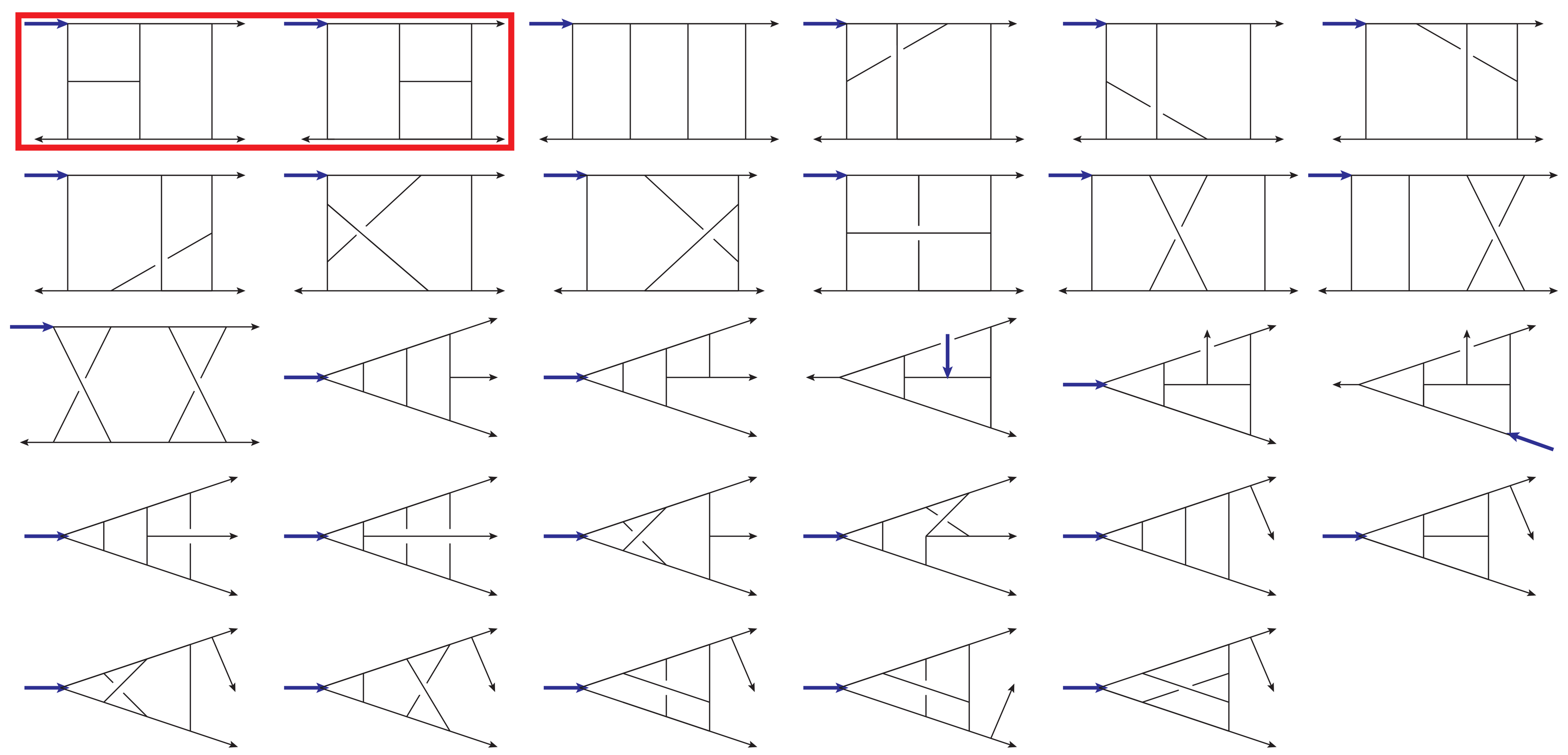

Master numerators $\xrightarrow{\text{dual Jacobi relation}}$ All numerators

2.Write down Minimal Ansatz for master numerators

3.Impose all dual Jacobi relations and graphic symmetries

☐ **Solve Ansatz**

Physical condition on integrands: Unitarity

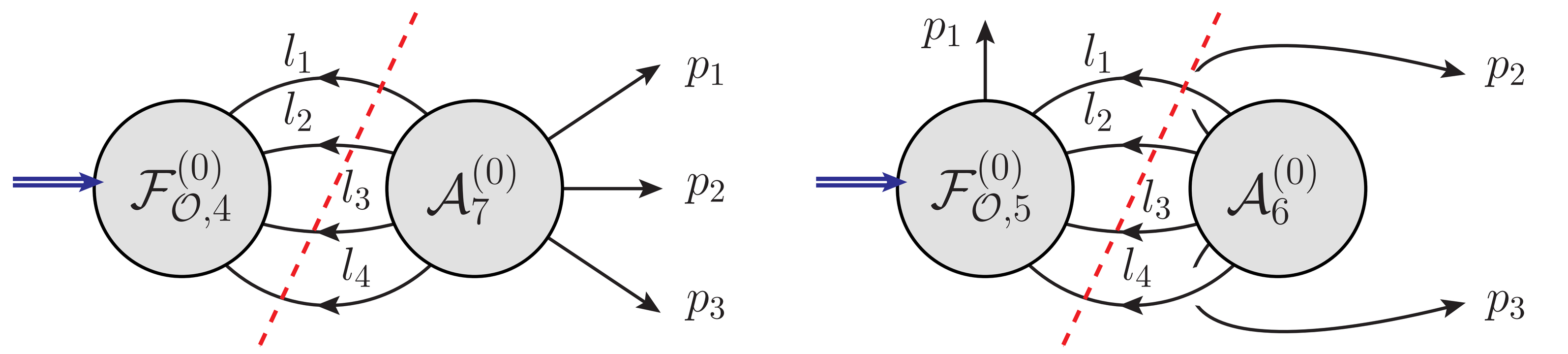

Interestingly, after considering all cut channels, the CK dual representation is still not completely fixed. Discuss later.

☐ **Integration & Check Solution**

1. Numerical Integration

Improve numerical efficiency by considering UT integrals, *e.g.*

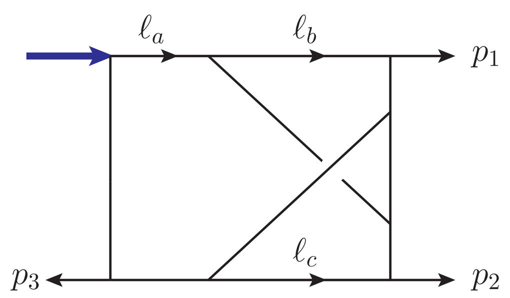

$$s_{12}s_{13}(\ell_a-p_1)^2\big((\ell_a-p_1)^2+s_{12}-\ell_a^2-(\ell_a-p_2-p_1)^2\big)$$

2. IR structure

The full-color IR divergence factor $\mathbf{Z}$ takes the form [5, 6]

$$\mathbf{Z}(p_i,\epsilon)=\exp\left\{\sum_{\ell=1}^{\infty}g^{2\ell}\left[\frac{\gamma^{(\ell)}_{\mathrm{cusp}}}{(\ell\epsilon)^2}\mathbf{D}_0-\frac{\gamma^{(\ell)}_{\mathrm{cusp}}}{\ell\epsilon}\mathbf{D}-n\frac{\mathcal{G}^{(\ell)}_{\mathrm{coll}}}{\ell\epsilon}\mathbf{1}+\frac{1}{\ell\epsilon}\mathbf{\Delta}^{(\ell)}\right]\right\}$$

where $\mathbf{\Delta}$ refers to non-dipole terms starting from 3 loops. We find the IR divergence with complete color dependence of our result is consistent with the above formula.

3.Finite Remainders

Leading color part of our result is consistent with the 3-loop FFOPE computation[4]. We also obtain the non-planar three-loop remainder function.

DISCUSSION & OUTLOOK

☐ **Discussion:** The solution space and parameters

The solution of the integrand in CK-dual representation is not unique. The undetermined parameters cancel at the **Integrand** level, based on **generalized gauge transformation**(GGT)[2].

For form factors, the insertion of local operator can induce a novel type of GGTs. For example, at 2 loops, we allow the following deformation (given the condition $C_{\rm a}=C_{\rm b}$)

$$N_{\rm a}\to N_{\rm a}+\ell_A^2\Delta,\quad N_{\rm b}\to N_{\rm b}-\ell_B^2\Delta$$

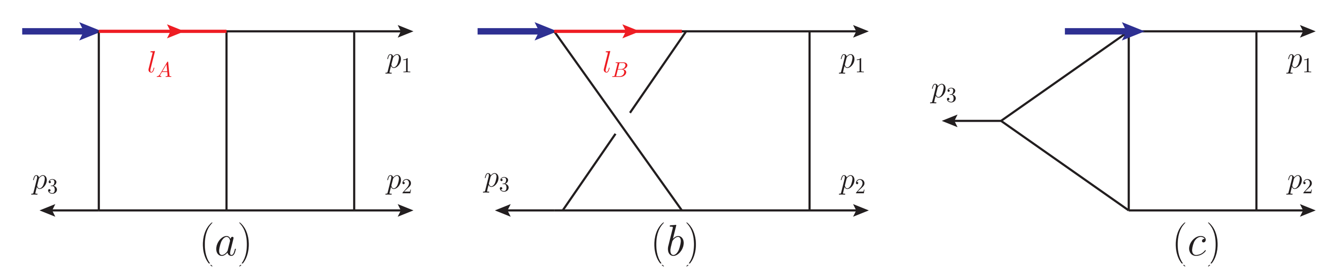

The large solution space of CK-dual integrand indicates **constructibility**(via CK duality) at four or even higher loops.

☐ **Outlook(i):** The double copy

A mathematically consistent double copy requires N_i to satisfy both dual Jacobi relations and operator induced relations

$$C_{\rm a}=C_{\rm b}\Rightarrow N_{\rm a}=N_{\rm b}\,,$$

where we find no local solutions. So the question is what can be the double copy of a form factor like quantity?

☐ **Outlook(ii):** Relation to QCD

Does the maximal transcendental principle (MTP) still hold at 3 loops, especially for N_c subleading parts?

Analytic expressions based on for example complete UT basis and canonical differential equations are interesting projects.

REFERENCES

[1] Z. Bern, J.J.M.Carrasco, and H. Johansson, *Phys. Rev. D78, 080511(2008).*
[2] Z. Bern, J.J.M.Carrasco, and H. Johansson, *Phys. Rev. Lett. 105, 061602 (2010).*
[3] A. Brandhuber, G. Travaglini, and G. Yang, *JHEP 1205(2012), 082.*
[4] L. J. Dixon, A. J. McLeod, and M. Wilhelm, *JHEP 04(2021), 147.*
[5] Ø. Almelid, C. Duhr, and E. Gardi *Phys. Rev. Lett. 117, 172002 (2016).*
[6] J. M. Henn and B. Mistlberger, *Phys. Rev. Lett. 117, 171601 (2016).*

A NEW WILSON LINE BASED ACTION FOR GLUODYNAMICS

AGH

H. Kakkad
AGH University of Science and Technology, *Krakow, Poland.*
In collaboration with P. Kotko, A. Stasto

Introduction

The subject of interest of the following work are scattering amplitudes, in particular the pure gluonic amplitudes. Despite the fact that gluon fields are regarded fundamental, they are not the most effective degrees of freedom when calculating amplitudes. Interestingly, in [1], the Maximally Helicity Violating (MHV) vertices used in the Cachazo-Svrcek-Witten (CSW) method [2] were shown to be connected with straight infinite Wilson lines on certain complex plane (self-dual plane). These Wilson lines emerge as the transformation of the positive helicity field appearing in the light cone Yang-Mills action, to a new action (often called as the 'MHV action') where the MHV vertices are explicit [3, 4, 5, 6]. Following that, in [7], we showed that the minus helicity field is given by a similar Wilson line, but with an insertion of the minus helicty gluon field somewhere on the line. Additionally, we postulated, that it should be a part of a bigger structure, extending beyond the self-dual plane. Indeed, in [8], we derived a new classical action for gluodynamics in which the fields are directly related to Wilson line functionals extending over both the self-dual and the anti-self-dual planes. The action is most easily derived through a canonical transformation of the anti-self-dual part of the MHV action, but we also discuss a direct link between the new action and the Yang-Mills action. The key property of the new action is that it does not have the triple-gluon vertices at all. This is because the triple-gluon vertices have been effectively resummed inside the Wilson lines. Thus, the lowest multiplicity vertex is the four-point MHV vertex. Higher-point vertices include not only the MHV vertices, but also other helicity configurations. The number of diagrams needed to obtain amplitudes beyond the MHV level is thus greatly reduced. We performed explicit calculations within the new formulation of several higher multiplicity amplitudes, to verify the consistency of the results.

MHV Lagrangian

The starting point is the full Yang-Mills action on the constant light-cone time x^+ in the light-cone gauge $\hat{A}^+ = 0$. We denote $\hat{A} = A_a t^a$, here t^a are color generators in the fundamental representation satisfying $\left[t^a, t^b\right] = i\sqrt{2} f^{abc} t^c$ and $\mathrm{Tr}(t^a t^b) = \delta^{ab}$. Integrating out the $\hat{A}^-$ fields (appearing quadratically) from the partition function [9], leaves only two complex fields $\hat{A}^\bullet$, $\hat{A}^\star$ that correspond to plus-helicity and minus-helicity gluon fields. We use the so-called 'double-null' coordinates defined as $v^+ = v\cdot\eta$, $v^- = v\cdot\tilde{\eta}$, $v^\bullet = v\cdot\varepsilon_\perp^+$, $v^\star = v\cdot\varepsilon_\perp^-$ with the two light-like basis four-vectors $\eta = (1,0,0,-1)/\sqrt{2}$, $\tilde{\eta} = (1,0,0,1)/\sqrt{2}$, and two space like complex four-vectors spanning the transverse plane $\varepsilon_\perp^\pm = \frac{1}{\sqrt{2}}(0,1,\pm i,0)$. The action reads

$$S_{\mathrm{Y-M}}^{(\mathrm{LC})}[A^\bullet, A^\star] = \int dx^+ \int d^3\mathbf{x} \left\{ -\mathrm{Tr}\,\hat{A}^\bullet \Box \hat{A}^\star - 2ig\,\mathrm{Tr}\,\partial_-^{-1}\partial_\bullet \hat{A}^\bullet \left[\partial_-\hat{A}^\star, \hat{A}^\bullet\right] - 2ig\,\mathrm{Tr}\,\partial_-^{-1}\partial_\star \hat{A}^\star \left[\partial_-\hat{A}^\bullet, \hat{A}^\star\right] - 2g^2\,\mathrm{Tr}\left[\partial_-\hat{A}^\bullet, \hat{A}^\star\right]\partial_-^{-2}\left[\partial_-\hat{A}^\star, \hat{A}^\bullet\right] \right\}, \quad (1)$$

where $\Box = 2(\partial_+\partial_- - \partial_\bullet\partial_\star)$. Thus we see, there are $(++-)$, $(--+)$ and $(++--)$ vertices in the action. Above, the bold position vector is defined as $\mathbf{x} \equiv (x^-, x^\bullet, x^\star)$.

The MHV action [3], implementing the CSW rules [2] is obtained from the Yang-Mills action Eq. (1) by canonically transforming both the fields to a new pair of fields $(\hat{B}^\bullet, \hat{B}^\star)$ with a requirement that the kinetic term and the $(++-)$ triple-gluon vertex in Eq. (1) is mapped to the kinetic term in the new action:

$$\mathrm{Tr}\,\hat{A}^\bullet\Box\hat{A}^\star + 2ig\,\mathrm{Tr}\,\partial_-^{-1}\partial_\bullet\hat{A}^\bullet\left[\partial_-\hat{A}^\star, \hat{A}^\bullet\right] \longrightarrow \mathrm{Tr}\,\hat{B}^\bullet\Box\hat{B}^\star . \quad (2)$$

Solving the above transformation for $\hat{A}^\bullet$, $\hat{A}^\star$ and substituting it in Eq. (1) results in the MHV action consisting of an infinite set of MHV vertices

$$S_{\mathrm{Y-M}}^{(\mathrm{LC})}[B^\bullet, B^\star] = \int dx^+ \left(-\int d^3\mathbf{x}\,\mathrm{Tr}\,\hat{B}^\bullet\Box\hat{B}^\star + \mathcal{L}_{--+}^{(\mathrm{LC})} + \dots + \mathcal{L}_{--+\dots+}^{(\mathrm{LC})} + \dots \right), \quad (3)$$

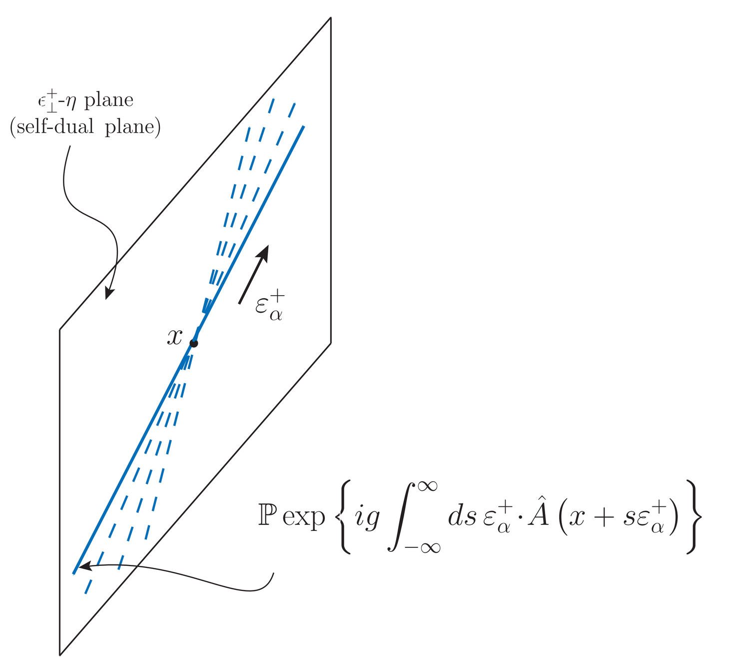

Fig. 1: $B_a^\bullet(x)$ is given by the straight infinite Wilson line lying on the plane spanned by $\varepsilon_\alpha^+ = \varepsilon_\perp^+ - \alpha\eta$ (with $\varepsilon_\perp^+ = (0,1,i,0)/\sqrt{2}$, $\eta = (1,0,0,-1)/\sqrt{2}$) and integrated over all α (the dashed lines represent tilted Wilson lines due to the change of α).

where $\mathcal{L}_{--+\dots+}^{(\mathrm{LC})}$ represents a generic n-point MHV vertex in the action, which in our conventions has the following form in the momentum space

$$\mathcal{L}_{--+\dots+}^{(\mathrm{LC})} = \int d^3\mathbf{p}_1 \dots d^3\mathbf{p}_n \delta^3\left(\mathbf{p}_1 + \dots + \mathbf{p}_n\right) \widetilde{\mathcal{V}}_{--+\dots+}^{b_1\dots b_n}\left(\mathbf{p}_1,\dots,\mathbf{p}_n\right) \widetilde{B}_{b_1}^\star\left(x^+;\mathbf{p}_1\right)\widetilde{B}_{b_2}^\star\left(x^+;\mathbf{p}_2\right)\widetilde{B}_{b_3}^\bullet\left(x^+;\mathbf{p}_3\right)\dots\widetilde{B}_{b_n}^\bullet\left(x^+;\mathbf{p}_n\right), \quad (4)$$

with the MHV vertices

$$\widetilde{\mathcal{V}}_{--+\dots+}^{b_1\dots b_n}\left(\mathbf{p}_1,\dots,\mathbf{p}_n\right) = \sum_{\substack{\text{noncyclic}\\ \text{permutations}}} \mathrm{Tr}\left(t^{b_1}\dots t^{b_n}\right)\frac{(-g)^{n-2}}{(n-2)!}\left(\frac{p_1^+}{p_2^+}\right)^2 \frac{\widetilde{v}_{21}^{*4}}{\widetilde{v}_{1n}^*\widetilde{v}_{n(n-1)}^*\widetilde{v}_{(n-1)(n-2)}^*\dots\widetilde{v}_{21}^*}, \quad (5)$$

where we introduced spinor-like variables

$$\tilde{v}_{ij} = p_i^+\left(\frac{p_j^\star}{p_j^+} - \frac{p_i^\star}{p_i^+}\right), \qquad \tilde{v}_{ij}^* = p_i^+\left(\frac{p_j^\bullet}{p_j^+} - \frac{p_i^\bullet}{p_i^+}\right). \quad (6)$$

The $\tilde{v}_{ij}$, $\tilde{v}_{ij}^*$ symbols are directly proportional to the spinor products $\langle ij\rangle$ and $[ij]$.

It is very interesting how the solution of the Mansfield's transformations Eq. (2) are related to straight infinite Wilson line spanning over the transverse complex plane [1, 7]. However, in the original work [3] the MHV action was constructed using only analytic properties of the transformations and equivalence theorem for the S-matrix. The explicit solution for $\hat{A}^\bullet$ and $\hat{A}^\star$ fields was found in [4] in momentum space.

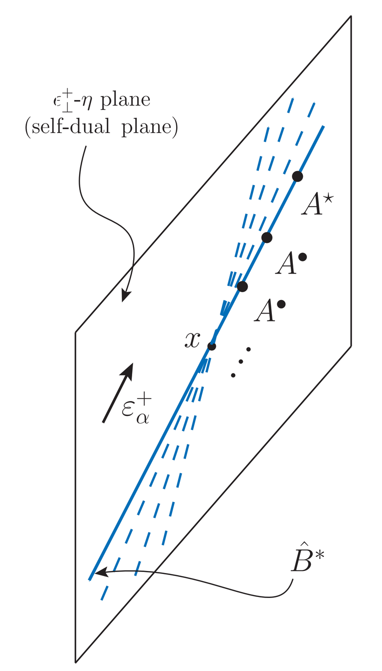

Fig. 2: The $B^\star$ field can be represented as the straight infinite Wilson line similar to the one from Fig. 1, but where one $A^\bullet$ field has been replaced by the $A^\star$ field.

Straight infinte Wilson Lines

The Wilson line interpretation of the new fields in the MHV action was first discussed in [1] where the plus helicity field, $B_a^\bullet[\hat{A}^\bullet](x)$, was shown to be the straight infinite Wilson line $B_a^\bullet[A^\bullet](x) = \mathcal{W}_{(+)}^a[A](x)$. For a generic vector field K^μ, the straight infinite Wilson line functional $\mathcal{W}_{(\pm)}[K]$ reads:

$$\mathcal{W}_{(\pm)}^a[K](x) = \int_{-\infty}^{\infty} d\alpha\,\mathrm{Tr}\left\{\frac{1}{2\pi g}t^a\partial_-\mathbb{P}\exp\left[ig\int_{-\infty}^{\infty} ds\,\varepsilon_\alpha^\pm\cdot\hat{K}\left(x+s\varepsilon_\alpha^\pm\right)\right]\right\}, \quad (7)$$

with $\varepsilon_\alpha^{\pm\mu} = \varepsilon_\perp^{\pm\mu} - \alpha\eta^\mu$. This four vector has the form of a gluon polarization vector. Indeed for $\alpha = p\cdot\varepsilon_\perp^\pm/p^+$, it is the transverse polarization vector for a gluon with momentum p.
For a given α, the Wilson line $B_a^\bullet[\hat{A}^\bullet](x)$, is along the plus helicity polarization vector ε_α^+. This implies, the line is on the so-called self-dual plane (the plane on which the tensors are self dual) spanned by $\varepsilon_\perp^+$ and η (see Fig. 1). However, on this plane, the Wilson line is not along a fixed direction. It is, rather, integrated over all possible directions α.
On the other hand, the minus helicity field, $B_a^\star[\hat{A}^\bullet, \hat{A}^\star](x)$ in the MHV action Eq. (3) was shown in [7] to be a similar Wilson line, but with an insertion of the minus helicty gluon field at certain point on the line (see Fig. 2).

$$B_a^\star[A^\bullet, A^\star](x) = \int d^3\mathbf{y}\left[\frac{\partial_-^2(y)}{\partial_-^2(x)}\frac{\delta\mathcal{W}_{(+)}^a[A](x^+;\mathbf{x})}{\delta A_c^\bullet(x^+;\mathbf{y})}\right]A_c^\star(x^+;\mathbf{y}), \quad (8)$$

where $\partial_-(x) = \partial/\partial x^-$. It is natural to think about the $A^\star$ fields as belonging to Wilson lines living within the anti-self-dual plane spanned by ε_α^- (recall that the $B^\bullet$ lives on the plane spanned by ε_α^+). Therefore, in [7], we conjectured that the solution (8) should just be a cut through a bigger structure, spanning over both planes.

A new Wilson Line based action

The canonical transformation, Eq. (2), maps the self-dual part of the Yang-Mills action to the kinetic term in the MHV action. This mapping eliminates one of the triple gloun vertex $(++-)$. The other triple gloun vertex $(+--)$ still exists in the MHV action ($\mathcal{L}_{--+}^{(\mathrm{LC})}$ term in Eq. (3)). The triple point vertex is not a very effective building block for calculating amplitudes. Moreover, in the on-shell limit they are zero (for real momenta). The smallest amplitude which is finite in the on-shell limit is the four-point MHV. In [8], motivated by the above arguments, we found a more general canonical transformation based on path ordered exponentials of the gauge fields, extending over both the self-dual and anti-self-dual planes

$$\left\{\hat{A}^\bullet, \hat{A}^\star\right\} \to \left\{\hat{Z}^\bullet[A^\bullet, A^\star], \hat{Z}^\star[A^\bullet, A^\star]\right\}, \quad (9)$$

It maps the kinetic term and both the triple-gluon vertices of the Yang-Mills action Eq. (1) into a free term in the new action. The requirement that the transformation is canonical is necessary in order to preserve the functional measure in the partition function, up to a field independent factor. Although the transformation (9) is rather complicated, we found that, quite amazingly, the generating functional $\mathcal{G}[A^\bullet, Z^\star]$ for the transformation can be written in the following simple form:

$$\mathcal{G}[A^\bullet, Z^\star](x^+) = -\int d^3\mathbf{x}\;\hat{\mathcal{W}}_{(-)}^{-1}[Z](x)\,\partial_-\hat{\mathcal{W}}_{(+)}[A](x), \quad (10)$$

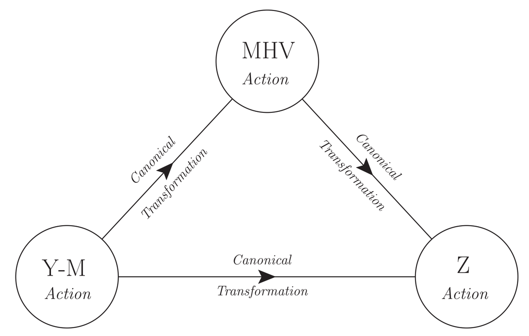

Fig. 3: Two ways to derive the new action. First is the direct method which involves the generating functional (10). Second involves two consecutive canonical field transformation.

However, we showed [8] that the transformation from the Yang-Mills action to the new action generated by the functional (10) is equivalent to two canonical transformations: first transforming the self-dual part of the Yang-Mills action to the kinetic term in MHV action, and then transforming the anti-self-dual part in the latter to kinetic term in the new action (see Fig. 3).
The transformation can be solved to obtain the explicit solutions for $\hat{Z}^\bullet[A^\bullet, A^\star]$ and $\hat{Z}^\star[A^\bullet, A^\star]$ fields [8]. We schematically depict the structure of the $Z^\star$ field in Fig. 4. Substituting the inverse of these fields in the Yang-Mills action Eq. (1) results in the new action. For convenience, we shall call the new action as *Z-field action* hereafter. It has the following generic structure:

$$S_{\mathrm{Y-M}}^{(\mathrm{LC})}[Z^\bullet, Z^\star] = \int dx^+\left\{-\int d^3\mathbf{x}\,\mathrm{Tr}\,\hat{Z}^\bullet\Box\hat{Z}^\star + \mathcal{L}_{--++}^{(\mathrm{LC})} + \mathcal{L}_{--+++}^{(\mathrm{LC})} + \mathcal{L}_{--++++}^{(\mathrm{LC})} + \dots + \mathcal{L}_{---++}^{(\mathrm{LC})} + \mathcal{L}_{---+++}^{(\mathrm{LC})} + \mathcal{L}_{---++++}^{(\mathrm{LC})} + \dots \;\vdots\; + \mathcal{L}_{---\dots-++}^{(\mathrm{LC})} + \mathcal{L}_{---\dots-+++}^{(\mathrm{LC})} + \mathcal{L}_{---\dots-++++}^{(\mathrm{LC})} + \dots\right\},$$

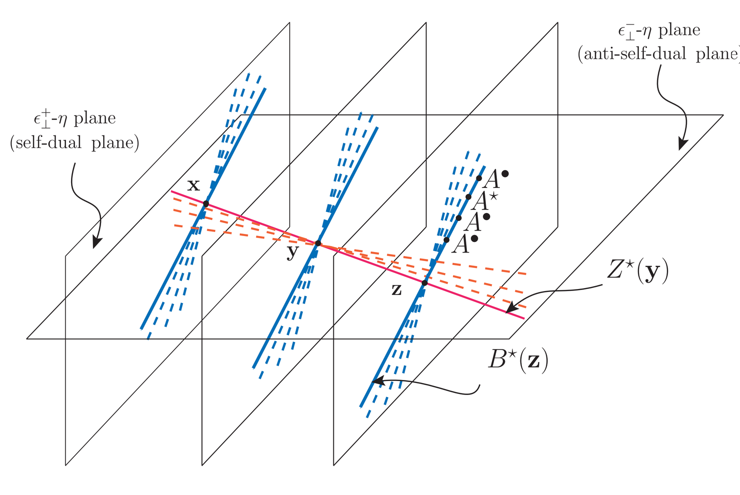

Fig. 4: Schematic presentation of the geometric structure of the $Z^\star$ field (the structure of $Z^\bullet$ is quite similar). $Z^\star$ field is a Wilson line (with exactly the same analytic form as $B^\bullet$) of only $B^\star$ fields on anti-self-dual plane. Notice, each vertical plane is self-dual plane with $B^\star$ embedded in it as was showin in Fig. 2 .

where the n-point interaction vertex, $n \geq 4$, that couples m minus helicity fields, $m \geq 2$, and $n-m$ plus helicity fields, has the following general form:

$$\mathcal{L}_{\underbrace{-\cdots-}_{m}\underbrace{+\cdots+}_{n-m}}^{(\mathrm{LC})} = \int d^3\mathbf{y}_1\dots d^3\mathbf{y}_n\,\mathcal{U}_{-\dots-+\dots+}^{b_1\dots b_n}\left(\mathbf{y}_1,\cdots\mathbf{y}_n\right)\prod_{i=1}^{m}Z_{b_i}^\star(x^+;\mathbf{y}_i)\prod_{j=1}^{n-m}Z_{b_j}^\bullet(x^+;\mathbf{y}_j). \quad (11)$$

The above action has the following properties:

i) There are no three point interaction vertices. The reason is that the triple-gluon vertices have been effectively resummed inside the Wilson lines. Thus, the lowest multiplicity vertex is the four-point MHV vertex.

ii) At the classical level there are no all-plus, all-minus, as well as $(-+\dots+)$, $(-\dots-+)$ vertices.

iii) There are MHV vertices, $(--+\dots+)$, corresponding to MHV amplitudes in the on-shell limit.

iv) There are $\overline{\mathrm{MHV}}$ vertices, $(-\dots-++)$, corresponding to $\overline{\mathrm{MHV}}$ amplitudes in the on-shell limit.

v) All vertices have the form which can be easily calculated. In the foloowing section we discuss the general form for any vertex (described by Eq. (11)) in the Z-field action.

Generic vertex in the action

As mentioned earlier, the transformation from the Yang-Mills action to the new action generated by the functional (10) is equivalent to two canonical transformations. Using the latter, we can readily write the relations between the Z fields and B fields in momentum space [8]. For the $B^\star$ field we have

$$\widetilde{B}_a^\star(x^+;\mathbf{P}) = \sum_{n=1}^{\infty}\int d^3\mathbf{p}_1\dots d^3\mathbf{p}_n\,\overline{\widetilde{\Psi}}{}_n^{a\{b_1\dots b_n\}}(\mathbf{P};\{\mathbf{p}_1,\dots,\mathbf{p}_n\})\prod_{i=1}^{n}\widetilde{Z}_{b_i}^\star(x^+;\mathbf{p}_i), \quad (12)$$

with

$$\overline{\widetilde{\Psi}}{}_n^{a\{b_1\cdots b_n\}}(\mathbf{P};\{\mathbf{p}_1,\dots,\mathbf{p}_n\}) = -(-g)^{n-1}\frac{\widetilde{v}_{(1\cdots n)1}}{\widetilde{v}_{1(1\cdots n)}}\frac{\delta^3(\mathbf{p}_1+\dots+\mathbf{p}_n-\mathbf{P})\,\mathrm{Tr}(t^a t^{b_1}\cdots t^{b_n})}{\widetilde{v}_{21}\widetilde{v}_{32}\cdots\widetilde{v}_{n(n-1)}}. \quad (13)$$

The expansion for the $B^\bullet$ field reads

$$\widetilde{B}_a^\bullet(x^+;\mathbf{P}) = \sum_{n=1}^{\infty}\int d^3\mathbf{p}_1\dots d^3\mathbf{p}_n\,\overline{\widetilde{\Omega}}{}_n^{ab_1\{b_2\cdots b_n\}}(\mathbf{P};\mathbf{p}_1,\{\mathbf{p}_2,\dots,\mathbf{p}_n\})\widetilde{Z}_{b_1}^\bullet(x^+;\mathbf{p}_1)\prod_{i=2}^{n}\widetilde{Z}_{b_i}^\star(x^+;\mathbf{p}_i), \quad (14)$$

where

$$\overline{\widetilde{\Omega}}{}_n^{ab_1\{b_2\cdots b_n\}}(\mathbf{P};\mathbf{p}_1,\{\mathbf{p}_2,\dots,\mathbf{p}_n\}) = n\left(\frac{p_1^+}{p_{1\cdots n}^+}\right)^2\overline{\widetilde{\Psi}}{}_n^{ab_1\cdots b_n}(\mathbf{P};\mathbf{p}_1,\dots,\mathbf{p}_n). \quad (15)$$

In order to derive the content of the Z-field action, we insert the expansions of B fields in terms of Z fields in the MHV action Eq. (3). Consider, in momentum space, the vertex in Eq. (11) which has n external legs with the momenta $\mathbf{p}_1\dots\mathbf{p}_n$, where $\mathbf{p}_1\dots\mathbf{p}_m$ correspond to the minus helicity legs (the negative helicity fields are considered adjacent for convenience). The color ordered vertex can be written as:

$$\mathcal{U}_{-\dots-+\dots+}^{b_1\dots b_n}(\mathbf{p}_1,\dots,\mathbf{p}_n) = \sum_{\substack{\text{noncyclic}\\ \text{permutations}}}\mathrm{Tr}\left(t^{b_1}\dots t^{b_n}\right)\mathcal{U}\left(1^-,\dots,m^-,(m+1)^+,\dots,n^+\right), \quad (16)$$

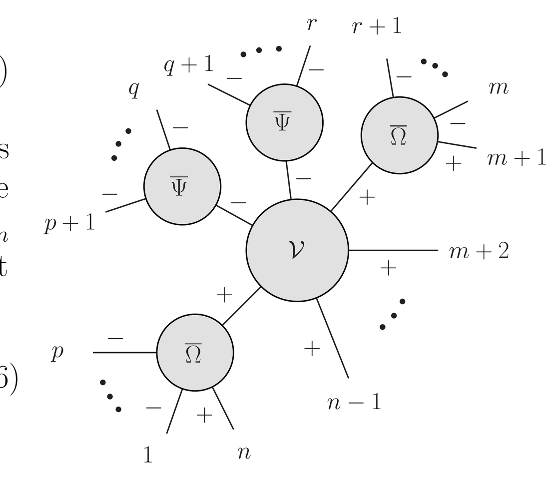

Fig. 5: A general contribution to the Z-theory vertex $\mathcal{U}\left(1^-,\dots,m^-,(m+1)^+,\dots,n^+\right)$. The central blob is the MHV vertex.

We introduce a collective index $[i, i+1,\dots,j]$ labeling the momentum, $\mathbf{p}_{i(i+1)\dots j} = \mathbf{p}_i + \mathbf{p}_{i+1} + \dots + \mathbf{p}_j$. Using this notation, the general form of the color ordered vertex can be written as [8] (see Fig. 5):

$$\mathcal{U}\left(1^-,\dots,m^-,(m+1)^+,\dots,n^+\right) = \sum_{p=0}^{m-2}\sum_{q=p+1}^{m-1}\sum_{r=q+1}^{m}\mathcal{V}\left([p+1,\dots,q]^-,[q+1,\dots,r]^-,[r+1,\dots,m+1]^+,(m+2)^+,\dots,(n-1)^+,[n,1,\dots,p]^+\right)\overline{\Omega}\left(n^+,1^-,\dots,p^-\right)\overline{\Psi}\left((p+1)^-,\dots,q^-\right)\overline{\Psi}\left((q+1)^-,\dots,r^-\right)\overline{\Omega}\left((r+1)^-,\dots,m^-,(m+1)^+\right) \quad (17)$$

Although the analytic formula do not seem to collapse, in general, to any simple form, the above expression is operational and can be readily applied in the actual amplitude calculation. We discuss this in the following section.

Pure gluonic amplitudes

Using this new action we computed several tree-level amplitudes. The MHV and $\overline{\mathrm{MHV}}$ vertices alone give the corresponding on-shell amplitudes. Consider the 5-point $\overline{\mathrm{MHV}}$. It is easily obtained from (17). In Fig. 6 we show the contributing terms. In the on-shell limit, the sum of these diagrams reduces to the known formula for the $\overline{\mathrm{MHV}}$ amplitude:

$$\mathcal{A}(1^-,2^-,3^-,4^+,5^+) = g^3\left(\frac{p_4^+}{p_5^+}\right)^2\frac{\widetilde{v}_{54}^4}{\widetilde{v}_{15}\widetilde{v}_{54}\widetilde{v}_{43}\widetilde{v}_{32}\widetilde{v}_{21}}. \quad (18)$$

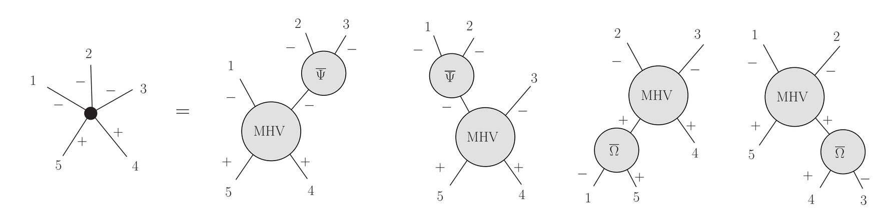

Fig. 6: The contributions to the color-ordered $\overline{\mathrm{MHV}}$ vertex, with helicity $(---++)$.

For the 6-point Next-To-MHV (NMHV) amplitude with helicity configuration $(---+++)$ we have just three contributing diagrams depicted in Fig. 7. The sum of these diagrams reproduce in the on-shell limit the known result [10].
For 7-point NNMHV amplitude $(----+++)$ we had just five contributing diagrams depicted in Fig. 8. Furthermore, the higher multiplicity amplitudes, up to 8-point NNMHV $(----++++)$, were calculated and shown to be in agreement with the standard methods. The maximum number of diagrams we encountered in that case was 13. The absence of triple-gluon vertices resulted in fewer diagrams required to compute amplitudes, when compared to the CSW method and, obviously, considerably fewer than in the standard Yang-Mills action.

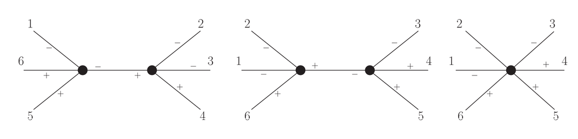

Fig. 7: Diagrams contributing to 6-point NMHV amplitude $(---+++)$.

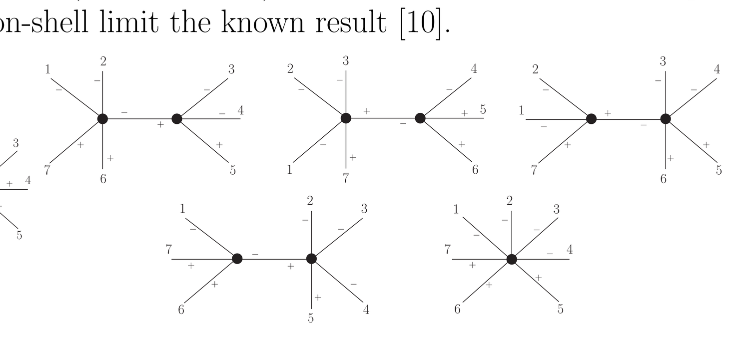

Fig. 8: Diagrams contributing to 7-point NNMHV amplitude $(----+++)$.

Acknowledgement

H.K. and P.K. are supported by the National Science Centre, Poland grant no. 2018/31/D/ST2/02731. A.M.S. is supported by the U.S. Department of Energy Grant DE-SC-0002145 and in part by National Science Centre in Poland, grant 2019/33/B/ST2/02588.

References

[1] P Kotko and A M Stasto. "Wilson lines in the MHV action". In: *J. High Energy Phys.* 2017.9 (2017), p. 47. ISSN: 1029-8479.
[2] Freddy Cachazo, Peter Svrcek, and Edward Witten. "MHV Vertices And Tree Amplitudes In Gauge Theory". en. In: *J. High Energy Phys.* 2004.09 (2004), pp. 006–006. ISSN: 1029-8479.
[3] Paul Mansfield. "The lagrangian origin of MHV rules". en. In: *J. High Energy Phys.* 2006.03 (2006), pp. 037–037. ISSN: 1029-8479.
[4] James H Ettle and Tim R Morris. "Structure of the MHV-rules lagrangian". In: *J. High Energy Phys.* 2006.08 (2006), pp. 003–003. ISSN: 1029-8479.
[5] James H Ettle et al. "S-matrix equivalence theorem evasion and dimensional regularisation with the canonical MHV lagrangian". In: *J. High Energy Phys.* 2007.05 (2007), pp. 011–011. ISSN: 1029-8479.
[6] James H Ettle, Tim R Morris, and Zhiguang Xiao. "The MHV QCD Lagrangian". en. In: *J. High Energy Phys.* 2008.08 (2008), pp. 103–103. ISSN: 1029-8479.
[7] Hiren Kakkad, Piotr Kotko, and Anna Stasto. "Exploring straight infinite Wilson lines in the self-dual and the MHV Lagrangians". In: *Phys. Rev. D* 102.9 (2020), p. 094026. ISSN: 2470-0010.
[8] Hiren Kakkad, Piotr Kotko, and Anna Stasto. "A new Wilson line-based action for gluodynamics". In: *Journal of High Energy Physics* 2021.7 (July 2021). DOI: 10.1007/jhep07(2021)187.
[9] J. Scherk and John H. Schwarz. "Gravitation in the light cone gauge". In: *Gen. Relativ. Gravit.* 6.6 (1975), pp. 537–550. ISSN: 00017701.
[10] David A Kosower. "Light-cone recurrence relations for QCD amplitudes". In: *Nucl. Phys. B* 335.1 (1990), pp. 23–44. ISSN: 05503213.

Tree BCJ implies loop BCJ for almost any field theory

(S)YM(–matter) · NLSM · BLG · strings

2007.13803 2102.11390 2108.03030 21??.?????

Hyungrok Kim

with L. Borsten, B. Jurčo, T. Macrelli, C. Saemann, M. Wolf

Gravity Batalin–Vilkovisky action

$$\frac{1}{2}R + \frac{1}{12}H^2 + \frac{1}{2}\varphi\,\Box\,\varphi + B^*\nabla\Lambda + g^*\nabla X + \cdots$$

Ricci scalar · Kalb–Ramond field strength · dilaton · KR ghost · graviton antifield · diffeo. ghost

Cubic gravity action with auxiliaries

$$\frac{1}{2}\phi_{AA'}\,\Box\,\phi^{AA'} + \frac{1}{6}F^A_{BC}F^{A'}_{B'C'}\phi_{AA'}\phi^{BB'}\phi^{CC'} + \frac{1}{2}(F^A_{BC}Q^{A'}_{B'C'} + Q^A_{BC}F^{A'}_{B'C'})\phi^*_{AA'}\phi^{BB'}\phi^{CC'}$$

where $\phi^{AA'} = (h_{\mu\nu}, B_{\mu\nu}, \varphi, X^\mu, \bar{X}_\mu, \dots, \varpi^\mu, \dots, G_{\mu\nu\rho\sigma}, \dots)$ — (anti)ghosts, Nakanishi–Lautrup, auxiliaries

GR = kinematic ⊗ kinematic ⊗ cubic scalar theory

← *integrate out auxiliaries, redefine (anti)fields, introduce Schwartz part of dilaton*

↑ *double copy*

Yang–Mills Batalin–Vilkovisky action

↓ (from title)

$$\frac{1}{4}F^2 + A^*_a \cdot D_A c^a + \bar{c}^* b + \frac{1}{2} f^a_{bc} c^*_a c^b c^c$$

antifield · ghost · Nakanishi–Lautrup · antighost antifield

YM = colour ⊗ colour-stripped YM (L_∞-algebra; colour: Lie alg.; colour-stripped YM: C_∞-algebra)

$d^2 = 0$, $d[x,y] = [dx,y] \pm [x,dy]$, $[x,y] = \pm[x,y]$

$[x,[y,z]] = [[x,y],z] \pm [y,[x,z]] \pm d\mu_3(x,y,z) \pm \mu_3(dx,y,z) \pm \mu_3(x,dy,z) \pm \mu_3(x,y,dz)$

⋮

→ *redefine fields, add terms summing to 0 (Tolotti–Weinzierl), nonlinear gauge*

Gauge-fixed action manifests BCJ

$$\sum_{n=2}^{\infty}\sum_{i\in\Gamma_n}\frac{f^{n-2}(\partial^{n-2}\phi^n + \partial^{n-3}\phi^*\phi^{n-1})}{\prod_{e\in\mathrm{Edges}(i)}\Box_e}$$

colour factor built using i's topology · n-linear pseudodifferential operator · n-leg cubic trees

at $n = 2$, '−1 edges' yields $\phi_{aA}\,\Box\,\phi^{aA} + Q^A_B\phi^*_{aA}\phi^{aB}$

where $\phi^{aA} = (A^a_\mu, c^a, \bar{c}^a, b^a)$

YM = colour ⊗ colour-stripped YM ($BV^\Box_\infty$-algebra)

→ *introduce aux. fields*

Cubic action manifests perfect BCJ

$$\frac{1}{2}\phi_{aA}\,\Box\,\phi^{aA} + \phi^*_{aA}Q^A_B\phi^{aB} + f^a_{bc}\left(\frac{1}{6}F^A_{BC}\phi_{aA} + \frac{1}{2}Q^A_{BC}\phi^*_{aA}\right)\phi^{bB}\phi^{cC}$$

linear part of BRST · antifield · colour structure constant · kinematic structure constant · cubic part of BRST

where $\phi^{aA} = (A^a_\mu, c^a, \bar{c}^a, b^a, G^a_{\mu\nu\rho}, \dots)$ — (anti)ghost, Nakanishi–Lautrup, auxiliaries

YM = colour ⊗ kinematic ⊗ cubic scalar theory (colour: gametic alg.; kinematic: gametic alg.; kinematic ⊗ cubic scalar theory: $BV^\Box$-algebra)

↑ *needed to define* (from Gametic algebra)

$BV^\Box_\infty$-algebra

Algebra of on-shell BCJ

$BV^\Box$ axioms hold *up to homotopy*

↖ *underlies* (Gauge-fixed action manifests BCJ)

↑ *Koszul duality*

Twisted Hopf algebras

Hopf algebra: coproduct is homom. $H \to H \otimes H$

Twisted Hopf: coproduct is homom. $H \to H \otimes_\tau H$

where τ is a *twist* defining alternative assoc. alg. structure on $H \otimes H$

Unrelated to quasitriangular Hopf algebras!

→ *needed to define*

Hodge complexes

Like chain complexes (V,d), but with (V,d,h) where

$dh + hd = \Box$, $d^2 = h^2 = 0$

Chain complex: mod. over Hopf alg. $\mathbb{R}[d]/(d^2)$

Hodge complex: mod. over *twisted* Hopf alg.

$\mathbb{R}[\partial_0, \dots, \partial_{d-1}]\langle d,h\rangle/(d^2, h^2, dh + hd - \Box)$

Hopf means well defined ⊗ (←coproduct),

$1_\otimes$ (←counit), dual (←antipode)

→ *needed to define*

$BV^\Box$-algebra

Algebra of perfect BCJ

$[,]$ given by F^A_{BC}; $(\cdot)$ by $F^A_{BC} + Q^A_{BC}$

$d^2 = h^2 = 0$, $dh + hd = \Box$, $xy = \pm yx$, $(xy)z = x(yz)$

$d(xy) = dx \cdot y \pm x \cdot dy$, $d[x,y] = [dx,y] \pm [x,dy] + \Box(xy) - \Box x \cdot y - x \cdot \Box y$

$h(xy) - hx \cdot y \pm x \cdot hy = [x,y]$, $h[x,y] = -[hx,y] \pm [x,hy]$

$[x,y] = \pm[y,x]$, $[x,[y,z]] = \pm[[x,y],z] \pm [y,[x,z]]$, $[x,yz] = [x,y]z \pm y[x,z]$

↗ *underlies* (Cubic action manifests perfect BCJ)

Gametic algebra

Common structure of colour and kinematic algebras

Lie algebra equipped with info about BRST

$([,], d, \{,\})$ encodes $(f^a_{bc}, 0, 0)$ or $(F^A_{BC}, Q^A_B, Q^A_{BC})$

$d^2 = 0$, $d[x,y] - [dx,y] \pm [x,dy] = \{x,y\}$, $d\{x,y\} + \{dx,y\} \pm \{x,dy\} = 0$

$[x,y] = \pm[y,x]$, $[x,[y,z]] = [[x,y],z] \pm [y,[x,z]]$

$\{x,y\} = \pm\{y,x\}$, $2\{x,\{y,z\}\} = \{\{x,y\},z\} \pm \{y,\{x,z\}\}$

$-2\{x,[y,z]\} = [\{x,y\},z] \pm [y,\{x,z\}]$, $-2[x,\{y,z\}] = \{[x,y],z\} \pm \{y,[x,z]\}$

Progress in two-loop five-point Feynman Integrals

Dhimiter D. Canko[1], Adam Kardos[2], Costas G. Papadopoulos[1], Alexander V. Smirnov[3], Nikoloas Syrrakos[1] and Christopher Wever[4]

1. Institute of Nuclear and Particle Physics, NCSR 'Demokritos', Agia Paraskevi, 15310, Greece
2. University of Debrecen, Faculty of Science and Technology, Department of Experimental Physics, 4010, Debrecen, PO Box 105, Hungary
3. Research Computing Center, Moscow State University, 119991 Moscow, Russia
4. Physik-Department T31, Technische Universitat Munchen, James-Franck Strasse 1, D-85748 Garching, Germany

Abstract

A review of recent results on two-loop five-point Feynman Integrals with up to one off-shell external leg is presented. The three planar families have been fully expressed in terms of Goncharov poly-logarithms. From the three hexa-box families, the first one has also been fully expressed as above, whereas the current effort is to complete the same task for the other two families, studying new methods to cope with algebraic letters. In the near future we hope that the two double-pentagon families will also be fully resolved. The achievements so far, based on the Simplified Differential Equations (SDE) approach, include also multi-scale Feynman Integrals with internal masses.

Introduction

When considering multiloop Feynman integrals involving many external particles, the current frontier lies at two-loop five-point integrals with up to one off-shell leg and massless internal lines. For the fully massless case, all Master integrals are by now known up to transcendental weight four [1, 2, 3, 4, 5, 6, 7] and their solutions have been implemented in a fast C++ library known as *pentagon functions* [8]. When one of the external particles is considered off-shell, the planar topologies have been recently solved using two different computational approaches for the solution of canonical differential equations, numerically [9] and analytically [10]. The numerical calculation was performed using a generalised power-series method [11, 12], while the analytical solution was achieved through the use of the Simplified Differential Equations approach (SDE) [13], with the results given in terms of Goncharov polylogarithms of up to transcendental weight four. These results are relevant to many $2 \to 3$ scattering processes studied experimentally at the LHC, e.g. $W + 2$ jets production. For the computation of the relevant scattering amplitudes, one-loop five-point Feynman integrals with one off-shell leg also have to be known up to transcendental weight four [14]. These results were recently used for the calculation of two-loop QCD corrections to $Wb\bar{b}$ production [15]. First results for one of the non-planar topologies have also appeared using a numerical approach [16]. Recently, numerical results for the non-planar hexabox topologies were presented in [17]. On the multi-scale frontier, analytic results for several one-loop five-point families involving up to three external masses and up to one internal mass were recently presented in [18] based on the SDE approach.

Computational framework

The standard approach for the calculation of Feynman integrals involves obtaining a complete set of Master integrals through the use of Integration-By-Part identities [19], constructing a pure basis of Master integrals [20] and then deriving and solving differential equations [21, 22, 23, 24] in canonical form [25]. This approach has yielded numerous results [26], in part due to the fact that we have a solid understanding of the special class of functions, known as multiple or Goncharov polylogarithms [27, 28, 29, 30], in terms of which many Feynman integrals can be expressed. In more complicated cases however, this class of functions is not enough and important steps have been made in getting a better understanding of a more general class of functions, Elliptic integrals [31, 32, 33, 34, 35, 36, 37], which appear in solutions of multiloop Feynman integrals with many scales, especially when several internal masses are introduced.

More specifically, assuming that we have a pure basis of Master integrals $\mathbf{g}$, the SDE in canonical form satisfied by this basis is

$$\partial_x \mathbf{g} = \epsilon \left(\sum_{i=1}^{l_{max}} \frac{\mathbf{M}_i}{x - l_i} \right) \mathbf{g} \tag{1}$$

where $\mathbf{M}_i$ are the residue matrices corresponding to each letter l_i and l_{max} is the length of the alphabet. In order to solve (1) we need to provide boundary terms. We start with the residue matrix corresponding to the letter $\{0\}$, $\mathbf{M}_1$ and through its Jordan Decomposition we rewrite it as follows,

$$\mathbf{M}_1 = \mathbf{SDS}^{-1} \tag{2}$$

Then we define the *resummation matrix* $\mathbf{R}$ as follows

$$\mathbf{R} = \mathbf{S} e^{\epsilon \mathbf{D} \log(x)} \mathbf{S}^{-1} \tag{3}$$

The next step is to use IBP identities to write the pure basis $\mathbf{g}$ in the following form

$$\mathbf{g} = \mathbf{TG} \tag{4}$$

Using the expansion-by-regions method [38] implemented in the `asy` code which is shipped along with `FIESTA4` [39], we can obtain information for the asymptotic behaviour of the Feynman integrals in terms of which we express the pure basis of Master integrals (4) in the limit $x \to 0$,

$$G_i \underset{x \to 0}{=} \sum_j x^{b_j + a_j \epsilon} G_i^{(b_j + a_j \epsilon)} \tag{5}$$

where a_j and b_j are integers and G_i are the individual members of the basis $\mathbf{G}$ of Feynman integrals in (4). As explained in [10], we can construct the relation

$$\mathbf{Rb} = \lim_{x \to 0} \mathbf{TG} \Big|_{\mathcal{O}(x^{0 + a_i \epsilon})} \tag{6}$$

where $\mathbf{b} = \sum_{i=0}^{n} \epsilon^i \mathbf{b}_0^{(i)}$ are the boundary terms that we need to compute. The right-hand-side of (6) implies that, apart from the terms $x^{a_i \epsilon}$ coming from (5), we expand around $x = 0$, keeping only terms of order x^0.

After obtaining the relevant boundary terms we can write the solution of (1) in the following compact form,

$$\begin{aligned}
\mathbf{g} = {} & \epsilon^0 \mathbf{b}_0^{(0)} + \epsilon \left(\sum \mathcal{G}_a \mathbf{M}_a \mathbf{b}_0^{(0)} + \mathbf{b}_0^{(1)} \right) \\
& + \epsilon^2 \left(\sum \mathcal{G}_{ab} \mathbf{M}_a \mathbf{M}_b \mathbf{b}_0^{(0)} + \sum \mathcal{G}_a \mathbf{M}_a \mathbf{b}_0^{(1)} + \mathbf{b}_0^{(2)} \right) \\
& + \epsilon^3 \left(\sum \mathcal{G}_{abc} \mathbf{M}_a \mathbf{M}_b \mathbf{M}_c \mathbf{b}_0^{(0)} + \sum \mathcal{G}_{ab} \mathbf{M}_a \mathbf{M}_b \mathbf{b}_0^{(1)} + \sum \mathcal{G}_a \mathbf{M}_a \mathbf{b}_0^{(2)} + \mathbf{b}_0^{(3)} \right) \\
& + \epsilon^4 \left(\sum \mathcal{G}_{abcd} \mathbf{M}_a \mathbf{M}_b \mathbf{M}_c \mathbf{M}_d \mathbf{b}_0^{(0)} + \sum \mathcal{G}_{abc} \mathbf{M}_a \mathbf{M}_b \mathbf{M}_c \mathbf{b}_0^{(1)} \right. \\
& \left. + \sum \mathcal{G}_{ab} \mathbf{M}_a \mathbf{M}_b \mathbf{b}_0^{(2)} + \sum \mathcal{G}_a \mathbf{M}_a \mathbf{b}_0^{(3)} + \mathbf{b}_0^{(4)} \right)
\end{aligned} \tag{7}$$

were $\mathcal{G}_{ab\ldots} := \mathcal{G}(l_a, l_b, \ldots; x)$ represent the Goncharov polylogarithms.

Planar Pentaboxes

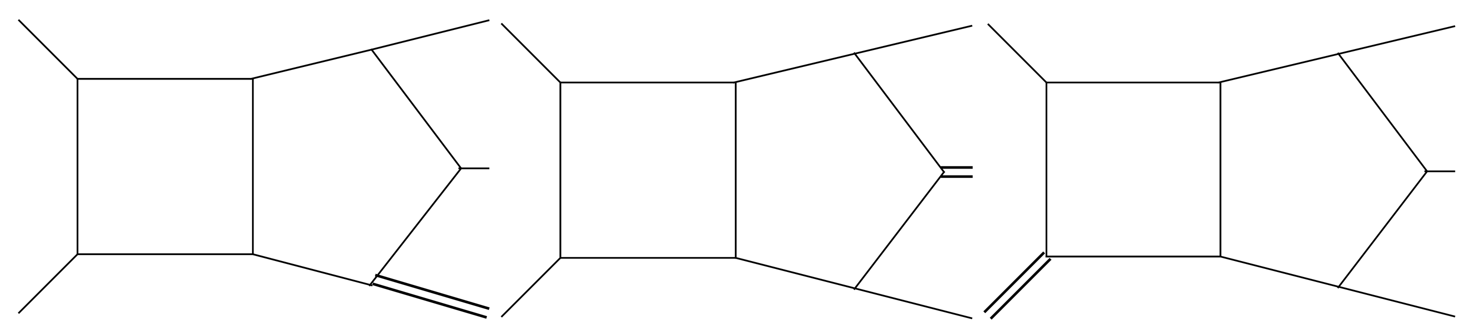

Figure 1: The two-loop diagrams representing the top-sector of the planar pentabox family P_1(74 MI), P_2(75 MI) and P_3(86 MI). All external momenta are incoming.

Hexaboxes

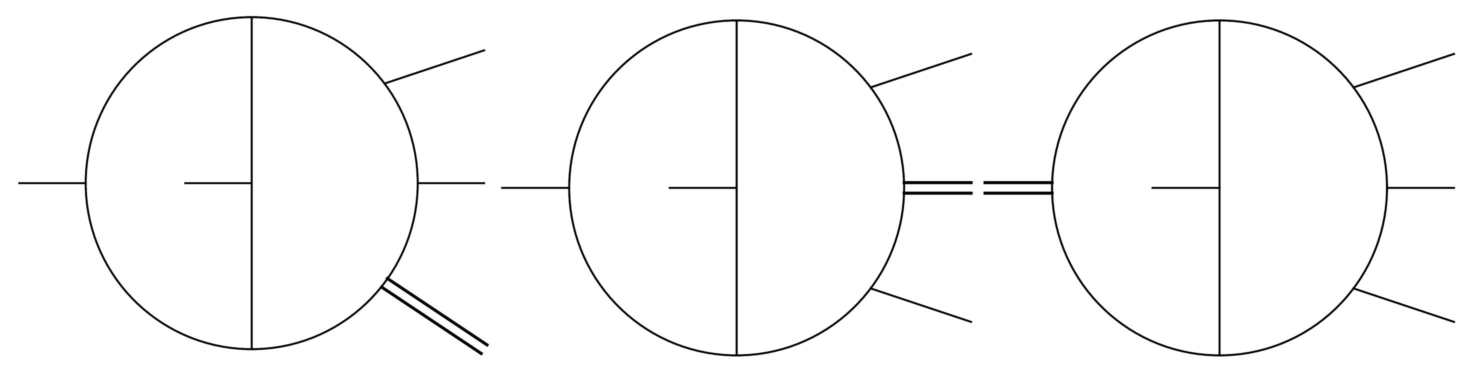

Figure 2: The two-loop diagrams representing the top-sector of the non-planar hexabox family N_1(86 MI), N_2(86 MI) and N_3(135 MI). All external momenta are incoming.

Multi-scale pentagons

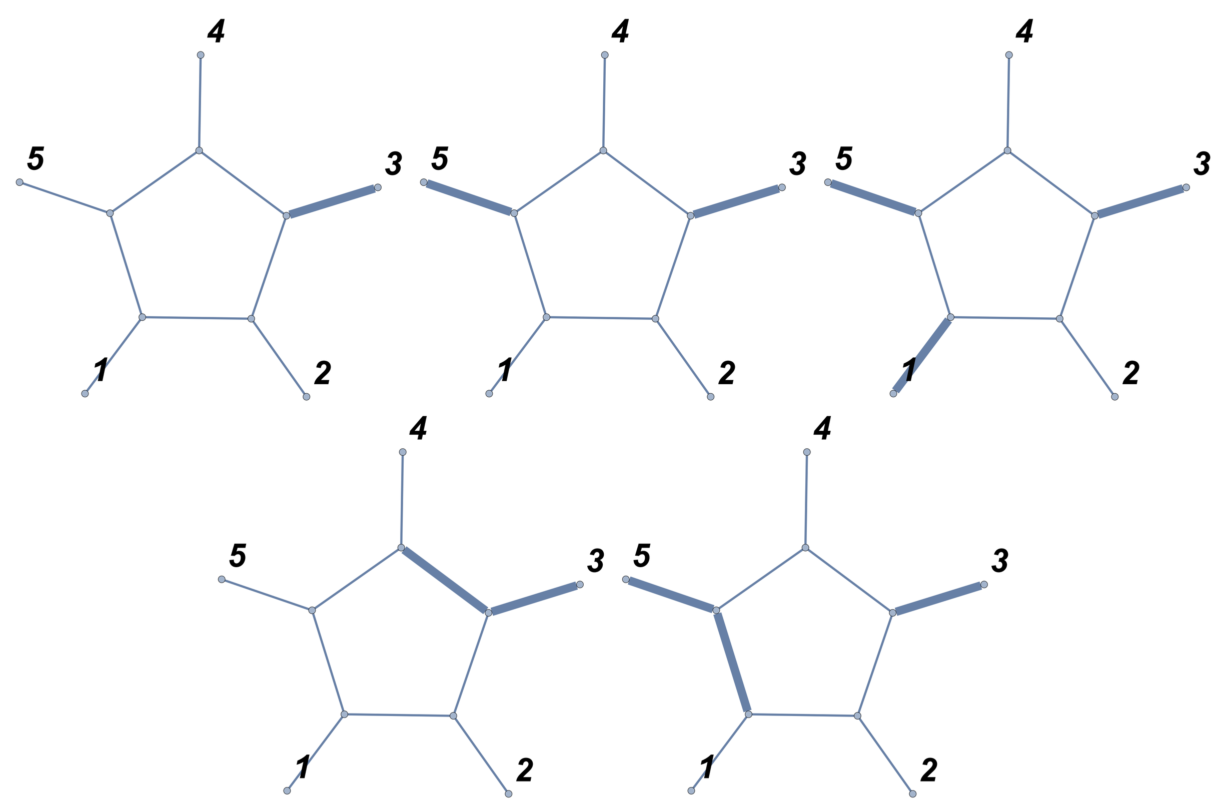

Figure 3: The one-loop diagrams representing the top-sector of the multiscale pentagon families. All external momenta are incoming. Bold external lines represent particles with $p^2 \neq 0$. Bold internal lines represent particles with $m \neq 0$.

Results

P_3	g_{84}	ϵ^0: 1/2 ϵ^1: 3.2780415861887284967738281876762 ϵ^2: 0.11455863130537720411162743574627 ϵ^3: -16.979642659429606120982671925458 ϵ^4: -48.101985355625914648042310964575

Table 1: Numerical results for the non-zero top sector element of each family with 32 significant digits.

The computation of GPs is performed using their implementation in `GiNaC`. This implementation is capable to evaluate the GPs at an arbitrary precision. The computational cost to numerically evaluate a GP function, depends of course on the number of significant digits required as well as on their weight and finally on their structure, namely how many of its letters, Eq. (7), satisfy $l_a \in [0, x]$. We refer to reference [40] for more details.For the following Euclidean point $S_{12} \to -2, S_{23} \to -3, S_{34} \to -5, S_{45} \to -7, S_{51} \to -11, x \to \frac{1}{4}$, all GP functions with real letters are real, namely no letter is in $[0, x]$, and moreover the boundary terms are by construction all real. The result is given in Table 1, with timings, running the `GiNaC` Interactive Shell `ginsh`, given by 1.9, 3.3, and 2 seconds for P_1, P_2 and P_3 respectively and for a precision of 32 significant digits. More results including physical phase-space points can be found in [10, 14, 18].

Conclusions

The SDE approach has been proven very successful in expressing many multi-scale two-loop integrals in terms of GPLs. We are currently working on the two last hexa-box families. In the near future, when the canonical basis for the two double-pentagon families becomes available, we plan to complete the analytic representation of all two-loop five-point Feynman Integrals with up to one off-shell external leg.

References

[1] C. G. Papadopoulos, D. Tommasini and C. Wever, JHEP **04** (2016), 078 doi:10.1007/JHEP04(2016)078 [arXiv:1511.09404 [hep-ph]].

[2] T. Gehrmann, J. M. Henn and N. A. Lo Presti, Phys. Rev. Lett. **116** (2016) no.6, 062001 [erratum: Phys. Rev. Lett. **116** (2016) no.18, 189903] doi:10.1103/PhysRevLett.116.062001 [arXiv:1511.05409 [hep-ph]].

[3] D. Chicherin, J. Henn and V. Mitev, JHEP **05** (2018), 164 doi:10.1007/JHEP05(2018)164 [arXiv:1712.09610 [hep-th]].

[4] T. Gehrmann, J. M. Henn and N. A. Lo Presti, JHEP **10** (2018), 103 doi:10.1007/JHEP10(2018)103 [arXiv:1807.09812 [hep-ph]].

[5] D. Chicherin, T. Gehrmann, J. M. Henn, N. A. Lo Presti, V. Mitev and P. Wasser, JHEP **03** (2019), 042 doi:10.1007/JHEP03(2019)042 [arXiv:1809.06240 [hep-ph]].

[6] S. Abreu, B. Page and M. Zeng, JHEP **01** (2019), 006 doi:10.1007/JHEP01(2019)006 [arXiv:1807.11522 [hep-th]].

[7] D. Chicherin, T. Gehrmann, J. M. Henn, P. Wasser, Y. Zhang and S. Zoia, Phys. Rev. Lett. **123** (2019) no.4, 041603 doi:10.1103/PhysRevLett.123.041603 [arXiv:1812.11160 [hep-ph]].

[8] D. Chicherin and V. Sotnikov, JHEP **12** (2020), 167 doi:10.1007/JHEP12(2020)167 [arXiv:2009.07803 [hep-ph]].

[9] S. Abreu, H. Ita, F. Moriello, B. Page, W. Tschernow and M. Zeng, JHEP **11** (2020), 117 doi:10.1007/JHEP11(2020)117 [arXiv:2005.04195 [hep-ph]].

[10] D. D. Canko, C. G. Papadopoulos and N. Syrrakos, JHEP **01** (2021), 199 doi:10.1007/JHEP01(2021)199 [arXiv:2009.13917 [hep-ph]].

[11] F. Moriello, JHEP **01** (2020), 150 doi:10.1007/JHEP01(2020)150 [arXiv:1907.13234 [hep-ph]].

[12] M. Hidding, [arXiv:2006.05510 [hep-ph]].

[13] C. G. Papadopoulos, JHEP **07** (2014), 088 doi:10.1007/JHEP07(2014)088 [arXiv:1401.6057 [hep-ph]].

[14] N. Syrrakos, JHEP **06** (2021), 037 doi:10.1007/JHEP06(2021)037 [arXiv:2012.10635 [hep-ph]].

[15] S. Badger, H. B. Hartanto and S. Zoia, Phys. Rev. Lett. **127** (2021) no.1, 012001 doi:10.1103/PhysRevLett.127.012001 [arXiv:2102.02516 [hep-ph]].

[16] C. G. Papadopoulos and C. Wever, JHEP **02** (2020), 112 doi:10.1007/JHEP02(2020)112 [arXiv:1910.06275 [hep-ph]].

[17] S. Abreu, H. Ita, B. Page and W. Tschernow, [arXiv:2107.14180 [hep-ph]].

[18] N. Syrrakos, [arXiv:2107.02106 [hep-ph]].

[19] K. G. Chetyrkin and F. V. Tkachov, Nucl. Phys. B **192** (1981), 159-204 doi:10.1016/0550-3213(81)90199-1.

[20] J. M. Henn, J. Phys. A **48** (2015), 153001 doi:10.1088/1751-8113/48/15/153001 [arXiv:1412.2296 [hep-ph]].

[21] A. V. Kotikov, Phys. Lett. B **254** (1991), 158-164.

[22] A. V. Kotikov, Phys. Lett. B **259** (1991), 314-322.

[23] A. V. Kotikov, Phys. Lett. B **267** (1991), 123-127 [Erratum: Phys. Lett. B **295** (1992), 409].

[24] T. Gehrmann and E. Remiddi, Nucl. Phys. B **580** (2000), 485-518 [arXiv:hep-ph/9912329 [hep-ph]].

[25] J. M. Henn, Phys. Rev. Lett. **110** (2013), 251601 doi:10.1103/PhysRevLett.110.251601 [arXiv:1304.1806 [hep-th]].

[26] A. V. Kotikov, [arXiv:2102.07424 [hep-ph]].

[27] A. B. Goncharov, Math. Res. Lett. **5** (1998), 497-516 doi:10.4310/MRL.1998.v5.n4.a7 [arXiv:1105.2076 [math.AG]].

[28] C. Duhr, H. Gangl and J. R. Rhodes, JHEP **10** (2012), 075 doi:10.1007/JHEP10(2012)075 [arXiv:1110.0458 [math-ph]].

[29] C. Duhr, JHEP **08** (2012), 043 doi:10.1007/JHEP08(2012)043 [arXiv:1203.0454 [hep-ph]].

[30] C. Duhr, doi:10.1142/9789814678766_0010 [arXiv:1411.7538 [hep-ph]].

[31] E. Remiddi and L. Tancredi, Nucl. Phys. B **925** (2017), 212-251 doi:10.1016/j.nuclphysb.2017.10.007 [arXiv:1709.03622 [hep-ph]].

[32] J. Broedel, C. Duhr, F. Dulat and L. Tancredi, JHEP **05** (2018), 093 doi:10.1007/JHEP05(2018)093 [arXiv:1712.07089 [hep-th]].

[33] J. Broedel, C. Duhr, F. Dulat and L. Tancredi, Phys. Rev. D **97** (2018) no.11, 116009 doi:10.1103/PhysRevD.97.116009 [arXiv:1712.07095 [hep-ph]].

[34] J. Broedel, C. Duhr, F. Dulat, B. Penante and L. Tancredi, JHEP **08** (2018), 014 doi:10.1007/JHEP08(2018)014 [arXiv:1803.10256 [hep-th]].

[35] J. Broedel, C. Duhr, F. Dulat, B. Penante and L. Tancredi, JHEP **01** (2019), 023 doi:10.1007/JHEP01(2019)023 [arXiv:1809.10698 [hep-th]].

[36] J. Broedel, C. Duhr, F. Dulat, B. Penante and L. Tancredi, JHEP **05** (2019), 120 doi:10.1007/JHEP05(2019)120 [arXiv:1902.09971 [hep-ph]].

[37] C. Duhr and L. Tancredi, JHEP **02** (2020), 105 doi:10.1007/JHEP02(2020)105 [arXiv:1912.00077 [hep-th]].

[38] B. Jantzen, A. V. Smirnov and V. A. Smirnov, Eur. Phys. J. C **72** (2012), 2139 doi:10.1140/epjc/s10052-012-2139-2 [arXiv:1206.0546 [hep-ph]].

[39] A. V. Smirnov, Comput. Phys. Commun. **204** (2016), 189-199 doi:10.1016/j.cpc.2016.03.013 [arXiv:1511.03614 [hep-ph]].

[40] J. Vollinga and S. Weinzierl, *Numerical evaluation of multiple polylogarithms*, *Comput.Phys.Commun.* **167** (2005) 177, [hep-ph/0410259].

Scattering Amplitudes for Binary Systems beyond GR

AMPLITUDES 2021
AUGUST 16th–20th
NIELS BOHR INSTITUTE COPENHAGEN

Mariana Carrillo Gonzalez, Claudia de Rham, Andrew J. Tolley
Imperial College London

Imperial College London

Why Go beyond GR?

- The **gravitational waves** observed by the LIGO and Virgo collaborations[1,2] provide a unique opportunity **to test General Relativity** (GR).
- Models beyond GR generically involve **new graviton polarizations** that in some cases can give rise to the **accelerated expansion** observed today[3].
- Extra degrees of freedom lead to **fifth forces** that can be highly constrained from solar system tests[4,5]. **Screening mechanism** help avoid these bounds[3].

Decoupling Limit and the Helicity-0 Mode

Amplitude techniques have recently been used to compute the **Post-Minkowskian Hamiltonians** in GR that describe the **inspiral phase** and are used to build **waveforms.**
As a first step towards using these techniques beyond GR, we consider a theory involving an **extra d.o.f. given by a helicity-0 mode**. We focus on the **decoupling limit** where the **helicity-0 and helicity-2 modes do not interact**[6,7] and consider a **conformal coupling** to the matter sector. As an example, we consider the cubic Galileon:

$$S=\int \mathrm{d}^4x\left(-\frac{1}{2}(\partial\pi)^2-\frac{1}{\Lambda^3}\Box\pi(\partial\pi)^2-\frac{1}{2}A^2(\pi)(\partial\phi_i)^2-\frac{1}{2}A^4(\pi)m^2\phi_i^2\right)$$

$$A(\pi)=1+\sum_n D_n g^n\pi^n/M_{\rm Pl}^n\,.$$

The theory is screened inside the radius:

$$r_{V_i}=\frac{1}{\Lambda}\left(\frac{|D_1|g\,m_i}{M_{\rm Pl}}\right)^{1/3}$$

From Amplitudes to Potentials

We consider **gravitational scattering of massive matter** (scalar ϕ_a). Then, we extract the **classical limit** of the scattering amplitudes by taking $\hbar\to 0$ and considering small transferred momenta (large impact parameter, b):

$$q\ll|p|,m_1,m_2 \quad \text{(p, external momenta)}$$

To obtain the potential we can use two equivalent methods:

- **Matching to scalars EFT** [8]: We match the full theory amplitudes to the EFT.
  $$\mathcal{M}^{\rm EFT}=\frac{\mathcal{M}}{4E_1E_2}$$
  Then, we identify the Wilson coefficients of the EFT with the potential.
- **Born Approximation**: The relation between the potential and the amplitudes is constructed from the Lippmann-Schwinger equation.

$$V(\mathbf{p},\mathbf{p}+\mathbf{q})\big|_{\mathcal{O}(g^n)}=-\frac{1}{4E_1(\mathbf{p})E_2(\mathbf{p})}\mathcal{M}_4(\mathbf{p},\mathbf{p}+\mathbf{q})\Big|_{\mathcal{O}(g^n)}-\frac{1}{4E_1(\mathbf{p})E_2(\mathbf{p})}\int_k\frac{\mathcal{M}_4(\mathbf{p},\mathbf{k})\mathcal{M}_4(\mathbf{k},\mathbf{p}+\mathbf{q})}{4E_1(\mathbf{k})E_2(\mathbf{k})(E_p-E_k+i\epsilon)}\Bigg|_{\mathcal{O}(g^n)}+\cdots$$

Full theory describing gravitational scattering:

Massive objects (scalars) coupled to a gravitational helicity-0 mode (Galileon).

EFT for compact objects

Is constructed in the CM frame, describes self-interaction of compact objects which are described by scalar fields.

Probe particle limit:

Is the limit where one object is much heavier than the other. Can be described by a point-particle living in a scalar field background.

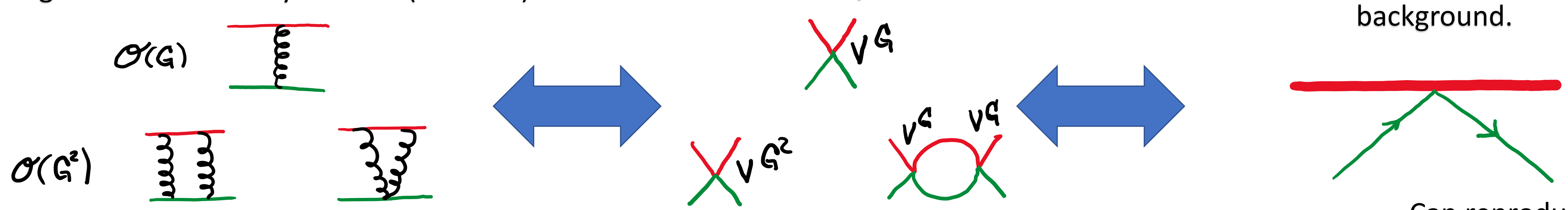

Can reproduce known field profile $\pi(r)$.

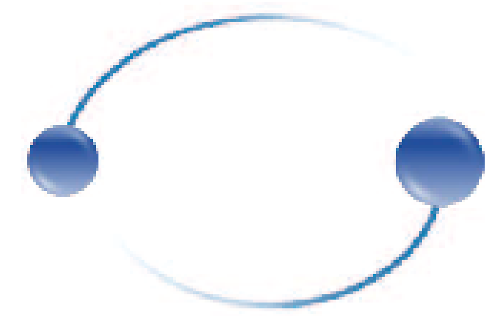

$$V^{\mathcal{O}(G)}(\mathbf{p},r)=-\frac{2D_1^2g^2Gm_a^2m_b^2}{E_aE_br}\left(1-\left(\frac{r_{V_a}^3+r_{V_b}^3}{4\pi r^3}\right)\right.$$
$$\left.+\frac{2}{7\pi^2r^6}\left(r_{V_a}^6+r_{V_b}^6+\frac{399m_am_b}{32E_aE_b}r_{V_a}^3r_{V_b}^3\left(1-\frac{25}{42}\frac{(3E_a^2+4E_aE_b+3E_b^2)}{E_a^2E_b^2}|\mathbf{p}|^2+\mathcal{O}(|\mathbf{p}|^4)\right)\right)\right),$$

Valid outside Vainshtein radius r_V.

Figure 1. Sketch of the matching procedure.

Delicate Matching for Conformal Coupling

Consider **correct scattering states** when matching EFTs:

$$\tilde{\phi}_i=A(\pi)\phi_i$$

$$\tilde{\phi}_i(x)\left|0\right\rangle=\int_p\frac{1}{\sqrt{2E(p)}}a_p^\dagger\left|0\right\rangle e^{-ix\cdot p}$$

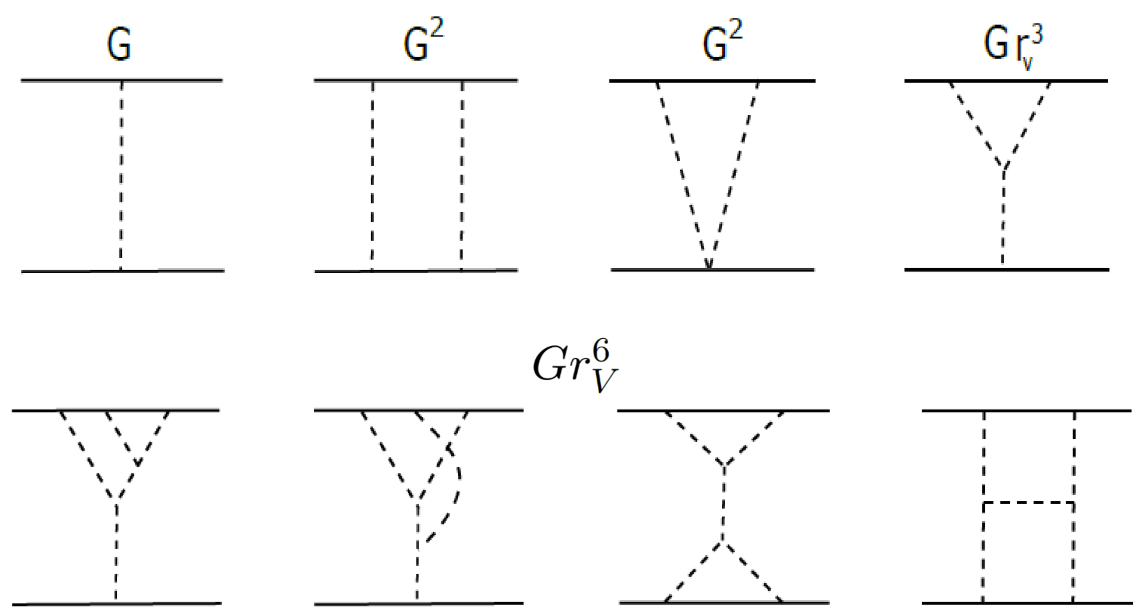

Figure 2. Feynman graph that can contain classical contributions.

Scattering Angle from Amplitudes

Surprisingly **simple relation**[9,10,11]:

$$\chi=\sum_{k=1}^{\infty}\widetilde{\chi}_k(b),\quad \widetilde{\chi}_k(b)\equiv\frac{2b}{k!}\int_0^\infty \mathrm{d}u\left(\frac{\mathrm{d}}{\mathrm{d}b^2}\right)^k\frac{1}{2^k(E_a+E_b)^k}\frac{\mathcal{M}^k_{\rm cl.}(|\mathbf{p}_\infty|,\sqrt{u^2+b^2})(u^2+b^2)^{(k-1)}}{|\mathbf{p}_\infty|^{2k}}\,.$$

In the probe-particle limit:

$$\chi=\frac{\epsilon_{\rm Gb}\epsilon_M}{\epsilon_{\rm pm}}\left(1-\frac{3}{16}\,\epsilon_{\rm Vb}^3+\frac{32}{35\pi^2}\,\epsilon_{\rm Vb}^6+\cdots\right)-\frac{\epsilon_{\rm Gb}^2\epsilon_M^2\epsilon_{\rm Vb}^3}{\pi\epsilon_{\rm pm}^2}$$

NLO can become relevant for supermassive black holes

$$\epsilon_{Gb}=g^2r_{\rm Sch}/b\qquad \epsilon_M\equiv m_b/m_a.$$
$$\epsilon_{Vb}=r_V/b\qquad \epsilon_{pm}\equiv(E-m_a-m_b)/\mu$$

Final Remarks

- **Amplitude methods can be applied beyond GR.**
- The perturbative expansions for V and χ **depend non-trivially on the momentum** of the scattered objects away from the probe-particle limit.
- Non-minimal couplings require a **careful matching** where the correct scattering states should be identified.
- Calculations outside the screened region are **relevant in backgrounds where** $r_V^{\rm redressed}\ll r_V$, e.g. 3 body problem with one heavier object and a binary system[12].

Based on:
arXiv: 2107.11384

Contact
Mariana Carrillo Gonzalez
m.carrillo-gonzalez@imperial.ac.uk.

Acknowledgements
The research of MCG is supported by STFC grants ST/P000762/1 and ST/T000791/1, and the European Union's Horizon 2020 Research Council grant 724659 MassiveCosmo ERC-2016-COG.

References

1. B.P. Abbott et al. (LIGO Scientific, Virgo), Observation of Gravitational Waves from a Binary Black Hole Merger, Phys. Rev. Lett. 116, 061102 (2016), arXiv:1602.03837 [gr-qc].
2. B.P. Abbott et al. (LIGO Scientific, Virgo), GW170817: Observation of Gravitational Waves from a Binary Neutron Star Inspiral, Phys. Rev. Lett. 119, 161101 (2017), arXiv:1710.05832 [gr-qc].
3. A. Joyce, B. Jain, J. Khory, M. Trodden, Beyond the Cosmological Standard Model, Phys. Rept. 568 (2015)), arXiv:1407.0059 [astro-ph.CO].
4. Clifford M. Will, The Confrontation between General Relativity and Experiment, Living Rev. Rel. 17, 4 (2014), arXiv:1403.7377 [gr-qc].
5. B. Bertotti, L. Iess, and P. Tortora, A test of general relativity using radio links with theCassini spacecraft, Nature 425, 374{376 (2003).
6. K.Hinterbichler, Theoretical Aspects of Massive Gravity, Rev. Mod. Phys. 84 (2012), arXiv:1105.3735 [hep-th]
7. C. de Rham, Massive Gravity, Living Rel. Rev. 17 (2014), arXiv:1401.4173 [hep-th]
8. Clifford Cheung, Ira Z. Rothstein, and Mikhail P. Solon, From Scattering Amplitudes to Classical Potentials in the Post-Minkowskian Expansion, Phys. Rev. Lett. 121, 251101 (2018), arXiv:1808.02489 [hep-th].
9. N. E. J. Bjerrum-Bohr, Andrea Cristofoli, and Poul H. Damgaard, Post-Minkowskian Scattering Angle in Einstein Gravity, JHEP 08, 038 (2020), arXiv:1910.09366 [hep-th].
10. Gregor Kalin and Rafael A. Porto, From Boundary Data to Bound States, JHEP 01, 072 (2020), arXiv:1910.03008 [hep-th].
11. Thibault Damour, High-energy gravitational scattering and the general relativistic two-body problem, Phys. Rev. D 97, 044038 (2018), arXiv:1710.10599 [gr-qc].
12. Philippe Brax, Lavinia Heisenberg, and Adrien Kuntz, Unveiling the Galileon in a three-body system : scalar and gravitational wave production, JCAP 05, 012 (2020), arXiv:2002.12590 [gr-qc].

Munich Institute for Theoretical Physics
Nick Early (earlnick@gmail.com)

Scattering Amplitudes, Worldsheet Associahedra and Root Systems

Parameterization $\mathbb{CP}^{n-3} \hookrightarrow \mathbb{G}(2,n)/(\mathbb{C}^*)^n$

Consider the map $\mathbb{C}^{n-2} \hookrightarrow \mathrm{Mat}(2,n)$,

$$x \mapsto g = \begin{pmatrix} 1 & 0 & x_1 & x_1+x_2 & x_1+x_2+x_3 & \cdots \\ 0 & 1 & 1 & 1 & 1 & \end{pmatrix}.$$

- Fact: this induces a generic embedding $\mathbb{CP}^{n-3} \hookrightarrow G(2,n)/(\mathbb{C}^*)^n$.
- Now we can define *dihedral cross ratios* u_{ij} in terms of 2×2 minors:

$$u_{i,j} = \frac{p_{i,j+1}p_{i+1,j}}{p_{i,j}p_{i+1,j+1}}!$$

See e.g. [Bardakci-Ruegg, Koba-Nielsen, Brown, Arkani-Bai-He-Yan].

- We generalize both constructions for an embedding of $(\mathbb{CP}^{n-k-1})^{\times(k-1)}$ into $G(k,n)/(\mathbb{C}^*)^n$ and define a new worldsheet associahedron $\mathcal{W}^{(+)}_{3,n}$ ($k \geq 4$ as well, but more detailed).

Worldsheet Associahedron: planar/positive part of $\mathcal{M}_{0,n}$

Now let $\{u_{i,j} : i<j,\ i+1 \neq j \text{ cyclically}\}$ be real variables on $\mathbb{R}^{\binom{n}{2}-n}$.

- **Definition.** The worldsheet associahedron $\mathcal{W}^+_{2,n}$ is

$$\mathcal{W}^+_{2,n} = \left\{ (u_{i,j}) \in [0,1]^{\binom{n}{2}-n} : u_{i,j} + \prod_{(k,\ell)} u_{k\ell} = 1 : (i+1<j) \right\}$$

where each product is over all pairs (k,ℓ) that cross (i,j), such that either $i<k<j<\ell$ or $k<i<\ell<j$.

- **Corollary.** If $u_{ij}=0$ then $u_{k\ell}=1$ for all k,ℓ that cross (i,j). **Example.** $\mathcal{W}_{2,6}$

$$u_{13}+u_{24}u_{25}u_{26}=1, \quad u_{14}+u_{25}u_{26}u_{35}u_{36}=1$$

- Well-known: can parameterize the $u_{i,j}$ with the dihedrally invariant cross-ratios on $\mathbb{CP}^1$!

Planar Basis of linear functions on the kinematic space

Define linear functions $L_1,\ldots,L_n$ on an auxiliary space $\mathbb{R}^n$ by

$$L_j(y) = y_{j+1} + 2y_{j+2} + \cdots + (n-1)y_{j-1}.$$

Definition. For any $J=\{j_1,\ldots,j_k\}$ denote by $\eta_{j_1\cdots j_k}$ the linear function on the kinematic space $\mathcal{K}(k,n)$,

$$\eta_J = -\frac{1}{n}\sum_{I\in\binom{[n]}{k}} \rho\left(\sum_{i\in I} e_i - \sum_{j\in J} e_j\right) s_I.$$

Proposition[E2019]. The functions $\binom{n}{k}-n$ linear functions η_J (for J not a cyclic interval $\{j,j+1,\ldots,j+k-1\}$) are linearly independent. In particular, they define a **planar basis** of linear functions on $\mathcal{K}(k,n)$. One has $\eta_{j,j+1,\ldots,j+k-1}=0$.
Example. $(k,n)=(2,4)$: here $\{\eta_{13},\eta_{24}\}$ is a basis. The other four η_{ij}'s are identically zero when the linear relations ("momentum conservation") on the s_{ij}'s are taken into account:

$$\eta_{24} = \frac{1}{4}\left(3s_{1,2}+2s_{1,3}+s_{1,4}+s_{2,3}+3s_{3,4}\right) = s_{12},$$

$$\eta_{12} = \frac{1}{4}\left(3s_{1,3}+2s_{1,4}+2s_{2,3}+s_{2,4}+4s_{3,4}\right) = 0$$

Biadjoint scalar partial amplitudes

Fix a planar orders α_1,α_2. Now sum over all planar cubic scalar Feynman diagrams for ϕ^3 compatible with both α_1,α_2; this is the *biadjoint partial amplitude* $m(\alpha_1,\alpha_2)$, studied by Cachazo-He-Yuan. Now put $\alpha_1=\alpha_2=(12\cdots n)$.
Fact. The biadjoint scalar partial amplitude $m^{(2)}_n := m^{(2)}_n(12\cdots n, 12\cdots n)$ can be written in terms of the *planar basis* as follows:

$$m^{(2)}_n = \sum_{\{(i_1j_1),\ldots,(i_{n-3}j_{n-3})\}} \prod_{t=1}^{n-3} \frac{1}{\eta_{i_1j_1}\cdots\eta_{i_{n-3}j_{n-3}}},$$

where the sum is over all pairwise *noncrossing* collections of $n-3$ pairs $\{(i_1,j_1),\ldots,(i_{n-3},j_{n-3})\}$.

- The Catalan-many $C_{n-2}=2,5,14,42,132,\ldots$ terms are in bijection with the set of tree-level Feynman diagrams for the cubic scalar theory, given a fixed planar order $(12\cdots n)$.
- Equivalently, in bijection with triangulations of a polygon with cyclically labeled vertices.

Associahedron in the Root Lattice via Root Kinematics

In this kinematics, linear relations among the poles reduce $m^{(2)}_6$ to the reduced form

$$\begin{aligned} m^{(2)}_6 = {} & \frac{1}{(\alpha_1+1)(\alpha_4+1)(\alpha_{34}+1)} + \frac{1}{(\alpha_2+1)(\alpha_4+1)(\alpha_{34}+1)} + \frac{1}{(\alpha_1+1)(\alpha_2+1)(\alpha_4+1)} \\ & + \frac{1}{(\alpha_1+1)(\alpha_{34}+1)(\alpha_{123}+1)} + \frac{1}{(\alpha_2+1)(\alpha_{34}+1)(\alpha_{123}+1)} + \frac{1}{(\alpha_1+1)(\alpha_2+1)(\alpha_{123}+1)}. \end{aligned}$$

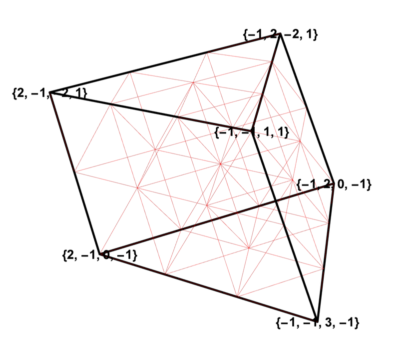

Here $\alpha_1,\ldots,\alpha_{n-2}$ are *roots*.

Dual picture: $m^{(k)}_n$ from subdivisions of Root Polytopes

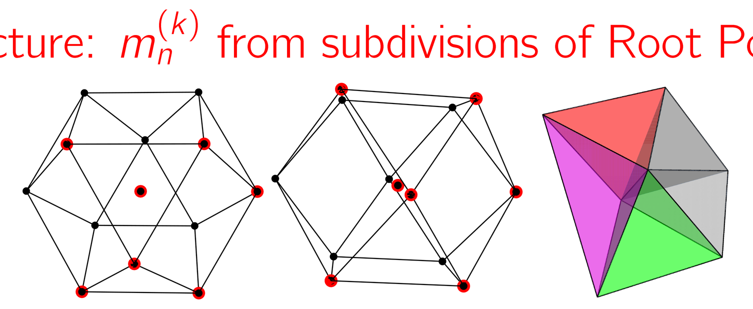

$$\hat{\mathcal{R}}^{(2)}_3 = \text{convex hull}\{0,\gamma_{13},\gamma_{14},\gamma_{24},\gamma_{25},\gamma_{35},\gamma_{15}\}$$

$$\mathcal{R}^{(2)}_3 = \text{convex hull}\{\overline{\gamma}_{13},\overline{\gamma}_{14},\overline{\gamma}_{24},\overline{\gamma}_{25},\overline{\gamma}_{35}\}.$$

- Root Kinematics: Planar Feynman Diagrams $\Leftrightarrow$ simplices in a triangulation of the **root polytope**.

Noncrossing property: $k \geq 3$ (but here, $k=3$)

Definition. Subsets $\{i_1,i_2\},\{j_1,j_2\}\subset\{1,\ldots,n\}$ with $i_1<i_2$ and $j_1<j_2$, say, are said to be *crossing* if

$$i_1<j_1<i_2<j_2 \text{ or } j_1<i_1<j_2<i_2.$$

Two triples $I=\{i_1,i_2,i_3\}$ and $J=\{j_1,j_2,j_3\}$ are *noncrossing* provided that none of the following situations holds:

$$(i_1,i_2),(j_1,j_2) \text{ is crossing, or}$$
$$(i_2,i_3),(j_2,j_3) \text{ is crossing, or}$$
$$(i_1,i_3),(j_1,j_3) \text{ is crossing and } i_2=j_2.$$

Denote by $\mathbf{NC}_{3,n}$ the (po)set of all collections of pairwise noncrossing triples $\{i,j,k\}$, where i,j,k is not a cyclic interval, ordered by inclusion.
Note: "Purity" (c.f. [Petersen, Pylyavskyy, Speyer]) All maximal (by inclusion) collections have exactly $(3-1)(n-3-1)$ triples.

Binary noncrossing relations for $k=3$

For any $J\in\binom{[n]}{3}^{nf}$, we have the binary equation

$$u_J = 1 - \prod_{\{I:\ (I,J)\notin\mathbf{NC}_{3,n}\}} \hat{u}_I^{c_{I,J}}, \tag{1}$$

where for any crossing pair $(I,J)=(i_1i_2i_3, j_1j_2j_3)\notin\mathbf{NC}_{3,n}$, exponents are

$$c_{(i_1i_2i_3),(j_1j_2j_3)} = \begin{cases} 2 & \text{if } i_1<j_1<i_2<j_2<i_3<j_3 \text{ or } j_1<i_1<j_2<i_2<j_3<i_3 \\ 1 & \text{otherwise.}\end{cases} \tag{2}$$

Definition. [E2021] The type (3,n) *generalized worldsheet associahedron* $\mathcal{W}^+_{3,n}$ is the solution in the u-space to Equations (1).

Parameterizing $\mathcal{W}^+_{3,n}$: (Planar) Face polynomials: case $k=3$

Define $\tau_{1,2,j}=1$ for all $j=3,\ldots,n$. For $\{1,j,k\}$ such that $3\leq j<k\leq n$, then let

$$\tau_{1,j,k} := \sum_{a\in[j-1,k-2]} x_{2,a}.$$

Whenever $\{i,j,k\}$ satisfies $2\leq i\leq j<k\leq n$, then put

$$\tau_{i,j,k} := \sum_{\{(a,b)\in[i-1,j-1]\times[j-2,k-3],\ a\leq b\}} x_{1,a}x_{2,b}$$

Example. We have

$$\tau_{136} = x_{2,1}+x_{2,2}+x_{2,3}, \quad \tau_{356} = \left(x_{1,2}+x_{1,3}\right)x_{2,3}$$

$$\tau_{468} = x_{1,3}x_{2,4}+x_{1,4}x_{2,4}+x_{1,3}x_{2,5}+x_{1,4}x_{2,5}+x_{1,5}x_{2,5}$$
$$\tau_{338} = x_{1,2}\left(x_{2,2}+x_{2,3}+x_{2,4}+x_{2,5}\right)$$

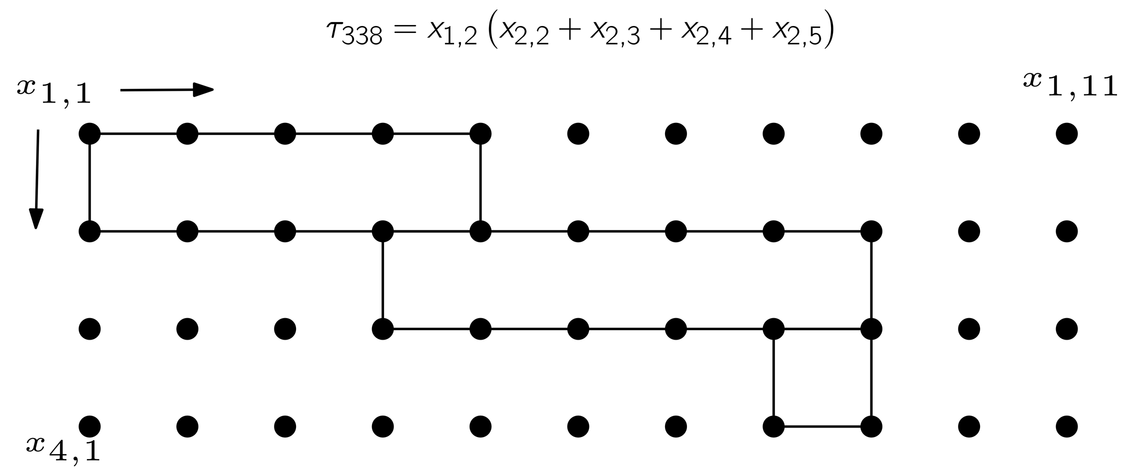

$$\tau_{2,6,11,12,14} = x_{1,1}x_{2,4}x_{3,8}x_{4,8} + x_{1,2}x_{2,4}x_{3,8}x_{4,8} + \cdots + x_{1,4}x_{2,9}x_{3,9}x_{4,9} + x_{1,5}x_{2,9}x_{3,9}x_{4,9}$$

A planar face variable.

Preview, The Staircase: successive levels from the top should be right-moving and should overlap by exactly one square.

Planar Face ratios: case $k=3$

For any $\{i,j,k\}\subset\{1,\ldots,n\}$ that is not one of the n cyclic intervals $\{j,j+1,j+2\}$, define a face ratio $u_{ijk}:\mathbb{CP}^{n-4}\times\mathbb{CP}^{n-4}\to\mathbb{CP}^1$, by

$$u_{ijk} = \begin{cases} \frac{\tau_{i,n-1,n}}{\tau_{i-1,n-1,n}}, & (i,j,k)=(i,n-1,n) \\ \frac{\tau_{i+1,j,k}\tau_{i,j+1,j+2}}{\tau_{i,j,k}\tau_{i+1,j+1,j+2}}, & j+1<k, \quad k=n, \\ \frac{\tau_{i+1,j,k}\tau_{i,j,k+1}}{\tau_{i,j,k}\tau_{i+1,j,k+1}}, & k<n. \end{cases}$$

Note. When $x_{i,j}$ are real and positive, then the planar face ratios u_{ijk} take values in the open interval $(0,1)$.

Note. We've defined analogous planar face ratios u_J in $(\mathbb{CP}^{n-k-1})^{\times(k-1)}$ for all k and have evidence that our definition is correct: we've checked (some) binary relations for (k,n) including $(3,15),(4,12),(5,10)$. Remains to determine exponents to get the full ideal of relations, defining the worldsheet associahedra $\mathcal{W}_{k,n}$!
Claim. With the u_{ijk} variables defined as above, they solve the noncrossing binary equations. (Combinatorial proof?)

14 noncrossing binary equations for $(3,6)$

$$\begin{aligned}
u_{124} &= 1-u_{135}u_{136}u_{235}u_{236}\\
u_{125} &= 1-u_{136}u_{146}u_{236}u_{246}u_{346}\\
u_{134} &= 1-u_{235}u_{236}u_{245}u_{246}u_{256}\\
u_{135} &= 1-u_{124}u_{146}u_{236}u_{245}u_{256}u_{346}u_{246}^2\\
u_{136} &= 1-u_{124}u_{125}u_{245}u_{246}u_{256}\\
u_{145} &= 1-u_{246}u_{256}u_{346}u_{356}\\
u_{146} &= 1-u_{125}u_{135}u_{235}u_{256}u_{356}\\
u_{235} &= 1-u_{124}u_{134}u_{146}u_{246}u_{346}\\
u_{236} &= 1-u_{124}u_{125}u_{134}u_{135}\\
u_{245} &= 1-u_{134}u_{135}u_{136}u_{346}u_{356}\\
u_{246} &= 1-u_{125}u_{134}u_{136}u_{145}u_{235}u_{356}u_{135}^2\\
u_{256} &= 1-u_{134}u_{135}u_{136}u_{145}u_{146}\\
u_{346} &= 1-u_{125}u_{135}u_{145}u_{235}u_{245}\\
u_{356} &= 1-u_{145}u_{146}u_{245}u_{246}.
\end{aligned}$$

Generalized positive roots

Definition. [CE2020; E2021] Put $\alpha_{i,[a,b]}=\sum_{j=a}^b\alpha_{i,j}$. Let $J=\{j_1,\ldots,j_k\}$, with order $1\leq j_1<\cdots<j_k\leq n$. The generalized positive root γ_J is the following sum of simple roots $\alpha_{i,j}$:

$$\gamma_J(\alpha) = \sum_{i=1}^{k-1}\alpha_{i,[j_i-(i-1),j_{i+1}-i-1]}.$$

Main Example. For simplicity we'll stick to $k=3$: $\gamma_{ijk}=\alpha_{1,[i,j-2]}+\alpha_{2,[j-1,k-3]}$.

$\gamma_{134}=\alpha_{1,1}$, $\gamma_{124}=\alpha_{2,1}$, $\gamma_{356}=\alpha_{1,3}$, $\gamma_{135}=\alpha_{1,1}+\alpha_{2,2}$, $\gamma_{269}=\alpha_{1,[2,4]}+\alpha_{2,[5,7]}=(\alpha_{1,2}+\alpha_{1,3}+\alpha_{1,4})+(\alpha_{2,5}+\alpha_{2,6})$.

Generalized positive roots: on the grid

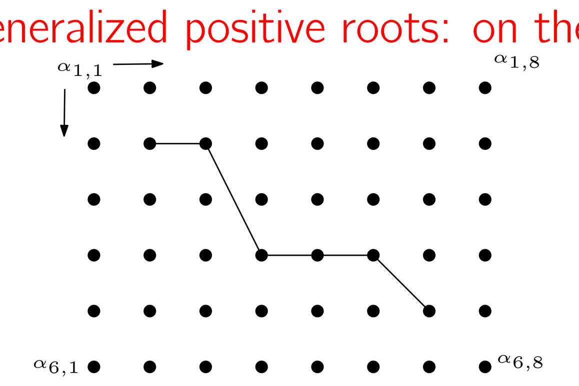

$$\begin{aligned}\gamma_{2,3,6,7,11,13,14} &= \alpha_{2,[2,3]}+\alpha_{4,[4,6]}+\alpha_{5,7}\\ &= \alpha_{2,2}+\alpha_{2,3}+\alpha_{4,4}+\alpha_{4,5}+\alpha_{4,6}+\alpha_{5,7}\end{aligned}$$

Each dot is a simple root. Each row is a simple root system of type A_{n-k}.

Generalized Root Polytopes

Let $\overline{\gamma}_J$ be the restriction of γ_J to $\mathcal{H}_{k,n}$, where $\sum_{j=1}^{n-k}\alpha_{i,j}=0$ for all $i=1,\ldots k-1$.
Define a ((k-1)(n-k)-dimensional) polytope $\hat{\mathcal{R}}^{(k)}_{n-k}$ *in the space of linear functions on* $\mathbb{R}^{(k-1)\times(n-k)}$:

$$\hat{\mathcal{R}}^{(k)}_{n-k} = \text{convex hull}\left(\{0\}\cup\left\{\gamma_J : J\in\binom{[n]}{k}\right\}\right)$$

and a dimension $(k-1)(n-k-1)$ polytope

$$\mathcal{R}^{(k)}_{n-k} = \text{convex hull}\left\{\overline{\gamma}_J : J\in\binom{[n]}{k}^{nf}\right\}.$$

Fact. $\mathcal{R}^{(k)}_{n-k}$ has $\binom{n}{k}-n$ vertices. $\overline{\gamma}_J=0$ exactly when J is a *cyclic* interval $\{i,i+1,\ldots,i+k-1\}$.

Planar Kinematics potential Function and PK polytope

Let $p_{j_1,\ldots,j_k}$ be Plucker variable on $G(k,n)$ with column set $\{j_1,\ldots,j_k\}$
Definition [CE2020] The *Planar Kinematics* potential function $\mathcal{S}^{(PK)}_{k,n}$ on the Grassmannian $G(k,n)$ is given by

$$\mathcal{S}^{(PK)}_{k,n} = \sum_{j=1}^n \log\left(\frac{p_{j,j+1,\ldots,j+k-2,j+k-1}}{p_{j,j+1,\ldots,j+k-2,j+k}}\right)$$

Let's evaluate this on the standard planar (BCFW) parameterization (of $G(k,n)/(\mathbb{C}^*)^n$). For instance for $k=4$ this is:

$$\begin{bmatrix} 1 & 0 & 0 & 0 & x_{1,1}x_{2,1}x_{3,1} & x_{1,1}\left(x_{2,1}\left(x_{3,1}+x_{3,2}\right)+x_{2,2}x_{3,2}\right)+x_{1,2}x_{2,2}x_{3,2} & \\ 0 & 1 & 0 & 0 & x_{2,1}x_{3,1} & x_{2,1}\left(x_{3,1}+x_{3,2}\right)+x_{2,2}x_{3,2} & \\ 0 & 0 & 1 & 0 & x_{3,1} & x_{3,1}+x_{3,2} & \cdots \\ 0 & 0 & 0 & 1 & 1 & 1 & \end{bmatrix}$$

Evaluating $\mathcal{S}^{(PK)}_{k,n}$ on the positive parameterization gives

$$\mathcal{S}^{(PK)}_{k,n} = \log\left(\frac{\prod_{(i,j)\in[1,k-1]\times[1,n-k]}x_{i,j}}{P_1\cdots P_{k-1}Q_1\cdots Q_{n-k-1}}\right)$$

where

$$P_i = \sum_{j=1}^{n-k}x_{i,j}, \quad Q_j = \sum_{\{(t_i)\in\{0,1\}^{k-1}:\ t_1\leq\cdots\leq t_{k-1}\}} x_{1,j+t_1}x_{2,j+t_2}\cdots x_{k-1,j+t_{k-1}}.$$

Example (3,6).

$$P_1 = x_{1,1}+x_{1,2}+x_{1,3}, \quad P_2 = x_{2,1}+x_{2,2}+x_{2,3}$$

$$Q_1 = x_{1,1}x_{2,1}+x_{1,1}x_{2,2}+x_{1,2}x_{2,2}, \quad Q_2 = x_{1,2}x_{2,2}+x_{1,2}x_{2,3}+x_{1,3}x_{2,3}$$

is a Minkowski sum of four *triangles*.
General fact: $\Pi^{(k)}_{n-k}$ is a Minkowski sum of $n-2$ *simplices*. There are $k-1$ simplices of dimension $n-k-1$ and $n-k-1$ simplices of dimension $k-1$. It is *not* a simple[1] polytope in general!

PK polytope and Noncrossing Generalized Amplitude (specialized to $k=3$)

Theorem[E2021] We have the following miracle:

$$\mathrm{Newt}\left(\exp\left(-\mathcal{S}^{(PK)}_{k,n}\right)\right) = \left\{(\alpha_{i,j})\in\mathbb{R}^{(k-1)\times(n-k)} : \sum_{j=1}^{n-k}\alpha_{i,j}=0,\ \gamma_J(\alpha)+1\geq 0\right\}.$$

Why useful for amplitudes???
$\hookrightarrow$ compatibility rules for poles can be extracted from the facet inequalities; possible to reconstruct amplitude from the volume of the dual polytope.
Defn. The **noncrossing amplitude** $m^{(3,NC)}_n$ is

$$m^{(3,NC)}_n = \sum_{\{J_1,\ldots,J_{(k-1)(n-k-1)}\}\text{is noncrossing}} \frac{1}{\prod_{j=1}^{(k-1)(n-k-1)}\eta_{J_j}}$$

Open Problems. Given that there is a noncrossing analog of the CHY scattering equations...

1. Is there a nice formula for the critical point enumeration?
2. Prove that this combinatorial formula matches the scattering equations formulation of the noncrossing amplitude?
3. Note well: the noncrossing generalized amplitude lacks cyclic symmetry... not clear what this could mean physically!
4. Explore relations to CEGM generalized biadjoint amplitudes?

Stay tuned...

[**CEGM2019**] Scattering Equations: From Projective Spaces to Tropical Grassmannians (1903.08904).
[**CE2020**] Planar Kinematics: Cyclic Fixed Points, Mirror Superpotential, k-Dimensional Catalan Numbers, and Root Polytopes (2010.09708)
[**E2021**] Planarity in Generalized Scattering Amplitudes: PK Polytope, Generalized Root Systems and Worldsheet Associahedra (2106.07142)

Compton Scattering of Kerr Black Holes

Marco Chiodaroli, Henrik Johansson, **Paolo Pichini**
Based on **arXiv:2107.14779** paolo.pichini@physics.uu.se
NORDITA
UPPSALA UNIVERSITET

Kerr Observables

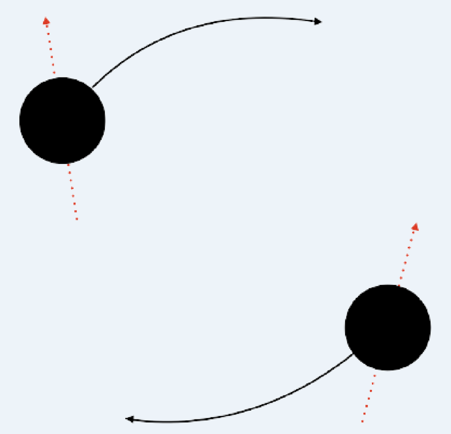

Kerr Energy-Momentum Tensor: [Vines, ...]

$$\varepsilon_{\mu\nu}(k)T^{\mu\nu}_{Kerr}(-k) \sim (\varepsilon \cdot p)^2 \exp\left(\frac{k \cdot S}{m}\right)$$

Two-Body Scattering:

$$\Delta p\,,\ \Delta S \sim$$ 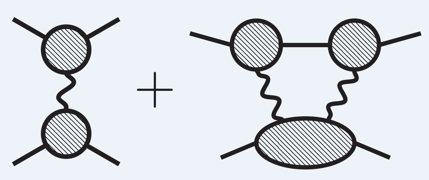 $$+\ \mathcal{O}(G^3)$$

Covariant Amplitudes

Gauge theory bosons:

$$\sum_{s=0}^{\infty} A_3(1\phi^s, 2\phi^s, 3A) =$$

$$A_{\phi\phi A} + \frac{A_{WWA} - (\varepsilon_1 \cdot \varepsilon_2)^2 A_{\phi\phi A}}{(1+\varepsilon_1\cdot\varepsilon_2)^2 + \frac{2}{m^2}\varepsilon_1\cdot p_2 \varepsilon_2 \cdot p_1}$$

Fermions and gravity: similar expressions.

Spin-1 Example

Gauge Theory Lagrangian:

$$2D_{[\mu}\overline{W}_{\nu]}D^{\mu}W^{\nu} - m^2\overline{W}^{\mu}W_{\mu} + ieF_{\mu\nu}\overline{W}^{\mu}W^{\nu}$$

Propagator:

$$\Delta_{(1)} = \frac{1}{p^2 - m^2}\left(\eta_{\mu\nu} - \frac{p_\mu p_\nu}{m^2}\right)$$

Tree-level unitarity: $p \cdot J = \mathcal{O}(m)$ fixes the non-minimal term and cures the mass pole in $\Delta_{(1)}$.

Spin-5/2 Compton

Diagrams:

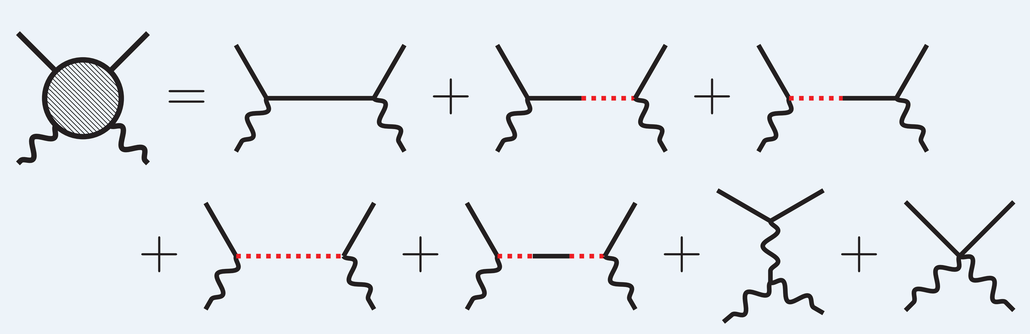

Ingredients:

1. Field content: physical $\psi_{\mu\nu}$, auxiliary λ, graviton h.
2. Free equations of motion: $(i\partial\!\!\!/ - m)\psi_{\mu\nu} = \gamma^{\mu}\psi_{\mu\nu} = \partial^{\mu}\psi_{\mu\nu} = \lambda = 0$.
3. $\mathcal{L}(\psi,\lambda) \supset m(\bar{\psi}^{\mu}_{\mu}\lambda + \bar{\lambda}\psi^{\mu}_{\mu})$ non-diagonal kinetic term.
4. Need propagators of both fields.
5. $\mathcal{L} \supset \bar{\lambda}(i\partial\!\!\!/ + 3m)\lambda$. Spurious poles from the λ propagator cancel out in the amplitude.

Summary

High-energy properties of higher spin theory are used to derive three-point and Compton amplitudes relevant to spinning black hole scattering, up to spin-5/2.

1. Massive Spinor-Helicity [Arkani-Hamed, Huang, ...; Guevara, Ochirov, Vines; ..., O'Connell]

The **classical limit** of scattering amplitudes is used to compute Kerr observables.

1. Leading order: match Kerr energy-momentum tensor from three-point amplitudes:

$$\mathcal{M}_3(1\phi^s, 2\phi^s, 3h^-) = \frac{m^{2-2s}}{x^2}[\mathbf{12}]^{2s} \xrightarrow{\hbar\to 0} (\varepsilon\cdot p)^2 \exp\left(\frac{k\cdot S}{m}\right)$$

2. Next-to-leading order: Compton amplitudes from BCFW recursion:

$$\mathcal{M}_4(1\phi^s, 2\phi^s, 3h^-, 4h^+) = \frac{[4|p_1|3\rangle^{4-2s}([4\mathbf{1}]\langle 3\mathbf{2}\rangle + [4\mathbf{2}]\langle 3\mathbf{1}\rangle)^{2s}}{s_{12}t_{13}t_{14}}$$

$$\mathcal{M}_4(1\phi^s, 2\phi^s, 3h^+, 4h^+) = \frac{\langle \mathbf{12}\rangle^{2s}[34]^4}{m^{2s-4}s_{12}t_{13}t_{14}}$$

Remark: Spurious pole appearing for $s \geq 5/2$, leading to contact term ambiguity.

2. Higher-Spin Theory [Ferrara, Porrati, Telegdi; Cucchieri, Deser, ...]

Coupling to gauge/gravity:

Minimal coupling $\partial \to \nabla$ is **not** the right choice for elementary particles (see spin-1 example).

High-energy (tree-level) unitarity:

- Define the three-point current $J^{\vec{\mu}} \equiv J^{\mu_1\cdots\mu_s}$ appearing in amplitudes (propagator: $\Delta_{\vec{\nu}\vec{\mu}}$):

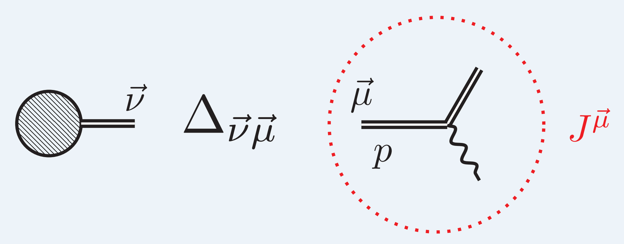

- **Current constraint**: interaction terms are constrained to restore tree-level unitarity.

$$p \cdot J|_{traceless} = \mathcal{O}(m)$$

Outcome:

Non-minimal terms linear in $R_{\mu\nu\rho\sigma}$ fixed, including a subset of four-point contact terms.
Non-minimal terms quadratic in $R_{\mu\nu\rho\sigma}$ excluded by **derivative counting** up to $s \leq 5/2$.

3. Higher-Spin Amplitudes

Unique results via current constraint and derivative counting.

Shorthand: $N_2 \equiv [4\mathbf{1}]\langle 3\mathbf{2}\rangle + [4\mathbf{2}]\langle 3\mathbf{1}\rangle$, $N_4 \equiv [4\mathbf{1}]\langle 3\mathbf{2}\rangle[4\mathbf{2}]\langle 3\mathbf{1}\rangle$, $t_{ij} \equiv s_{ij} - m^2$

Spin-3/2 gauge theory: a unique non-minimal interaction term is needed:

$$\mathcal{L}_{3/2} = \mathcal{L}_{3/2,min} + \frac{ie}{m}\bar{\psi}_\mu\left(F^{\mu\nu} - \frac{i}{2}\gamma^5\epsilon^{\mu\nu\rho\sigma}F_{\rho\sigma}\right)\psi_\nu$$

$$A_4(1\phi^{3/2}, 2\phi^{3/2}, 3A^-, 4A^+) = \frac{N_2}{[4|p_1|3\rangle}\left(\frac{N_2^2}{t_{13}t_{14}} - \frac{N_4}{m^4}\right)$$

Spin-5/2 gravity: a unique non-minimal term similar to the above is needed:

$$\mathcal{L}_{5/2} = \mathcal{L}_{5/2,min} - \frac{1}{m}\sqrt{-g}\,\bar{\psi}_{\mu\rho}\left(R^{\mu\nu\rho\sigma} - \frac{i}{2}\gamma^5\epsilon^{\rho\sigma\alpha\beta}R^{\mu\nu}{}_{\alpha\beta}\right)\psi_{\nu\sigma}$$

$$\mathcal{M}_4(1\phi^{5/2}, 2\phi^{5/2}, 3h^-, 4h^+) = \frac{N_2}{[4|p_1|3\rangle}\left(\frac{N_2^4}{s_{12}t_{13}t_{14}} - \frac{N_4^2}{m^6}\right)$$

Remark: The same-helicity Compton amplitudes match the known BCFW results.

Conclusion

Summary:

1. Current constraint: fixes three-point and $\mathcal{O}(R_{\mu\nu\rho\sigma})$ four-point terms up to spin-5/2.
2. Derivative counting: $\mathcal{O}(R^2_{\mu\nu\rho\sigma})$ terms excluded up to spin-5/2.
3. Kerr and higher-spin: high-energy properties of QFT seem related to black-holes.

Outlook:

1. Classical limit: Use the spin-5/2 amplitude to compute Kerr observables.
2. Higher spins: Extend the methods to $s \geq 3$.
3. Compare: other well-behaved theories (e.g. strings) should obey the current constraint.

Soft gauge symmetry implies the ***soft theorem***.

Martin Beneke, Patrick Hager, Robert Szafron

Isolating the Soft

- Split fields into soft and energetic modes.
- Modes are described using soft-collinear effective theory (SCET).
- Construct **SCET Gravity** to subleading orders.
- Soft field realised as special background field with **soft gauge symmetry**:
  $\rightarrow$ organises interactions,
  $\rightarrow$ constrains operators.
- New insight in Gravity: Translations and Rotations form the soft gauge symmetry.
- Momentum p^μ and angular momentum $J^{\mu\nu}$ correspond to color-generator t^a.

Observations

- Extremely similar structure of soft-collinear interactions in gauge theory and gravity.
- Leading soft emission completely determined by **universal** Lagrangian interactions.
- Process-dependence: soft building blocks $F_s^{\mu\nu}$, R_s are **absent** for the leading two (three) terms.

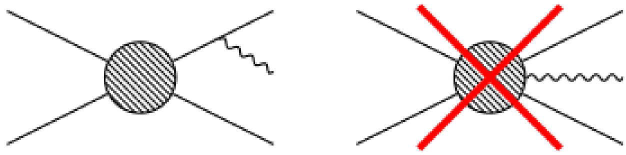

- Only these leading terms are **universal**.

Technical Details

- Energetic fields are expressed in terms of gauge-invariant **physical** variables.
- Soft fields are **multipole-expanded** around the large $x_- = n_+ x \frac{n_-}{2}$.
- Structure of Lagrangians for gauge and gravity (need up to $\mathcal{L}^{(4)}_{\text{grav}}$ for the computation):

$$\mathcal{L}^{(0)}_{\text{QCD}} = \frac{1}{2} n_+ D_c \Phi n_- D \Phi + \frac{1}{2} D_{c\perp}\Phi D_{c\perp}\Phi \qquad \mathcal{L}^{(0)}_{\text{grav}} = \frac{1}{2} n_+ \partial \Phi n_- D \Phi + \frac{1}{2}\partial_\perp \Phi \partial_\perp \Phi$$

$$\mathcal{L}^{(1)}_{\text{QCD}} = +\frac{1}{2} x_\perp^\mu n_-^\nu g F^s_{\mu\nu} n_+ J_c \qquad \mathcal{L}^{(2)}_{\text{grav}} \mathrel{\widehat{=}} -\frac{1}{4} x_\perp^\alpha x_\perp^\beta \kappa R_{\alpha-\beta-} T_{++}$$

$$n_- D = n_- \partial - i g t^a n_- A_s \qquad n_- D = n_- \partial - \frac{\kappa}{2}\left(s_{-\alpha}\partial^\alpha - [\partial_\alpha s_{\beta-}] J^{\alpha\beta}\right) + \dots$$

- Soft-covariant derivative in gravity related to Vierbein (translations) and Spin-Connection (rotations).
- The soft theorem is realised as an **operatorial statement** in SCET visible in the Lagrangian.
- The soft-covariant derivative generates the eikonal terms in the soft theorem.
- The subleading Lagrangian generates the subleading term.

$$\mathcal{A}^{\text{QCD}}_{\text{rad}} = \sum_i t^a \left(\frac{\varepsilon_\mu p_i^\mu}{p_i \cdot k} + \frac{k_\nu \varepsilon_\mu J_i^{\mu\nu}}{p_i \cdot k} \right) \mathcal{A}_0$$

$$\mathcal{A}^{\text{grav}}_{\text{rad}} = -\frac{\kappa}{2} \sum_i \left(p_i^\mu \frac{\varepsilon_{\mu\nu} p_i^\nu}{p_i \cdot k} + J_i^{\mu\nu} \frac{k_\nu \varepsilon_{\mu\rho} p_i^\rho}{p_i \cdot k} + J_i^{\mu\rho} \frac{1}{2} \frac{k_\rho k_\sigma \varepsilon_{\mu\nu} J_i^{\nu\sigma}}{p_i \cdot k} \right) \mathcal{A}_0$$

- Beyond this, non-universal process-dependent soft building blocks are available.

More details: $\rightarrow$
https://t1p.de/Amplitudes

Truncated Cluster Algebras & Feynman Integrals with Algebraic Letters

Qinglin Yang, with Song He and Zhenjie Li

1. Introduction

As observed in [1], alphabets of ladder integrals are related to finite-type cluster algebras. Moreover, surprisingly their alphabets are purely determined by the external kinematics. One natural question is whether we can find any relations between external kinematics of certain integrals and cluster algebras, such that having an algorithm to predict their alphabets.

2. General Algorithm

Our algorithm consists of four steps as

1. We relate external kinematics for certain integral to positroid cell Γ of $G_+(4,n)$ by imposing proper conditions on Plücker coordinates. Corresponding plabic graph gives a positive parametrization $\mathbf{Z}_\Gamma$ for momentum twistors (after modding out torus action). We only consider the case when Γ/T is still a boundary of $G_+(4,n)/T$
2. Applying mutations on the dual graph of its plabic graph with the internal facet variables f_i being the principal coefficients, we get a cluster algebra together with its F-polynomials, which either form a finite alphabet for finite-type algebra or need a truncation for infinite-type.
3. Evaluating all Plücker coordinates by matrix $\mathbf{Z}_\Gamma$ and taking the Minkowski sum [4] of Newton polytopes of these polynomials, we get the polytopal realization for this $G_+(4,n)/T$ boundary.
4. Select all the g-vectors coinciding with the normal vectors of the polytope. Rational alphabet is then the associated F-polynomials. Those normal vectors that are not g-vectors correspond to limit vectors, which after algorithm in [3] give algebraic letters.

3. Warm up: D_n cluster algebras

Consider the one-mass hexagon kinematics:

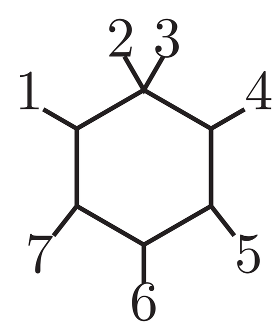

For the massive corner (23), we impose two conditions $\langle 7123\rangle=\langle 2345\rangle=0$ [5], leading to a $4(7-4)-6-2=4$ dimensional boundary of $G_+(4,n)/T$. Corresponding plabic graph and its dual graph read

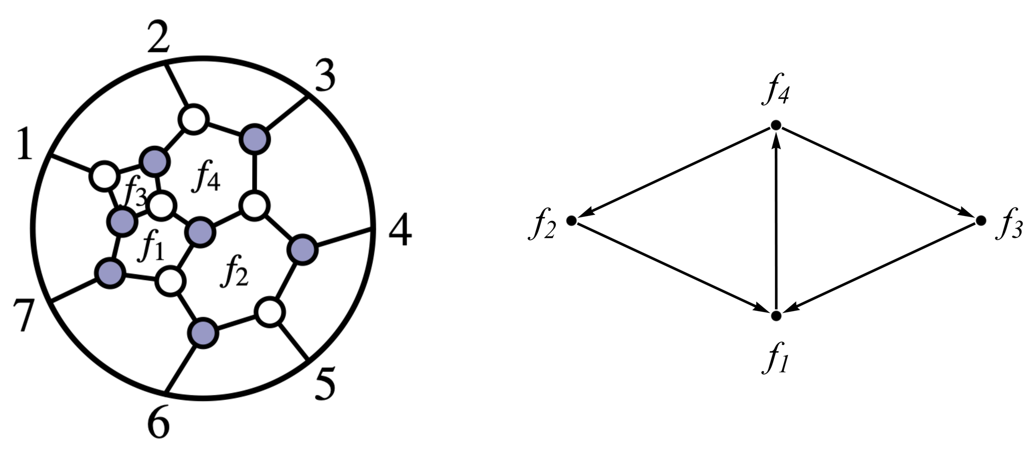

and the resulting $\mathbf{Z}_\Gamma$ matrix which positively parametrizes the kinematics is

$$\begin{pmatrix} f_3f_4 & (1+f_3)\,f_4 & 1+f_4+f_3f_4 & 1 & 0 & 0 & 0 \\ 0 & f_1f_2f_4 & f_2\,(1+f_1+f_1f_4) & 1+f_2+f_1f_2 & 1 & 0 & 0 \\ 0 & 0 & f_2 & 1+f_2 & 1 & 0 & -1 \\ 0 & 0 & 0 & 1 & 1 & 1 & 0 \end{pmatrix}.$$

Beginning with the quiver, we get a D_4 cluster algebra with 16 F-polynomials in variables f_i. As checked in [1], at least up to 4 loops, alphabet produced by these F-polynomials applies to the double-pentagon ladder integrals for $n=7$, even with various different numerators. Same for two- and three-mass-easy hexagon kinematics for $n=8$ and 9, and they correspond to D_5 and D_6 cluster algebras.

Geometrically, by taking the Minkowski sum of the Newton polytopes of the Plücker coordinates, we get "truncated D_n polytopes" , whose normal vectors are exactly those g-vectors of D_n but co-dimensional k-boundaries for $k\geq 3$ are slightly different from D_n cluster polytopes. For instance, truncated D_4 polytope has the f-vector as $\mathbf{f}=(1,49,99,66,16,1)$, differing from the D_4 cluster polytope with $\mathbf{f}=(1,50,100,66,16,1)$.

4. Affine D_4 and bootstrapping $\Omega_L(1458)$

Our main example is the double-pentagon ladder $\Omega_L(1458)$ involving algebraic letters, whose kinematics is drawn as the two-mass-opposite hexagon:

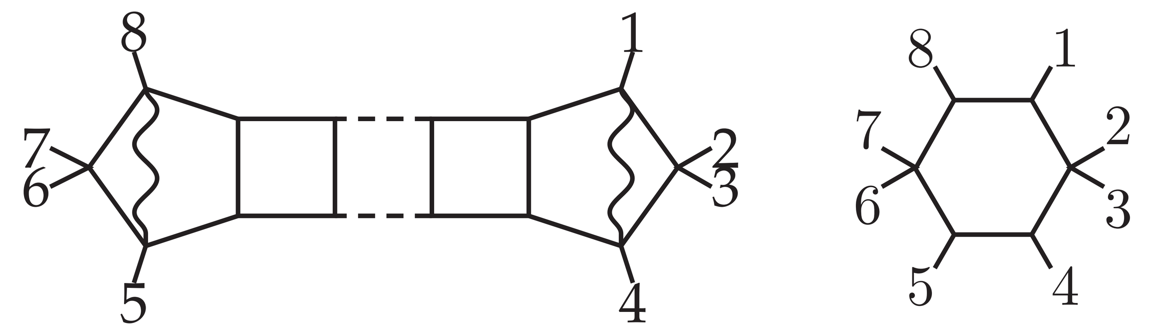

corresponding to plabic graph and the dual graph as

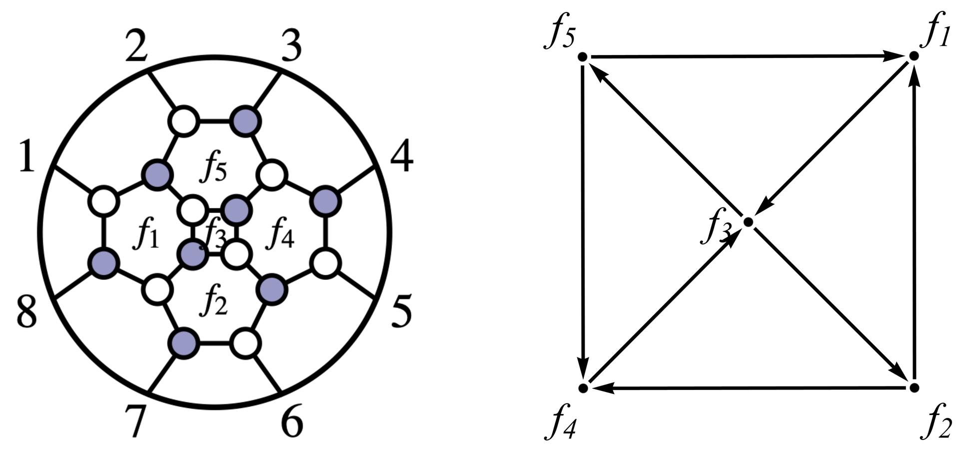

which is related to affine D_4 cluster algebra (infinite-type). On the other hand, Minkowski sum gives us a 5-dimensional polytope with $\mathbf{f}=(1,280,739,694,272,39,1)$, 38 normal vectors of whose facets are g-vector of the algebra, determining all 38 rational letters $W_1\cdots W_{38}$; while the rest one is the limit ray, leading to 5 algebraic letters $L_1\cdots L_5$, according to the algorithm in [3]. Note that square root from the computation is exactly the one for four-mass-box $F(2,4,6,8)$.

Following the prediction of alphabet and bootstrapping strategies, we can localize $\Omega_L(1458)$ for $L=2,3,4$ in the integrable symbol space generated by $\{W_i,L_j\}_{i=1\cdots 38,j=1\cdots 5}$ Conditions we impose to determine the results are

1. First-entry condition: First entries of the result can only be the physical discontinuities $\langle i\, i{+}1\, j\, j{+}1\rangle$
2. Last-entry condition: Last entries, which can be proved by symbol integration algorithm, can only be five combinations of W_i, denoted as $\{z_i\}_{i=1\cdots 5}$.
3. Two axial symmetries.
4. Boundary condition from Wilson-loop $\mathrm{d}\log$ picture: Following [2], Ω_L satisfies the recursive relation (with the initial $\Omega_1(1458)$ being the two-mass-opposite chiral hexagon):
$$\Omega_L(1458){=}\int_{\mathbb{R}^2_{\geq 0}} d\log\langle 148Y\rangle\, d\log\frac{\langle 1X4Y\rangle}{t}\,\Omega_{L-1}(1458)\big|_{\substack{Z_2\to X=Z_8+tZ_2\\ Z_3\to Y=Z_2+sZ_4}}$$
requiring $\Omega_L(Z_2{\to}Z_8){=}0$ to make sure the convergence at $t=0$
5. Differential equation: Derived from the recursion that
$$\Omega_L=(z_4{-}1)(z_1\partial_{z_1}{+}z_4\partial_{z_4}{+}z_5\partial_{z_5})(z_2\partial_{z_2}{+}z_4\partial_{z_4}{+}z_5\partial_{z_5})\Omega_{L+1}$$

We obtained $\mathcal{S}(\Omega_L(1458))$ up to $L=4$ and find out that their alphabet is $\{W_i,L_j\}_{i=1\cdots 25,j=1\cdots 5}$. Moreover, algebraic letters for these results always read: $\mathcal{W}_L=\sum_{i=1}^5\mathcal{S}(F(2,4,6,8))\otimes L_i\otimes\mathcal{S}(h_i)$, where h_i are weight-$(2L{-}3)$ polylogrithmic functions with only rational letters.

Outlook

- Consider integrals with kinematics that cannot be labelled by positroids of $G_+(4,n)$, *e.g.* kinematics with two adjacent massive corners.
- Extend these discussions to non-DCI situations, *e.g.* L-loop box ladders with one-,two- and three-massive corners.

References

[1] S.He, Z.Li and Q.Yang, Notes on cluster algebra and some all-loop Feynman integrals, *JHEP 06 (2021) 119.*

[2] S. He Z.Li,Y.Tang and Q.Yang, The Wilson-loop $\mathrm{d}\log$ representation for Feynman integrals, *JHEP 05 (2021) 052.*

[3] J.Drummond, J. Foster, and Ö. Gürdogan, Algebraic singularities of scattering amplitudes from tropical geometry, *JHEP 04 (2021) 002.*

[4] N.Arkani-Hamed, S.He and T.Lam, Stringy Canonial Forms, *JHEP 02 (2021) 069*

[5] J. L. Bourjaily, A. J. McLeod, M. von Hippel, and M. Wilhelm, Rationalizing Loop Integration, *JHEP 08 (2018) 184*

Thermalization Phenomena in Quenched Quantum Brownian Motion in De Sitter Space

Subhashish Banerjee, Sayantan Choudhury, Satyaki Chowdhury, Johannes Knaute, Sudhakar Panda, K.Shirish
School of Physical Sciences, National Institute of Science Education and Research, Jatni, Bhubaneswar, India.
Homi Bhabha National Institute, Training School Complex, Anushakti Nagar, Mumbai, India.
E-mail: sayantan.choudhury@niser.ac.in

Based on: arXiv:2104.10692 [hep-th], Poster Session, Amplitudes 2021, Niels Bohr Institute, Copenhagen.

ABSTRACT

In this work, we study the QFT version of the Caldeira-Leggett model to describe the Brownian Motion in De Sitter space considering interactions between two scalar fields. The thermalization phenomena using quantum quench from one scalar field model obtained from effective action. We consider a sudden quench mass protocol of the field of our interest. We find that the dynamics of the field post-quench is described in terms of the state of the generalized Calabrese-Cardy (gCC). We found the conserved charges of W_∞ algebra for the gCC state and it is different from flat space. We found that irrespective of the pre-quench state, the post quench state can be written in terms of the gCC state showing that the subsystem of our interest thermalizes. Furthermore, we study thermalization from a thermal Generalized Gibbs ensemble (GGE).

INTRODUCTION

- The study of Brownian motion of a particle coupled to a thermal bath has assumed great significance owing to its relevance as a robust model for open quantum systems in the context of macroscopic properties of a particle in a general environment. This has been used to study quantum dissipation and quantum decoherence due to the system's interaction with the environment.
- This model of QBM has proven to be useful not only in studies of open quantum systems but also in the field of quantum cosmology, quantum correlation problems, among others. It has also been extensively used in the context of AdS/CFT.
- The usual approach of tackling this problem involves use of the influence functional technique developed by Feynman and Vernon. The contribution of the environment degrees of freedom is quantified by the influence functional and one obtains the reduced subsystem of interest whose dynamics is of particular interest. A very well-known model in this direction was given by Caldeira and Leggett.
- Quantum quench is one such technique where the process of thermalization can be realized in the system in the post-quench phase. In a quantum quench, some parameter of the Hamiltonian change over a finite duration of time, and the initial wave function in the pre-quench function evolves to a state after the quench that is not stationary.
- Due to the growing interest in studying thermalization for integrable systems, there has been huge progress in the understanding of thermalization in scalar fields and extensive studies in the direction.
- This quench protocol has also found its applications in the cosmology of the early universe. It has been used to study the characteristics of fast phase transitions, under the settings of early cosmology where temperature promptly decreases.

QUANTUM QUENCH IN DS

$$S^{\rm eff}_{\rm free}[\chi]=\frac{1}{2}\int d\tau\ d^3\mathbf{x}\ a^2(\tau)\left[(\partial_\tau\chi(\mathbf{x},\tau))^2-(\partial_i\chi(\mathbf{x},\tau))^2-m^2(\tau)a^2(\tau)\chi^2(\mathbf{x},\tau)\right]$$

Field redefinition

Quench protocol:

$$m^2(\tau)=\left(m^2_\chi-\frac{2c^2(\tau)}{m^2_\phi}\right)=m_0^2\Theta(-\tau)=\begin{cases}m_0^2 & \textbf{Before quench}:\ \tau<\eta;\\ 0 & \textbf{After quench}:\ \tau\geq\eta,\end{cases}$$

$$S^{\rm eff}_{\rm free}[\chi]=\frac{1}{2}\int d\tau\ d^3\mathbf{x}\left[(\partial_\tau v(\mathbf{x},\tau))^2-(\partial_i v(\mathbf{x},\tau))^2-\left(m^2(\tau)a^2(\tau)-\frac{a''(\tau)}{a(\tau)}\right)v^2(\mathbf{x},\tau)\right]\quad v(\mathbf{x},\tau):\equiv a(\tau)\chi(\mathbf{x},\tau)$$

Fourier Transform $v(\mathbf{x},\tau):=\int\frac{d^3\mathbf{k}}{(2\pi)^3}\exp(i\mathbf{k}.\mathbf{x})\ v(\mathbf{k},\tau)$

$$S^{\rm eff}_{\rm free}[\chi]=\int d\tau\ d^3\mathbf{k}\ \left[|v'(\mathbf{k},\tau)|^2-\omega^2(\mathbf{k},\tau)|v(\mathbf{k},\tau)|^2\right],$$

EOM in Fourier space

Before quench: $\left[\frac{d^2}{d\tau^2}+\omega^2_{\rm eff,in}(k,\tau)\right]v_{in}(\mathbf{k},\tau)=0,$

After quench: $\left[\frac{d^2}{d\tau'^2}+\omega^2_{\rm eff,out}(k,\tau')\right]v_{out}(\mathbf{k},\tau')=0$

$\omega^2_{\rm eff,in}(k,\tau):=\left(k^2-\frac{\nu^2_{in}-\frac{1}{4}}{\tau^2}\right)$ with $\nu_{in}=\sqrt{\frac{9}{4}-\frac{m_0^2}{H^2}},$

$\omega^2_{\rm eff,out}(k,\tau'):=\left(k^2-\frac{\nu^2_{out}-\frac{1}{4}}{\tau'^2}\right)$ with $\nu_{out}=\frac{3}{2}$

Bunch – Davies vacuum :	$d_1=1,$	$d_2=0,$
α vacua :	$d_1=\cosh\alpha,$	$d_2=\sinh\alpha,$
Motta – Allen vacua :	$d_1=\cosh\alpha,$	$d_2=\exp(i\gamma)\sinh\alpha.$

Quench protocol

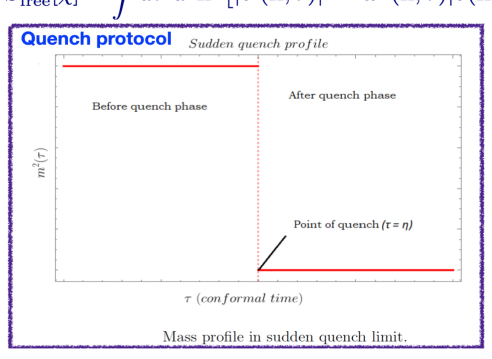

Mass profile in sudden quench limit.

Asymptotic solution

Before quench: $v_{in}(\mathbf{k},\tau)=\frac{2^{\nu_{in}-\frac{3}{2}}\ i\ (-k\tau)^{\frac{3}{2}-\nu_{in}}}{\sqrt{2}k^{3/2}\tau}\left|\frac{\Gamma(\nu_{in})}{\Gamma(3/2)}\right|\times\left[d_1(1+ik\tau)\exp\left(-i\left\{k\tau+\frac{\pi}{2}(\nu_{in}+\frac{1}{2})\right\}\right)-d_2(1-ik\tau)\exp\left(i\left\{k\tau+\frac{\pi}{2}(\nu_{in}+\frac{1}{2})\right\}\right)\right],$

After quench: $v_{out}(\mathbf{k},\tau)=\frac{2^{\nu_{out}-\frac{3}{2}}\ i\ (-k(\tau+\eta))^{\frac{3}{2}-\nu_{out}}}{\sqrt{2}k^{3/2}(\tau+\eta)}\left|\frac{\Gamma(\nu_{out})}{\Gamma(3/2)}\right|\times\left[d_3(1+ik(\tau+\eta))\exp\left(-i\left\{k(\tau+\eta)+\frac{\pi}{2}\left(\nu_{out}+\frac{1}{2}\right)\right\}\right)-d_4(1-ik(\tau+\eta))\exp\left(i\left\{k(\tau+\eta)+\frac{\pi}{2}\left(\nu_{out}+\frac{1}{2}\right)\right\}\right)\right].$

Hence using the continuity of the modes and the canonically conjugate momenta one can able to express the outgoing coefficients (after quench) in terms of the incoming coefficients (before quench).

$$v_{in}(\mathbf{k},\tau)=\alpha(k,\eta)\ v_{out}(\mathbf{k},\tau)+\beta(k,\eta)\ v^*_{out}(-\mathbf{k},\tau),\qquad a_{in}(\mathbf{k})=\alpha^*(k,\eta)a_{out}(\mathbf{k})-\beta^*(k,\eta)a^\dagger_{out}(-\mathbf{k}),$$
$$v_{out}(\mathbf{k},\tau)=\alpha^*(k,\eta)\ v_{in}(\mathbf{k},\tau)-\beta(k,\eta)\ v^*_{in}(-\mathbf{k},\tau)\qquad a_{out}(\mathbf{k})=\alpha^*(k,\eta)a_{in}(\mathbf{k})+\beta^*(k,\eta)a^\dagger_{in}(-\mathbf{k})$$

$$\alpha(k,\eta)=\left.\frac{v'_{out}(\mathbf{k},\tau)v^*_{in}(\mathbf{k},\tau)-v_{out}(\mathbf{k},\tau)v'^*_{in}(\mathbf{k},\tau)}{2i}\right|_\eta,\qquad \beta^*(k,\eta)=\left.\frac{v'_{out}(\mathbf{k},\tau)v_{in}(\mathbf{k},\tau)-v_{out}(\mathbf{k},\tau)v'_{in}(\mathbf{k},\tau)}{2i}\right|_\eta$$

Bogoliubov coefficients

$$\gamma(k)=\frac{\beta^*(k,\eta)}{\alpha^*(k,\eta)}$$

For Dirichlet boundary state: $\kappa(k)=-\frac{1}{2}\log(-\gamma(k))=\left(\kappa_{0,\mathbf{DB}}+\sum_{n=1}^\infty\kappa_{n+1,\mathbf{DB}}|k|^n\right),$

For Neumann boundary state: $\kappa(k)=-\frac{1}{2}\log(\gamma(k))=\left(\kappa_{0,\mathbf{NB}}+\sum_{n=1}^\infty\kappa_{n+1,\mathbf{NB}}|k|^n\right)$

$$\kappa_{0,\mathbf{DB}}=\left(\kappa_{0,\mathbf{NB}}+\frac{i\pi}{2}\right),\quad\text{and}\quad\kappa_{n+1,\mathbf{DB}}=\kappa_{n+1,\mathbf{NB}}\quad\forall\quad n=1,2,3,\cdots,\infty$$

Without squeezing:

1.Pre quench state: $|0,in\rangle=\frac{1}{\sqrt{|d_1|}}\exp\left(-\frac{id_2^*}{2d_1^*}\int\frac{d^3\mathbf{k}}{(2\pi)^3}a^\dagger_{in}(\mathbf{k})a^\dagger_{in}(-\mathbf{k})\right)|0,in\rangle_{\mathbf{BD}}$

2.Post quench gCC state:

$|\psi_{gCC}\rangle_{\mathbf{DB}}=\frac{1}{\sqrt{|d_1|}}\exp\left(-\kappa_{0,\mathbf{DB}}W_0-\sum_{n=2}^\infty\kappa_{2n,\mathbf{DB}}W_{2n,\mathbf{DB}}\right)|D\rangle\qquad|D\rangle=\exp\left[-\frac{1}{2}\int\frac{d^3\mathbf{k}}{(2\pi)^3}a^\dagger_{out}(\mathbf{k})a^\dagger_{out}(-\mathbf{k})\right]|0,out\rangle,$

$|\psi_{gCC}\rangle_{\mathbf{NB}}=\frac{1}{\sqrt{|d_1|}}\exp\left(-\kappa_{0,\mathbf{NB}}W_0-\sum_{n=2}^\infty\kappa_{2n,\mathbf{NB}}W_{2n}\right)|N\rangle\qquad|N\rangle=\exp\left[\frac{1}{2}\int\frac{d^3\mathbf{k}}{(2\pi)^3}a^\dagger_{out}(\mathbf{k})a^\dagger_{out}(-\mathbf{k})\right]|0,out\rangle.$

→ Before thermalization

3.Usual thermal state: → **After thermalization**

$$\alpha(k,\eta)=\left.\frac{v'_{out}(\mathbf{k},\tau)v^*_{in}(\mathbf{k},\tau)-v_{out}(\mathbf{k},\tau)v'^*_{in}(\mathbf{k},\tau)}{2i}\right|_\eta,\qquad\beta^*(k,\eta)=\left.\frac{v'_{out}(\mathbf{k},\tau)v_{in}(\mathbf{k},\tau)-v_{out}(\mathbf{k},\tau)v'_{in}(\mathbf{k},\tau)}{2i}\right|_\eta$$

Bogoliubov coefficients

$$\gamma^{\rm eff}(k)=\exp(i\delta(k))\left(\frac{\gamma(k)+f(k)\exp(i\delta(k))}{1+\exp(i\delta(k))f(k)\gamma^*(k)}\right)\qquad\exp(i\delta(k))=\frac{\alpha(k)}{\alpha^*(k)}$$

For Dirichlet boundary state: $\kappa_{\rm eff}(k)=-\frac{1}{2}\log(-\gamma^{\rm eff}(k))=\left(\kappa^{\rm eff}_{0,\mathbf{DB}}+\sum_{n=1}^\infty\kappa^{\rm eff}_{n+1,\mathbf{DB}}|k|^n\right),$

For Neumann boundary state: $\kappa_{\rm eff}(k)=-\frac{1}{2}\log(\gamma^{\rm eff}(k))=\left(\kappa^{\rm eff}_{0,\mathbf{NB}}+\sum_{n=1}^\infty\kappa^{\rm eff}_{n+1,\mathbf{NB}}|k|^n\right)$

$$\kappa^{\rm eff}_{0,\mathbf{DB}}=\left(\kappa^{\rm eff}_{0,\mathbf{NB}}+\frac{i\pi}{2}\right),\quad\text{and}\quad\kappa^{\rm eff}_{n+1,\mathbf{DB}}=\kappa^{\rm eff}_{n+1,\mathbf{NB}}\quad\forall\quad n=1,2,3,\cdots,\infty$$

With squeezing:

1.Pre quench state: $|f\rangle=\exp\left(\frac{1}{2}\int\frac{d^3k}{(2\pi)^3}f(k)a^\dagger_{in}(\mathbf{k})a^\dagger_{in}(\text{-}\mathbf{k})\right)|0,in\rangle\qquad f(k)=\exp\left(-\frac{k^2}{2\sigma^2}\right)$

2.Post quench gCC state:

$|\psi^{\rm eff}_{gCC}\rangle_{\mathbf{DB}}=\frac{1}{\sqrt{|d_1|}}\exp\left(-\kappa^{\rm eff}_{0,\mathbf{DB}}W_0-\sum_{n=2}^\infty\kappa^{\rm eff}_{2n,\mathbf{DB}}W_{2n,\mathbf{DB}}\right)|D\rangle\qquad|D\rangle=\exp\left[-\frac{1}{2}\int\frac{d^3\mathbf{k}}{(2\pi)^3}a^\dagger_{out}(\mathbf{k})a^\dagger_{out}(-\mathbf{k})\right]|0,out\rangle,$

$|\psi^{\rm eff}_{gCC}\rangle_{\mathbf{NB}}=\frac{1}{\sqrt{|d_1|}}\exp\left(-\kappa^{\rm eff}_{0,\mathbf{NB}}W_0-\sum_{n=2}^\infty\kappa^{\rm eff}_{2n,\mathbf{NB}}W_{2n}\right)|N\rangle\qquad|N\rangle=\exp\left[\frac{1}{2}\int\frac{d^3\mathbf{k}}{(2\pi)^3}a^\dagger_{out}(\mathbf{k})a^\dagger_{out}(-\mathbf{k})\right]|0,out\rangle.$

→ Before thermalization

3.Usual thermal state: → **After thermalization** (Not affected by squeezing)

CALDEIRA-LEGGETT MODEL IN QM

- In the Caldeira-Leggett (CL) model the phenomenon of quantum dissipation was discussed and closed equations for such a quantum system were obtained. For the purpose of studying such phenomenon, a particular model describing such system-bath interaction was chosen and the parameters of the model were fitted in such a way that the classical equations of Brownian motion were reproduced.

CL model:

$$H=H_S+H_B+H_I \leftarrow \textbf{Total Hamiltonian}$$
$$H_S=\frac{p^2}{2M}+V(x), \leftarrow \textbf{System Hamiltonian}$$
$$H_B=\sum_k\frac{p_k^2}{2m_k}+\sum_k\frac{1}{2}m\omega_k^2R_k^2, \leftarrow \textbf{Bath/environment Hamiltonian}$$
$$H_I=x\sum_k C_kR_k. \leftarrow \textbf{Interaction Hamiltonian}$$

- One must note that the construction of the density matrix does not provide any evidence that the chosen system of interest will behave like a Brownian particle in the classical regime. However, in the continuum limit with a suitable distribution of the bath oscillators, it is possible to realize the brownian motion of the system particle.

QFT OF BROWNIAN MOTION IN DS

QFT generalized CL model:

$$S_{\rm CL}[\phi,\chi]=\int d^4x\sqrt{-g(x)}\left[\underbrace{\left(-\frac{1}{2}(\partial\phi(x))^2+\frac{m_\phi^2}{2}\phi^2(x)\right)}_{\text{Free theory of }\phi}+\underbrace{\left(-\frac{1}{2}(\partial\chi(x))^2+\frac{m_\chi^2}{2}\chi^2(x)\right)}_{\text{Free theory of }\chi}+\underbrace{c(x)\phi(x)\chi(x)}_{\text{Interaction}}\right],$$

Effective potential for signal field: $V(\phi(x),\chi(x))=\left(\frac{m_\phi^2}{2}\phi^2(x)+\frac{m_\chi^2}{2}\chi^2(x)+c(x)\phi(x)\chi(x)\right).$

$$\left(\frac{\partial V(\phi(x),\chi(x))}{\partial\phi(x)}\right)=m_\phi^2\phi(x)+c(x)\chi(x)=0\quad\Longrightarrow\quad\phi(x)=-\frac{c(x)\chi(x)}{m_\phi^2},$$
$$\left(\frac{\partial^2V(\phi(x),\chi(x))}{\partial\phi^2(x)}\right)=m_\phi^2>0\ \Longrightarrow\ \text{minimum.}\qquad V_{\rm eff}(\chi(x))=\frac{m^2(x)}{2}\chi^2(x)\quad\text{where}\quad m^2(x)=\left(m_\chi^2-\frac{2c^2(x)}{m_\phi^2}\right)$$

$$S_{\rm CL}[\phi,\chi]=\int d^4x\sqrt{-g(x)}\left[\left(-\frac{1}{2}(\partial\phi(x))^2+\frac{m_\phi^2}{2}\phi^2(x)\right)+\left(-\frac{1}{2}(\partial\chi(x))^2+V_{\rm eff}(\chi(x))\right)+c(x)\phi(x)\chi(x)\right]$$

Path integral and effective action in De Siitter:

$$\mathcal{Z}_{\rm eff}[\chi]:=\int\mathfrak{D}\phi\ \exp\left[-S^E_{\rm CL}[\phi,\chi]\right]=\exp\left[-S^E_{\rm eff}[\chi]\right]\quad ds^2=a^2(\tau)\left(-d\tau^2+d\mathbf{x}^2\right)\quad\text{where}\quad a(\tau)=-\frac{1}{H\tau}\quad\text{and}\quad\sqrt{-g(\tau)}=a^4(\tau)$$

$$S^E_{\rm eff}[\chi]=\ln\left[2\sinh\left(\frac{m_\phi}{2H_T}\ln\left(-\frac{1}{H_T\tau_T}\right)\right)\right]+\int d^4x\sqrt{-g(x)}\left\{\left(-\frac{1}{2}(\partial\chi)^2+V_{\rm eff}(\chi)\right)\right\}+\int d^3\mathbf{x}\int_{-1/H}^{-\exp(-TH)/H}d\tau\sqrt{-g(\tau)}\int_{-1/H'}^{-\exp(-TH')/H'}d\tau'\sqrt{-g(\tau')}\times\mathcal{K}_\phi(\tau,\tau')\times c(\tau)\chi(\mathbf{x},\tau)\ c(\tau')\chi(\mathbf{x},\tau')$$

Noise kernel

$$\mathcal{K}_\phi(\tau,\tau')=\left(\frac{1}{m_\phi^2}\right)\exp\left(-m_\phi\left|\frac{1}{H}\ln\left(-\frac{1}{H\tau}\right)-\frac{1}{H'}\ln\left(-\frac{1}{H'\tau'}\right)\right|\right)$$

$$\lim_{\tau\to0}\lim_{\tau'\to0}\mathcal{K}_\phi(\tau,\tau')=0$$

Kernel vanishes At late time limit

SUBSYSTEM THERMALIZATION

Reduced density matrix of region A (by partially tracing region B) for the post-quench gCC type of quantum states (which can be the expansion coefficients of the W conserved charges)

↓ **Late time limit**

Thermal density matrix for GGE

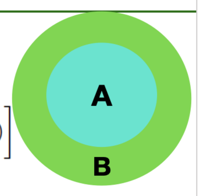

For Dirichlet boundary state:

$$\text{Tr}_\mathcal{B}\left[\exp(-iH\tau)\,|\psi(\kappa_n)\rangle\langle\psi(\kappa_n)|\exp(iH\tau)\right]$$
$$=\text{Tr}_\mathcal{B}\left[\exp(-iH\tau)\exp\left(-\int\frac{d^3\mathbf{k}}{(2\pi)^3}\kappa(k)\hat{N}(k)\right)|D\rangle\langle D|\exp\left(-\int\frac{d^3\mathbf{k}}{(2\pi)^3}\kappa(k)\hat{N}(k)\right)\exp(iH\tau)\right]$$
$$\xrightarrow{\tau\to0}\text{Tr}_\mathcal{B}\left[\frac{1}{Z(\tau)}\exp\left(-\int\frac{d^3\mathbf{k}}{(2\pi)^3}4\kappa(k)\hat{N}(k)\right)\right]$$
$$=\text{Tr}_\mathcal{B}\left[\rho_{\rm GGE}(\beta,4\kappa_{n,\mathbf{DB}})\right]\quad\text{where}\quad\rho_{\rm GGE}(\beta,4\kappa_{n,\mathbf{DB}})=\frac{1}{Z(\tau)}\exp\left(-\beta H-4\sum_n\kappa_{n,\mathbf{DB}}W_n\right)$$

For Neumann boundary state:

$$\text{Tr}_\mathcal{B}\left[\exp(-iH\tau)\,|\psi(\kappa_n)\rangle\langle\psi(\kappa_n)|\exp(iH\tau)\right]$$
$$=\text{Tr}_\mathcal{B}\left[\exp(-iH\tau)\exp\left(\int\frac{d^3\mathbf{k}}{(2\pi)^3}\kappa(k)\hat{N}(k)\right)|N\rangle\langle N|\exp\left(\int\frac{d^3\mathbf{k}}{(2\pi)^3}\kappa(k)\hat{N}(k)\right)\exp(iH\tau)\right]$$
$$\xrightarrow{\tau\to0}\text{Tr}_\mathcal{B}\left[\frac{1}{Z(\tau)}\exp\left(\int\frac{d^3\mathbf{k}}{(2\pi)^3}4\kappa(k)\hat{N}(k)\right)\right]$$
$$=\text{Tr}_\mathcal{B}\left[\rho_{\rm GGE}(\beta,4\kappa_{n,\mathbf{NB}})\right]\quad\text{where}\quad\rho_{\rm GGE}(\beta,4\kappa_{n,\mathbf{NB}})=\frac{1}{Z(\tau)}\exp\left(-\beta H-4\sum_n\kappa_{n,\mathbf{NB}}W_n\right)$$

$$W_n=|k|^{n-1}\ N(\hat{k})\quad\text{where}\quad N(\hat{k})=a^\dagger_{out}(\mathbf{k})a_{out}(\mathbf{k})$$

$$\langle W_0\rangle:=\int\frac{d^3\mathbf{k}}{(2\pi)^3}\langle0,in|a^\dagger_{out}(\mathbf{k})a_{out}(\mathbf{k})|0,in\rangle=\int\frac{d^3\mathbf{k}}{(2\pi)^3}\langle N(k)\rangle,$$
$$\langle W_{n+1}\rangle:=\int\frac{d^3\mathbf{k}}{(2\pi)^3}|k|^n\langle0,in|a^\dagger_{out}(\mathbf{k})a_{out}(\mathbf{k})|0,in\rangle=\int\frac{d^3\mathbf{k}}{(2\pi)^3}|k|^n\langle N(k)\rangle,$$
$$\forall\ n=1,2,\cdots,\infty\quad\text{where}\quad\langle N(k)\rangle=|\beta(k,\eta)|^2$$

$$\langle W_n\rangle_{\rm gCC}=\langle W_n\rangle_{\rm GGE}$$
$$\langle N(k)\rangle_{\rm gCC}=|\beta(k)|^2=\frac{|\gamma(k)|^2}{1-|\gamma(k)|^2},$$
$$\langle N(k)\rangle_{\rm GGE}=\frac{1}{\exp(4\kappa(k))-1},$$
$$\langle N(k)\rangle_{\rm gCC}=\langle N(k)\rangle_{\rm GGE}$$

TWO-POINT FUNCTIONS

From pre quenched ground state:

$$\langle0,in|\chi(\mathbf{k},\tau)\chi(\mathbf{k}',\tau)|0,in\rangle=(2\pi)^3\delta^3(\mathbf{k}+\mathbf{k}')\mathcal{P}^0_{\chi\chi}(\mathbf{k},\tau),$$
$$\langle0,in|(ik\chi(\mathbf{k},\tau))(ik\chi(\mathbf{k}',\tau))|0,in\rangle=(2\pi)^3\delta^3(\mathbf{k}+\mathbf{k}')\mathcal{P}^0_{\partial_j\chi\partial_j\chi}(\mathbf{k},\tau)$$
$$\langle0,in|\Pi(\mathbf{k},\tau)\Pi(\mathbf{k}',\tau)|0,in\rangle=(2\pi)^3\delta^3(\mathbf{k}+\mathbf{k}')\mathcal{P}^0_{\Pi_\chi\Pi_\chi}(\mathbf{k},\tau)$$

$$\mathcal{P}^0_{\chi\chi}(\mathbf{k},\tau)=\frac{1}{a^2(\tau)}\frac{1}{|d_1|}\left[\sum_{b=1}^4\Delta_b(\mathbf{k},\tau)\right],$$
$$\mathcal{P}^0_{\partial_j\chi\partial_j\chi}(\mathbf{k},\tau)=-k^2\ \mathcal{P}^0_{\chi\chi}(\mathbf{k},\tau),$$
$$\mathcal{P}^0_{\Pi_\chi\Pi_\chi}(\mathbf{k},\tau)=\left[\frac{(a'(\tau))^2}{a^2(\tau)}\mathcal{P}^0_{\chi\chi}(\mathbf{k},\tau)-\frac{a'(\tau)}{(a^3(\tau)}\frac{1}{|d_1|}\left(\sum_{b=5}^{12}\Delta_b(\mathbf{k},\tau)\right)+\frac{1}{a^2(\tau)}\frac{1}{|d_1|}\left(\sum_{b=13}^{16}\Delta_b(\mathbf{k},\tau)\right)\right]$$

From post quenched gCC state:

A. Dirichlet boundary state:

$${}_{\mathbf{DB}}\langle gCC|\chi(\mathbf{k},\tau)\chi(\mathbf{k}',\tau)|gCC\rangle_{\mathbf{DB}}=(2\pi)^3\delta^3(\mathbf{k}+\mathbf{k}')\mathcal{P}^{gCC_{\mathbf{DB}}}_{\chi\chi}(\mathbf{k},\tau),$$
$${}_{\mathbf{DB}}\langle gCC|(ik\chi(\mathbf{k},\tau))(ik\chi(\mathbf{k}',\tau))|gCC\rangle_{\mathbf{DB}}=(2\pi)^3\delta^3(\mathbf{k}+\mathbf{k}')\mathcal{P}^{gCC_{\mathbf{DB}}}_{\partial_j\chi\partial_j\chi}(\mathbf{k},\tau)$$
$${}_{\mathbf{DB}}\langle gCC|\Pi(\mathbf{k},\tau)\Pi(\mathbf{k}',\tau)|gCC\rangle_{\mathbf{DB}}=(2\pi)^3\delta^3(\mathbf{k}+\mathbf{k}')\mathcal{P}^{gCC_{\mathbf{DB}}}_{\Pi_\chi\Pi_\chi}(\mathbf{k},\tau).$$

$$\mathcal{P}^{gCC_{\mathbf{DB}}}_{\chi\chi}(\mathbf{k},\tau)=\frac{1}{a^2(\tau)}\frac{1}{|d_1|}\exp\left(-(\kappa^*_{0,\mathbf{DB}}+\kappa_{0,\mathbf{DB}})\langle N(k)\rangle-\sum_{n=2}^\infty(\kappa^*_{2n,\mathbf{DB}}+\kappa_{2n,\mathbf{DB}})|k|^{2n-1}\langle N(k)\rangle\right)\left[\sum_{c=1}^4\Theta_c(\mathbf{k},\tau)\right],$$
$$\mathcal{P}^{gCC_{\mathbf{DB}}}_{\partial_j\chi\partial_j\chi}(\mathbf{k},\tau)=-k^2\ \mathcal{P}^{gCC_{\mathbf{DB}}}_{\chi\chi}(\mathbf{k},\tau),$$
$$\mathcal{P}^{gCC_{\mathbf{DB}}}_{\Pi_\chi\Pi_\chi}(\mathbf{k},\tau)=\left[\frac{(a'(\tau))^2}{a^2(\tau)}\mathcal{P}^{gCC_{\mathbf{DB}}}_{\chi\chi}(\mathbf{k},\tau)-\exp\left(-(\kappa^*_{0,\mathbf{DB}}+\kappa_{0,\mathbf{DB}})\langle N(k)\rangle-\sum_{n=2}^\infty(\kappa^*_{2n,\mathbf{DB}}+\kappa_{2n,\mathbf{DB}})|k|^{2n-1}\langle N(k)\rangle\right)\left\{\frac{a'(\tau)}{(a^3(\tau)}\frac{1}{|d_1|}\left(\sum_{c=5}^{12}\Theta_c(\mathbf{k},\tau)\right)-\frac{1}{a^2(\tau)}\frac{1}{|d_1|}\left(\sum_{b=13}^{16}\Theta_c(\mathbf{k},\tau)\right)\right\}\right]$$

B. Neumann boundary state:

$${}_{\mathbf{NB}}\langle gCC|\chi(\mathbf{k},\tau)\chi(\mathbf{k}',\tau)|gCC\rangle_{\mathbf{NB}}=(2\pi)^3\delta^3(\mathbf{k}+\mathbf{k}')\mathcal{P}^{gCC_{\mathbf{DB}}}_{\chi\chi}(\mathbf{k},\tau),$$
$${}_{\mathbf{NB}}\langle gCC|(ik\chi(\mathbf{k},\tau))(ik\chi(\mathbf{k}',\tau))|gCC\rangle_{\mathbf{NB}}=(2\pi)^3\delta^3(\mathbf{k}+\mathbf{k}')\mathcal{P}^{gCC_{\mathbf{DB}}}_{\partial_j\chi\partial_j\chi}(\mathbf{k},\tau)$$
$${}_{\mathbf{NB}}\langle gCC|\Pi(\mathbf{k},\tau)\Pi(\mathbf{k}',\tau)|gCC\rangle_{\mathbf{NB}}=(2\pi)^3\delta^3(\mathbf{k}+\mathbf{k}')\mathcal{P}^{gCC_{\mathbf{DB}}}_{\Pi_\chi\Pi_\chi}(\mathbf{k},\tau).$$

$$\mathcal{P}^{gCC_{\mathbf{NB}}}_{\chi\chi}(\mathbf{k},\tau)=\frac{1}{a^2(\tau)}\frac{1}{|d_1|}\exp\left(-(\kappa^*_{0,\mathbf{NB}}+\kappa_{0,\mathbf{NB}}))\langle N(k)\rangle-\sum_{n=2}^\infty(\kappa^*_{2n,\mathbf{NB}}+\kappa_{2n,\mathbf{NB}}))|k|^{2n-1}\langle N(k)\rangle\right)\left[\sum_{c=1}^4\Theta_c(\mathbf{k},\tau)\right],$$
$$\mathcal{P}^{gCC_{\mathbf{NB}}}_{\partial_j\chi\partial_j\chi}(\mathbf{k},\tau)=-k^2\ \mathcal{P}^{gCC_{\mathbf{NB}}}_{\chi\chi}(\mathbf{k},\tau),$$
$$\mathcal{P}^{gCC_{\mathbf{NB}}}_{\Pi_\chi\Pi_\chi}(\mathbf{k},\tau)=\left[\frac{(a'(\tau))^2}{a^2(\tau)}\mathcal{P}^{gCC_{\mathbf{NB}}}_{\chi\chi}(\mathbf{k},\tau)-\exp\left(-(\kappa^*_{0,\mathbf{NB}}+\kappa_{0,\mathbf{NB}}))\langle N(k)\rangle-\sum_{n=2}^\infty(\kappa^*_{2n,\mathbf{NB}}+\kappa_{2n,\mathbf{NB}}))|k|^{2n-1}\langle N(k)\rangle\right)\left\{\frac{a'(\tau)}{(a^3(\tau)}\frac{1}{|d_1|}\left(\sum_{c=5}^{12}\Theta_c(\mathbf{k},\tau)\right)-\frac{1}{a^2(\tau)}\frac{1}{|d_1|}\left(\sum_{b=13}^{16}\Theta_c(\mathbf{k},\tau)\right)\right\}\right],$$

(Without/With Squeezing)

From thermal state:

$$\mathcal{P}^{GGE}_{+,\chi\chi}(\beta,\mathbf{k},\tau)=\frac{v_{out}(\mathbf{k},\tau)v^*_{out}(-\mathbf{k},\tau)}{2a^2(\tau)}\exp\left(\frac{\beta E_k(\tau)}{2}\right)\text{cosech}\left(\frac{\beta E_k(\tau)}{2}\right),$$
$$\mathcal{P}^{GGE}_{-,\chi\chi}(\beta,\mathbf{k},\tau)=\frac{v^*_{out}(-\mathbf{k},\tau)v_{out}(\mathbf{k},\tau)}{2a^2(\tau)}\exp\left(-\frac{\beta E_k(\tau)}{2}\right)\text{cosech}\left(\frac{\beta E_k(\tau)}{2}\right),$$
$$\mathcal{P}^{GGE}_{+,\partial_i\chi\partial_i\chi}(\beta,\mathbf{k},\tau)=-k^2\ \mathcal{P}^{GGE}_{+,\chi\chi}(\beta,\mathbf{k},\tau),$$
$$\mathcal{P}^{GGE}_{-,\partial_i\chi\partial_i\chi}(\beta,\mathbf{k},\tau)=-k^2\ \mathcal{P}^{GGE}_{-,\chi\chi}(\beta,\mathbf{k},\tau),$$
$$\mathcal{P}^{GGE}_{+,\Pi_\chi\Pi_\chi}(\beta,\mathbf{k},\tau)=\frac{v'_{out}(\mathbf{k},\tau)v^{*\prime}_{out}(-\mathbf{k},\tau)}{2a^2(\tau)}\exp\left(\frac{\beta E_k(\tau)}{2}\right)\text{cosech}\left(\frac{\beta E_k(\tau)}{2}\right)-\frac{\mathcal{P}^{GGE}_{+,\chi\chi}(\beta,\mathbf{k},\tau)}{a^2(\tau)}a'^2(\tau),$$
$$\mathcal{P}^{GGE}_{-,\Pi_\chi\Pi_\chi}(\beta,\mathbf{k},\tau)=\frac{v^{*\prime}_{out}(-\mathbf{k},\tau)v'_{out}(\mathbf{k},\tau)}{2a^2(\tau)}\exp\left(-\frac{\beta E_k(\tau)}{2}\right)\text{cosech}\left(\frac{\beta E_k(\tau)}{2}\right)-\frac{\mathcal{P}^{GGE}_{-,\chi\chi}(\beta,\mathbf{r},\tau)}{a^2(\tau)}a'^2(\tau)$$

Dispersion relation:

$$E_k(\tau_1)=\left[|\Pi_{out}(\mathbf{k},\tau_1)|^2+\omega^2_{out}(k,\tau_1)|v_{out}(\mathbf{k},\tau_1)|^2\right]\quad\omega^2_{out}(k,\tau_1)=\left(k^2-\frac{2}{\tau_1^2}\right)\quad\text{where}\quad\tau_1=\tau+\eta$$

Partition function:

$$Z=\frac{1}{2|d_1|}\exp\left(-\frac{i}{2}\left\{\frac{d_2^*}{d_1^*}-\frac{d_2}{d_1}\right\}\right)\exp\left(\frac{\beta E_k(\tau_1)}{2}\right)\text{cosech}\left(\frac{\beta E_k(\tau_1)}{2}\right),$$

Bunch – Davies vacuum :	$d_1=1,$	$d_2=0,$
α vacua :	$d_1=\cosh\alpha,$	$d_2=\sinh\alpha,$
Motta – Allen vacua :	$d_1=\cosh\alpha,$	$d_2=\exp(i\gamma)\sinh\alpha.$

NUMERICAL RESULTS

Spectrum before quench:

Consistent with Planck 2018 data with 95% CL

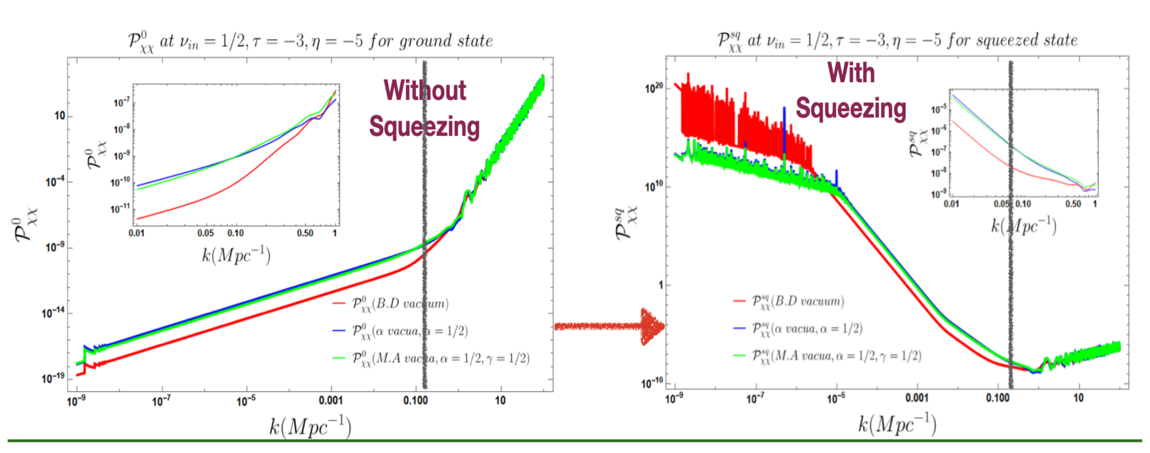

Spectrum after thermalization (at high temperature):

$\beta=\frac{1}{T}$ with $k_B=1$

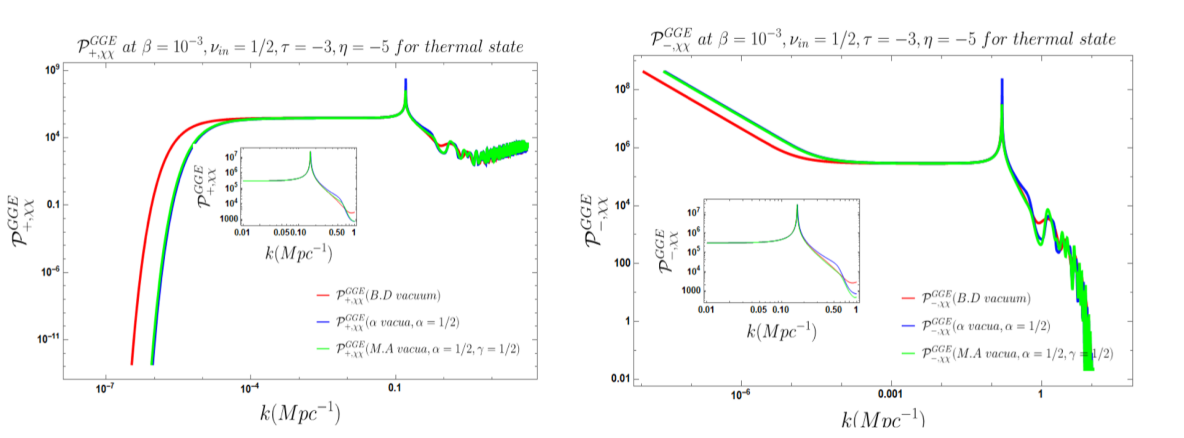

Spectrum after quench:

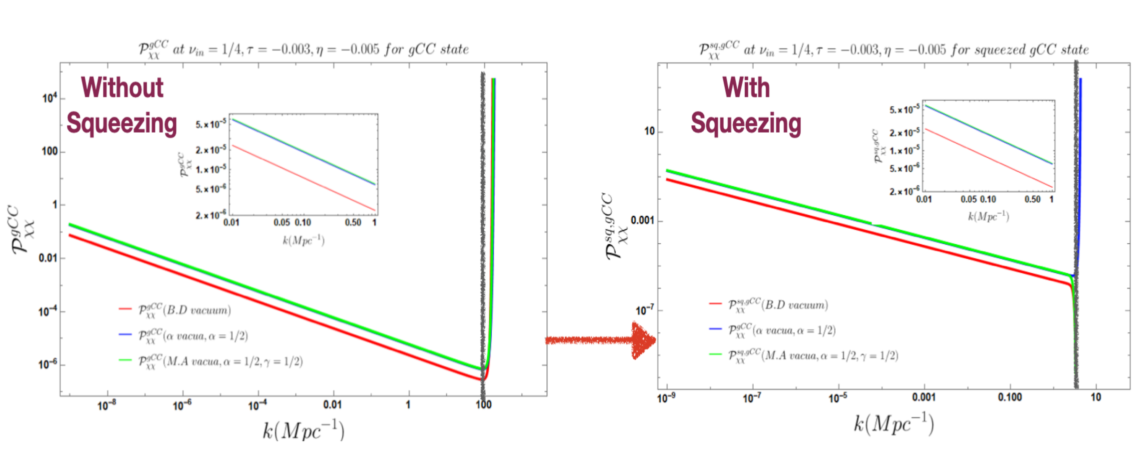

Spectrum after thermalization (at low temperature):

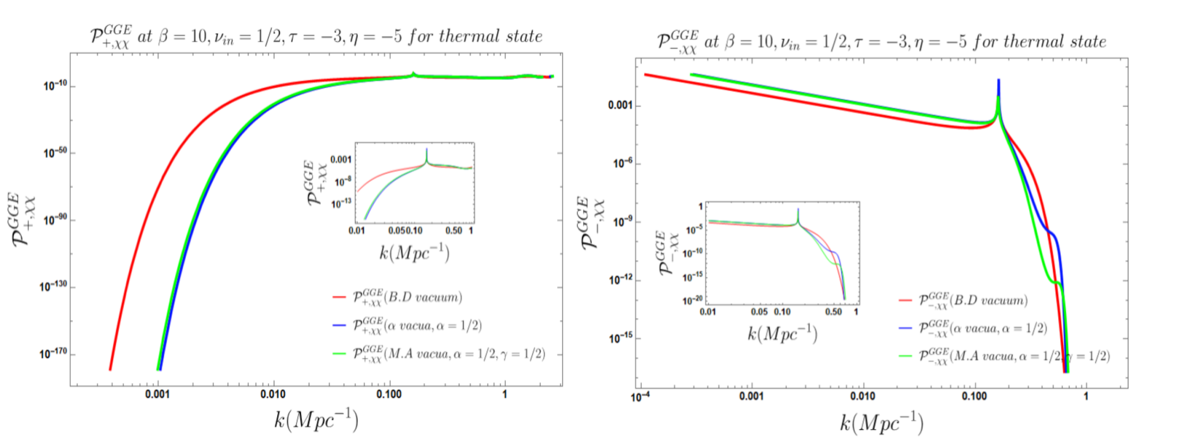

Next-to-leading power two-loop soft functions for the Drell-Yan process at threshold

Alessandro Broggio,[a,b] Sebastian Jaskiewicz,[c] and Leonardo Vernazza[b,d,e]
[a] Università degli Studi di Milano-Bicocca, [b] INFN, [c] Durham University and IPPP,
[d] Università di Torino, [e] CERN.
sebastian.jaskiewicz@durham.ac.uk based on arXiv: 2107.07353

Introduction

We calculate the generalized soft functions at $\mathcal{O}(\alpha_s^2)$ at next-to-leading power accuracy for the Drell-Yan process at threshold. The operator definitions of these objects contain explicit insertions of soft gauge and matter fields, giving rise to a dependence on additional convolution variables with respect to the leading power result. These soft functions constitute the last missing ingredient for the validation of the bare factorization theorem to NNLO accuracy. We carry out the calculations by reducing the soft squared amplitudes into a set of canonical master integrals and we employ the method of differential equations to evaluate them. We retain the exact d-dimensional dependence of the convolution variables at the integration boundaries in order to regulate the fixed-order convolution integrals. After combining the soft functions with the relevant collinear functions, we perform checks of the results at the cross-section level against the literature and expansion-by-regions calculations, at NNLO and partly at N^{3}LO, finding agreement.

Factorization

We consider the diagonal channel of the DY process, $q\bar{q} \to \gamma^*[\to \ell\bar{\ell}] + X$, in the kinematic region $z = Q^2/\hat{s} \to 1$. The NLP partonic cross-section has the following structure [M. Beneke, A.Broggio, **SJ**, L. Vernazza, 1912.01585]

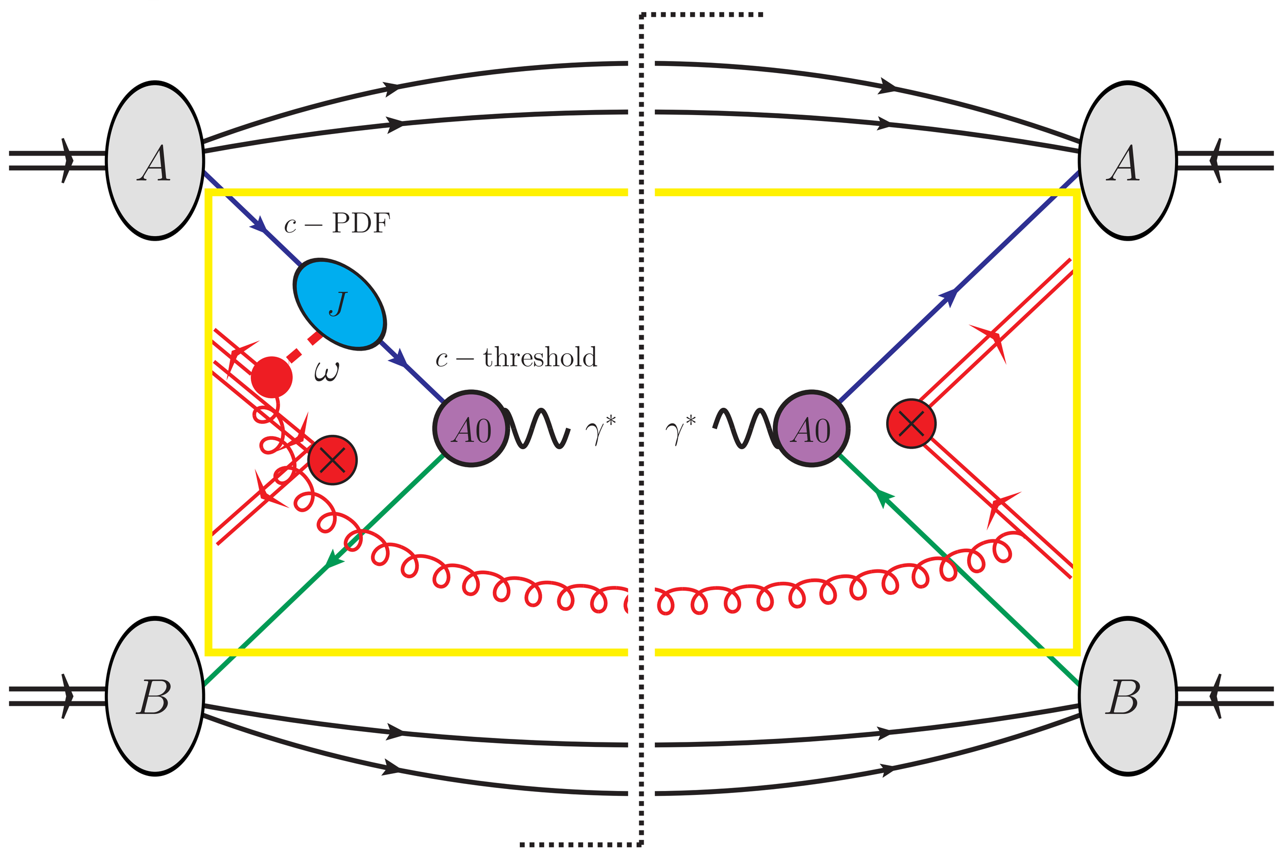

$$\Delta^{dyn}_{\rm NLP}(z) = -\frac{2}{(1-\epsilon)}\, Q \left[\left(\frac{\not{n}_-}{4}\right)\gamma_{\perp\rho}\left(\frac{\not{n}_+}{4}\right)\gamma_\perp^\rho\right]_{\beta\gamma} \times \int d(n_+p)\, C^{A0,A0}(n_+p, x_b n_- p_B)\, C^{*A0A0}(x_a n_+ p_A, x_b n_- p_B) \times \sum_{i=1}^{5} \int \{d\omega_j\}\, J_{i,\gamma\beta}(n_+p, x_a n_+ p_A; \{\omega_j\})\, S_i(\Omega;\{\omega_j\}) + \text{h.c.}$$

Here we focus on $\mathcal{O}(\alpha_s^2)$ calculation of the soft functions

$$S_i(\Omega;\{\omega_j\}) = \int \frac{dx^0}{4\pi}\, e^{i\Omega x^0/2} \int \left\{\frac{dz_{j-}}{2\pi}\right\} e^{-i\omega_j z_{j-}}\, S_i(x_0;\{z_{j-}\})$$

Soft functions

Example operator definitions, using building block $\mathcal{B}^\mu_\pm = Y^\dagger_\pm\, [i D^\mu_s Y_\pm]$:

$$S_1(x^0;z_-) = \frac{1}{N_c}\mathrm{Tr}\langle 0|\bar{\mathbf{T}}\left[Y^\dagger_+(x^0)Y_-(x^0)\right]\mathbf{T}\left(\left[Y^\dagger_-Y_+\right](0)\frac{i\partial^\nu_\perp}{in_-\partial}\mathcal{B}^+_{\nu_\perp}(z_-)\right)|0\rangle$$

$$S_3(x^0;z_-) = \frac{1}{N_c}\mathrm{Tr}\,\langle 0|\bar{\mathbf{T}}\left[Y^\dagger_+(x^0)Y_-(x^0)\right] \times \mathbf{T}\left(\left[Y^\dagger_-(0)Y_+(0)\right]\frac{1}{(in_-\partial)^2}\left[\mathcal{B}^{+\mu_\perp}(z_-),\left[in_-\partial\mathcal{B}^+_{\mu\perp}(z_-)\right]\right]\right)|0\rangle$$

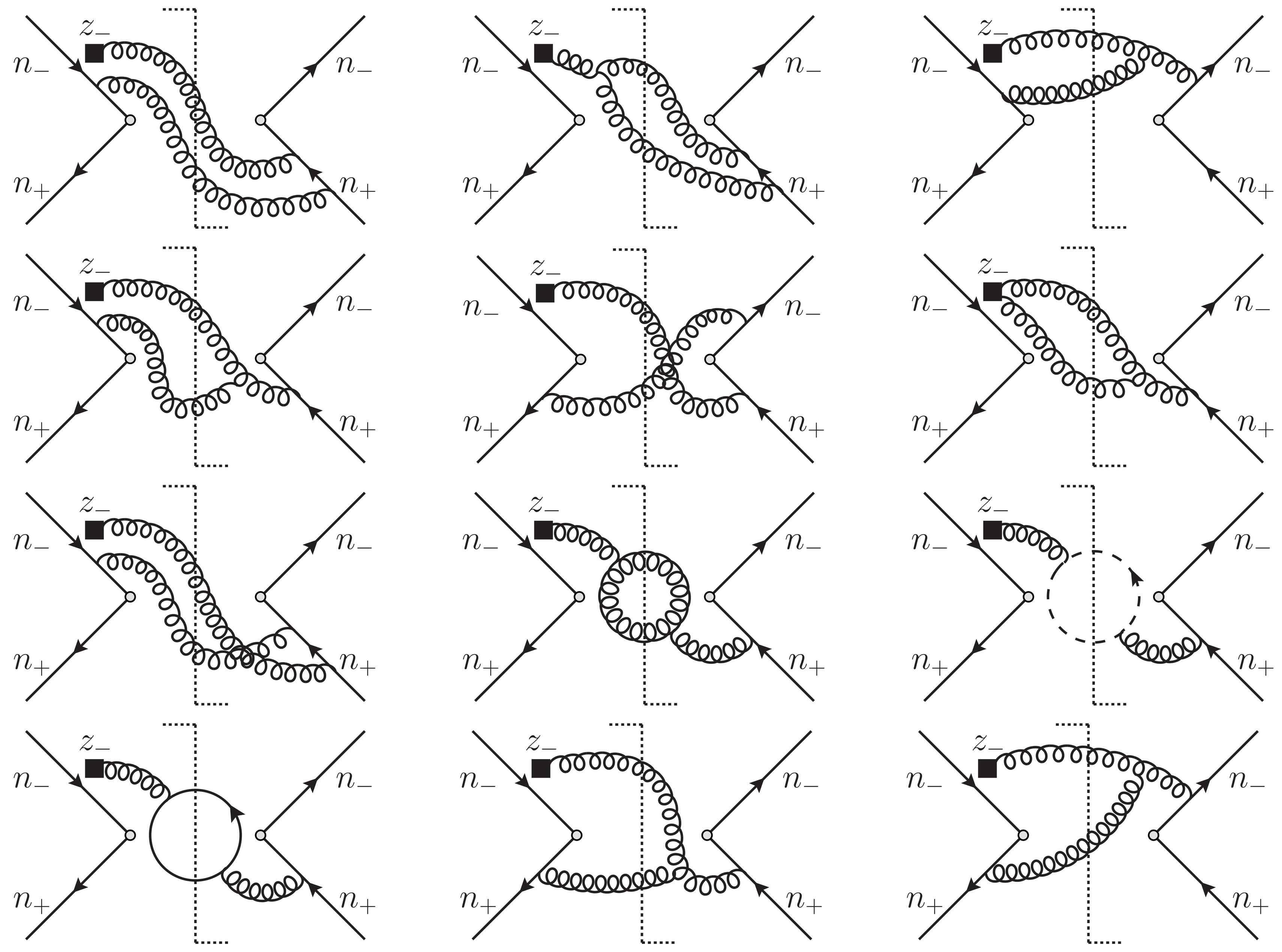

Reduction

The integrals are written as

$$\hat{I}_{\mathcal{T}}(\alpha_1,\alpha_2,\alpha_3,\alpha_4,\alpha_5,\alpha_6,\alpha_7) = (4\pi)^4\left(\frac{e^{\gamma_E}\mu^2}{4\pi}\right)^{2\epsilon}\int\frac{d^dk_1}{(2\pi)^{d-1}}\frac{d^dk_2}{(2\pi)^{d-1}}\prod_{i=1}^{7}\frac{1}{P_i^{\alpha_i}}$$

We find the 9 relevant topologies for the reduction. For example:

$$P_1 = (k_1+k_2)^2,\quad P_2 = n_+k_2,\quad P_3 = n_-(k_1+k_2),\quad P_4 = k_1^2,$$
$$P_5 = k_2^2,\quad P_6 = (\Omega - n_-k_1 - n_-k_2 - n_+k_1 - n_+k_2),\quad P_7 = (\omega - n_-k_1)$$

The four propagators in blue boxes are cut propagators. S_1 is given by

$$S_1^{(2)2r0v}(\Omega,\omega) = \frac{\alpha_s^2}{(4\pi)^2}C_F^2\frac{8\left(2-9\epsilon+9\epsilon^2\right)}{\epsilon^2\,\omega\,(\Omega-\omega)^2}\hat{I}_1$$
$$+\frac{\alpha_s^2}{(4\pi)^2}C_FC_A\Bigg[\frac{(2-3\epsilon)\left(-4\Omega+\epsilon\,(\omega+19\Omega)+4\epsilon^2\,(\omega-7\Omega)-16\epsilon^3(\omega-\Omega)\right)}{\epsilon^2(1-2\epsilon)\,\omega\,\Omega\,(\Omega-\omega)^2}\hat{I}_1$$
$$-\frac{(1-4\epsilon^2)}{\epsilon\,\omega\,\Omega}\hat{I}_2+\frac{(3\Omega-10\epsilon\,\Omega+16\epsilon^2(\omega+\Omega))}{2(1-2\epsilon)\,\omega\,\Omega}\hat{I}_3+\frac{(\Omega-3\omega)}{2\omega}\hat{I}_4$$
$$+\Omega\,\hat{I}_5+\frac{(9-20\epsilon+12\epsilon^2-2\epsilon^3)}{\epsilon^2\,(3-2\epsilon)\omega^2(\Omega-\omega)}\hat{I}_6+(\Omega-\omega)\hat{I}_7\Bigg]$$
$$-\frac{\alpha_s^2}{(4\pi)^2}C_F\,n_f\,\frac{4(1-\epsilon)^2}{\epsilon\,(3-2\epsilon)\omega^2(\Omega-\omega)}\hat{I}_6$$

Master Integrals

Four master integrals we calculate directly. The rest of master integrals form a system of DEs, which can be put into canonical form [J. Henn, 1304.1806]

$$\frac{d\vec{I}(r)}{dr} = \epsilon\,A(r)\cdot\vec{I}(r)\quad\text{with}\quad \mathrm{A(r)} = \begin{pmatrix} -\frac{1}{r}+\frac{3}{1-r} & 0 & 0 & 0\\ \frac{2}{r} & -\frac{2}{r} & 0 & 0\\ \frac{2}{r} & \frac{2}{r} & \frac{4}{1-r} & 0\\ \frac{1}{r} & \frac{1}{r} & \frac{1}{r} & -\frac{2}{r}\end{pmatrix}$$

$$I_1'(r) = \frac{2(1-r)^2}{2-9\epsilon+9\epsilon^2}I_1(r),\qquad I_3'(r) = \frac{1}{\epsilon^2}I_3(r),$$
$$I_4'(r) = -\frac{1}{\epsilon^2(1-r)}I_4(r),\qquad I_5'(r) = -\frac{1+r}{2\epsilon^2(1-r)r}I_4(r)+\frac{1}{\epsilon^2 r}I_5(r)$$

We solve iteratively, keeping d-dimensional information at boundaries. For example:

$$I_4(r) = -(1-r)^{-4\epsilon}\,e^{2\epsilon\gamma_E}\Gamma(1-\epsilon)\left[\frac{2\,\Gamma(1-2\epsilon)\Gamma(1+\epsilon)}{\Gamma(1-4\epsilon)} + \frac{\epsilon\,r^{-1-\epsilon}(1-r)^{1+\epsilon}}{(1+\epsilon)\Gamma(1-3\epsilon)}\,{}_3F_2\left(1,1-\epsilon,1+\epsilon;\,1-3\epsilon,2+\epsilon;\,\frac{r-1}{r}\right)\right]\theta(r)\theta(1-r)$$

Combining with tree-level collinear functions and integrating over ω gives cross-section results. Summing with NNLO results in [M. Beneke, A. Broggio, **SJ**, L. Vernazza, 1912.01585] we reproduce the full NNLO cross section in [R. Hamberg, W. L. van Neerven, T. Matsuura, Nucl. Phys. B359(1991) 343–405].

Cwebs beyond three loops in multiparton amplitudes

AMPLITUDES 2021

Neelima Agarwal[1], **Lorenzo Magnea**[2,3], **Sourav Pal**[4,†], **Anurag Tripathi**[4]

[1]Department of Physics, Chaitanya Bharathi Institute of Technology, Gandipet, Hyderabad, Telangana State 500075, India; [2] Theoretical Physics Department, CERN, CH-1211 Geneva 23, Switzerland; [3] Dipartimento di Fisica and Arnold-Regge Center, Università di Torino and INFN, Sezione di Torino, Via Pietro Giuria 1, I-10125 Torino, Italy; [4] Department of Physics, Indian Institute of Technology Hyderabad, Kandi, Sangareddy, Telangana State-502284, India

spalexam@gmail.com

IIT Hyderabad
Indian Institute of Technology Hyderabad

Abstract

Correlators of Wilson-line operators in non-abelian gauge theories are known to exponentiate, and their logarithms can be organised in terms of collections of Feynman diagrams called webs. We introduce the concept of Cweb, or correlator web, which is a set of skeleton diagrams built with connected gluon correlators, and we computed the mixing matrices for all Cwebs at four loops. Our results complete the required colour building blocks for the calculation of the soft anomalous dimension matrix at four-loop order. We also demonstrate that low-dimensional mixing matrices can be uniquely determined to all orders in perturbation theory from their known properties.

Introduction

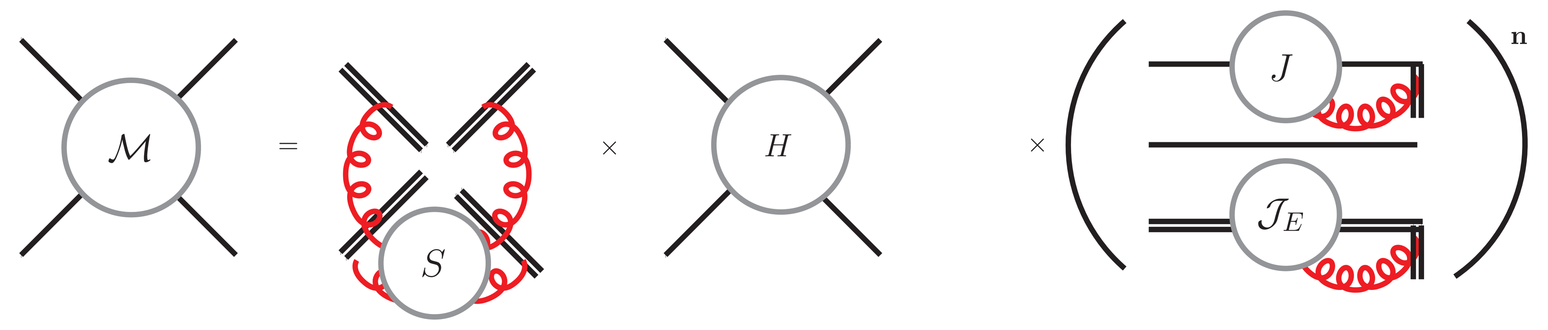

- Soft function obeys diagrammatic exponentiation in terms of webs $\mathcal{W}$, $S = \exp[\mathcal{W}]$
- A web in the multiparton case is a set of diagrams which differ only by the order of the gluon attachment on each Wilson line.

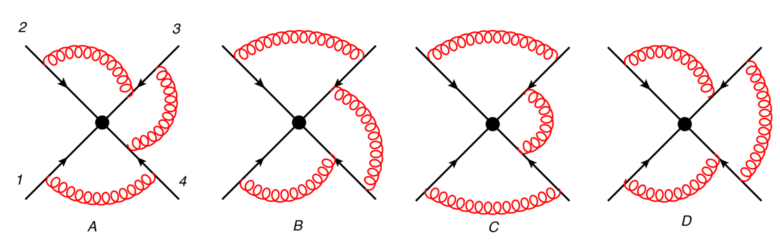

- For a diagram $D = F(D)C(D)$ a Web $\mathcal{W}$ is:

$$\mathcal{W} = \sum_D F(D)\tilde{C}(D) = \sum_{D,D'} F(D)R_{DD'}C(D)$$

Web mixing matrices

- A well known replica trick algorithm determines the mixing matrix R.
- R has following properties
  - Idempotence: $R^2 = R$, eigenvalues 1 or 0.
  - Zero-sum rows.
  - Conjecture: $\sum_D c(D)s(D) = 0$.
- All three loop mixing matrices and exponentiated colour factors are known

Cwebs

A Cweb is a set of skeleton diagrams, built out of connected gluon correlators attached to Wilson lines, closed under shuffles of gluon attachments to each Wilson line.

- Recursive algorithm to generate higher order Cwebs from lower orders

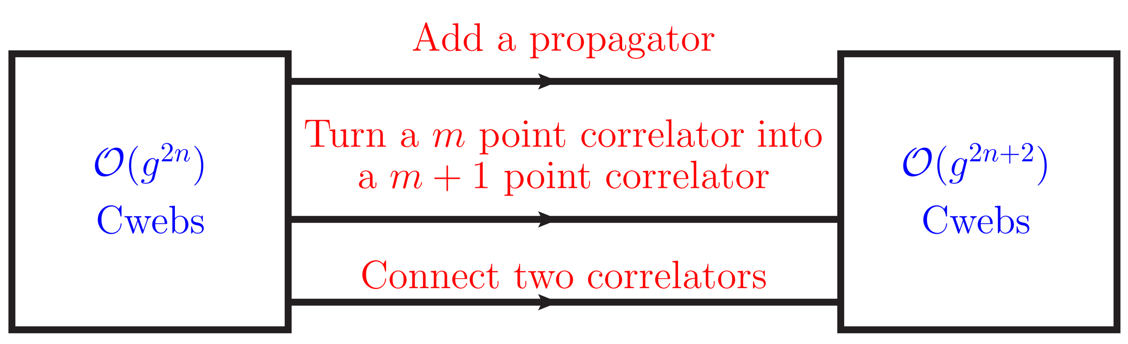

Challenges at 4 loops

- Calculation of number of Cwebs.
- At 4-loop we have 60 Cwebs .
- The largest dimension of the mixing matrix for the Cweb is 36×36.
- Results available for 3-loop has largest dimension of mixing matrix as 16×16.

Sample Results

$\mathbf{W}_4^{(1,0,1)}(1,1,2,2)$

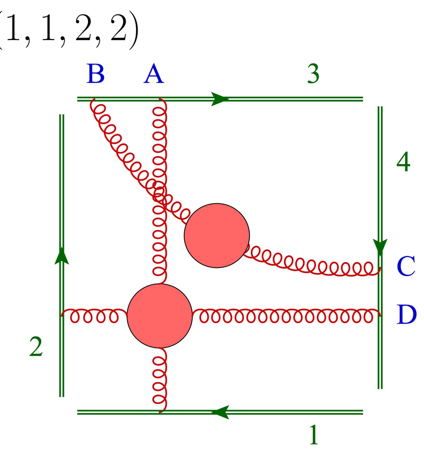

Diagrams	Sequences	S-factors
C_1	$\{\{BA\},\{CD\}\}$	1
C_2	$\{\{BA\},\{DC\}\}$	0
C_3	$\{\{AB\},\{CD\}\}$	0
C_4	$\{\{AB\},\{DC\}\}$	1

$$(YC)_1 = if^{abg}f^{cdg}f^{edh}\mathbf{T}_1^a\mathbf{T}_2^b\mathbf{T}_3^e\mathbf{T}_3^c\mathbf{T}_4^h - if^{abg}f^{cdg}f^{cej}\mathbf{T}_1^a\mathbf{T}_2^b\mathbf{T}_3^j\mathbf{T}_4^d\mathbf{T}_4^e,$$

$$(YC)_2 = -if^{abg}f^{cdg}f^{cej}\mathbf{T}_1^a\mathbf{T}_2^b\mathbf{T}_3^j\mathbf{T}_4^d\mathbf{T}_4^e,$$

$$(YC)_3 = if^{abg}f^{cdg}f^{edh}\mathbf{T}_1^a\mathbf{T}_2^b\mathbf{T}_3^e\mathbf{T}_3^c\mathbf{T}_4^h - f^{abg}f^{cdg}f^{cej}f^{edh}\mathbf{T}_1^a\mathbf{T}_2^b\mathbf{T}_3^j\mathbf{T}_4^h.$$

$$R = \begin{pmatrix} \frac{1}{2} & 0 & 0 & -\frac{1}{2} \\ -\frac{1}{2} & 1 & 0 & -\frac{1}{2} \\ -\frac{1}{2} & 0 & 1 & -\frac{1}{2} \\ -\frac{1}{2} & 0 & 0 & \frac{1}{2} \end{pmatrix}, \qquad Y = \begin{pmatrix} -1 & 0 & 0 & 1 \\ -1 & 0 & 1 & 0 \\ -1 & 1 & 0 & 0 \\ 1 & 0 & 0 & 1 \end{pmatrix}$$

- General colour structure at four loops

Direct Construction

- Construction of mixing matrices using known properties, without applying the replica trick.
- Consider generic matrix
- Apply row-sum, column-sum rule and idempotent property to fix all the elements.

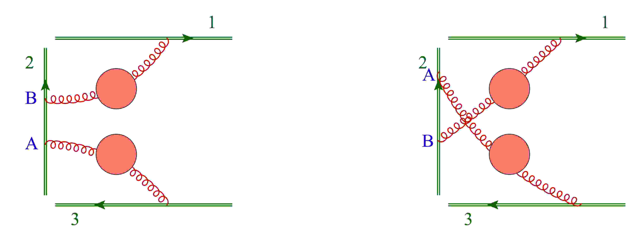

(a) s=1 (b) s=1

Diagrams for mixing matrix R_1

All order 2×2 mixing matrix:

$$R_{\text{generic}} = \begin{pmatrix} a & b \\ c & d \end{pmatrix} \quad R_1 = \begin{pmatrix} \frac{1}{2} & -\frac{1}{2} \\ -\frac{1}{2} & \frac{1}{2} \end{pmatrix} \quad R_2 = \begin{pmatrix} 1 & -1 \\ 0 & 0 \end{pmatrix}.$$

All order 3×3 mixing matrix:

$$R = \begin{pmatrix} \frac{1}{2} & 0 & -\frac{1}{2} \\ -\frac{1}{2} & 1 & -\frac{1}{2} \\ -\frac{1}{2} & 0 & \frac{1}{2} \end{pmatrix}$$

All order $p \times p$ mixing matrix (p is a prime number)

$$R = \begin{pmatrix} \frac{1}{2} & 0\,0\ldots0 & -\frac{1}{2} \\ -\frac{1}{2} & 1\,0\ldots0 & -\frac{1}{2} \\ & \ldots & \\ -\frac{1}{2} & 0\,0\ldots1 & -\frac{1}{2} \\ -\frac{1}{2} & 0\,0\ldots0 & \frac{1}{2} \end{pmatrix}.$$

Conclusions

- We have introduced Cwebs or correlator webs.
- We have developed a recursive algorithm to generate Cwebs at higher orders starting from lower orders.
- 60 Mixing matrices at four-loop were computed.
- Direct construction of all 2×2, 3×3 and $p \times p$ matrices are complete, p is prime.
- All the mixing matrices are idempotent and obey row sum rule and the column sum conjecture.
- In future determination of kinematics will complete the calculation of soft anomalous dimension at four loops.

References

[1] N. Agarwal, L. Magnea, S. Pal and A. Tripathi, JHEP **03** (2021), 188 doi:10.1007/JHEP03(2021)188 [arXiv:2102.03598 [hep-ph]].

[2] N. Agarwal, A. Danish, L. Magnea, S. Pal and A. Tripathi, JHEP **05** (2020), 128 doi:10.1007/JHEP05(2020)128 [arXiv:2003.09714 [hep-ph]].

† presenter

One-loop polytope from generalised scattering equations

Md. Abhishek, Subramanya Hegde, & Arnab Priya Saha, arXiv: 2012.10916[hep-th]

[1] Harish-Chandra Research Institute, Allahabad, India - 211019

mdabhishek@hri.res.in, subramanyahegde@hri.res.in, arnabpriyasaha@hri.res.in

Introduction

- CHY formalism maps kinematics of n scattering particles to the moduli space of n punctured $\mathbb{CP}^1$. CEGM formalism generalises this to scalar amplitudes defined as integrals on the moduli space of n punctured $\mathbb{CP}^{k-1}$. These are called amplitudes for generalised bi-adjoint scalars.
- Genralised scattering potential:

$$\mathcal{S}^{(k)} = \sum_{a_1<a_2<\cdots<a_k} s_{a_1a_2\cdots a_k} \log |a_1a_2\cdots a_k|, \tag{1}$$

where $|a_1a_2\cdots a_k|$ is the determinant of the $k\times k$ matrix with the inhomogeneous coordinates of punctures $a_1, a_2, \cdots, a_k$ as entries.

- Scattering equations:

$$E^i_a := \frac{\partial \mathcal{S}^{(k)}}{\partial x^a_i} = 0. \tag{2}$$

- The amplitude is given by,

$$m^{(k)}_n(\alpha|\beta) = \frac{1}{vol(SL(k,\mathbb{C}))}\int \prod_{a=1}^{n}\prod_{i=1}^{k-1} dx^a_i \prod_{a=1}^{n}\prod_{i=1}^{k-1}\delta(E^i_a) PT^{(k)}(\alpha) PT^{(k)}(\beta), \tag{3}$$

where for canonical ordering,

$$PT^{(k)}(\mathbb{I}) = \frac{1}{|12\cdots k||2\cdots k+1|\cdots|n-k+1\; n-k+2\cdots n|}. \tag{4}$$

- Bi-adjoint scalar amplitudes for n particle scattering are related to $\mathcal{A}_{n-3}$ polytopes which are in turn related to $Gr(2,n)$ cluster algebra. In general, CEGM amplitudes for a given k and n, are related to $Gr(k,n)$ cluster algebra. These $k>2$ amplitudes do not have a physical intepretation, as of yet.
- We provide the interpretation for $k=3, n=6$ amplitudes as polytope for the four point one-loop amplitude for the bi-adjoint scalar theory. We use the equivalence of $Gr(3,6)$ to $\mathcal{D}_4$ cluster algebra and the recent description of one-loop polytopes in terms of the $\mathcal{D}_n$ cluster algebras.

Cluster algebra and cluster fans

- An example: $Gr(2,6)$. Initial cluster is,

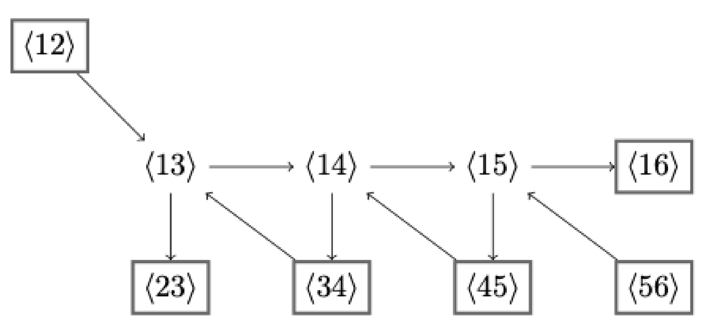

- Mutation rules define further clusters.
- Adjacency matrix: b_{ij} = (No. of arrows from i to j) − (No. of arrows from j to i).
- Cluster $\mathcal{A}$-coordinates: Determinants of the $\mathbb{CP}^{k-1}$ coordinates. Eg. $\langle 12\rangle = \epsilon^{ab}\sigma^{(1)}_a\sigma^{(2)}_b$. This is a highly redundant coordinatisation of $Gr(k,n)$.
- Cluster χ-coordinates: Eg. $x_1 = \frac{\langle 12\rangle\langle 34\rangle}{\langle 23\rangle\langle 14\rangle}$. Their number equals the number of unfrozen nodes.
- Rays and fan: Associate the rays $\mathbf{g}_i = \mathbf{e}_i$ to the unfrozen nodes of initial cluster where $\mathbf{e}_i$ are the basis of $\mathbb{R}^m$, m being the number of unfrozen nodes. There is a specific rule for the mutation of the rays. Collection of rays is called the cluster fan.

Tropicalisation and basis kinematic variables

- Tropicalisation: Multiplication becomes addition and addition becomes minimum.
- In this tropicalised description, rays of the fan separate different regions of linearity of the tropicalised cluster $\mathcal{A}$-coordinates in the tropicalised χ-coordinate space
- For eg: ray associated with $\langle 13\rangle$ unfrozen node in $Gr(2,6)$ is $\mathbf{e}_1 = (1,0,0)$ where the components are along the tropicalised χ-coordinates. The same ray can be given in tropicalised $\mathcal{A}$ coordinates as $\text{ev}(\mathbf{e}_1) = (0,0,0,0,0,0,0,0,0,1,1,1,1,1,1)$. We can obtain the associated Mandelstam variable by taking the dot product of the above vector with $\mathbf{y} = (s_{12}, s_{13}, s_{14}, s_{15}, s_{16}, s_{23}, s_{24}, s_{25}, s_{26}, s_{34}, s_{35}, s_{36}, s_{45}, s_{46}, s_{56})$. Using momentum conservation we get for the above ray,

$$\mathbf{y}\cdot \text{ev}(\mathbf{e}_1) = s_{12}. \tag{5}$$

- All the Mandelstam variables that appear as poles in the amplitude can be obtained this way by using the rays associated with the unfrozen cluster coordinates.
- Further one can write,

$$\sum_{1\le i<j\le 6} s_{ij}\log\langle ij\rangle = \sum_{\alpha} v_\alpha \log u_\alpha, \tag{6}$$

where v_α are the basis Mandelstam variables and u_α are diherdral coordinates which are useful to study the boundaries of the Moduli space.

- Rays of the fan can also be used to give the constraints for the kinematic associahedron.

$Gr(3,6)$ amplitude

- For $Gr(3,6)$ the association of rays of the fan with basis variables and $\mathcal{A}$ coordinates is no longer true as the numbers do not match.
- Remedy to this was proposed in [3] by generalising the scattering potential as,

$$F = \sum_{1\le i<j<k\le 6} s_{ijk}\log\langle ijk\rangle + s_{q_1}\log q_1 + s_{q_2}\log q_2, \tag{7}$$

where,

$$\begin{aligned} q_1 &= \langle 12[34]56\rangle = \langle 124\rangle\langle 356\rangle - \langle 123\rangle\langle 456\rangle,\\ q_1 &= \langle 23[45]61\rangle = \langle 235\rangle\langle 461\rangle - \langle 234\rangle\langle 561\rangle. \end{aligned} \tag{8}$$

.

- Basis variables were found to be

$$\begin{aligned} v_a = \{&s_{123}, s_{234}, s_{345}, s_{456}, s_{156}, s_{126},\\ &t_{1234}+s_{q_1}, t_{2345}+s_{q_2}, t_{3456}+s_{q_1}, t_{4561}+s_{q_2}, t_{5612}+s_{q_1}, t_{6123}+s_{q_2},\\ &r_{123456}+s_{q_1}, r_{234561}+s_{q_2}, r_{341256}+s_{q_1}, r_{452361}+s_{q_2}\}, \end{aligned} \tag{9}$$

- The u-coordinates are,

$$\begin{aligned} u_a = \Bigg\{&\frac{\langle 123\rangle\langle 246\rangle}{\langle 124\rangle\langle 236\rangle}, \frac{\langle 234\rangle\langle 135\rangle}{\langle 134\rangle\langle 235\rangle}, \frac{\langle 345\rangle\langle 246\rangle}{\langle 245\rangle\langle 346\rangle}, \frac{\langle 456\rangle\langle 135\rangle}{\langle 145\rangle\langle 356\rangle}, \frac{\langle 156\rangle\langle 246\rangle}{\langle 146\rangle\langle 256\rangle}, \frac{\langle 126\rangle\langle 135\rangle}{\langle 125\rangle\langle 136\rangle},\\ &\frac{\langle 12[34]56\rangle}{\langle 125\rangle\langle 346\rangle}, \frac{\langle 23[45]61\rangle}{\langle 145\rangle\langle 236\rangle}, \frac{\langle 12[34]56\rangle}{\langle 134\rangle\langle 256\rangle}, \frac{\langle 23[45]61\rangle}{\langle 136\rangle\langle 245\rangle}, \frac{\langle 12[34]56\rangle}{\langle 124\rangle\langle 356\rangle}, \frac{\langle 23[45]61\rangle}{\langle 146\rangle\langle 235\rangle},\\ &\frac{\langle 124\rangle\langle 256\rangle\langle 346\rangle}{\langle 246\rangle\langle 12[34]56\rangle}, \frac{\langle 136\rangle\langle 145\rangle\langle 235\rangle}{\langle 135\rangle\langle 23[45]61\rangle}, \frac{\langle 125\rangle\langle 134\rangle\langle 356\rangle}{\langle 135\rangle\langle 12[34]56\rangle}, \frac{\langle 146\rangle\langle 236\rangle\langle 245\rangle}{\langle 246\rangle\langle 23[45]61\rangle}\Bigg\}. \end{aligned} \tag{10}$$

- Using the above u-coordinates, we associate the kinematic basis variables for CEGM amplitudes with the kinematic variables for the one-loop $\mathcal{D}_4$ polytope according to [2] as,

$$\begin{array}{llll} X_1 \leftrightarrow s_{456} & X_2 \leftrightarrow t_{6123}+s_{q_2} & X_3 \leftrightarrow s_{123} & X_4 \leftrightarrow t_{3456}+s_{q_1}\\ \tilde{X}_1 \leftrightarrow s_{234} & \tilde{X}_2 \leftrightarrow t_{2345}+s_{q_2} & \tilde{X}_3 \leftrightarrow s_{561} & \tilde{X}_4 \leftrightarrow t_{5612}+s_{q_1}\\ X_{12} \leftrightarrow r_{234561}+s_{q_2} & X_{13} \leftrightarrow t_{4561}+s_{q_2} & X_{23} \leftrightarrow r_{452361}+s_{q_2} & X_{24} \leftrightarrow s_{345}\\ X_{34} \leftrightarrow r_{123456}+s_{q_1} & X_{31} \leftrightarrow t_{1234}+s_{q_1} & X_{41} \leftrightarrow r_{341256}+s_{q_1} & X_{42} \leftrightarrow s_{612}. \end{array} \tag{11}$$

.

- We also obtain the constraints that define the polytope in the kinematic space, they differ from that of [2] due to the choice of a different initial cluster. We have found the appropriate choice of initial clusters to relate the two descriptions.

Factorisations of the $Gr(3,6)$ amplitude

- We have used the CEGM classification of boundaries of the moduli space and mapped them to the factorisations of the $\mathcal{D}_4$ polytope.
- Eg. Let us consider the facet $X_1 = 0$ which corresponds to the propagator s_{456}. In the worldsheet the boundary is $u_1 = 0$. In terms of the punctures, there are two possibilities: 1. σ_1, σ_2 and σ_3 collide together simultaneously. In this case we have,

$$\langle 123\rangle \sim \mathcal{O}\left(\varepsilon^2\right), \qquad \langle 12a\rangle \approx \langle 13a\rangle \approx \langle 23a\rangle \sim \mathcal{O}(\varepsilon), \qquad \langle abc\rangle \sim \mathcal{O}\left(\varepsilon^0\right), \qquad a,b,c\in\{4,5,6\} \tag{12}$$

2. σ_4, σ_5 and σ_6 are collinear to each other at a rate ε. In this case we have $\langle 456\rangle \sim \mathcal{O}(\varepsilon)$ and all other determinants are of $\mathcal{O}\left(\varepsilon^0\right)$. It immediately follows that $u_1 = \frac{\langle 456\rangle\langle 135\rangle}{\langle 145\rangle\langle 356\rangle} \sim \mathcal{O}(\varepsilon)$ and goes to 0. It can also be checked that the incompatible variables, $\{\tilde{u}_2, \tilde{u}_3, \tilde{u}_4, u_{23}, u_{24}, u_{34}\} \to 1$.

- At the boundaries $X_i = 0$ or $\tilde{X}_i = 0$, $i = 1,2,3,4$, the amplitude can be expressed as a forward limit of tree-level amplitudes leading to one-loop four-point amplitudes in the bi-adjoint scalar theory.
- We use the CEGM classification of boundaries of the moduli space to reduce the $k=3, n=6$ CEGM integral into an integral over 6 punctured $\mathbb{CP}^1$.

Conclusions and future directions

- We have made explicit the relation between the $Gr(3,6)$ CEGM amplitude with the polytope for four point one loop bi-adjoint scalar amplitude.
- Factorisations of the amplitude can be given in the moduli space using the CEGM classification of boundaries of the moduli space.
- We have presented the constraints in the kinematic space for the one-loop polytope and the appropiate choice of the initial cluster using the $Gr(3,6)$ description.
- For the case of $k=3, n=7$, the $Gr(3,7)$ cluster algebra is equivalent to E_6 cluster algebra. Therefore in this case $\mathcal{D}_5$ is only a sub algebra.
- Study of subalgebras of cluster algebra from CEGM moduli space maybe interesting for applications to $Gr(4,n)$ amplitudes relevant for the study of SYM amplitudes.

References

[1] Md. Abhishek, Subramanya Hegde, and Arnab Priya Saha. One-loop integrand from generalised scattering equations. *JHEP*, 05:012, 2021.

[2] Nima Arkani-Hamed, Song He, Giulio Salvatori, and Hugh Thomas. Causal Diamonds, Cluster Polytopes and Scattering Amplitudes. 12 2019.

[3] James Drummond, Jack Foster, Ömer Gürdogan, and Chrysostomos Kalousios. Tropical Grassmannians, cluster algebras and scattering amplitudes. *JHEP*, 04:146, 2020.

Protected states in AdS_3 backgrounds from integrability (2103.16972)

Suvajit Majumder, City, University of London

PhD Supervisor: Bogdan Stefanski
Collaborators: Alessandro Torrielli, Olof Ohlsson Sax.

Introduction

- Integrability offers a novel way to prove non-renormalization theorems
- In the planar limit, integrable $\mathrm{AdS}_5 \times \mathrm{S}^5$ and $\mathrm{AdS}_4 \times \mathrm{CP}^3$ backgrounds have only one protected multiplet for each value of global charges. The corresponding string state, which maps to a half-BPS operator in the dual field theory, is often written as
$$|Z^L\rangle\,.$$
- The protected-spectrum of integrable $\mathrm{AdS}_3/\mathrm{CFT}_2$ backgrounds is much richer, with several multiplets for a given set of charges. In the integrable formulation, these extra multiplets appear because the worldsheet theory has fermionic massless excitations [6].
- Results hold across entire 20, respectively 2 dimensional moduli space for $\mathrm{AdS}_3 \times \mathrm{S}^3 \times \mathcal{M}_4$ backgrounds with $\mathcal{M}_4 = \mathrm{T}^4$ and $\mathcal{M}_4 = \mathrm{S}^3 \times \mathrm{S}^1$.
- The AdS_3 backgrounds considered in this paper have *small* $(4,4)$ superconformal symmetry. Protected states satisfy shortening conditions on both the left- and right-moving parts of the algebra
$$D_{\mathrm{L}} = J_{\mathrm{L}}\,, \qquad D_{\mathrm{R}} = J_{\mathrm{R}}\,.$$
Such half-BPS multiplets are often written in the following notation
$$(2D_{\mathrm{L}}+1, 2D_{\mathrm{R}}+1)_{\mathrm{s}}$$
- In the case of $\mathrm{AdS}_3 \times \mathrm{S}^3 \times \mathrm{T}^4$, the protected multiplets organise themselves into a family of Hodge diamonds labelled by L, which we write following [1] as
$$\begin{array}{ccccc} & & |Z^L\rangle & & \\ & |Z^L\chi^{\dot a}\rangle & & |Z^L\tilde\chi^{\dot a}\rangle & \\ \epsilon_{\dot a\dot b}\,|Z^L\chi^{\dot a}\chi^{\dot b}\rangle & & |Z^L\chi^{\dot a}\tilde\chi^{\dot b}\rangle & & \epsilon_{\dot a\dot b}\,|Z^L\tilde\chi^{\dot a}\tilde\chi^{\dot b}\rangle \\ & \epsilon_{\dot a\dot b}\,|Z^L\chi^{\dot a}\chi^{\dot b}\tilde\chi^{\dot c}\rangle & & \epsilon_{\dot a\dot b}\,|Z^L\chi^{\dot a}\tilde\chi^{\dot b}\tilde\chi^{\dot c}\rangle & \\ & & \epsilon_{\dot a\dot b}\epsilon_{\dot c\dot d}\,|Z^L\chi^{\dot a}\chi^{\dot b}\tilde\chi^{\dot c}\tilde\chi^{\dot d}\rangle & & \end{array}$$
- The protected spectrum of the $\mathrm{AdS}_3 \times \mathrm{S}^3 \times \mathrm{K3}$ theory(where $\mathrm{K3} = \mathrm{T}_4/\mathrm{Z}_n$, $n = 2,3,4,6$) is a family of Hodge diamonds labelled by integer L, with $h^{0,0} = h^{2,2} = h^{2,0} = h^{0,2} = 1$ and $h^{1,1} = 20$.

Algebraic Bethe ansatz for $\mathrm{AdS}_3 \times \mathrm{S}^3 \times \mathrm{T}^4$

- Relevant symmetry algebras: $\mathrm{psu}(1|1)^2_{\text{c.e.}}$ and $\mathrm{psu}(1|1)^4_{\text{c.e.}}$. Generators satisfy the commutation relations
$$\{\mathrm{Q}_{\mathrm{L}},\mathrm{S}_{\mathrm{L}}\} = \mathrm{H}_{\mathrm{L}}, \qquad \{\mathrm{Q}_{\mathrm{R}},\mathrm{S}_{\mathrm{R}}\} = \mathrm{H}_{\mathrm{R}}, \qquad \{\mathrm{Q}_{\mathrm{L}},\mathrm{Q}_{\mathrm{R}}\} = \mathrm{C}, \qquad \{\mathrm{S}_{\mathrm{L}},\mathrm{S}_{\mathrm{R}}\} = \bar{\mathrm{C}}\,.$$
- Exact $\mathrm{psu}(1|1)^2_{\text{c.e.}}$-invariant R matrices
$$R^{\mathrm{LL}}(p,q) = \begin{pmatrix} A_{pq} & 0 & 0 & 0 \\ 0 & B_{pq} & E_{pq} & 0 \\ 0 & C_{pq} & D_{pq} & 0 \\ 0 & 0 & 0 & -F_{pq} \end{pmatrix}, \qquad R^{\tilde{\mathrm{L}}\tilde{\mathrm{L}}}(p,q) = \begin{pmatrix} A_{pq} & 0 & 0 & 0 \\ 0 & B_{pq} & -E_{pq} & 0 \\ 0 & -C_{pq} & D_{pq} & 0 \\ 0 & 0 & 0 & -F_{pq} \end{pmatrix},$$
where the entries are functions of Zhukovski variables $x^{\pm}_p, x^{\pm}_q$. For e.g. in the normalisation where $A_{pq} = 1$, we have $B_{pq} = \left(\frac{x^-_p}{x^+_p}\right)^{1/2} \frac{x^+_p - x^+_q}{x^-_p - x^+_q}$.
- The Zhukovski variables $x^{\pm}_p$ are related to the momentum p through the relations
$$\frac{x^+_p}{x^-_p} = e^{ip}, \qquad x^+_p + \frac{1}{x^+_p} - x^-_p - \frac{1}{x^-_p} = \frac{2i(|m| + \hbar p)}{h}.$$
which are solved in the physical region by
$$x^{\pm}_p = \frac{(|m| + \hbar p) + \sqrt{(|m| + \hbar p)^2 + 4h^2 \sin^2\frac{p}{2}}}{2h \sin\frac{p}{2}} e^{\pm\frac{ip}{2}}, \qquad \hbar = \frac{k}{2\pi}.$$
- The $\mathrm{psu}(1|1)^4$ R-matrix is the graded tensor product of the $\mathrm{psu}(1|1)^2$ R-matrices
$$R_{\mathrm{psu}(1|1)^4} = R^{\mathrm{LL}}_{\mathrm{psu}(1|1)^2} \otimes R^{\tilde{\mathrm{L}}\tilde{\mathrm{L}}}_{\mathrm{psu}(1|1)^2}.$$
- The $\mathrm{psu}(1|1)^2_{\text{c.e.}}$ algebra, the $\mathrm{psu}(1|1)^4_{\text{c.e.}}$ monodromy matrix can be written as a product of two 2×2 $\mathrm{psu}(1|1)^2_{\text{c.e.}}$ monodromy matrices. We denote the components of this smaller matrix, and the associated transfer matrix by
$$\mathcal{M}^I(p_0) = \begin{pmatrix} \mathcal{A}^I(p_0) & \mathcal{B}^I(p_0) \\ \mathcal{C}^I(p_0) & \mathcal{D}^I(p_0) \end{pmatrix}, \qquad \mathcal{T}^I(p_0) = \mathrm{str}_0\, \mathcal{M}^I(p_0)\,.$$
where the index $I = 1,3$ labels the two copies of $\mathrm{psu}(1|1)^2_{\text{c.e.}}$
- Eigenstates built from
$$|\vec p; \vec{y_1}; \vec{y_3}\rangle \equiv \mathcal{B}^1(y_{1,1}) \cdots \mathcal{B}^1(y_{1,N_1}) \mathcal{B}^3(y_{3,1}) \cdots \mathcal{B}^3(y_{3,N_3})\, |\chi_{p_1} \cdots \chi_{p_{N_0}}\rangle\,.$$
where $\vec p = \{p_1, \dots, p_{N_0}\}$ and $\vec{y_I} = \{y_{I,1}, \dots, y_{I,N_I}\}$
- Bethe equations
$$1 = \prod_{j=1}^{N_0} \sqrt{\frac{x^+_j}{x^-_j}} \frac{y_{I,k} - x^-_j}{y_{I,k} - x^+_j}, \qquad k = 1, \dots, N_I, \qquad I = 1,3\,.$$
$$\left(\frac{x^+_k}{x^-_k}\right)^L = \prod_{\substack{j=1\\ j\neq k}}^{N_0} \sqrt{\frac{x^-_k}{x^+_k}\frac{x^+_j}{x^-_j}} \frac{x^+_k - x^-_j}{x^-_k - x^+_j} (\sigma^{\circ\circ}_{kj})^2 \prod_{j=1}^{N_1} \sqrt{\frac{x^+_k}{x^-_k}} \frac{x^-_k - y_{1,j}}{x^+_k - y_{1,j}} \prod_{j=1}^{N_3} \sqrt{\frac{x^+_k}{x^-_k}} \frac{x^-_k - y_{3,j}}{x^+_k - y_{3,j}}\,.$$

Protected states from Bethe ansatz wave functions

- Protected states do not receive corrections to their energies and since the dispersion relation depends on the magnon momentum p_k, protected states come from zero-momentum magnons only
- We can label protected states by the number of momentum-carrying and auxiliary roots
$$|N_0, N_1, N_3\rangle \equiv |\vec p = \vec 0; \vec{y_1} = \vec s_{\pm}; \vec{y_3} = \vec s_{\pm}\rangle\,.$$
- Auxiliary roots $y_{I,j}$ also take special values for protected states $y_{I,j} = s_{\pm}$ with $s_{\pm}$ defined below
$$s_+ \equiv \lim_{p\to 0^+} x^{\pm}_p = \frac{\hbar + \sqrt{\hbar^2 + h^2}}{h}, \qquad s_- \equiv \lim_{p\to 0^-} x^{\pm}_p = \frac{\hbar - \sqrt{\hbar^2 + h^2}}{h} = -\frac{1}{s_+},$$
which become ± 1 for $\hbar = 0$.
- We can equivalently write the above states in the following notation(c.f. SUGRA calculations of Boer et al)
$$|N_0, N_1, N_3\rangle \equiv (L + N_1 + N_3 - N_0 + 1, L + 1)_{\mathrm{s}}\,.$$
- The protected states can be summarised as follows, where superscripts indicate the $\mathrm{su}(2)_\circ$ representations
$$\begin{array}{ccccc} & & |0,0,0\rangle^1 & & \\ & |1,0,0\rangle^2 & & |1,1,1\rangle^2 & \\ |2,0,0\rangle^1 & & |2,1,1\rangle^{1\oplus 3} & & |2,2,2\rangle^1 \\ & |3,1,1\rangle^2 & & |3,2,2\rangle^2 & \\ & & |4,2,2\rangle^1 & & \end{array}$$
which leads to Hodge numbers $h^{0,0} = h^{2,2} = h^{2,0} = h^{0,2} = 1\,, h^{1,0} = h^{0,1} = h^{2,1} = h^{1,2} = 2\,, h^{1,1} = 4$
- These states match the Hodge diamond of the seed T^4 theory and, since they depend additionally on L through the BMN vacuum $|0,0,0\rangle$, we match the expected protected spectrum.

Protected states in $\mathrm{AdS}_3 \times \mathrm{S}^3 \times \mathrm{K3}$ orbifolds

- The $n = 2$ untwisted sector protected spectrum is
$$\begin{array}{ccccc} & & |0,0,0\rangle & & \\ & \varnothing & & \varnothing & \\ |2,0,0\rangle & & |2,1,1\rangle^{\oplus 4} & & |2,2,2\rangle \\ & \varnothing & & \varnothing & \\ & & |4,2,2\rangle & & \end{array}$$
- The $n > 2$ untwisted sector protected spectrum is
$$\begin{array}{ccccc} & & |0,0,0\rangle & & \\ & \varnothing & & \varnothing & \\ |2,0,0\rangle & & |2,1,1\rangle^{\oplus 2} & & |2,2,2\rangle \\ & \varnothing & & \varnothing & \\ & & |4,2,2\rangle & & \end{array}$$
- We have dropped the superscript denoting the $\mathrm{su}(2)_\circ$ representations, since $\mathrm{su}(2)_\circ$ is broken by the orbifold and each multiplet above has multiplicity one.
- Twisted sectors: only the massless momentum-carrying Bethe equations change. The twisted-sector boundary conditions are implemented in the Bethe equations by an additional phase $e^{-i\phi_0}$ where ϕ_0 is
$$\phi_0 = \pm\frac{2\pi}{n}\,.$$
- Counting of protected multiplets in the twisted sectors matches the Hodge number counting: there are 16, respectively 18, twisted sector multiplets in the Z_2, respectively $\mathrm{Z}_{n>2}$, orbifolds.

References

[1] Marco Baggio, Olof Ohlsson Sax, Alessandro Sfondrini, Bogdan Stefański jr., and Alessandro Torrielli. "Protected string spectrum in $\mathrm{AdS}_3/\mathrm{CFT}_2$ from worldsheet integrability". In: *JHEP* 04 (2017), p. 091. DOI: 10.1007/JHEP04(2017)091. arXiv: 1701.03501 [hep-th].

[2] Jan de Boer. "Six-dimensional supergravity on $\mathrm{S}^3 \times \mathrm{AdS}_3$ and 2d conformal field theory". In: *Nucl. Phys.* B548 (1999), pp. 139–166. DOI: 10.1016/S0550-3213(99)00160-1. arXiv: hep-th/9806104 [hep-th].

[3] Diego Bombardelli, Bogdan Stefański, and Alessandro Torrielli. "The low-energy limit of $\mathrm{AdS}_3/\mathrm{CFT}_2$ and its TBA". In: *JHEP* 10 (2018), p. 177. DOI: 10.1007/JHEP10(2018)177. arXiv: 1807.07775 [hep-th].

[4] Riccardo Borsato, Olof Ohlsson Sax, Alessandro Sfondrini, and Bogdan Stefański jr. "The complete $\mathrm{AdS}_3 \times \mathrm{S}^3 \times \mathrm{T}^4$ worldsheet S-matrix". In: *JHEP* 1410 (2014), p. 66. DOI: 10.1007/JHEP10(2014)066. arXiv: 1406.0453 [hep-th].

[5] Thomas Lloyd, Olof Ohlsson Sax, Alessandro Sfondrini, and Bogdan Stefański jr. "The complete worldsheet S matrix of superstrings on $\mathrm{AdS}_3 \times \mathrm{S}^3 \times \mathrm{T}^4$ with mixed three-form flux". In: *Nucl. Phys.* B891 (2015), pp. 570–612. DOI: 10.1016/j.nuclphysb.2014.12.019. arXiv: 1410.0866 [hep-th].

[6] Olof Ohlsson Sax, Bogdan Stefański jr., and Alessandro Torrielli. "On the massless modes of the $\mathrm{AdS}_3/\mathrm{CFT}_2$ integrable systems". In: *JHEP* 1303 (2013), p. 109. DOI: 10.1007/JHEP03(2013)109.

ster

LAPLACE METHOD FOR SINGLE-LOOP DIAGRAMS OF ELASTIC PROTON SCATTERING

T. Yushkevych, N. Chudak, O. Potiienko, I. Sharph

e-mail: zebra2368@gmail.com
Odessa State Polytechnic University

Problem statement

Due to the strong interaction, the processes of proton collision are described by phenomenological theories Our aim is to describe such processes by the dynamic theory. We suggest the multiparticle fields theory for this purpose. Here we wish to describe the elastic proton collision. Namely, the differential cross section of proton scattering, because it has a characteristic non-monotonic form.

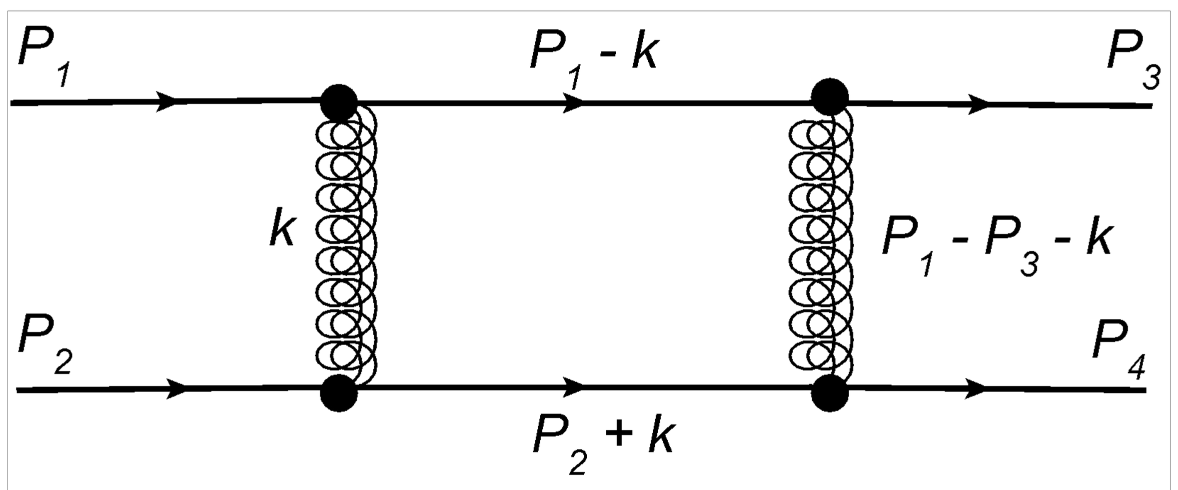

Fig. 2: The simplest loop diagram of elastic proton scattering. P_1, P_2 - four-momenta of input protons, P_3, P_4 - four-momenta of output protons, k, $P_1 - k$, $P_2 + k$, $P_1 - P_3 - k$ - four-momenta of virtual particles. The double lines correspond to the bound state of gluons - glueballs.

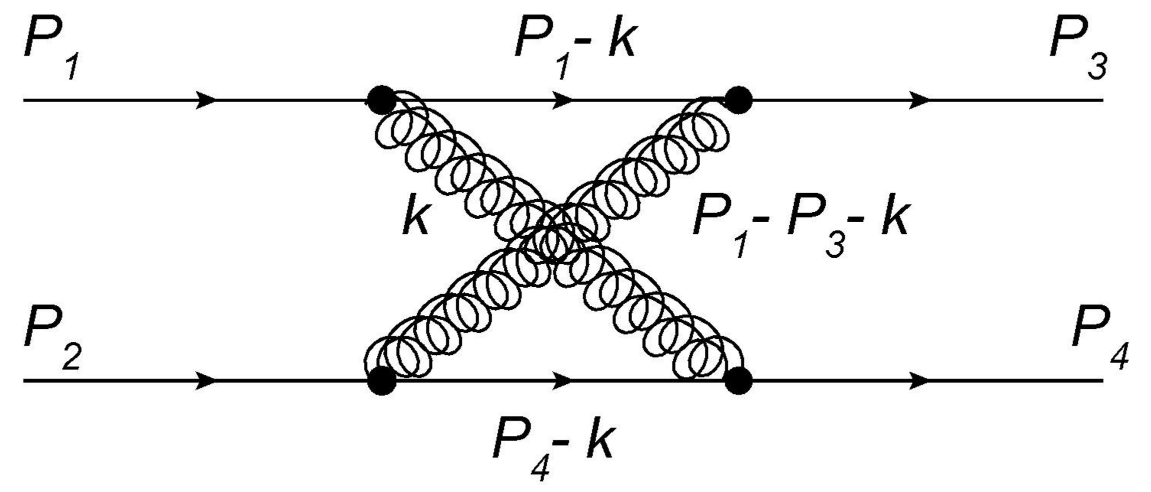

Fig. 3: The simplest loop diagram of elastic proton scattering. P_1, P_2 - four-momenta of input protons, P_3, P_4 - four-momenta of output protons, k, $P_1 - k$, $P_4 - k$, $P_1 - P_3 - k$ - four-momenta of virtual particles. The double lines correspond to the bound state of gluons - glueballs.

In order to describe the differential cross section of scattering, we need to describe loop diagrams. The purpose of this work is to calculate the model of the differential cross section of elastic scattering within the method of multiparticle fields, based on the non-loop diagrams as well as diagrams of Fig. 2, Fig. 3, and the diagrams obtained from Fig. 2, Fig. 3 by permutation of particle lines in the final state. We aim to compare the results of the calculation with the known experimental data and to find out whether it is possible to describe the experimentally observed effects of non-monotonicity in the differential cross section dependence on the square of the transmitted four-momentum within the considered model.

Here we calculate only single-loop diagrams, but later we plan to apply this method for more loops.

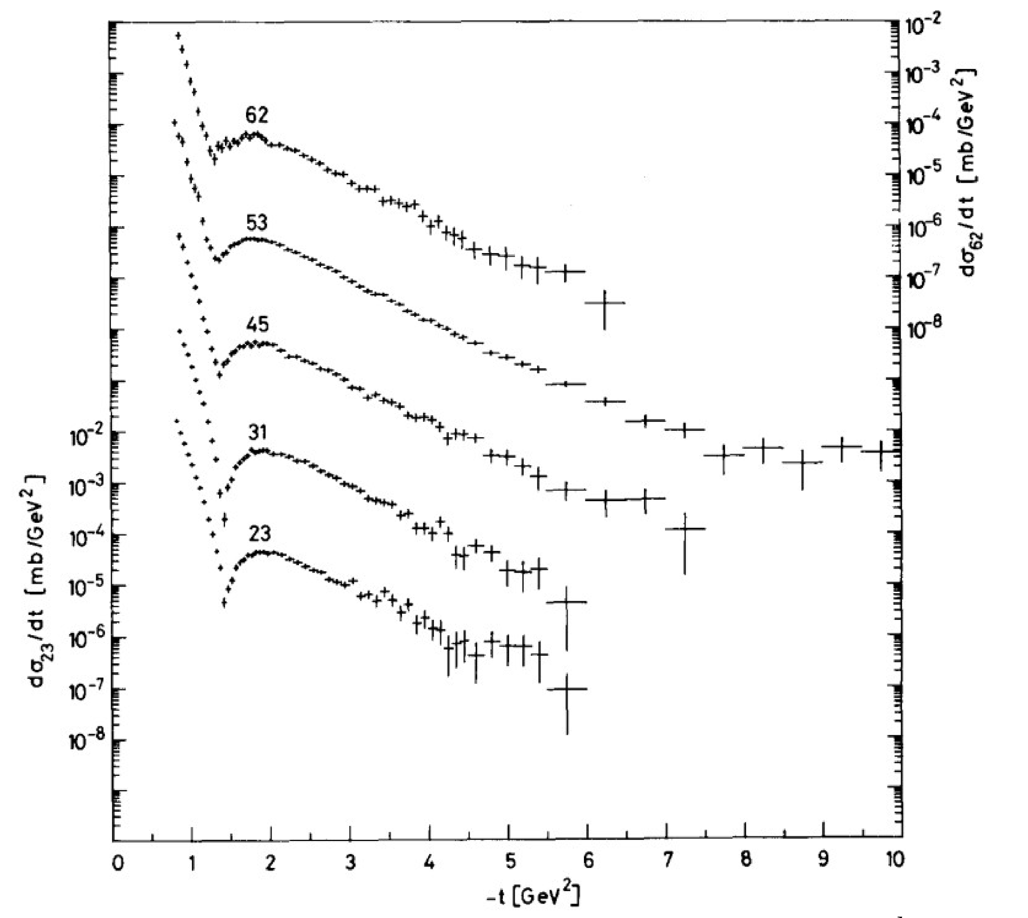

Fig. 1: Graph of the dependence of the differential cross section $\frac{d\sigma_{el}}{dt}(x)$ on the square of the transmitted four-momentum t, taken from [1]

The analytical expression for the diagram of Fig. 2 has the form:

$$A=\lim_{\varepsilon\to+0}\frac{(ig)^4}{(2\pi)^6}\left(\bar{v}^{+}_{\nu_3}(P_4)\right)_{s_4}\gamma^{a}_{s_4 s_2}\left(\bar{v}^{-}_{\nu_2}(P_2)\right)_{s_2}\left(\bar{v}^{+}_{\nu_4}(P_3)\right)_{s_3}\gamma^{b}_{s_3 s_1}\left(\bar{v}^{-}_{\nu_1}(P_1)\right)_{s_1}\times\delta\left((P_3+P_4)-(P_1+P_2)\right)\times$$

$$\times\int d^4k\,(k_a+2P_{2a})(2P_{1b}-k_b)\frac{1}{M_p^2-(P_1-k)^2-i\varepsilon}\frac{1}{M_p^2-(P_1+k)^2-i\varepsilon}\times$$

$$\times\frac{1}{M_G^2-k^2-i\varepsilon}\frac{1}{M_G^2-(P_1-P_3-k)^2-i\varepsilon}$$

Here g is the effective coupling constant, M_p and M_G – masses of proton and glueball, respectively, $\left(\bar{v}^{+}_{\nu_3}(P_4)\right)_{s_4}$, $\left(\bar{v}^{-}_{\nu_2}(P_2)\right)_{s_2}$, $\left(\bar{v}^{+}_{\nu_4}(P_3)\right)_{s_3}$, $\left(\bar{v}^{-}_{\nu_1}(P_1)\right)_{s_1}$ are the solutions of Dirac's equations, $\gamma^{a}_{s_4 s_2}$ - elements of Dirac matrices. All quantities are normalized by the mass of proton. M_G and g are considered as adjustable parameters. We need to calculate the limits of four-dimensional integrals over virtual four momenta k, which determine the tensor components at $\varepsilon \to +0$. We will denote it further as a tensor t_{ab}:

$$t_{ab}=\lim_{\varepsilon\to+0}\int d^4k\,(k_a+2P_{2a})(2P_{1b}-k_b)\frac{1}{M_p^2-(P_1-k)^2-i\varepsilon}\frac{1}{M_p^2-(P_1+k)^2-i\varepsilon}\times\frac{1}{M_G^2-k^2-i\varepsilon}\times\frac{1}{M_G^2-(P_1-P_3-k)^2-i\varepsilon}.$$

Each of the indices a and b takes four values from 0 to 3.

The problem is not in the large dimensionality of the integrals, but in the fact that **it is actually necessary to calculate the limit from the multidimensional integral when approaching zero parameters that bypass the poles of the integrand**. In this case, the passage to the limit cannot be performed before the calculation of the integral, because the poles are falling inside the integration domain and the integral loses its meaning. The need to calculate the integral before the boundary transition limits the possibility of applying numerical methods to calculate the integral. This is because the passage to the limit will require calculation at small parameter values at which the poles become close to the integration domain. It complicates the numerical calculation.

Consider an arbitrary Feynman diagram. Let us denote the number of integration variables as n, and the integration variables as $x_1, x_2, \ldots, x_n$. Their whole set will be denoted as $\{x\}$. Then we write the tensor of dimension k for this diagram:

$$t_{a_1 a_2 \ldots a_k}=\lim_{\varepsilon\to+0}\int dx_1\,dx_2\ldots dx_n\frac{f_{a_1 a_2\ldots a_k}(x)}{(z_1(x)-i\varepsilon)(z_2(x)-i\varepsilon)\ldots(z_l(x)-i\varepsilon)}$$

Here l is the number of Feynman denominators corresponding to the diagram (according to the number of internal lines of the diagram), $f_{a_1 a_2\ldots a_k}(x)$ - the tensor which is determined by the numerators of Feynman propagation functions (chronological pairings), $z_a(x)$, $a=1,2,\ldots,l$ - functions from integration variables that determine Feynman denominators.

We represent the denominators as an exponent in the power of the logarithm and get the epsilon parameter in the denominator. Further, integration substituting the integration variable, according to the relation $x_1 = x_1(x_1, x_2, \ldots, x_n) + \varepsilon y_1$, we get the epsilon in the numerator. Thus, we can reduce the epsilon in the numerator and denominator and direct the remaining parameters of the epsilon to zero.

But then there is the problem that **maybe several denominators equal to zero on a subset on which the first denominator is zero**.

To avoid this problem, instead of the equation $z_1(x)=0$, one could similarly consider a system of equations of the form:

$$\begin{cases} z_{a_1}(x)=0, \\ z_{a_2}(x)=0, \\ \ldots\ldots\ldots\ldots, \\ z_{a_r}(x)=0 \end{cases}.$$

Here $a_1, a_2, \ldots, a_r$ is some subset of the set of indices 1,2,..., l of expressions $z_a(x)$. The number of these expressions r and the values of the indices $a_1, a_2, \ldots, a_r$ are chosen so that the system of equations was consistent. However, adding another equation of the form $z_{a_{r+1}}(x)=0$ yields an incompatible system, i.e. the system without solutions. The system of equations defines such a subset of the integration domain on which the maximum number of denominators at $\varepsilon\to+0$ would take zero values.

Calculation of analytical expressions of a Feynman diagram with one loop using the Laplace method

Now let us apply the Laplace's method to pass to the limit. To do this, we introduce the notation $f_{ab}(k^0,\vec{k})$ for the tensor numerator, choose the center-of-mass system, and write the tensor:

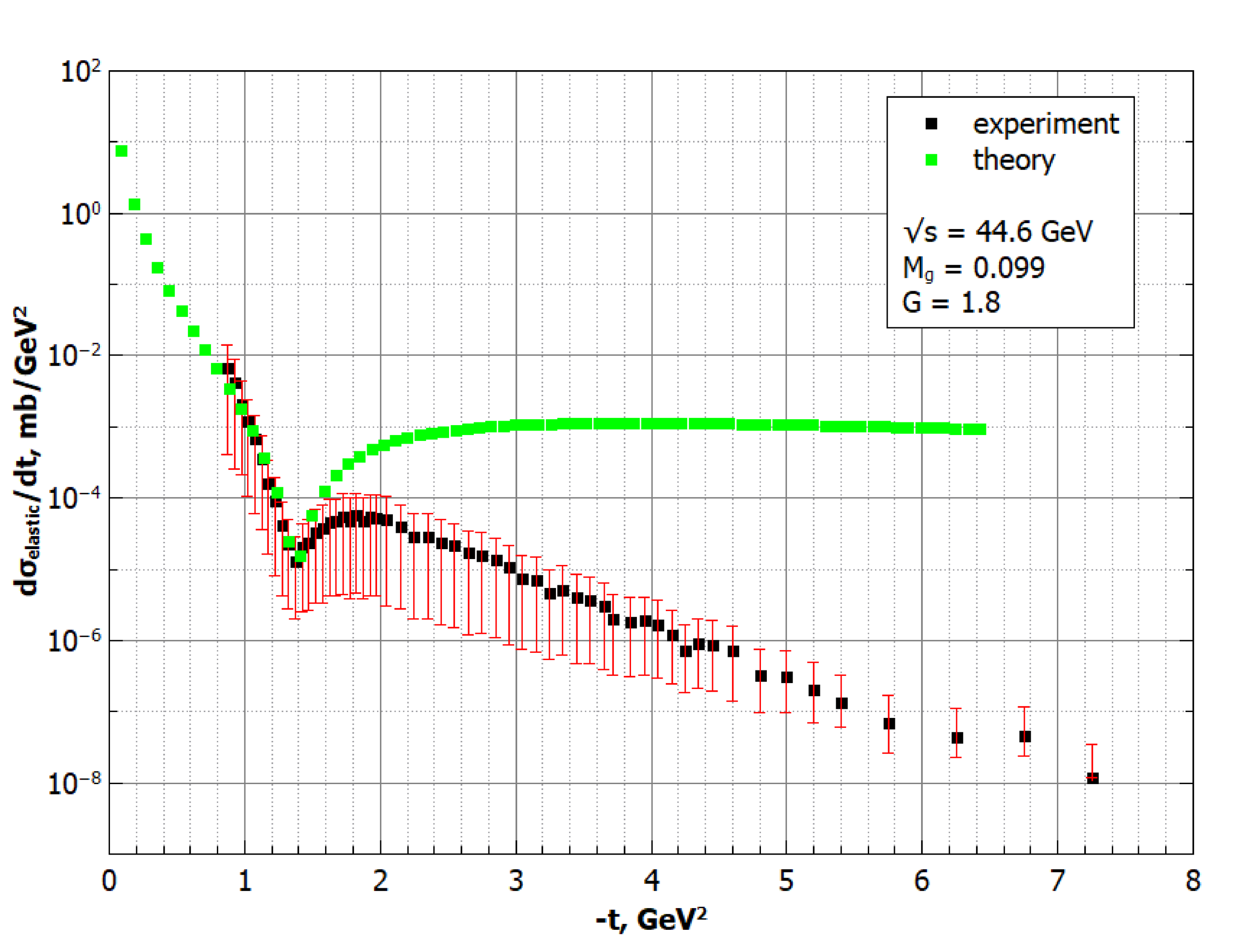

Fig. 4: Comparison of the dependence of the differential cross section dσ/dt on the square of the transmitted four-momentum t at energy $\sqrt{s}$ = 44.6 GeV calculated according to the model described in this work (green dots) with the experiment (black dots) [1]

$$t_{ab}=\int_{-\infty}^{\infty}dk^0\int d\vec{k}\,f_{ab}(k^0,\vec{k})\;\frac{1}{M_p^2-(\frac{\sqrt{s}}{2}+k^0)^2+(\vec{k}-\vec{P}_1)^2-i\varepsilon}\,\frac{1}{M_p^2-(\frac{\sqrt{s}}{2}-k^0)^2+(\vec{k}-\vec{P}_1)^2-i\varepsilon}\,\frac{1}{M_G^2-(k^0)^2+\vec{k}^2-i\varepsilon}\,\frac{1}{M_G^2-(k^0)^2+\vec{P}_1-\vec{P}_3-\vec{k}^2-i\varepsilon}$$

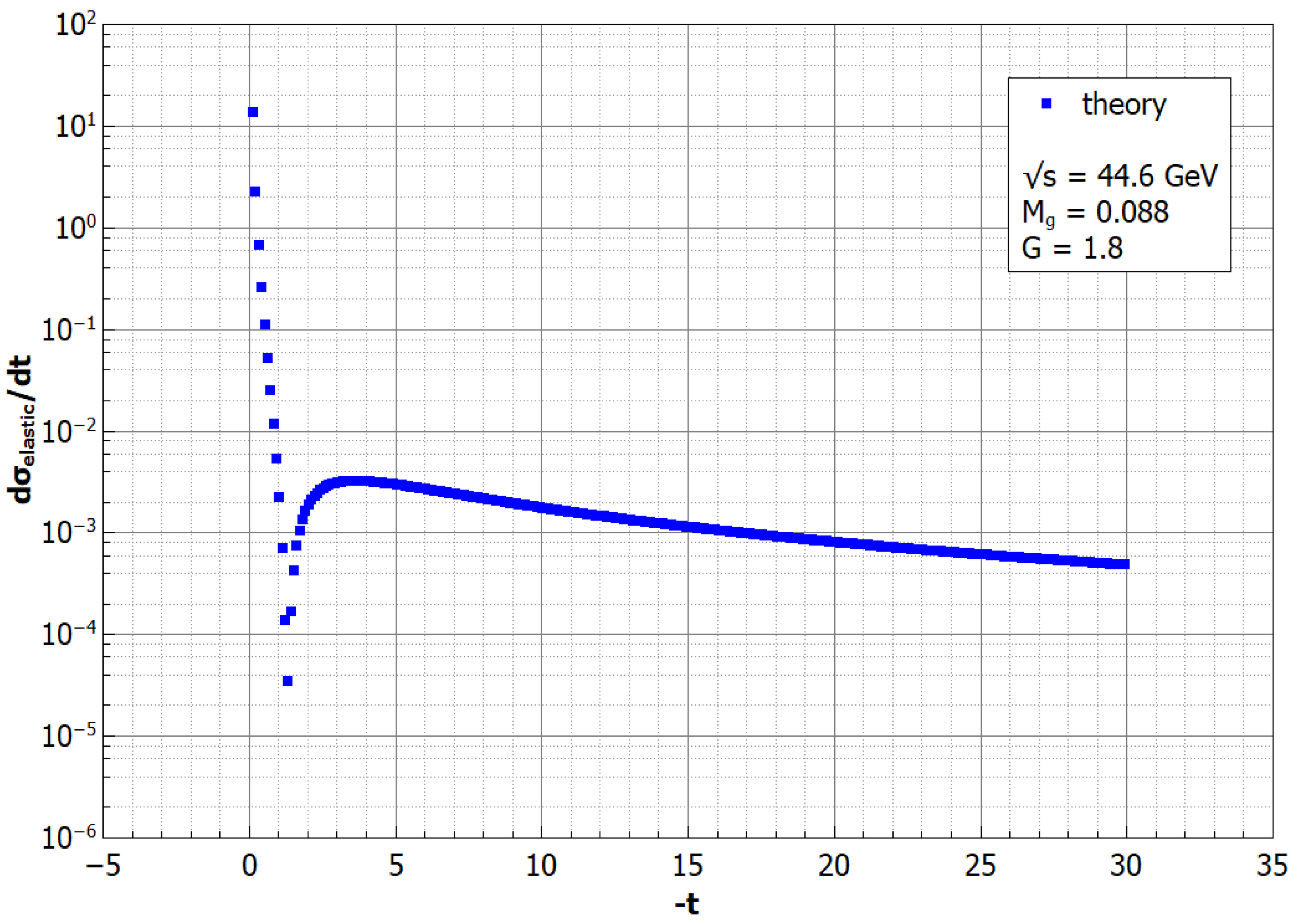

Fig. 5: Comparison of the dependence of the differential cross section dσ/dt on the square of the transmitted four-momentum t at energy $\sqrt{s}$ = 44.6 GeV calculated according to the model described in this work (t is non-dimensioned by the square of the proton mass and dσ/dt - on the inverse square of the proton mass)

In [4] it was shown that either the first pair of denominators, which correspond to the horizontal lines in the diagram Fig. 2, or the second pair of denominators, corresponding to two vertical lines, can become zero at the same time. Consider the system of equations of the first two denominators. Put the real parts equal to zero, then $1/\varepsilon^2$ remains, which gives the maximum contribution to the integrand.

Next, we apply the Laplace method to calculate the denominators of the horizontal and vertical lines of the Feynman diagram separately.

The model has two adjustable parameters: M_G - the mass of the glueball and G - the strong interaction constant. We also plotted the diagrams for energies of 22,4 and 30.5 GeV and compared these plots with the same adjustable parameters.

Conclusions

- We show that the method of multiparticle fields leads to dynamic models that can be used to describe experiments on the scattering of multiquark systems and to achieve agreement with experimental data at least at the level of qualitative coincidence.
- The application of the Laplace method to calculate loop diagrams allows their approximate calculation, but is still quite tedious and needs further improvement.
- The experimentally observed effects of non-monotonicity of the dependence of the differential cross section of elastic proton scattering on the square of the transmitted four-momentum in our model are the consequences of spin effects. Taking these effects into account in the non-loop and simplest loop diagrams led to the qualitative coincidence with the experiment. The obtained results suggest that further consideration of more complex loop diagrams with more than one loop will allow to achieve a quantitative coincidence with the experimental results.

[1] Nagy E. at al. Measurements of elastic proton-proton scattering at large momentum transfer at the CERN intersecting storage rings//Nuclear Physics B.-1979-Vol.150.-P.244
[2] I.M. Dremin, Advances in physical sciences, **187**, 353 (2017).
[3] D.A. Ptashynskiy et al., arXiv:1905.07233 [physics.gen-ph] (2019).
[4] Sharph I. V., Zelentsova T. M., Chudak N. O. et al. Laplace method for the simplest diagrams of elastic scattering of scalar particles. – 2020. – 2003.07321.
[5] D.A. Ptashynskiy et al., Ukrainian Journal of Physics, **64**, 732 (2019).
[6] Nicolaas G De Bruijn, Asymptotic methods in analysis; 1st ed. Bibl. Matematica. North-Holland, Amsterdam (1958).

Celestial Dual Superconformal Symmetry, MHV Amplitudes and Differential Equations

Yangrui Hu, Lecheng Ren, Akshay Yelleshpur Srikant and Anastasia Volovich

Department of Physics, Brown University

Based on arXiv: 2106.16111

Abstract

Celestial and momentum space amplitudes for massless particles are related to each other by a change of basis provided by the Mellin transform. Therefore properties of celestial amplitudes have counterparts in momentum space amplitudes and vice versa. In this work, we study the celestial avatar of dual superconformal symmetry of $\mathcal{N}=4$ Yang-Mills theory. We also analyze various differential equations known to be satisfied by celestial n-point tree-level MHV amplitudes and identify their momentum space origins.

Motivations

The quest for flat space holography has recently received a boost owing to the realization that scattering amplitudes in 4D flat spacetime can be recast as correlation functions of a 2D conformal field theory living on the celestial sphere [1]–[3]. Then the celestial CFT (CCFT) becomes a potential candidate for a holographic description of the flat space S-matrix. A path towards a better understanding of CCFTs involves translating well understood aspects of momentum space amplitudes into statements about celestial correlators, as well as mapping momentum space amplitudes onto the celestial sphere.

In this work, we look at this problem from the both sides: we study the celestial avatar of the dual superconformal symmetry of $\mathcal{N}=4$ Yang-Mills; we also identify the momentum space origins of various differential equations satisfied by celestial n-point tree level MHV amplitudes.

Celestial Dual Superconformal Symmetry

Let us first rewrite the expression for the generators $K^{\alpha\dot{\alpha}}$ and $\mathcal{S}_\alpha^A$ given in [4] in a more compact form

$$\mathcal{K}^{\alpha\dot{\alpha}} = -\sum_{i<j}\left(\tilde{\lambda}_i^{\dot{\alpha}}\lambda_j^{\alpha}D_{j,i} + \lambda_i^{\alpha}\tilde{\lambda}_i^{\dot{\alpha}}\right),$$

$$\mathcal{S}_\alpha^A = -\sum_{i<j}\left(\lambda_{j,\alpha}\eta_i^A D_{j,i} + \lambda_{i,\alpha}\eta_i^A\right).$$

where we have made use of momentum conservation and also introduced the operator

$$D_{i,j} \;=\; \lambda_j^\alpha\frac{\partial}{\partial\lambda_i^\alpha} \;-\; \tilde{\lambda}_{i,\dot{\beta}}\frac{\partial}{\partial\tilde{\lambda}_{j,\dot{\beta}}} \;-\; \sum_A \eta_i^A\frac{\partial}{\partial\eta_j^A},$$

Let $\mathcal{O}$ be an operator acting on the amplitude. The corresponding operator $\tilde{\mathcal{O}}$, which acts on the celestial amplitude is defined by

$$\tilde{\mathcal{O}}\tilde{\mathcal{A}}_n := \int\left(\prod_{i=1}^n \frac{d\omega_i}{\omega_i}\omega_i^{\Delta_i}\right)\mathcal{O}\mathcal{A}_n.$$

Then the operator $\tilde{\mathcal{K}}^{\alpha\dot{\alpha}}$ and $\tilde{\mathcal{S}}_\alpha^A$ act on the celestial amplitude as

$$\begin{aligned}\tilde{\mathcal{K}}^{\alpha\dot{\alpha}} =& \sum_{i<j}\Bigg\{\begin{pmatrix}1 & \bar{z}_i\\ z_j & \bar{z}_i z_j\end{pmatrix}\Bigg[2\epsilon_i e^{\frac{\partial}{\partial\Delta_i}}\left(\Delta_j + J_j - z_{ij}\frac{\partial}{\partial z_j}\right) + 2\epsilon_j e^{\frac{\partial}{2\partial\Delta_i}+\frac{\partial}{2\partial\Delta_j}}\sum_A \eta_j^A\frac{\partial}{\partial\eta_i^A}\\ &-2\epsilon_j e^{\frac{\partial}{\partial\Delta_j}}\left(\Delta_i - J_i + \bar{z}_{ij}\frac{\partial}{\partial\bar{z}_i}\right)\Bigg] - 2\epsilon_i e^{\frac{\partial}{\partial\Delta_i}}\begin{pmatrix}1 & \bar{z}_i\\ z_i & z_i\bar{z}_i\end{pmatrix}\Bigg\}\end{aligned}$$

$$\begin{aligned}\tilde{\mathcal{S}}_\alpha^A =& \sqrt{2}\sum_{i<j}\Bigg\{\begin{pmatrix}-z_j\\ 1\end{pmatrix}\Bigg[\epsilon_i\eta_i^A e^{\frac{\partial}{2\partial\Delta_i}}\left(\Delta_j + J_j - z_{ij}\frac{\partial}{\partial z_j}\right) + \epsilon_j e^{\frac{\partial}{2\partial\Delta_j}}\eta_i^A\sum_B \eta_j^B\frac{\partial}{\partial\eta_i^B}\\ &-\epsilon_j\eta_i^A e^{\frac{\partial}{\partial\Delta_j}-\frac{\partial}{2\partial\Delta_i}}\left(\Delta_i - J_i + \bar{z}_{ij}\frac{\partial}{\partial\bar{z}_i}\right)\Bigg] - \epsilon_i\eta_i^A e^{\frac{\partial}{2\partial\Delta_i}}\begin{pmatrix}-z_i\\ 1\end{pmatrix}\Bigg\}.\end{aligned}$$

Differential Equations

- **The celestial tree-level MHV n-point amplitude** is given by the Mellin transform of the amplitude w.r.t. to ω_i [3], [5]

$$\begin{aligned}\tilde{\mathcal{M}}_n(J_i,\Delta_i,z_i,\bar{z}_i) \;=&\; \int\left[\prod_{i=1}^n\frac{d\omega_i}{\omega_i}\omega_i^{\Delta_i}\right]\mathcal{M}_n(h_i,\omega_i,z_i,\bar{z}_i)\\ :=&\; \mathcal{N}(z_i,\bar{z}_i)\,\delta\left(\sum_i(\Delta_i-1)\right)F\left(x_{a,b},\Delta_i\right),\end{aligned}$$

  where $F\left(x_{a,b},\Delta_i\right)$ is the Aomoto-Gelfand hypergeometric function. We find that momentum conservation and $GL(n-4)$ transformations reduce to the well-known first-order defining PDEs of AG function.

- **Momentum conservation**: the total momentum celestial operator is $\tilde{\mathbb{P}}^\mu = \sum_{i=1}^n \epsilon_i\, q_i^\mu e^{\frac{\partial}{\partial\Delta_i}}$ and we define 4 vectors v_b^μ s.t. $v_b^\mu\,\epsilon_a\, q_{a\mu} = -U x_{a,b}$, $b = \{n-3,\, n-2,\, n-1,\, n\}$.

$$\tilde{\mathbb{P}}^\mu\tilde{\mathcal{M}}_n = 0 \;\Rightarrow\; \sum_{i=1}^n \epsilon_i\, v_{b\mu}\, q_i^\mu e^{\frac{\partial}{\partial\Delta_i}}\tilde{\mathcal{M}}_n = 0 \;\Rightarrow\; \sum_{a=1}^{n-4} x_{a,b}\frac{\partial F}{\partial x_{a,b}} = \alpha_b F$$

- $GL(n-4)$ **transformations:** using the momentum conserving delta function we can solve for arbitrary 4 ω's and these are equivalent representations up to $GL(n-4)$ transformations. This property of $\tilde{\mathcal{M}}_n$ gives rises to

$$\alpha_a F + \sum_{b=n-3}^{n} x_{a,b}\frac{\partial F}{\partial x_{a,b}} \;=\; -F \;\;,\;\; 1 \le a \le n-4$$

- **Generalized Banerjee-Ghosh (BG) equation**
  We derive momentum space generalizations of the differential equations found in [6] by connecting them to the behaviour of amplitudes under BCFW shifts:

$$\lambda_i \;\to\; \hat{\lambda}_i \;=\; \lambda_i + z\,\lambda_j \qquad \tilde{\lambda}_j \;\to\; \hat{\tilde{\lambda}}_j \;=\; \tilde{\lambda}_j - z\,\tilde{\lambda}_i.$$

  For infinitesimal z, this shift is implemented on $\mathcal{M}_n$ by the $D_{i,j}$ operator we introduced before.

$$D_{i,j}\,\mathcal{M}_n \;=\; \mathcal{M}_n\left(-\frac{\langle i-1,j\rangle}{\langle i-1,i\rangle} - \frac{\langle i+1,j\rangle}{\langle i+1,i\rangle} + 4\frac{\langle j,t\rangle}{\langle i,t\rangle}\delta_{i,s} + 4\frac{\langle j,s\rangle}{\langle i,s\rangle}\delta_{i,t}\right)$$

  Mapping this to the celestial sphere and taking $J_i = +$, we get

$$\begin{aligned}&\left[-\left(\Delta_i + z_{ij}\frac{\partial}{\partial z_i}\right) + \frac{z_{i-1,j}}{z_{i-1,i}} + \frac{z_{i+1,j}}{z_{i+1,i}} - 1\right]\tilde{\mathcal{M}}_n\\ &+\;\epsilon_i\epsilon_j\left(\Delta_j - J_j - 1 + \bar{z}_{ji}\frac{\partial}{\partial\bar{z}_j}\right)e^{\frac{\partial}{\partial\Delta_i}-\frac{\partial}{\partial\Delta_j}}\tilde{\mathcal{M}}_n \;=\; 0\end{aligned}$$

  which generalizes the color-stripped BG equation.

- **Connect to BG equation:** without loss of generality, we choose $i=1$. After some manipulation, the color-stripped BG equation can be brought to the form

$$\begin{aligned}\Bigg[&\left(\alpha_1 + 1 + \sum_{b=n-3}^{n} x_{1,b}\frac{\partial}{\partial x_{1,b}}\right) - \sum_b\frac{\epsilon_2}{\epsilon_1}\left(x_{2,b} + \bar{z}_{1,2}\frac{\partial x_{2,b}}{\partial\bar{z}_2}\right)\left(\frac{\partial}{\partial x_{1,b}} - \frac{\partial}{\partial x_{2,b}}e^{\frac{\partial}{\partial\Delta_1}-\frac{\partial}{\partial\Delta_2}}\right)\\ &-\frac{\epsilon_2}{\epsilon_1}e^{\frac{\partial}{\partial\Delta_1}-\frac{\partial}{\partial\Delta_2}}\left(\alpha_2 + 1 + \sum_b x_{2,b}\frac{\partial}{\partial x_{2,b}}\right)\Bigg]F = 0\end{aligned}$$

  which shows that it reduces to combinations of the hypergeometric equations. The orange term is identically zero based on the integral representation of F.

References

[1] S. Pasterski, S.-H. Shao, and A. Strominger, "Flat Space Amplitudes and Conformal Symmetry of the Celestial Sphere," *Phys. Rev. D*, vol. 96, no. 6, p. 065026, 2017. DOI: `10.1103/PhysRevD.96.065026`. arXiv: `1701.00049 [hep-th]`.

[2] S. Pasterski and S.-H. Shao, "Conformal basis for flat space amplitudes," *Phys. Rev. D*, vol. 96, no. 6, p. 065022, 2017. DOI: `10.1103/PhysRevD.96.065022`. arXiv: `1705.01027 [hep-th]`.

[3] S. Pasterski, S.-H. Shao, and A. Strominger, "Gluon Amplitudes as 2d Conformal Correlators," *Phys. Rev. D*, vol. 96, no. 8, p. 085006, 2017. DOI: `10.1103/PhysRevD.96.085006`. arXiv: `1706.03917 [hep-th]`.

[4] J. M. Drummond, J. M. Henn, and J. Plefka, "Yangian symmetry of scattering amplitudes in N=4 super Yang-Mills theory," *JHEP*, vol. 05, F. Liu, Z. Xiao, and P. Zhuang, Eds., p. 046, 2009. DOI: `10.1088/1126-6708/2009/05/046`. arXiv: `0902.2987 [hep-th]`.

[5] A. Schreiber, A. Volovich, and M. Zlotnikov, "Tree-level gluon amplitudes on the celestial sphere," *Phys. Lett. B*, vol. 781, pp. 349–357, 2018. DOI: `10.1016/j.physletb.2018.04.010`. arXiv: `1711.08435 [hep-th]`.

[6] S. Banerjee and S. Ghosh, "MHV Gluon Scattering Amplitudes from Celestial Current Algebras," Oct. 2020. arXiv: `2011.00017 [hep-th]`.

AMPLITUDES 2021
AUGUST 16th–20th

The Wilson-loop *dlog* Representation for Feynman Integrals

Song He, Zhenjie Li, Yichao Tang, and Qinglin Yang

Introduction

The duality between scattering amplitudes and (super-)Wilson-loops (WL) [1] in planar $\mathcal{N}=4$ super-Yang-Mills theory (SYM) prompts the study of individual Feynman integrals from this point of view. Our attempts in this direction reveal that:

- Put in $\mathrm{d}\log$ forms, integrals become easily computable;
- Integrals such as the "ladders" have rich analytic structures.

Example: Pentagon

To illustrate our method, consider the chiral pentagon integral Ω_1.

$$\Omega_1 = \int \mathrm{d}^4\ell \frac{\langle \ell \bar{i} \cap \bar{j}\rangle\langle Iij\rangle}{\langle\!\langle \ell i\rangle\!\rangle\langle\!\langle \ell j\rangle\!\rangle\langle \ell I\rangle} = \int \mathrm{d}^4\ell \int_0^\infty \mathrm{d}^2\tau \frac{\langle \ell \bar{i}\cap\bar{j}\rangle\langle Iij\rangle}{\langle \ell iX\rangle^2\langle \ell jY\rangle^2\langle \ell I\rangle} = \int_0^\infty \mathrm{d}^2\tau \frac{\langle I\bar{i}\cap\bar{j}\rangle\langle Iij\rangle}{\langle iXjY\rangle\langle iXI\rangle\langle jYI\rangle}. \quad (*)$$

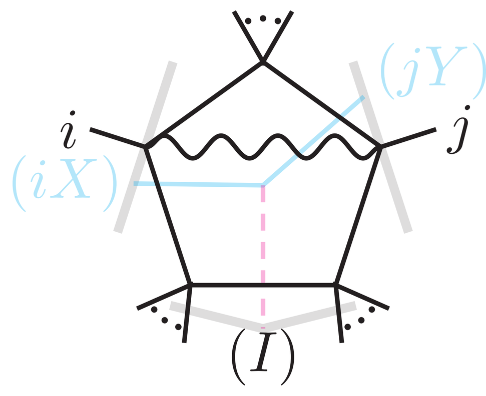

Here, we have performed a partial Feynman parametrization on $\frac{1}{\langle\!\langle \ell i\rangle\!\rangle} := \frac{1}{\langle \ell i{-}1 i\rangle\langle \ell i i{+}1\rangle} = \int_0^\infty \frac{\mathrm{d}\tau_X}{\langle \ell iX\rangle^2}$, where $X := Z_{i-1} - \tau_X Z_{i+1}$, and similarly for $\frac{1}{\langle\!\langle \ell j\rangle\!\rangle}$. These have the interpretation of fermion insertions along WL edges i and j. The remaining propagator $\frac{1}{\langle \ell I\rangle}$ acts as a scalar interacting with the fermions through Yukawa coupling in the dual spacetime. In the last step, we have used the famous star-triangle identity to perform the loop integral.

The above integral is easily put in $\mathrm{d}\log$ form by partial fractioning:

$$\Omega_1 = \int \mathrm{d}\log \frac{\langle jYI\rangle}{\langle jYiI\cap\bar{i}\rangle}\,\mathrm{d}\log\frac{\langle iXjY\rangle}{\langle iXI\rangle}.$$

Moreover, since the Feynman parameters $\tau_{X,Y}$ are projective, we may rescale $\tau \mapsto \alpha\tau$ arbitrarily. Choosing α wisely, we espress the $\mathrm{d}\log$ form using dual-conformally-invariant (DCI) variables only:

$$\Omega_1 = \int \mathrm{d}\log \frac{\tau_Y+1}{v(1-uw)\tau_Y + (1-u)}\,\mathrm{d}\log\frac{\tau_X+1}{u(\tau_Y+vw)\tau_X + (\tau_Y+v)}.$$

From this expression, it is straightforward to get a manifestly DCI result—the symbol and function can be obtained from linearly-reducible $\mathrm{d}\log$ integrals purely algebraically.

Application: Double Pentagon

The most general double pentagon and its degenerations consititute the entire 2-loop MHV amplitudes in planar $\mathcal{N}=4$ SYM. They also give many components of NMHV amplitudes [2]. By applying $(*)$ to one of the loops, we can reduce the most general double pentagon to a two-fold integral of a hexagon:

$$I_{\text{dp}} = [\text{diagram}] = \int_0^\infty \mathrm{d}^2\tau \frac{\langle ijkl\rangle}{\langle iXjY\rangle} \times [\text{diagram}]$$

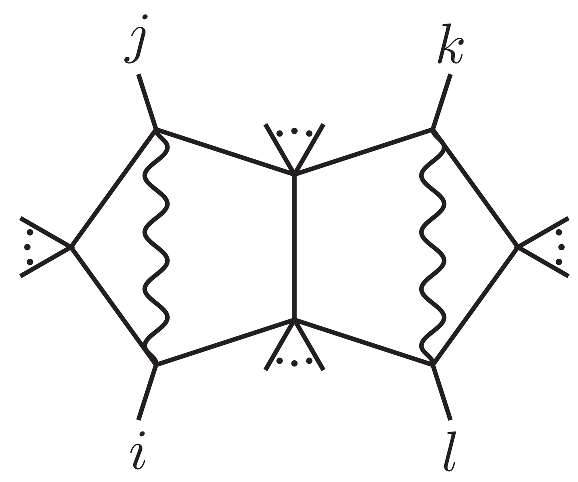

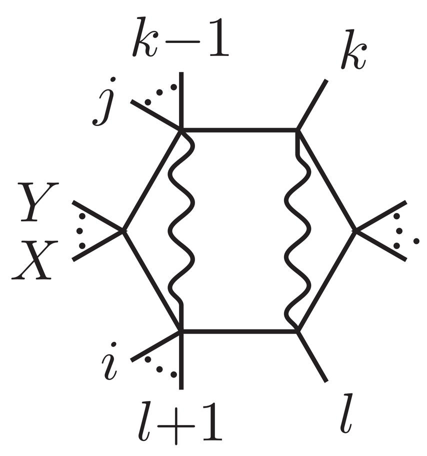

To put it in $\mathrm{d}\log$ form, expand the remaining hexagon to a linear combination of weight-2 scalar box integrals. Miraculously, the coefficients combine with the prefactor $\frac{\langle ijkl\rangle}{\langle iXjY\rangle}$ into nice $\mathrm{d}\log$ forms:

$$I_{\text{dp}} = \int [x, x_k] I_{x,x_k} - (k{-}1 \leftrightarrow k{+}1) - (\bar{k} \leftrightarrow \bar{l}) + [x,y] I_{x,y},$$

where $I_{a,b}$ are scalar box integrals with propagators a and b shrinked, and $[a,b]$ denote the corresponding $\mathrm{d}\log\wedge\mathrm{d}\log$ prefactors [3]. The symbol is easily computed, once proper rationalization is done to make $\mathrm{d}\log$ arguments linearly-reducible. The result contains 164 rational letters and 96 algebraic letters, and the algebraic part cancels out between $I_{\text{dp}}(i,j,k,l)$ and $I_{\text{dp}}(j,k,l,i)$ in the NMHV amplitudes.

Penta-Ladder-Type Integrals

An interesting class of Feynman integrals is the penta-ladder-type, whose defining feature is a chiral pentagon subgraph at the end of a ladder. We consider only the IR-finite integrals for simplicity.

Penta-ladder-type integrals satisfy a recursion relation [4]:

$$\mathcal{I}_L = [\text{diagram}]$$

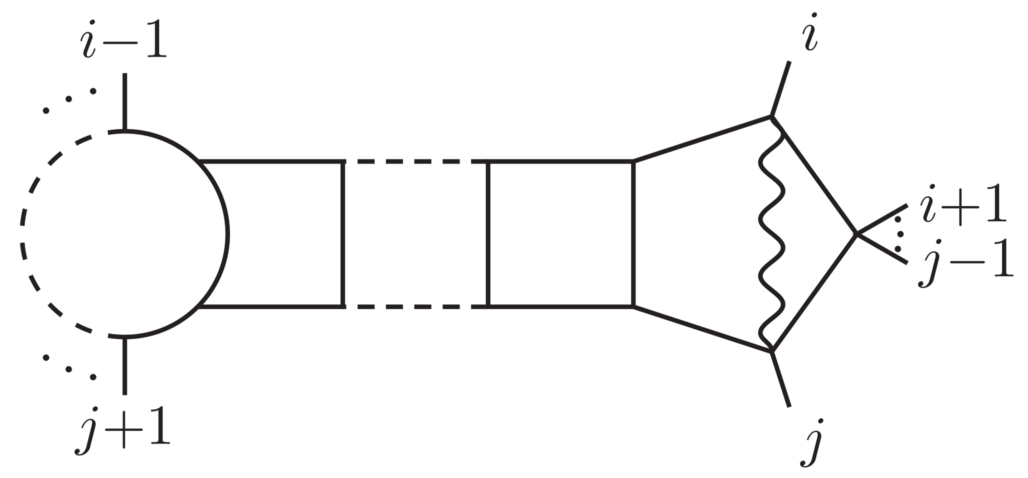

$$= \int [\text{diagram}] \times \mathrm{d}\log(\tau_Y{+}1)\,\mathrm{d}\log\frac{\tau_X{+}1}{\tau_X}$$

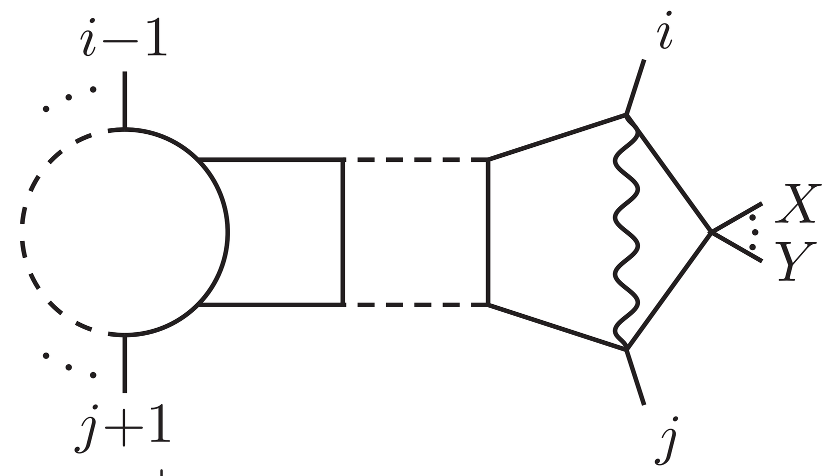

$$= \int \mathcal{I}_{L-1}\Big|_{\substack{i+1\to X\\ j-1\to Y}} \times \mathrm{d}\log(\tau_Y{+}1)\,\mathrm{d}\log\frac{\tau_X{+}1}{\tau_X}.$$

The deform-then-integrate can be performed for X and Y separately:

$$\mathcal{I}_L = \int \mathrm{d}\log(\tau_Y{+}1) \times \mathcal{I}_{L-\frac{1}{2}}\,|_{j-1\to Y}\,,\qquad \mathcal{I}_{L-\frac{1}{2}} = \int \mathrm{d}\log\frac{\tau_X{+}1}{\tau_X} \times \mathcal{I}_{L-1}\,|_{i+1\to X}\,,\qquad \mathcal{I}_1 = [\text{diagram}].$$

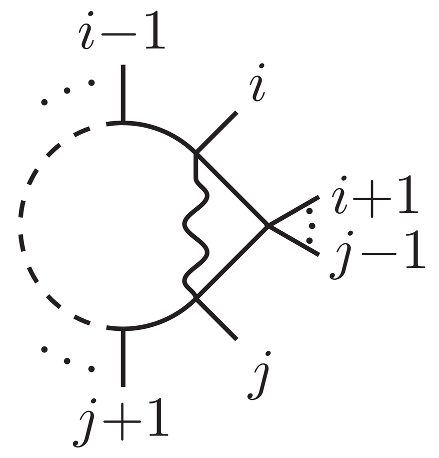

The thus-defined "$(L-\frac{1}{2})$-loop" integrals have odd transcendental weight, and their physical meaning is generally unclear.

It is always possible to expand $\mathcal{I}_1$ to scalar boxes. Thus, a penta-ladder-type integral can be written as $2(L-1)$-fold $\mathrm{d}\log$ integrals of weight-2 functions. In the special case of penta-ladder, the 1-loop integral Ω_1 has its own $\mathrm{d}\log$ form, so the integral becomes a $2L$-fold recursive $\mathrm{d}\log$ integral.

In the cases of penta-ladder and double-penta-ladder, the $\mathrm{d}\log$ representation allows us to recursively prove that their symbol alphabets form certain cluster algebras [5]:

	8pt penta-	7pt double-penta-	8pt double-penta-
$\mathcal{I}_L$	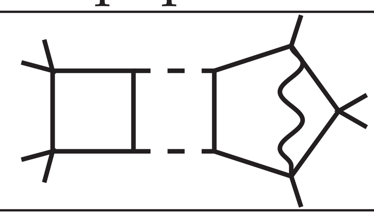	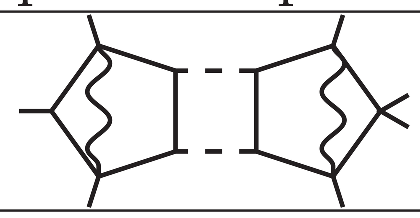	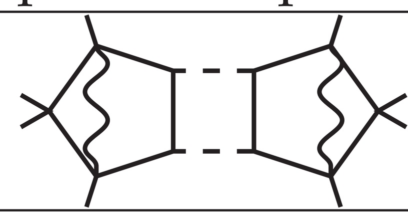
$\mathcal{I}_1$	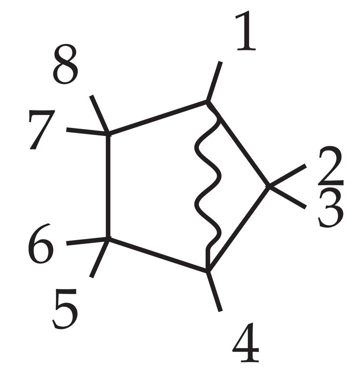	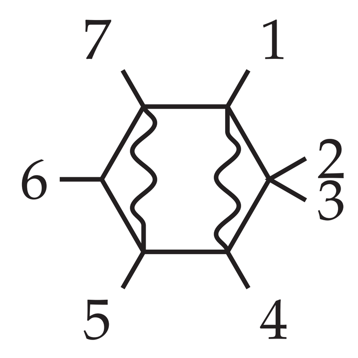	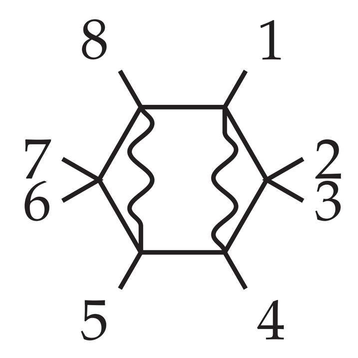
cluster algebra	D_3	D_4	affine D_4 (trunc.)

Outlook

- Study the IR-divergent integrals with proper regularization;
- Find applications to the study of amplitudes (e.g., in 2d);
- Search for a geometric interpretation of the $\mathrm{d}\log$ form;
- Explore the origin of cluster structures.

References

[1] S. Caron-Huot, *JHEP 07 (2011) 058.*
[2] N. Arkani-Hamed, J. L. Bourjaily, F. Cachazo, and J. Trnka, *JHEP 06 (2012) 125.*
[3] S. He, Z. Li, Q. Yang, and C. Zhang, *Phys.Rev.Lett. 126 (2021) 231601.*
[4] S. He, Z. Li, Y. Tang, and Q. Yang, *JHEP 05 (2021) 052.*
[5] S. He, Z. Li, and Q. Yang, arxiv: *2106.09314.*

Wave scattering in Black Hole backgrounds

Yilber Fabian Bautista [1,2]
With Alfredo Guevara, Chris Kavanagh and Justin Vines.
[1] *Perimeter Institute for Theoretical Physics*
[2] *Department of Physics & Astronomy, York University*

Abstract

We revisit the scattering of waves of helicity $h < 2$ in the Schwarzschild and Kerr backgrounds in the long-wave regime. The classical wave scattering is computed in terms of $2 \to 2$ QFT amplitudes in flat spacetime, which are shown to correspond to Newmann-Penrose amplitudes obtained from solving the Regge-Wheeler/Teukolsky equation in the spinless/spinning scenario. Finally, in the small scattering angle limit, we argue that the wave scattering admits a universal point particle description, determined by the eikonal approximation. The scattering phase at 2PM (G^2) for a spinning and 3PM (G^3) for a spinless BH is provided and shown to agree with known results in the literature.

1.Schwarzschild scattering

The radiative content for wave perturbations of the Schwarzschild BH (SBH) is encoded by the asymptotic form of the Neumann-Penrose (NP) scalars

$$\Psi_h(t,r,\theta,\phi) \propto \frac{1}{r} e^{-iEt} \sum_{l=0}^{\infty} D_r^h R_\ell(r)\ {}_hY_{\ell 0}(\theta,\phi)\,,$$

where ${}_hY_{\ell m}$ are spherical harmonics of spin-weight/helicity h, $R_\ell(r)$ are solutions to the Regge-Wheeler equation and D_r^h is a differential operator trivial for $h=0$. A vacuum solution to the wave equation consist of an incoming plane wave $\Psi^{\rm PW}$ and an outgoing scattered wave $\Psi^{\rm S}$: $\Psi = \Psi^{\rm PW} + \Psi^{\rm S}$.
The key observable is the differential cross section, which measures the angular profile of the flux from the scattered wave $\frac{d\sigma}{d\Omega} = \lim_{r\to\infty} r^2 |\Psi^S|^2 = |f(\theta,\phi)|^2$. For instance, for scalar waves the amplitude function is

$$f(\theta) = \frac{2\pi}{i\omega} \sum_{l=0}^{\infty} Y_{l0}(0,0) Y_{l0}(\theta,0)\left(e^{2i\delta_l} - 1\right), \quad (1)$$

where the phase shift $e^{2i\delta_l}$ is directly related to R_l, once the boundary condition for the total wave of being purely 'ingoing' at the horizon is imposed.

Long wavelength scattering

The solution (1) is formally exact. In order to find closed expressions, we restrict to the long wave regime, where $\epsilon = 2GM\omega \ll 1$. To leading order in ϵ, the scalar solution is

$$f(\theta) = GM \frac{\Gamma(1-i\epsilon)}{\Gamma(1+i\epsilon)} \sin\left(\frac{\theta}{2}\right)^{-2+i2\epsilon}, \quad (2)$$

where $\frac{\Gamma(1-i\epsilon)}{\Gamma(1+i\epsilon)}$, is the 'Newtonian phase'. Crucially, it is not a phase for $\omega \in \mathbb{C}$. Its poles located at $\epsilon := 2GM\omega = in, n \in \mathbb{N}$ provide the spectrum of bounded states of the Newtonian problem [1]. (It can be recovered from an eikonal amplitude, see (5.13) in [2])
For waves of helicity $h \le 2$, the differential cross section can be obtained with the compact expression

$$\frac{d\sigma^h}{d\Omega} = \frac{G^2M^2}{\sin^4(\theta/2)}\left[\cos^{4h}(\theta/2) + \eta \sin^{4h}(\theta/2)\right], \quad (3)$$

where $\eta = 1$ for $h = 2$, and zero otherwise. For $\theta \to 0$, the differential cross section has a universal divergence, due to the long-range nature of the gravitational potential.

2.Kerr Scattering

Wave scattering off the Kerr BH (KBH) is analogous to the scattering off the SBH, with some complications arising from the BH's spin. The NP scalar is

$$\Psi_h(t,r,\theta,\phi) = e^{-i\omega t} \sum_{l=0}^{\infty} \sum_{m=-l}^{l} {}_{-h}S_{\ell m}(\theta,\phi; a\omega) R_{lm}(r)\,, \quad (4)$$

where now the angular dependence is captured by the spin weighted spheroidal harmonics, and the radial functions satisfy the $s = h$, radial Teukolsky equation. Analogous expression for the amplitude functions $f(\theta,\phi)$ in (1). and the phase shift $e^{2i\delta_{\ell m}}$, can be found.

Expansion parameters

The long wave (perturbative) parameter ϵ, the spheroidicity parameter $z = 2a\omega$ and the rotation rate parameter $a^\star = \frac{z}{\epsilon} = \frac{a}{GM}$.
The perturbative expansion is controlled by $\epsilon \ll 1$, and $a^\star \gg 1$. In practice, black hole perturbation theory (BHPT) assumes $a^\star \le 1$, and then the results are analytically continued to $a^\star \to \infty$. However, unlike for the SBH, finding closed expressions analogous to (2) is very difficult in almost every spin configuration.

3. Amplitudes ↔ BHPT dictionary

QFT scattering amplitudes with massless particles naturally encode the radiative content of a scattering process. For wave scattering off BHs, it is reasonable to propose that the a 4-pt amplitude $A_4^{a,h}$, with two massive spin $a = S/M$ legs, and two massless legs of helicity h, encode the radiative content of the NP-scalar, provided a prescription to take the classical limit is given

- For a given order in GM/r, Quantum corrections in $A_4^{a,h}$ appear through $\frac{E}{M} \sim \frac{1}{rM}$. Can disregard them using $E \to \hbar\omega$, $r \to r/\hbar$ and taking $\hbar \to 0$.
- Scaling $r \to \hbar^{-1} r$, is equivalent to a large angular moment expansion $L \to \hbar^{-1} L$. Therefore, for the KBH, the infinite spin limit is needed $a \to \hbar^{-1} a$.

With this prescription at hand one can check that:

- To leading order in G, $|A_4^{a=0,h}|^2$ easily recovers the results in (3).
- For KBH, $A_4^{a,h}$ provides a closed form for the partial wave expansion (see (3.8 -3.13) in [2]).

4. A classical Wave-Particle duality and the eikonal in Kerr

The universality for $\theta \to 0$ in (3) also appears for wave scattering off the KBH. In this regime, the same scattering function $\chi(b, m = \omega b)$, can be obtained from, the eikonal approximation, the phase shift $e^{2i\delta_{\ell m}}$ in the large ℓ-limit, and from the propagation of massless geodesic in Kerr. We obtain

- At 1PM, $\chi(b, m = \omega b) = -2GM\omega \log\left[b^2\omega^2 + a^2\omega^2 \sin^2\gamma + 2a\omega m\right] = 2\,\delta_{lm}^{\rm eik}(\gamma)$, ($\gamma$ is the angle between a and the direction of the incoming wave).
- At 2PM $\chi_{\text{1-loop}}(b, m = b\omega) = -\frac{\pi(GM)^2\omega}{2a^2}\left(b - 4a - \frac{(b-a)^4}{(b^2-a^2)^{3/2}}\right)$, for equatorial scattering $\gamma = \pi/2$, which agrees with the two body result of [3] in the massless limit for one of the BHs.
- At 3PM for wave scattering off the SBH
$\chi_{\text{2-loop}}(b, m = b\omega) = -4GM\omega\left(\log b - \frac{15\pi GM}{16b} - \frac{16G^2M^2}{3b^2} + \dots\right) + \mathcal{O}(a)$, which agrees with the probe limit result (6.29) of [4], in the massless limit.

5. Remarks & Conclusions

- There is a dictionary between QFT amplitudes and BHPT which allows to get new information in both sides. BHPT gives higher-spin data for amplitudes, and amplitudes resume BHPT.
- There is a 3-equality relation between the eikonal approximation, the phase shift from BHPT, and null geodesics motion in the Kerr background, in the $\theta \to 0$ limit.

References

[1] D. N. Kabat and M. Ortiz, *Eikonal quantum gravity and Planckian scattering*, *Nucl. Phys. B* **388** (1992) 570–592, [hep-th/9203082].
[2] Y. F. Bautista, A. Guevara, C. Kavanagh, and J. Vines, *From Scattering in Black Hole Backgrounds to Higher-Spin Amplitudes: Part I*, arXiv:2107.10179.
[3] A. Guevara, A. Ochirov, and J. Vines, *Scattering of Spinning Black Holes from Exponentiated Soft Factors*, *JHEP* **09** (2019) 056, [arXiv:1812.06895].
[4] P. Di Vecchia, C. Heissenberg, R. Russo, and G. Veneziano, *The Eikonal Approach to Gravitational Scattering and Radiation at $\mathcal{O}(G^3)$*, arXiv:2104.03256.

Reducing one-loop correlators to bases of worldsheet functions

Carlos Rodriguez, Oliver Schlotterer and **Yong Zhang**
Department of Physics and Astronomy, Uppsala University
yong.zhang@physics.uu.se

UPPSALA UNIVERSITET

Motivation

It's well-known that the tree-level open string integrand can be expanded onto $(n-3)!$ bases on the support of integration-by-parts (IBP). This expansion simplifies the study of string amplitudes in many aspects. In our paper to appear, we achieve this goal at one-loop level. We find a systematic way to reduce genus-one correlaters of bosonic, heterotic and super symmetric string theories to a universal bases of worldsheet functions.

A Brief Review: universal bases at tree level

Any n-point massless open string tree-level amplitude takes the form

$$A^{\text{tree}} = \int_{z_1<\cdots<z_n} \frac{d^n z}{\text{SL}(2)} \overbrace{\prod_{i<j} z_{ij}^{-s_{ij}}}^{:=\text{KN}} I_n(\{k_i,\epsilon_i,z_i\}) \,, \tag{1}$$

where $s_{ij} := -2\alpha' k_i{\cdot}k_j$, $z_{ij}=z_i-z_j$; one can fix three punctures, e.g. $(z_1, z_{n-1}, z_n) = (0,1,\infty)$, using $\text{SL}(2,\mathbb{R})$ redundancy. After stripping the Koba-Nielsen factor off, the (reduced) string correlator I_n is a rational function of z's which depends on details of vertex operators. There may be terms in I_n that are proportional to a single PT factor

$$\text{PT}(1,2,\cdots,n) := \frac{1}{z_{12}z_{23}\cdots z_{n1}} \,. \tag{2}$$

But in general, there would be a product of shorter PT factors in the string integrand, e.g.

$$\text{PT}(1,2,\cdots,m)\text{PT}(m+1,m+2,\cdots,n) \,. \tag{3}$$

As shown in [1], one can break a shorter PT factor this way

$$\text{PT}(12\cdots m)(\cdots) \overset{\text{IBP}}{=} \frac{1}{1+s_{12\cdots m}} \left(\sum_{\ell=2}^{m} \sum_{j=m+1}^{n-1} \sum_{\rho\in X\sqcup\!\sqcup Y^T} (-1)^{|Y|+1} \frac{s_{\ell j}}{z_{1\rho_1} z_{\rho_1\rho_2}\cdots z^{\ell}_{\rho_{|\rho|}} z_{\ell j}} \right) (\cdots) \,, \tag{4}$$

where X and Y are obtained by matching $(1,2\cdots m) = (1,X,\ell,Y)$. The ellipsis part is free of $z_2, z_3, \cdots, z_m$. Then eq.(3) is reduced as a linear combination of PT factors, which is easy to be further expanded onto the (n-3)! BCJ bases, for example $\text{PT}(1,\rho(2,3,\cdots,n-2),n-1,n)$. As discussed in [2], for a product of more shorter PT factors, one just needs to use the above identity recursively. Our essential task is to find the analog of eq.(4) at one-loop level.

Open-string integrals at genus one

At one-loop, we integrate (S)CFT correlators over a torus, which is equivalent to a parallelogram with identified edges. By suitable involutions of the torus, one obtains the surfaces describing the scattering of open-string states, the cylinder and the Möbius strip. Functions defined on this modular space should be doubly-periodic,

$$F(z+1) = F(z+\tau) = F(z) \,, \tag{5}$$

where τ is the modular parameter. Doubly-periodic Kronecker-Eisenstein series can generate such doubly-periodic functions

$$\begin{aligned}\Omega(z,\eta,\tau) &\equiv \exp\left(2\pi i\eta \frac{\text{Im}\, z}{\text{Im}\,\tau}\right) \frac{\theta'(0,\tau)\theta(z+\eta,\tau)}{\theta(z,\tau)\theta(\eta,\tau)} \\ &= \sum_{w=0}^{\infty} \eta^{w-1} f^{(w)}(z,\tau) \,,\end{aligned} \tag{6}$$

with lower point examples given by $f^{(0)}=1$ and $f^{(1)}(z,\tau) = \partial_z \log\theta(z,\tau) + 2\pi i \frac{\text{Im}\, z}{\text{Im}\,\tau}$. These $f^{(k)}$ functions appear in the string integrand. For example, the OPE of two Kac-Moody currents on torus reads $\langle J^{a_1}(z_1) J^{a_2}(z_2)\rangle \sim 2f^{(2)}_{12} - \left(f^{(1)}_{12}\right)^2 + (\text{free of } z)$, where $f^{(k)}_{ij}$ is the abbreviation of $f^{(k)}(z_{ij},\tau)$. Remind that at tree level, this OPE gives $\sim \text{PT}(12)$. The massless n-point one-loop amplitudes of the open string give rise to integrals of the form $(z_1=0)$ [3]

$$\int_{\mathcal{C}(*)} \left(\prod_{j=2}^{n} \mathrm{d}z_j\right) f^{(k_1)}_{i_1 j_1} f^{(k_2)}_{i_2 j_2} \cdots \overbrace{\exp\left(\sum_{i<j}^{n} s_{ij} G(z_{ij},\tau)\right)}^{:=\text{KN}^\tau} \,, \tag{7}$$

with different integration domains $\mathcal{C}(*)$ for the cylinder and the Möbius strips. The bosonic Green function in the one-loop Koba-Nielsen factor KN^τ satisfies $\partial_{z_i} G(z_{ij},\tau) = -f^{(1)}_{ij}$ and therefore

$$\partial_{z_i}\text{KN}^\tau = -\text{KN}^\tau \sum_{j\neq i}^{n} s_{ij} f^{(1)}_{ij} \,. \tag{8}$$

This can help us to reduce the string integrand at one-loop level.
Studying relations of generating functions is more efficient since it contains an infinite number of relations of $f^{(k)}_{ij}$. It's argued that any open string one-loop integrand can be reduced as a linear combination of functions generated by the following expression (with $\eta_{23\ldots n} = \eta_2 + \eta_3 + \ldots + \eta_n$)

$$\Omega_{12\cdots n} := \Omega(z_{12}, \eta_{23\ldots n}, \tau)\, \Omega(z_{23}, \eta_{3\ldots n}, \tau) \ldots \Omega(z_{n-1,n}, \eta_n, \tau) \,, \tag{9}$$

and its relabelling over $2,3,\cdots n$. However a practical way to realize this idea in general case was absent for a long time until we worked it out.

Identities of the Kronecker-Eisenstein series

There are three important identities of the Kronecker-Eisenstein series: Fay identity

$$\Omega(z_1,\alpha_1,\tau)\,\Omega(z_2,\alpha_2,\tau) = \Omega(z_1,\alpha_1+\alpha_2,\tau)\,\Omega(z_2-z_1,\alpha_2,\tau) + (1\leftrightarrow 2) \,, \tag{10}$$

its variant

$$\Omega(z_{12},\eta,\tau)\,\Omega(z_{21},\xi,\tau) = \Omega(z_{12},\eta-\xi,\tau)\left(\hat g^{(1)}(\xi,\tau) - \hat g^{(1)}(\eta,\tau)\right) + \partial_z \Omega(z_{12},\eta-\xi,\tau) \,, \tag{11}$$

where $\hat g^{(1)}(\eta,\tau) = \partial_\eta \log\theta(\eta,\tau) + \frac{\pi\eta}{\text{Im}\,\tau}$, and the last one about their derivatives

$$\partial_z\Omega(z,\eta,\tau) - \partial_\eta\Omega(z,\eta,\tau) = \left(\hat g^{(1)}(\eta,\tau) - f^{(1)}(z,\tau)\right)\Omega(z,\eta,\tau) \,. \tag{12}$$

Together with eq.(8), the above equations are enough to derive a formula to break a cycle

$$C_{(12\cdots m)} = \Omega_{1,2}(\eta_{2\cdots m,m+1})\Omega_{2,3}(\eta_{3\cdots m,m+1})\cdots\Omega_{m-1,m}(\eta_{m,m+1})\Omega_{m,1}(\eta_{m+1}) \quad \text{with } m\leq n \,, \tag{13}$$

as an analog of eq.(4). Here $\Omega_{ij}(\eta_{ab\ldots c}) := \Omega(z_{ij}, \eta_{ab\ldots c}, \tau)$. For simplicity, we only show the cases $n=m$ in the remaining content of this poster.

Length-2 cycle

According to (11), we have

$$C_{(12)} = \Omega_{1,2}(\eta_{2,3})\Omega_{2,1}(\eta_3) = \Omega_{1,2}(\eta_2)\left(\hat g^{(1)}(\eta_2,\tau) - \hat g^{(1)}(\eta_{23},\tau)\right) + \partial_{z_1}\Omega_{12}(\eta_2) \,. \tag{14}$$

Note that

$$\left(\partial_{z_1}\Omega_{12}(\eta_2)\right)\text{KN}^\tau \overset{\text{IBP}}{=} -\Omega_{12}(\eta_2)\left(\partial_{z_1}\text{KN}^\tau\right) = \Omega_{12}(\eta_2)\,\text{KN}^\tau s_{12} f^{(1)}_{12} \,. \tag{15}$$

Together with eq. (12), it can be used to solve $\partial_{z_1}\Omega_{12}(\eta_2)$ and $f^{(1)}_{12}\Omega_{12}(\eta_2)$. Hence we get

$$C_{(12)} \overset{\text{IBP}}{=} \frac{1}{1+s_{12}}\left(s_{12}\partial_{\eta_2} - \hat g_1(\eta_2) + (1+s_{12})\,\tilde V_1(\eta_2,\eta_3)\right)\Omega_{1,2}(\eta_2) \,, \tag{16}$$

where $\tilde V_1(\eta_I,\eta_J) := \hat g_1(\eta_I) + \hat g_1(\eta_J) - \hat g_1(\eta_{I,J})$.

Length-3 cycle

The first non-trivial example is to break $C_{(123)} = \Omega_{1,2}(\eta_{2,3,4})\Omega_{2,3}(\eta_{3,4})\Omega_{3,1}(\eta_4)$. We found

$$\begin{aligned}&(1+s_{123})C_{(123)} \\ &\overset{\text{IBP}}{=} \left((s_{13}+s_{23})\partial_{\eta_3} - s_{23}\partial_{\eta_2} - \hat g_1(\eta_3) - s_{12}\tilde V_1(\eta_3,\eta_2) + \left(1+s_{1,2,3}\right)\tilde V_1(\eta_3,\eta_4)\right)\Omega_{1,2,3} \\ &\quad - \left((s_{12}+s_{23})\partial_{\eta_2} - s_{23}\partial_{\eta_3} - \hat g_1(\eta_2) - s_{13}\tilde V_1(\eta_2,\eta_3) + \left(1+s_{1,2,3}\right)\tilde V_1\left(\eta_2,\eta_{3,4}\right)\right)\Omega_{1,3,2} \,.\end{aligned} \tag{17}$$

Note that $\Omega_{1,2,3} = \Omega_{1,2}(\eta_{23})\Omega_{2,3}(\eta_3)$.

Arbitrary cycle

We even found a formula to break a cycle of arbitrary multiplicity,

$$\begin{aligned}&(1+s_{12\cdots n})C_{(12\cdots n)} \\ &\overset{\text{IBP}}{=} \sum_{\ell=2}^{n} \sum_{\rho\in\{2,3,\cdots,\ell-1\}\sqcup\!\sqcup\{n,n-1,\cdots,\ell+1\}} (-1)^{n-\ell-1}\Bigg[\sum_{i=1}^{n} s_{i,\ell}\,\partial_{\eta_\ell} - \sum_{i=2}^{n} s_{i,\ell}\,\partial_{\eta_i} - \hat g_1(\eta_\ell) \\ &\qquad + (1+s_{12\cdots n})\tilde V_1(\eta_\ell,\, \eta_{\ell+1,\cdots,n+1}) - \sum_{i=2}^{\ell-1} S_{i,\rho}\tilde V_1(\eta_\ell,\, \eta_{i,i+1,\cdots,\ell-1}) \\ &\qquad - \sum_{i=\ell+1}^{n} S_{i,\rho}\tilde V_1(\eta_\ell,\, \eta_{\ell+1,\ell+2,\cdots,i})\Bigg]\Omega_{1,\rho,\ell} \\ &\quad + \sum_{1\leq p<u<v<w<q\leq n+1} \sum_{\substack{\rho\in\{2,3,\cdots,p\}\sqcup\!\sqcup\{n,n-1,\cdots,q\} \\ \gamma\in\{p+1,\cdots,u-1\}\sqcup\!\sqcup\{v-1,\cdots,u+1\} \\ \pi\in\{v+1,\cdots,w-1\}\sqcup\!\sqcup\{q-1,\cdots,w+1\}}} \sum_{\sigma\in\{\gamma,u\}\sqcup\!\sqcup\{\pi,w\}} \\ &\qquad (-1)^{n+u+v+w}\left(\sum_{i=q}^{n} s_{vi} + \sum_{i=1}^{p} s_{vi}\right) \\ &\qquad \times\left(\hat g_1(\eta_{u+1,\cdots,w-1}) - \hat g_1(\eta_{u+1,\cdots,w}) - \hat g_1(\eta_{u,\cdots,w-1}) + \hat g_1(\eta_{u,\cdots,w})\right)\Omega_{1,\rho,v,\sigma} \,,\end{aligned} \tag{18}$$

where $S_{i,\rho}$ is a sum of Mandelstam variables

$$S_{i,\rho} := s_{i,1} + \sum_{\substack{2\leq j\leq n \\ j \text{ precedes } i \text{ in } \rho}} s_{i,j} \,. \tag{19}$$

When $q=n+1$, $\{n,n-1,\cdots,q\}$ is understood as the empty set $\{\}$ and $\sum_{i=q}^{n} s_{vi} = 0$. The condition $1\leq p<u<v<w<q\leq n+1$ implies $p+4\leq q$ and $p+2\leq v\leq q-2$.
Similar to the tree-level case, for a product of cycles, e.g. $C_{(12\cdots m)}C_{(m+1,m+2\cdots n)}$, one can use the above identity recursively to reduce them onto bases.

Conclusions

We found a closed-form formula to break a cycle of Kronecker-Eisenstein series, which can be recursively used to reduce one-loop open string integrands onto bases. It also applies to closed strings by considering the anti-holomorphic version as well. Our work can simplify the study of one-loop string amplitudes, for example, the integration over punctures z_i's using modular graph forms [4] and the all-order α'-expansion of arbitrary one-loop open-string integrals [5].

References

[1] O. Schlotterer, JHEP **11** (2016), 074 [arXiv:1608.00130 [hep-th]].
[2] S. He, F. Teng and Y. Zhang, Phys. Rev. Lett. **122** (2019) no.21, 211603 [arXiv:1812.03369 [hep-th]].
[3] J. Broedel, C. R. Mafra, N. Matthes and O. Schlotterer, JHEP **07** (2015), 112 [arXiv:1412.5535 [hep-th]].
[4] E. D'Hoker and M. B. Green, J. Number Theor. **189** (2018), 25-80 doi:10.1016/j.jnt.2017.11.015 [arXiv:1603.00839 [hep-th]].
[5] C. R. Mafra and O. Schlotterer, Phys. Rev. Lett. **124** (2020) no.10, 101603 [arXiv:1908.09848 [hep-th]].

Bootstrapping the form factor with master integrals

Yuanhong Guo, Lei Wang, Gang Yang, arXiv:2106.01374
Institute of Theoretical Physics, Chinese Academy of Sciences, Beijing, China
中国科学院理论物理研究所 Institute of Theoretical Physics, Chinese Academy of Sciences

INTRODUCTION

- We consider a 2-loop 4-point form factor in planar $\mathcal{N}$=4 SYM, which may be understood as a supersymmetric version of the Higgs-plus-four-parton scattering, namely, 2-loop 5-point amplitudes with one color-singlet massive external leg:

$$\mathcal{F}_{\mathrm{tr}(\phi_{12}^3)}(1^\phi, 2^\phi, 3^\phi, 4^+; q) = \langle \phi(p_1)\phi(p_2)\phi(p_3)g_+(p_4)|\mathrm{tr}(\phi_{12}^3)|\Omega\rangle.$$

- We develop a new bootstrap strategy: starting with an ansatz expanded in terms of master integrals, then solving the master coefficients via various physical constraints:

$$\mathcal{F}^{(l),\mathrm{ansatz}} = \sum_i C_i I_i^{(l),\mathrm{master}}.$$

- Maximum topologies:

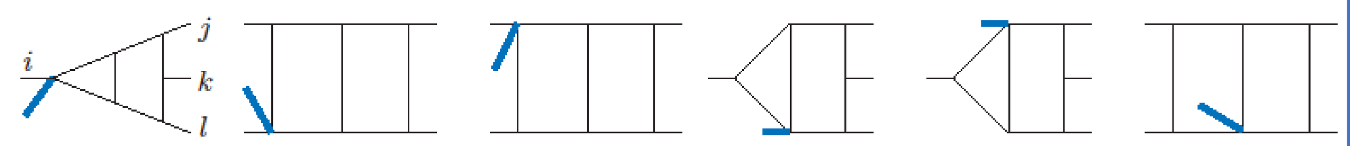

Master integrals are known in Symbol and Goncharov polylogarithms [1,2].

ANSATZ

The 2-loop 4-point form factor ansatz:

$$\mathcal{F}_4^{(2),\mathrm{ansatz}} = \mathcal{F}_4^{(0)} \sum_k (a_k B_1 + b_k B_2) I_k^{\mathrm{UT\ master}},$$

B_1, B_2 are spinor factor:

$$B_1 = \frac{\langle 12\rangle\langle 34\rangle}{\langle 13\rangle\langle 24\rangle}, B_2 = \frac{\langle 14\rangle\langle 23\rangle}{\langle 13\rangle\langle 24\rangle},$$ spurious pole

a_k, b_k are parameters belong to rational number field.

PHYSICS CONSTRAINTS

1. Symmetry: $\mathcal{F}_4^{(2)} = \mathcal{F}_4^{(2)}\big|_{p_1 \leftrightarrow p_3}$;
2. Infrared divergences(IR): which are captured by BDS ansatz [3], the infrared divergences and collinear factorization structure are uniform as follow by introducing $\mathcal{I}_n^{(L)} = \mathcal{F}_n^{(L)}/\mathcal{F}_n^{(0)}$, the remainder $\mathcal{R}_n^{(2)}$ is infrared finite, and 1-loop 4-point form factor is known [4],
$$\mathcal{I}_n^{(2)} = \frac{1}{2}\left(\mathcal{I}_n^{(1)}\right)^2 + f(\epsilon)\mathcal{I}_n^{(1)}(2\epsilon) + \mathcal{R}_n^{(2)} + \mathcal{O}(\epsilon).$$
3. Collinear limit: the remainder $\mathcal{R}_4^{(2)} \xrightarrow{p_3 \| p_4} \mathcal{R}_3^{(2)}$, 2-loop 3-point remainder is known [5], take the limit by introducing momentum twistor;

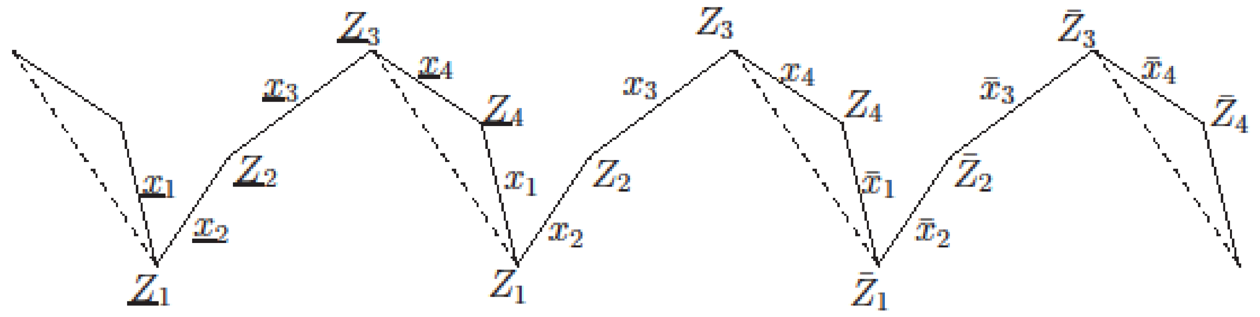

4. Spurious pole cancellation: $\mathcal{F}_4^{(2)} \xrightarrow{\langle 24\rangle \to 0}$ finite;
5. A convenient: the above steps can be done firstly at Symbol level, then repeating them at function level with numeric evaluation;
6. Unitarity cuts(see e.g. [6]): remaining parameters can be solved by one simple cut.

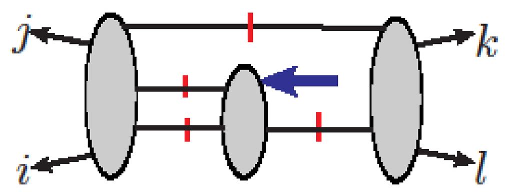

Finally, full analytic results in terms of both Symbol and Goncharov polylogarithms are provided.

Constraints		Parameters left
Symmetry		221
Symbol	IR	82
	Collinear limit	38
	Spurious pole	22
Function	IR	17
	Collinear limit	10
	Finite part	6
Unitarity cuts		0

SYMBOL LETTERS

$$u_{12}, u_{13}, u_{14}, u_{23}, u_{24}, u_{34},$$
$$u_{123}, u_{124}, u_{134}, u_{234},$$
$$u_{123}-u_{12}, u_{123}-u_{23}, u_{124}-u_{12}, u_{124}-u_{14},$$
$$u_{134}-u_{14}, u_{134}-u_{34}, u_{234}-u_{23}, u_{234}-u_{34},$$
$$1-u_{123}, 1-u_{124}, 1-u_{134}, 1-u_{234}.$$

$$\Delta_{3,ijkl} = -\mathrm{Gram}(p_i+p_j, p_k+p_l) = (q^2 - s_{ij} - s_{kl})^2 - 4s_{ij}s_{kl},$$

$$\mathrm{tr}_5^2 = \Delta_5 = \mathrm{Gram}(p_1,p_2,p_3,p_4) = (s_{12}s_{34} + s_{14}s_{23} - s_{13}s_{24})^2 - 4s_{12}s_{23}s_{34}s_{14}$$

$$x_{ijkl}^{\pm} = \frac{1 + u_{ij} - u_{kl} \pm \sqrt{\Delta_{3,ijkl}/s_{1234}}}{2u_{ij}},$$
$$y_{ijkl}^{\pm} = \frac{u_{ij}u_{kl} - u_{ik}u_{jl} + u_{il}u_{jk} \pm P(ijkl)\mathrm{tr}_5/(s_{1234})^2}{2u_{ij}u_{il}},$$
$$z_{ijkl}^{\pm\pm} = 1 + y_{ijkl}^{\pm} - x_{lijk}^{\pm},$$

$$U(p_i+p_j, p_k+p_l) = u_{ikl}u_{jkl} - u_{kl},$$
$$X_1(p_i+p_j, p_k, p_l) = \frac{u_{ij}x_{ijkl}^{+} - u_{ijl}}{u_{ij}x_{ijkl}^{-} - u_{ijl}},$$
$$X_2(p_i+p_j, p_k+p_l) = \frac{x_{ijkl}^{+}}{x_{ijkl}^{-}},$$
$$Y_1(p_i,p_j,p_k,p_l) = \frac{y_{ijkl}^{+}}{y_{ijkl}^{-}},$$
$$Y_2(p_i,p_j,p_k,p_l) = \frac{y_{ijkl}^{+}+1}{y_{ijkl}^{-}+1},$$
$$Z(p_i,p_j,p_k,p_l) = \frac{z_{ijkl}^{++}z_{ijkl}^{--}}{z_{ijkl}^{+-}z_{ijkl}^{-+}}.$$

42 letters, square roots: $\sqrt{\Delta_{3,ijkl}}$(even), tr_5(odd)

DISCUSS AND OUTLOOK

- Letters in each entry: (1) the first-entry contains 8 letters, corresponding to physical poles $u_{i,i+1}$ and $u_{i,i+1,i+2}$; (2) the second entry is free from $\{X_1, Y_1, Y_2, Z, u_{13}, u_{24}\}$, and there are 28 letters; (3) third entry contains all letters except u_{123}; (4) the last-entry is free from $\{X_1, X_2, Z, u_{ijk}, 1-u_{ijk}, u_{12}-u_{123}, u_{23}-u_{123}\}$, and there are 22 letters.
- Comparing to symbol bootstrap [7], we take the advantage of known master integrals: although containing more input comparing to the former, constraints from IR and unitarity cuts can be used. And it can be used to explain the observed universal maximally transcendental parts for form factors.
- Other physics constraints may fix more parameters of ansatz, such as form factor OPE, Regge limits and $\bar{Q}$-like equation.

REFERENCENS

1. Two-Loop Integrals for Planar Five-Point One-Mass Processes, S. Abreu, H. Ita, F. Moriello, B. Page, W. Tschernow, M. Zeng, arXiv:2005.04195.
2. Analytic representation of all planar two-loop five-point Master Integrals with one off-shell leg, D. Canko, C. Papadopoulos, N. Syrrakos, arXiv:2009.13917.
3. Iteration of Planar Amplitudes in Maximally Supersymmetric Yang-Mills Theory at Three Loops and Beyond, Z. Bern, L. Dixon, arXiv:hep-th/0505205.
4. On super form factors of half-BPS operators in N=4 super Yang-Mills, B. Penante, B. Spence, G. Travaglini, C. Wen, arXiv:1402.1300.
5. Analytic two-loop form factors in N = 4 SYM, A. Brandhuber, G. Travaglini, G. Yang, arXiv:1201.4170.
6. On-shell Methods for Form Factors in N=4 SYM and Their Applications, G. Yang, arXiv:1912.11454.
7. Bootstrapping the three-loop hexagon, L. Dixon, J. Drummond, J. Henn, arXiv:1108.4461.

Amplitudes of planar $\mathcal{N}=4$ super-Yang-Mills from $\bar{Q}$-equations

Song He, Zhenjie Li and Chi Zhang

中国科学院理论物理研究所
Institute of Theoretical Physics, Chinese Academy of Sciences

Introduction

We compute the symbol of three-loop MHV octagon [1] and some two-loop NMHV amplitudes [2, 3] in planar $\mathcal{N}=4$ super-Yang-Mills (sYM) from the $\bar{Q}$ equations [4] (the following figure also from [4]):

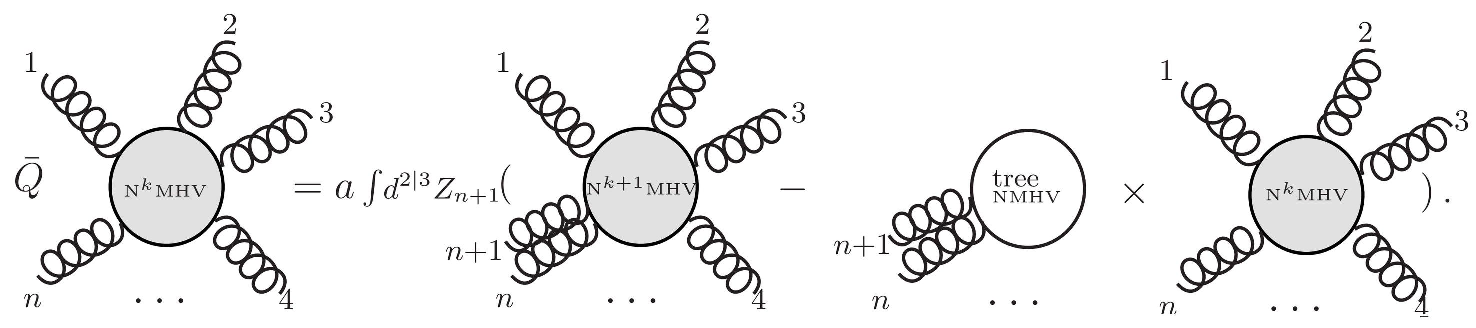

$$\bar{Q}^A_a R_{n,k} = \frac{1}{4}\Gamma_{\mathrm{cusp}} \operatorname*{Res}_{\epsilon=0} \int_{\tau=0}^{\tau=\infty} \left(\mathrm{d}^{2|3}\mathcal{Z}_{n+1}\right)^A_a [R_{n+1,k+1} - R_{n,k}R^{\mathrm{tree}}_{n+1,1}] + \text{cyc.}\,. \qquad (1)$$

It's an efficient first principle calculation from anomaly of dual superconformal symmetry. The results reveal new and rich structures beyond amplitudes of lower multiplicities, especially the appearance of algebraic letters.

Review of $\bar{Q}$ equations

The infrared divergences of planar $\mathcal{N}=4$ sYM can be captured by the so-called BDS anstaz, and we are interested in the infrared-finite object, the *BDS-subtracted amplitude*, $R_{n,k} = A_{n,k}/A_n^{\mathrm{BDS}}$, for n-point, N^kMHV amplitude $A_{n,k}$. As shown in [4], $R_{n,k}$ is a *dual conformal invariant* (DCI) but not invariant under the action of dual superconformal generators

$$\bar{Q}^A_a = \sum_{i=1}^{n} \chi_i^A \frac{\partial}{\partial Z_i^a}\,, \qquad (2)$$

where Z_i are momentum twistors and χ_i denote their Grassmann parts.

Nevertheless, this anomaly can be restored by an integral over collinear limits of higher-point amplitudes eq.(1), where Γ_{cusp} is the cusp anomalous dimension, and the particle $n+1$ is added in collinear limit with n whose (super-) momentum twistor $\mathcal{Z}_{n+1} = (Z_{n+1}, \chi_{n+1})$ is parametrized by τ and small ϵ:

$$\mathcal{Z}_{n+1} = \mathcal{Z}_n - \epsilon\mathcal{Z}_{n-1} + C\epsilon\tau\mathcal{Z}_1 + C'\epsilon^2\mathcal{Z}_2\,, \qquad (3)$$

where two constants C and C' fix the particle weight, and the integral measure is $(\mathrm{d}^{2|3}\mathcal{Z}_{n+1})^A_a := \varepsilon_{abcd} Z^b_{n+1}\mathrm{d}Z^c_{n+1}\mathrm{d}Z^d_{n+1}(\mathrm{d}^3\chi_{n+1})^A$. In this collinear limit, the bosonic integral reads

$$C(\bar{n})_a \operatorname{Res}_{\epsilon=0} \int \epsilon \mathrm{d}\epsilon \int_0^\infty \mathrm{d}\tau \qquad (4)$$

with $(\bar{n})_a := (n{-}1\,n\,1)_a$. The notation $\operatorname{Res}_{\epsilon=0}$ means to extract the coefficient of $\mathrm{d}\epsilon/\epsilon$ under the collinear limit of $\epsilon \to 0$.The perturbative expansion of (1) relates $R^{(L)}_{n,k}$ to $R^{(L-1)}_{n+1,k+1}$. After working out the integration,

$$\bar{Q}R^{(L)}_{n,k} = \textstyle\sum_\alpha Y^\alpha_{n,k}\ \bar{Q}\log(a_\alpha)\ \mathcal{I}^{(2L-1)}_\alpha\,, \qquad (5)$$

where $Y^\alpha_{n,k}$ are Yangian (superconformal & dual superconformal) invariants and $\mathcal{I}^{(2L-1)}_\alpha$ are DCI functions of weight $2L-1$.

There's no non-trivial DCI function living in the kernel of $\bar{Q}$ for $k=0,1$. Thus once a_α are DCI, taking the trace of $\bar{Q}$ in eq.(5), we get

$$\mathrm{d}R^{(L)}_{n,k} = \textstyle\sum_\alpha Y^\alpha_{n,k}\ \mathrm{d}\log(a_\alpha)\ \mathcal{I}^{(2L-1)}_\alpha\,, \qquad (6)$$

then the symbol of $R^{(L)}_{n,k}$ is $\mathcal{S}[R^{(L)}_{n,k}] = \sum_\alpha Y^\alpha_{n,k}\ \mathcal{S}[\mathcal{I}^{(2L-1)}_\alpha] \otimes (a_\alpha)$. Finally we want to calculate the functions $\mathcal{I}^{(2L-1)}_\alpha$ given by integrals of the form

$$\int_0^\infty \mathrm{d}\log f(\tau)\ I_{n+1}(\tau, \epsilon \to 0). \qquad (7)$$

Square root & four-mass box

However, there're Gram-determinant square roots in the integrand of eq.(7) when we calculate the two-loop 9-pt NMHV amplitude $R^{(2)}_{9,1}$ from 1-loop 10-pt N^2MHV amplitude $R^{(1)}_{10,2}$, and then three loop MHV octagon $R^{(3)}_{8,0}$ from $R^{(2)}_{9,1}$. These square roots come from the four-mass boxes in the box expansion of $R^{(1)}_{10,2}$:

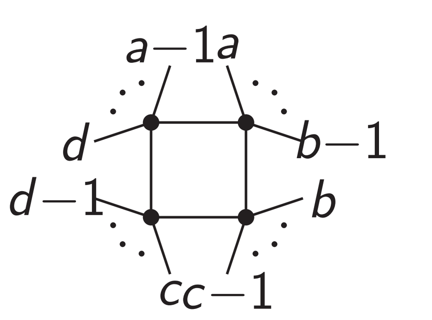

$$\begin{cases} x^2_{ab} := \dfrac{\langle a{-}1\,a\,b{-}1\,b\rangle}{\langle a{-}1\,a\rangle\langle b{-}1\,b\rangle},\ u_{abcd} = \dfrac{x^2_{ad}x^2_{bc}}{x^2_{ac}x^2_{bd}},\ v_{abcd} = \dfrac{x^2_{ab}x^2_{cd}}{x^2_{ac}x^2_{bd}}, \\ \Delta_{abcd} = \sqrt{(1-u_{abcd}-v_{abcd})^2 - 4u_{abcd}v_{abcd}}, \\ z_{abcd}\bar{z}_{abcd} = u_{abcd}, \quad (1-z_{abcd})(1-\bar{z}_{abcd}) = v_{abcd}, \\ F := \mathrm{Li}_2(1-z_{abcd}) - \mathrm{Li}_2(1-\bar{z}_{abcd}) + \frac{1}{2}\log(v_{abcd})\log(\frac{z_{abcd}}{\bar{z}_{abcd}}). \end{cases}$$

Rationalization of τ-integrals

The nontrivial τ-integrals involving square roots are in the form of

$$\int d\log(\tau - b)\, F(z(\tau), \bar{z}(\tau)) \otimes \frac{z(\tau)-a}{\bar{z}(\tau)-a},$$

where F is a (normalized) four-mass box function of pure transcendental weight 2. We need to rationalize it to perform the τ-integration.

The main observation here is that there're two rational constants p and q such that $pu(\tau) + qv(\tau) = 1$, which leads a Möbius transformation $\Lambda(z) = \frac{qz-q+1}{(p+q)z-q}$ such that $\Lambda(z) = \bar{z}$ and $\Lambda^2 = \mathrm{id}$. Thus, the transformation $\tau \to \tau(z)$ indeed rationalizes the above integral.

On the support $\bar{z} = \Lambda(z)$, it's also interesting to notice that the symbol of the function

$$F_x(z,\bar{z}) := \int d\log\frac{z-x}{\bar{z}-x}\, F(z,\bar{z})$$

is an integrable symbol with the minimal algebraic word $\mathcal{S}[F(z,\bar{z})] \otimes \frac{z-x}{\bar{z}-x}$:

$$\mathcal{S}[F_x(z,\bar{z})] = \mathcal{S}[F(z,\bar{z})] \otimes \frac{z-x}{\bar{z}-x} + \text{rational terms.} \qquad (8)$$

In our cases, the $d\log$ measure can always be written as

$$\int d\log\left(f(\tau) = c_0\frac{(z-c)(z-\bar{c})}{(z-1)(z-\bar{1})}\right) F(z,\bar{z}) \otimes \frac{z-a}{\bar{z}-a},$$

where we introduce the shorthand $\bar{x} := \Lambda(x)$. By calculating its total derivative by IBP, we get its symbol

$$\begin{aligned} &\left(\int d\log\frac{z-c}{z-\bar{c}}F\right) \otimes \frac{a-c}{a-\bar{c}} - \mathcal{S}[F_1] \otimes \frac{a-1}{a-\bar{1}} - \mathcal{S}[F_a] \otimes f(\tau_a) \\ &+ \frac{1}{2}\mathcal{S}[F_{\bar{\infty}}] \otimes \frac{f(\tau_a)(a-1)}{c_0(a-\bar{1})} + \mathcal{S}[F] \otimes \frac{z-a}{\bar{z}-a} \otimes f(\tau), \end{aligned} \qquad (9)$$

where τ_a is defined by $z(\tau = \tau_a) = a$.

Results & Comments

The symbol of three-loop MHV octagon can be written as $R^{(3)}_{8,0} = \sum_{i=2}^{5} P_i \otimes \langle 781i\rangle + \text{cyc.}$, each coefficient has around 10^8 terms.

The symbol alphabet of $R^{(3)}_{8,0}$ consists of 204 multiplicative-independent rational letters and 18 independent DCI algebraic letters. The 204 rational letters are organized as follows

- $\binom{8}{2} - 2 = 68$: all $\langle abcd\rangle$ except $\langle 1357\rangle$ and $\langle 2468\rangle$;
- 1 cyclic class of $\langle 12(345)\cap(678)\rangle$;
- 7 cyclic class of $\langle 1(ij)(kl)(mn)\rangle$ with $2 \le i < j < k < l < m < n \le 8$; 5 cyclic class of $\langle 1(28)(kl)(mn)\rangle$ with $2 < k < l < m < n < 8$;
- 5 cyclic class of $\langle \bar{2}\cap\bar{4}\cap(568)\cap\bar{8}\rangle$, $\langle \bar{2}\cap\bar{4}\cap\bar{6}\cap(681)\rangle$, $\langle (127)\cap(235)\cap\bar{5}\cap\bar{7}\rangle$, $\langle (127)\cap\bar{3}\cap(356)\cap\bar{7}\rangle$, $\langle \bar{2}\cap(278)\cap(346)\cap\bar{6}\rangle$.

The symbol alphabet of $R^{(2)}_{8,1}$ only consists of 180 rational letters, cyclic images of $\langle 1(23)(46)(78)\rangle$, $\langle \bar{2}\cap\bar{4}\cap(568)\cap\bar{8}\rangle$ and $\langle \bar{2}\cap\bar{4}\cap\bar{6}\cap(681)\rangle$ do not appear.

Algebraic letters can only appear at the second and third entry of $R^{(2)}_{n,1}$ and $R^{(3)}_{n,0}$ for $n \ge 8$, and the algebraic part with a given square root Δ_{abcd} of the symbol can be written as

$$\sum_\alpha \mathcal{S}[F(z_{abcd}, \bar{z}_{abcd})] \otimes \frac{z_{abcd}-\alpha}{\bar{z}_{abcd}-\alpha} \otimes R_\alpha,$$

where R_α is a weight $2L-3$ integrable symbol. For octagon ($n=8$), algebraic letters can be choosen as cyclic images of $(z_{2468}-\alpha)/(\bar{z}_{2468}-\alpha)$ for $\alpha = 0, \frac{\langle 1236\rangle\langle 5678\rangle}{\langle 1256\rangle\langle 3678\rangle}, \frac{\langle 1246\rangle\langle 5678\rangle}{\langle 1256\rangle\langle 4678\rangle}$.

Outlook

(1) Amplitudes beyond MHV and NMHV from anomaly ($Q^{(1)}$ equations), especially the two-loop N^2MHV octagon.

(2) Understand the structure of amplitudes involving square roots: Steinmann relations, extend Steinmann relations, limiting ray of infinite cluster algebra, cluster adjacency of irrational letters? & ...

Reference

[1] Zhenjie Li and Chi Zhang. to appear.
[2] Song He, Zhenjie Li, and Chi Zhang. *Phys. Rev. D*, 101(6):061701, 2020.
[3] Song He, Zhenjie Li, and Chi Zhang. *JHEP*, 03:278, 2021.
[4] Simon Caron-Huot and Song He. *JHEP*, 07:174, 2012.

lizhenjie@itp.ac.cn